The Stabilisation of Reduced Carboranes

Hugo Tricas Laliena

Submitted for the degree of Doctor of Philosophy at Heriot-Watt University, on completion of research in the School of Engineering and Physical Sciences.

September 2010

I hereby declare that the work presented in this thesis was carried out by myself at Heriot-Watt University, Edinburgh, except where due acknowledgement is made, and has not been submitted for any other degree.

_____

Hugo Tricas Laliena (Candidate)

_____

Prof. Alan J. Welch

_____

Date

ABSTRACT

Chapter 1 presents the most relevant literature in the fields of borane, carborane and metallacarborane chemistry, providing the reader with an overview of these topics. The area of supraicosahedral (hetero)carborane chemistry is covered in detail, focusing on the instability of reduced carborane dianions towards re-oxidation.

Chapter 2 reports the attempted stabilisation of reduced carborane dianions by control of the cage carbon atom movement. The design and preparation of a rigid tether and its attachment to *meta*-carborane are presented, accompanied by a detailed study of the reduction chemistry of the unprecedented tethered carborane formed.

Chapter 3 introduces the concept of reduced carborane stabilisation by inductive effects. A series of novel carboranes bearing electron withdrawing fluorinated aryl groups is reported. The influence of these substituents is investigated in detail by computational, structural, spectroscopic and electrochemical studies in order to select the best carborane precursor for polyhedral expansion chemistry.

Chapter 4 describes the polyhedral expansion of selected carboranes. The synthesis and characterisation of a series of novel supraicosahedral species are presented, together with an exhaustive discussion of the effect of fluorinated aryl groups in polyhedral expansion chemistry.

Chapter 5 gives full details of the experimental procedures undertaken and also provides spectroscopic and analytical data for all the new compounds reported herein.

Appendix 1 provides details of the crystal structure determinations of compounds synthesised.

Appendix 2 (provided on compact disc) gives the appropriate crystallographic files in RTF and CIF format.

ACADEMIC REGISTRY
Research Thesis Submission

Name*:*			
School/PGI:			
Version: *(i.e. First, Resubmission, Final)*		Degree Sought (Award **and** Subject area)	

Declaration

In accordance with the appropriate regulations I hereby submit my thesis and I declare that:

1) the thesis embodies the results of my own work and has been composed by myself
2) where appropriate, I have made acknowledgement of the work of others and have made reference to work carried out in collaboration with other persons
3) the thesis is the correct version of the thesis for submission and is the same version as any electronic versions submitted*.
4) my thesis for the award referred to, deposited in the Heriot-Watt University Library, should be made available for loan or photocopying and be available via the Institutional Repository, subject to such conditions as the Librarian may require
5) I understand that as a student of the University I am required to abide by the Regulations of the University and to conform to its discipline.

* *Please note that it is the responsibility of the candidate to ensure that the correct version of the thesis is submitted.*

Signature of Candidate*:*		Date:	

Submission

Submitted By *(name in capitals):*	
Signature of Individual Submitting:	
Date Submitted:	

For Completion in Academic Registry

Received in the Academic Registry by *(name in capitals):*			
Method of Submission *(Handed in to Academic Registry; posted through internal/external mail):*			
*E-thesis Submitted (**mandatory for final theses from January 2009)***			
Signature:		Date:	

“What we know is a drop, what we don't know is an ocean”
Isaac Newton

ACKNOWLEDGEMENTS

First of all I would like to thank my supervisor: Prof Alan J. Welch. The results presented in this thesis could have never been obtained without his enthusiastic advice, patience and guidance throughout this project. Besides the academic supervision, I would like to thank him for his great kindness and support in every aspect of life, especially for all the arrangements that made possible my short collaboration at the INEOS in Moscow. Being such as approachable person, he has made my time at his group infinitely more enjoyable.

I would like to thank all the members of the Boron Group, for making the laboratory such a nice and cheerful place to work. Dr David Ellis has been a continuous source of knowledge, usually after my common stupid questions. I also want to thank past members Drs Elena Lopez and Sergey Zlatogorsky for their help and guidance and for being such a good friends. Special thanks to Dr Peter Abram, Brian Hutton, Amelia McAnaw and Ross McLellan for all the countless cups of tea, football games, nights out and just good moments that we have shared over the last four years. I also want to thank the new lab members Gobika Thiripuranathar and Greig Scott, as well as the project students that worked next to me, Marta Colon and James Ward.

I also want to thank our collaborators for their contribution to the results presented in this thesis. Thanks to Prof Piero Zanello (University of Siena) for the electrochemistry and to David McKay for the DFT calculations. I want to express my sincere gratitude to Dr Dmitry Perekalin (INEOS, Moscow) for all his help and patience during my short stay at his institute. The experimental results could have never been obtained without the help and support of Dr Georgina Rosair for *X*-ray crystallography and mass spectrometry, Dr Alan Boyd for NMR and Christina Graham for elemental analysis.

Por último, y no por ello menos importante, infinitas gracias a mis padres por todo el apoyo económico y moral recibido durante mis cuatro años en Escocia, por todas las llamadas y emails, por todos los paquetes con provisiones enviados y sobre todo por haber venido a visitarme. Como no, gracias también para Emma, por su continuo apoyo, por poner un poco de orden en mi vida y especialmente por ser capaz de sacar lo mejor de mí en todo momento.

TABLE OF CONTENTS

ABBREVIATIONS

2c-2e	two centre two electron (bond)
3c-2e	three centre two electron (bond)
Ar_F	fluorinated aryl group(s)
BNCT	Boron Neutron Capture Therapy
br	broad
Cap	Capitation
CHN	elemental analysis (Carbon-Hydrogen-Nitrogen)
Cp	cyclopentadienyl (C_5H_5)
Cp*	pentamethylcyclopentadienyl (C_5Me_5)
CV	Cyclic Voltammetry
δ	chemical shift
d	doublet
DCM	dichloromethane
DSD	diamond-square-diamond
e	electron
E	Energy
EI	electron impact
Et	ethyl
g	gram(s)
HOMO	Highest Occupied Molecular Orbital
IR	Infra-red
LUMO	Lowest Unoccupied Molecular Orbital
m	multiplet
M^+	molecular ion
Me	methyl
Met	Metallation
mg	milligram(s)
min	minutes
ml	millilitre(s)
MHz	megahertz
mmol	millimole(s)

mol	mole(s)
MO	Molecular Orbital
MS	Mass spectrometry
MW	molecular weight
NMR	Nuclear Magnetic Resonance
petroleum ether	fraction of petroleum ether boiling between 40 and 60 ºC (unless otherwise stated)
Ph	phenyl
ppm	parts per million
PSEP	Polyhedral Skeletal Electron Pair
Red	Reduction
res	resolution
R_f	Retention factor
s	singlet
t	triplet
THF	tetrahydrofuran
TLC	Thin Layer Chromatography

ABBREVIATIONS FOR SPECIFIC COMPOUNDS

A	1,8-dichloroanthracene
B	1,8-bis[(trimethylsilyl)ethynyl]-anthracene
C	1,8-diethynylanthracene
D	1,7-$(CH_2OH)_2$-1,7-*closo*-$C_2B_{10}H_{10}$
E	C_6F_5-C≡C-Ph
F	4-$F_3CC_6H_4$-C≡C-Ph
G	1,2-Ph_2-1,2-*closo*-$C_2B_{10}H_{10}$
H	$F_3CC_6H_4$-C≡C-4'-$C_6H_4CF_3$
1	1,7-$(CH_2OSO_2CF_3)_2$-1,7-*closo*-$C_2B_{10}H_{10}$
2	1,7-$(CH_2I)_2$-1,7-*closo*-$C_2B_{10}H_{10}$
3	1,8-bis[(hydroxymethyl)ethynyl]-anthracene
4	1,8-bis[(bromomethyl)ethynyl]-anthracene
5	1,7-μ-[1',8'-$(C_2CH_2)_2$-$C_{14}H_8$)]-1,7-*closo*-$C_2B_{10}H_{10}$
6	1-C_6F_5-2-Ph-1,2-*closo*-$C_2B_{10}H_{10}$
7	1-(4'-$H_3CC_6F_4$)-2-Ph-1,2-*closo*-$C_2B_{10}H_{10}$
8	1-(4'-$F_3CC_6F_4$)-2-Ph-1,2-*closo*-$C_2B_{10}H_{10}$
9	1-(4'-$F_3CC_6H_4$)-2-Ph-1,2-*closo*-$C_2B_{10}H_{10}$
10	1,2-(4'-$F_3CC_6F_4)_2$-1,2-*closo*-$C_2B_{10}H_{10}$
11	1-(4'-$F_3CC_6F_4$)-1,2-*closo*-$C_2B_{10}H_{11}$
12	1-(4'-$F_3CC_6H_4$)-1,2-*closo*-$C_2B_{10}H_{11}$
13	1,2-(4'-$F_3CC_6H_4)_2$-1,2-*closo*-$C_2B_{10}H_{10}$
14	1,7-(4'-$F_3CC_6F_4)_2$-1,7-*closo*-$C_2B_{10}H_{10}$
15	1,12-(4'-$F_3CC_6F_4)_2$-1,12-*closo*-$C_2B_{10}H_{10}$
16	1,7-(4'-$F_3CC_6F_4)_2$-9,10-Ph_2-1,7-*closo*-$C_2B_{10}H_8$
17	1,12-(4'-$F_3CC_6F_4)_2$-4-Cp-4,1,12-*closo*-$CoC_2B_{10}H_{10}$
18A	μ-1,4-[2'-(η-C_5H_4)-4'-CF_3-C_6F_3]-6-Ph-4,1,6-*closo*-$CoC_2B_{10}H_{10}$
18B	1-Ph-μ-6,4-[2'-(η-C_5H_4)-4'-CF_3-C_6F_3]-4,1,6-*closo*-$CoC_2B_{10}H_{10}$
19	1-(4'-$F_3CC_6F_4$)-2-Ph-8-Cp-8,1,2-*closo*-$CoC_2B_9H_{11}$
20	1-Ph-4,5-Cp_2-6-(4'-$F_3CC_6F_4$)-4,5,1,6-c*loso*-$Co_2C_2B_9H_9$
21A	μ-1,4-[2'-(η-C_5H_4)-4'-CF_3-C_6F_3]-6-(4'-$F_3CC_6F_4$)-4,1,6-*closo*-$CoC_2B_{10}H_{10}$

21B 1-(4'-$F_3CC_6F_4$)-μ-6,4-[2'-(η-C_5H_4)-4'-CF_3-C_6F_3]-4,1,6-*closo*-$CoC_2B_{10}H_{10}$

22 1,2-(4'-$CF_2C_5Me_5$-C_6F_4)$_2$-1,2-*closo*-$C_2B_{10}H_{10}$

23 1,12-(4'-$F_3CC_6F_4$)$_2$-4-Cp*-4,1,12-*closo*-$CoC_2B_{10}H_{10}$

24 1-(4'-$F_3CC_6F_4$)-2,8-Cp*$_2$-12-(THF)-2,8,1-*closo*-$Co_2CB_9H_8$

25 1,2-(4'-$F_3CC_6F_4$)$_2$-3-(η-C_6H_6)-3,1,2-*pseudocloso*-$RuC_2B_9H_9$

26 1,12-(4'-$F_3CC_6F_4$)$_2$-4-(η-C_6H_6)-4,1,12-*closo*-$RuC_2B_{10}H_{10}$

27 1-(4'-$F_3CC_6F_4$)-4-(η-C_6H_6)-6-Ph-4,1,6-*closo*-$RuC_2B_{10}H_{10}$

CHAPTER 1. Introduction

1.1 Boron.

Boron is the only non-metal in group 13 of the periodic table. Boron is a relatively rare element in the earth's crust, representing only 0.001%. It does not occur free in nature but is found in a variety of minerals all related to borax, sodium tetraborate, $Na_2B_4O_7 \cdot 10H_2O$. These compounds have been known for thousands of years but elemental boron was not prepared until 1808 by the independent researches of Sir Humphry Davy in England and Gay-Lussac and Thenard in France.[1]

The element occurs naturally as 19.8% ^{10}B isotope and 80.2% ^{11}B isotope. The lighter isotope, ^{10}B, has a high neutron capture cross section for thermal neutron absorption and is used as a shield for nuclear radiation in instruments used for detecting neutrons and, more recently, in non-invasive cancer treatments such as BNCT (Boron Neutron Capture Therapy).[2,3] Both nuclei are NMR active with nuclear spin numbers 3 and 3/2 respectively. However, since ^{11}B is more abundant, it is the preferred nucleus. Thus, ^{11}B-NMR spectroscopy is a widely used technique for the study of boron-containing species.

Boron is electron-deficient, possessing a vacant p-orbital. Its chemical properties are determined by that fact giving boron the ability to form covalently bonded molecular clusters that involve delocalisation of electrons. In fact, boron exhibits extensive cluster chemistry, especially as boron hydrides (boranes). These compounds are constantly being developed along with new bonding theories and rules.

1.2 Boranes.

The chemical family of boron hydrides, also known as boranes, comprises the compounds that are composed solely of boron and hydrogen. Research into this field was first initiated by Stock.[4] Stock used newly developed glass vacuum lines to isolate a range of boranes from B_2H_6 to $B_{10}H_{14}$. These compounds were classified into two distinct homologous series: B_nH_{n+4} and B_nH_{n+6}. It soon became apparent that the bonding in boranes could not be directly compared with the classical bonding in alkanes due to the lower number of electrons involved. In order to explain the bonding of these compounds, in 1948 Longuet-Higgins proposed the theory of 3-centre 2-electron (3c-2e) bonding.[5] This led these boranes to be termed "electron deficient". The simplest boron hydride is diborane, B_2H_6. Diborane has two less bonding electrons available than its alkane analogue, C_2H_6. To overcome the electron deficiency B_2H_6 adopts a multicentre bonding structure as confirmed by *X*-ray diffraction techniques (see figure 1.2.1).[6,7]

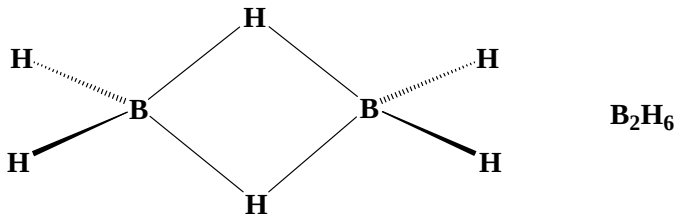

Figure 1.2.1 Structure of diborane, B_2H_6, the simplest example of 3c-2e bonding.

In the structure of diborane the four terminal hydrogen atoms are bonded to the boron atoms with classical 2c-2e bonds whereas the two bridging hydrogen atoms bind through a 3c-2e bond allowing each boron atom to achieve an octet.

In order to obtain a general theory of bonding in boranes, Lipscomb extended the 3c-2e model proposed by Longuet-Higgins and developed a set of rules known as the *styx* rules.[8] Lipscomb considered the number of 3c-2e B-H-B (*s*) and B-B-B (*t*) interactions, the number of 2c-2e B-B (*y*) bonds and the number of BH_2 units (*x*) to rationalise and predict structures of boranes. Although this theory was adequate for small boron hydrides it failed to predict the structures of larger boron clusters.

Wade developed the most complete method to predict the exact structure of boranes by counting the number of electrons involved in the skeletal bonding of the cluster.[9] This approach, known as Wade's rules, works for boranes, heteroboranes and also for other delocalised clusters and provides the basis of the Polyhedral Skeletal Electron Pair (PSEP) theory.[10] This theory recognises the ability of boron atoms to delocalise electrons and relates the number of electrons involved in the bonding within the polyhedral cluster to its structure.

In Wade's rules the number of polyhedral skeletal electron pairs (PSEP's) in a borane cluster can be calculated and this number, considering the number of vertices in the polyhedron, is associated with a type of structure.

The theory works as follows. The cluster can be broken into fragments denoted as: {fragment}. Each fragment in the polyhedron contributes a certain number of electrons to the skeletal bonding. For a main group vertex, for example {BH}, the electronic contribution(s) to the skeletal bonding is:

$$s = v + x - 2$$

where
s = number of electrons available for skeletal bonding.
v = number of valence electrons of the vertex atom.
x = number of electrons contributed by any exopolyhedral atom or group.

For a transition metal vertex, the electronic contribution needs to be adjusted and becomes:

$$s = v + x - 12 \text{ (for 18e species)}$$
$$s = v + x - 10 \text{ (for 16e species)}$$

The total number of skeletal electrons in the polyhedral cluster can be calculated by considering all the fragments, the bridging hydrogen atoms and any adjustment for the charge. The total number of PSEP's is given by halving this value.

The number of PSEP's is related to the number of vertices (n) in the polyhedron, allowing the structure prediction as follows (most common patterns underlined):

n	hypercloso
n+1	**<u>closo</u>**
n+2	**<u>nido</u>**
n+3	**<u>arachno</u>**
n+4	hypho
n+5	klado

According to these rules, different clusters of n vertices will present the same structure if they possess the same number of skeletal electrons, although they might have different isolobal[11] vertices (vertices which possess similar frontier molecular orbitals and the same number of bonding electrons) or an overall charge to compensate for the number of skeletal electrons. This can be illustrated by the substitution of {BH} vertices with {CH} and {$Ru(CO)_3$} fragments in the range of compounds *closo*-dodecaborate (2-)[12], *closo*-monocarbaundecaborate (1-)[13], 1,2-*closo*-dicarbadecaborane[14] and 3,3,3-tricarbonyl-3,1,2-*closo*-ruthenadicarbanonaborane[15] (figure 1.2.2).

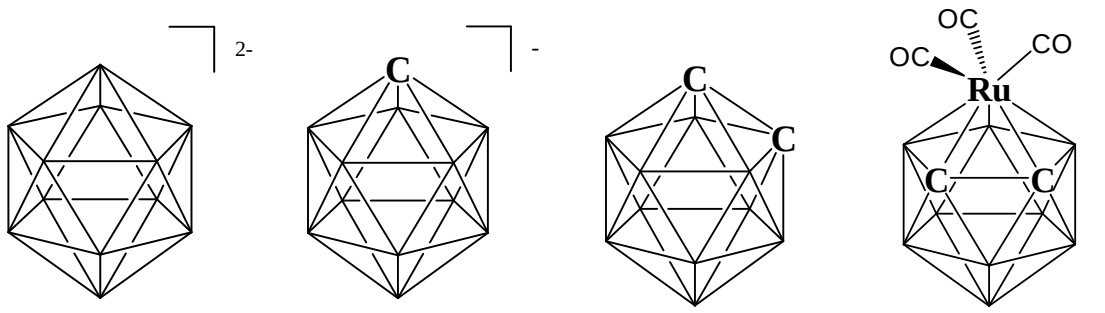

[*closo*-$B_{12}H_{12}$]$^{2-}$ [*closo*-$CB_{11}H_{12}$]$^{-}$ 1,2-*closo*-$C_2B_{10}H_{12}$ 3,3,3-$(CO)_3$-3,1,2-*closo*-$RuC_2B_9H_{11}$

Figure 1.2.2 Retention of icosahedral structure in different isostructural borane and heteroborane clusters. (N.B. Naked vertex = BH, C vertex = CH).

Williams was able to demonstrate the connection between the structures of many borane clusters by simply removing the highest connected vertex beginning with the closed parent polyhedron.[16] The highest connected vertex in a closo polyhedron is removed to afford a nido structure. The conversion from nido to arachno can be achieved by removing the highest connected vertex in the open face of the nido

fragment. This relationship is known as the Wade-Williams structural matrix, displayed in figure 1.2.3.

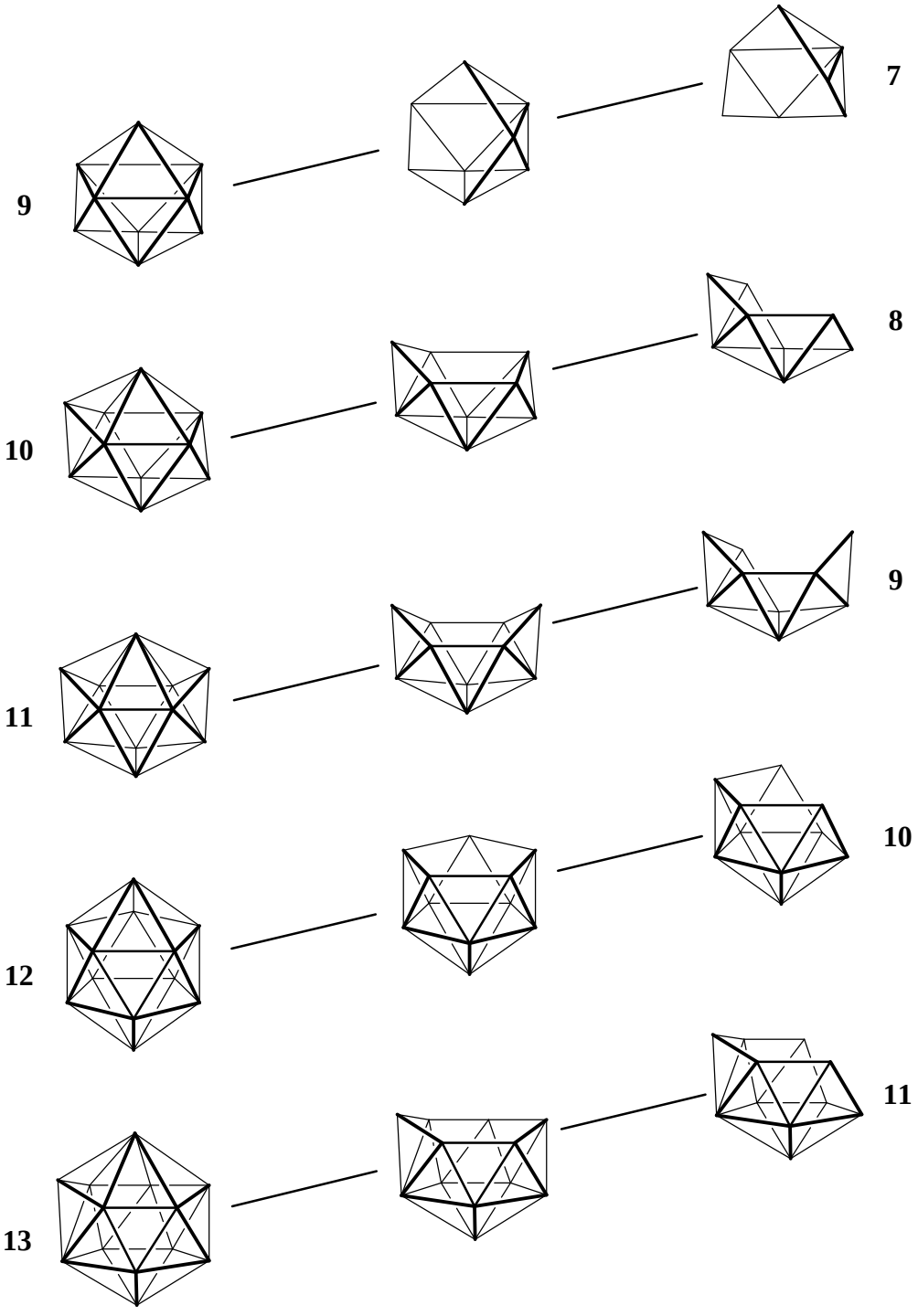

Figure 1.2.3 Part of the Wade-Williams structural matrix with an additional *closo*-13-vertex row. (N.B. alternative structures are also possible).

1.3 Carboranes.

One of the most studied heteroborane clusters is the carboranes. This large family comprises the polyhedral clusters composed of boron and carbon atoms. Since {CH} fragments are isolobal and isoelectronic with $\{BH\}^-$, successive substitution of vertices leads to neutral analogues of boranes. A really important subclass is the dicarbon series, with the general formula $C_2B_{n-2}H_n$ known for $5<n<12$.[17] The work presented in this thesis is focussed on the icosahedral dicarbon analogues of $[B_{12}H_{12}]^{2-}$, with general formula $C_2B_{10}H_{12}$ and called dicarbadecaboranes or more commonly carbaboranes or carboranes.

1.3.1 Synthesis.

Carboranes can be prepared by insertion of acetylenes into decaborane mediated by Lewis bases.[14a] This reaction can be utilised to synthesise carboranes and C-substituted carboranes (figure 1.3.1.1).

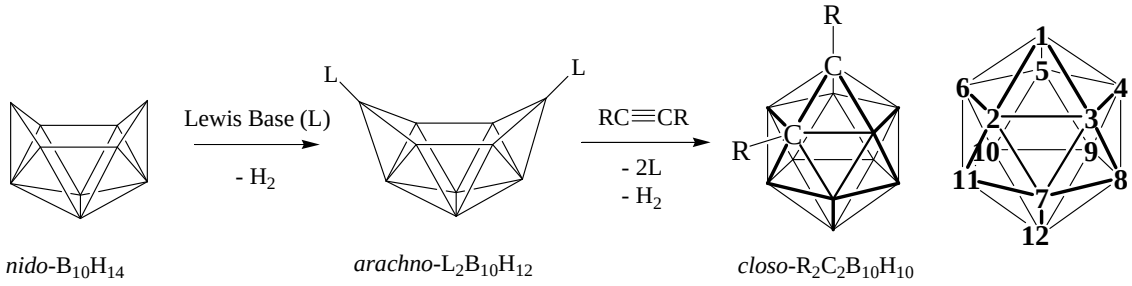

Figure 1.3.1.1 Preparation of carboranes by insertion of acetylenes into decaborane and numbering scheme for icosahedral clusters.

There are three possible isomers of icosahedral carborane depending on the positions of the carbon atoms in the cage: 1,2- (*ortho*), 1,7- (*meta*) and 1,12- (*para*) (figure 1.3.1.1). Soon after the discovery of *ortho*-carborane[14], its rearrangement at high temperatures to the 1,7- isomer was reported.[18]

At even higher temperatures, this new isomer decomposes with partial conversion into *para*-carborane.[19] Denoted as *ortho*-, *meta*-, and *para*-, the structures of the three isomers and their thermal rearrangements are shown in figure 1.3.1.2.

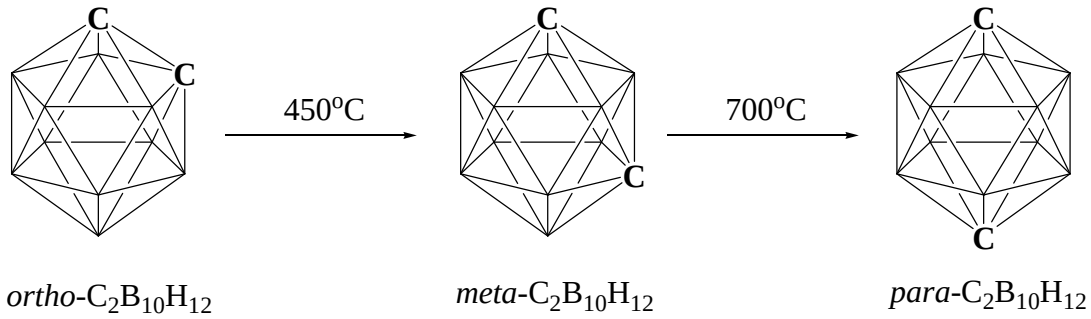

Figure 1.3.1.2 The three isomers of dicarbadecaborane and their thermal rearrangements.

1.3.2 Isomerisations.

Since some of the heteroboranes reported in this thesis undergo isomerisation, it is appropriate to introduce an overview of the best known mechanisms proposed to explain the isomerisation of icosahedral carboranes. The study of the thermal rearrangements from *ortho*- to *meta*-, and ultimately to *para*-carborane, is inhibited due to the high temperatures involved in these processes. Nevertheless, many theories pertaining to the mechanism have been postulated. The first one was Lipscomb's diamond-square-diamond (DSD) mechanism.[20] This consists of lengthening and subsequently breaking the common edge between two adjacent triangular faces, forming a square face which is divided again by a new bond orthogonal to the broken one. (Figure 1.3.2.1).

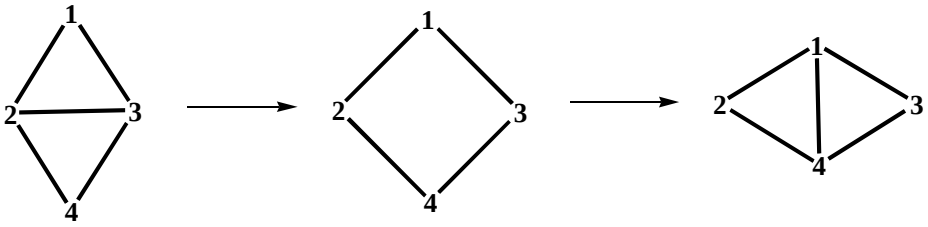

Figure 1.3.2.1 Schematic representation of the DSD mechanism in two adjacent triangular faces.

Lipscomb predicted a hextuple DSD process to explain the conversion of 1,2-$C_2B_{10}H_{12}$ to 1,7-$C_2B_{10}H_{12}$ through a cuboctahedral intermediate. However, this isomerisation mechanism cannot account for the formation of 1,12-$C_2B_{10}H_{12}$, starting from either *ortho*- or *meta*-carborane. In addition, Wales[21] has noted the hextuple

DSD process to form the cuboctahedral intermediate as involving an unfeasible high energy barrier.

The most universal postulated mechanism for the isomerisation of heteroboranes is Triangular Face Rotation (TFR).[22] It simply involves the 120º rotation of a single triangular face of the polyhedron, changing the position of the three vertices of that triangle (Figure 1.3.2.2).

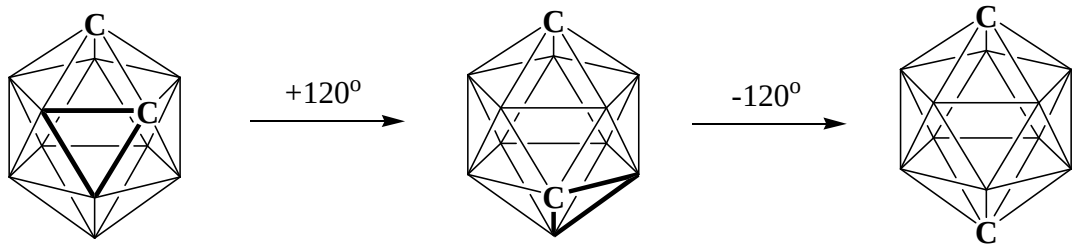

1,2-$C_2B_{10}H_{12}$ 1,7-$C_2B_{10}H_{12}$ 1,12-$C_2B_{10}H_{12}$

Figure 1.3.2.2 Isomerisation of 1,2- to 1,7- to 1,12-carborane by Triangular Face Rotation (TFR) mechanism.

This mechanism is very popular because all the isomerisation processes in deltahedral cages can be explained by several TFR steps. In addition, it has been computationally shown that in some cases it can be regarded as a low energy process. However, any TFR isomerisation can be explained as three consecutive DSD steps, giving the latter mechanism the greater generality to explain isomerisation in heteroboranes.[23]

1.3.3 Reactivity.

Icosahedral carboranes present a rich chemistry determined by their electron deficiency and the presence of the carbon atoms in the borane cluster. The two heteroatoms in the carborane are more electronegative than the rest of the boron atoms in the cage, and as a result, a gradient of relative natural charges appears in the molecule (see figure 1.3.3.1 for *ortho*-carborane).[24] The relative charge of each vertex is related to its reactivity.

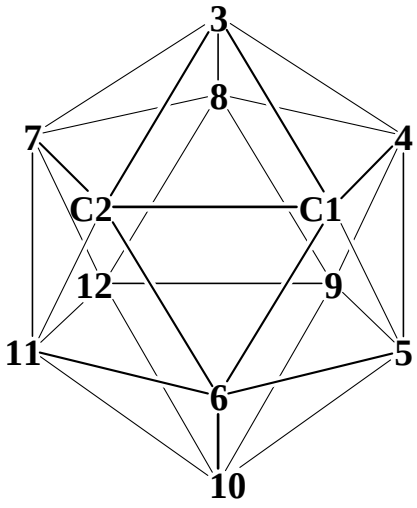

Boron vertex (B)	Charge (B)	Hydrogen atoms (H)	Charge (H)
C1, C2	-0.56	H1, H2	+0.36
B3, B6	+0.13	H3, H6	+0.08
B4, B5,		H4, H5,	
B7, B11	-0.03	H7, H11	+0.10
B10, B8	-0.17	H10, H8	+0.11
B9, B12	-0.19	H9, H12	+0.10

Figure 1.3.3.1 Computational prediction of the distribution of natural charges in *ortho*-carborane.

The protons of C-H groups are relatively acidic due to the greater electronegativity of carbon over boron. They can be easily removed by strong bases such BuLi to afford the lithiated derivatives of carboranes. The resultant deprotonated carboranes are strong nucleophiles able to attack suitable electrophiles like alkyl halides or carbonyl groups allowing the preparation of C-substituted carboranes.[25, 26] (figure 1.3.3.2).

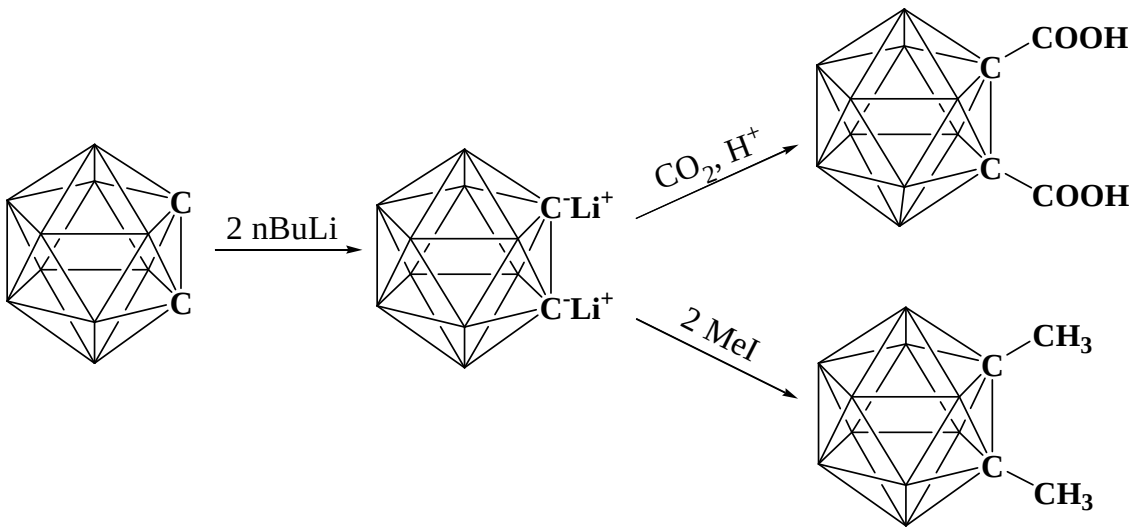

Figure 1.3.3.2 Reactions of deprotonated carborane with electrophiles.

In order to obtain C-aryl carboranes, lithium salts of carborane can react with copper (I) to form C-copper derivatives. Reaction of these species with aryl iodides in presence of pyridine gives C-aryl carboranes. This is a versatile procedure to functionalise carboranes although the reaction is limited to C-monosubstitution in the case of *ortho*-carborane.[27] The chemistry of carboranes is dominated by C-substituted compounds due to the relative difficulty to introduce functional groups selectively at cage B atoms.[28] Nevertheless, due to their relative charges in the cage some boron vertices are vulnerable to either nucleophilic or electrophilic substitutions.

Next to the carbon atoms in *ortho*-carborane are their immediate neighbours B3 and B6. These boron atoms are directly bonded to the most electronegative vertices in the cage, thus they bear a weak positive charge (figure 1.3.3.1). This fact makes them susceptible to nucleophilic attack and addition of base (KOH in ethanol, for example) affords a deboronated (decapitated) carborane.[29] The resulting nido carborane has an endo proton that can be removed by BuLi to yield a dicarbollide dianion, $[C_2B_9H_{11}]^{2-}$. This nido dianion can undergo recapitation with a functionalised boron fragment {BR} to afford B-substituted carboranes. This approach to carborane functionalisation is commonly known as cage subrogation (figure 1.3.3.3).[30]

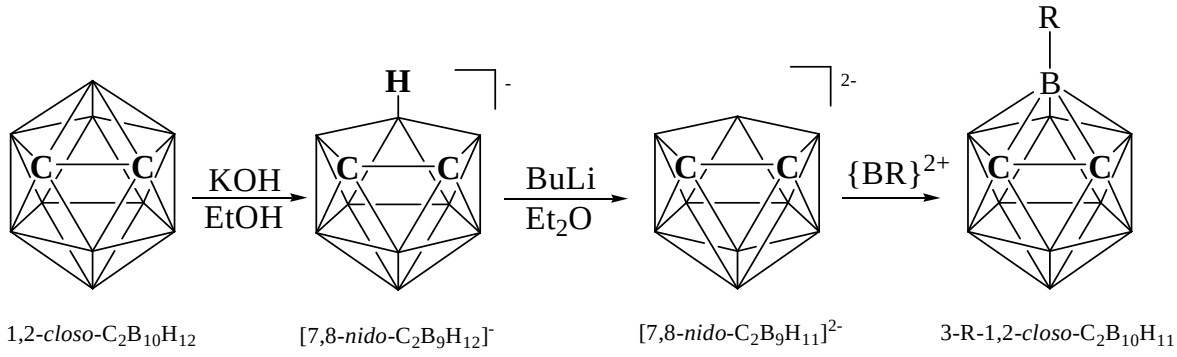

Figure 1.3.3.3 Deboronation and subsequent recapitation of carborane to afford B3-substituted carboranes (R= alkyl, aryl, allyl, halogen).

Depending on which isomer of carborane is deboronated and recapitated, the resulting products are the 3-R-1,2-, 2-R-1,7- and 2-R-1,12-C_2B_{10} isomers, from *ortho*-, *meta*- and *para*-carborane, respectively. In some cases, two subsequent cage subrogation processes are possible, allowing the preparation of B,B'-disubstituted carboranes.[31] Dicarbollide dianions can also be capitated with suitable metal fragments to prepare icosahedral metallacarboranes,[29,32] compounds that will be described in detail in section 1.5.1.

Opposite to the carbon atoms in the *ortho*-carborane cage are B9 and B12. Due to the fact that these vertices are the most distant to the carbon positions, they are the most nucleophilic boron atoms in the cluster (figure 1.3.3.1). Their weak negative charge leaves these positions vulnerable to undergo electrophilic substitution. An interesting example of this reaction is the selective iodination of carboranes by iodine or ICl catalysed by $AlCl_3$ (figure 1.3.3.4).[33]

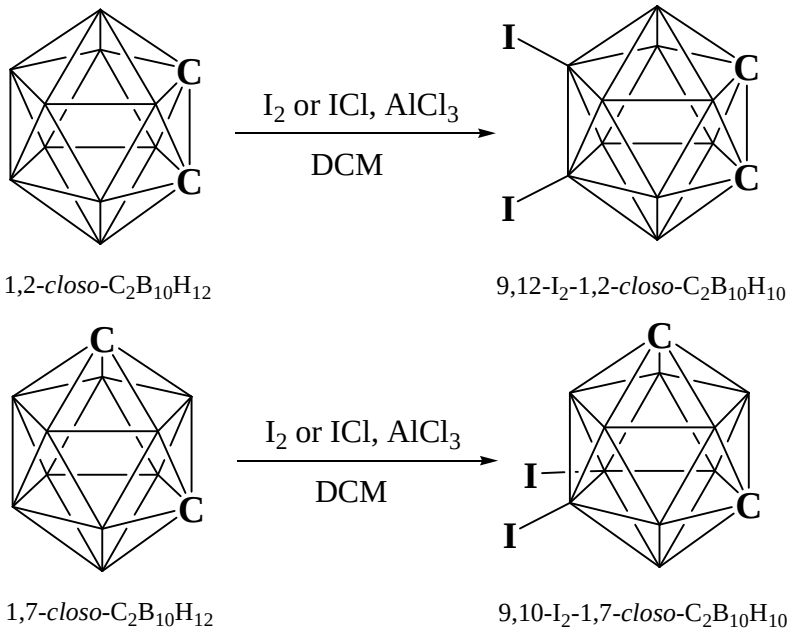

Figure 1.3.3.4 Selective electrophilic iodination of *ortho*- and *meta*-carborane.

Depending on the stoichiometry and the reaction time, this reaction can afford either mono- or di-substituted products. The resulting iodinated carboranes are important synthons for further reactions. These halogenated carboranes can undergo oxidative addition to palladium catalysts and therefore be utilised as counter partners for cross-coupling reactions with Grignard reagents (figure 1.3.3.5).[33]

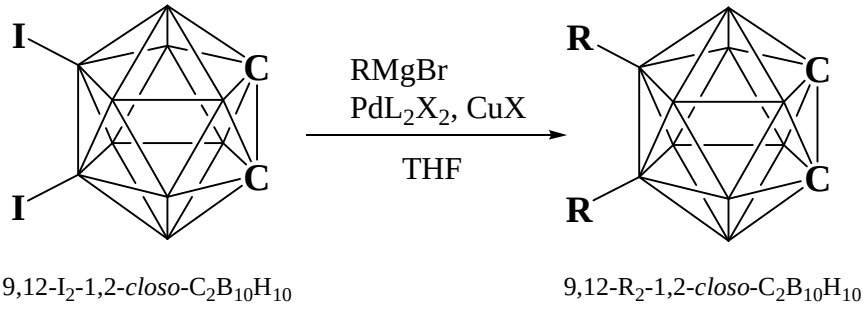

Figure 1.3.3.5 Cross coupling reactions of iodinated carboranes (R= alkyl, aryl, allyl).

The selectivity of the reaction of carborane with electrophiles is greater for *meta*-carborane since the relative charges at vertices B9 and B12 are quite distinctive. In *ortho*-carborane tri- and tetra-substitution at vertices B8 and B9 is sometimes also observed. The poorest selectivity is observed in disubstitution of *para*-carborane where the ten boron vertives are equally charged, thus there is no specific control in their reaction with electrophiles.

Since carborane cages can be regarded as electron deficient compounds, they are susceptible to reduction. As follows the Wade-Williams matrix, the addition of two electrons to an icosahedral cage results in the formation of a 12-vertex nido cluster, with an overall dinegative charge. This type of reductive opening of a closo cage can be observed when *ortho*-carborane is treated with two equivalents of sodium metal in THF solution to form [7,9-*nido*-$C_2B_{10}H_{12}]^{2-}$ [18] (figure 1.3.3.6).

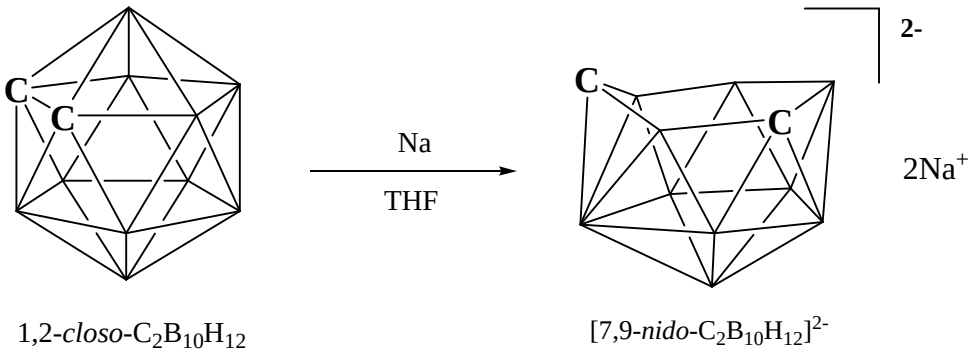

Figure 1.3.3.6 Two-electron reductive opening of icosahedral 1,2-*closo*-$C_2B_{10}H_{12}$ to [7,9-*nido*-$C_2B_{10}H_{12}]^{2-}$.

These di-anionic carboranes are air-sensitive compounds, although they can be isolated as the air-stable mono-protonated salt [*nido*-$C_2B_{10}H_{13}]^-$.[34] Reaction of 12-vertex di- anionic nido carboranes with suitable fragments isolobal to {BH} paves the way to supraicosahedral heteroboranes. This field of boron chemistry involves heteroborane polyhedral clusters beyond the icosahedron and is described in the following section.

1.4 Supraicosahedral boranes.

Although there are many examples of small boranes in the literature, borane clusters with more than 12 vertices still remain unknown. Nevertheless, the field of supraicosahedral boranes has been intriguing boron chemists for years. It was Lipscomb[35] who theoretically predicted the existence of stable boranes from the series $[B_nH_n]^{2-}$ where n≥13. Lipscomb found that the addition of a {BH} unit results in lower energy configurations; therefore the synthesis of larger boranes (and heteroboranes) should be a viable process. This work was later extended by Schleyer[36] when he described an increasing trend in the stability of boranes $[B_nH_n]^{2-}$ as *n* increases. Computing the cumulative {BH} addition energy versus the number of vertices (n) in the cluster, he reported the predicted stability of boranes $[B_nH_n]^{2-}$ for 5<n<17 as shown in figure 1.4.1.

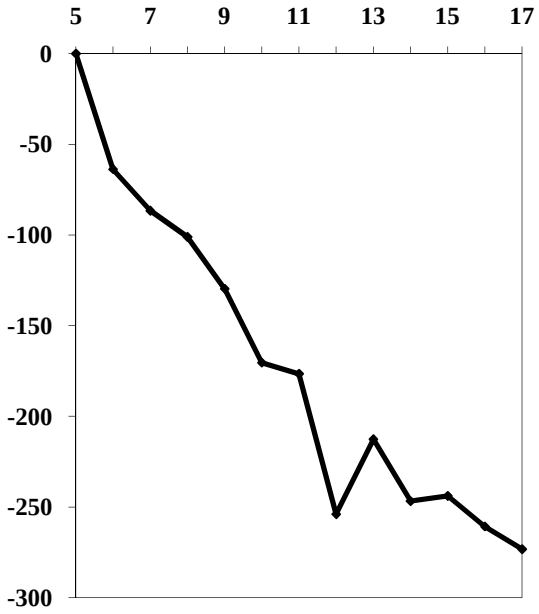

Figure 1.4.1 Plot of cumulative BH addition energy (kcal mol^{-1}, y-axis) vs. number of boron atoms (x-axis) for the *closo*-borane dianions $[B_nH_n]^{2-}$ (*n* = 5 – 17).

Although there is a general trend in stability as *n* increases, the extreme stability of icosahedral boranes (n =12) is noteworthy, making the addition of the thirteenth BH vertex an endothermic process. As shown in figure 1.4.1, the formation of supraicosahedral boranes $[B_{13}H_{13}]^{2-}$, $[B_{14}H_{14}]^{2-}$ and $[B_{15}H_{15}]^{2-}$ from $[B_{12}H_{12}]^{2-}$ are unfavourable endothermic processes. On the other hand, the formation of larger

boranes such as $[B_{16}H_{16}]^{2-}$ and $[B_{17}H_{17}]^{2-}$ from $[B_{12}H_{12}]^{2-}$ are exothermic processes, due to their relative stability over the known dodecaborate species.

The computationally predicted instability of some supraicosahedral boranes is explained by the structures that these large deltahedral clusters are expected to adopt. Boron atoms have contracted orbitals that do not stabilise highly connected cluster vertices. However, the predicted deltahedral structures (figure 1.4.2) for the unfavourable supraicosahedral boranes (n = 13, 14 and 15) involve in all cases more than one six-connected vertex. On the other hand, larger boranes whose formation is predicted to be more favourable (n = 16, 17…) are expected to adopt structures that only involve five-connected vertices as the highest degree atoms (figure 1.4.2).

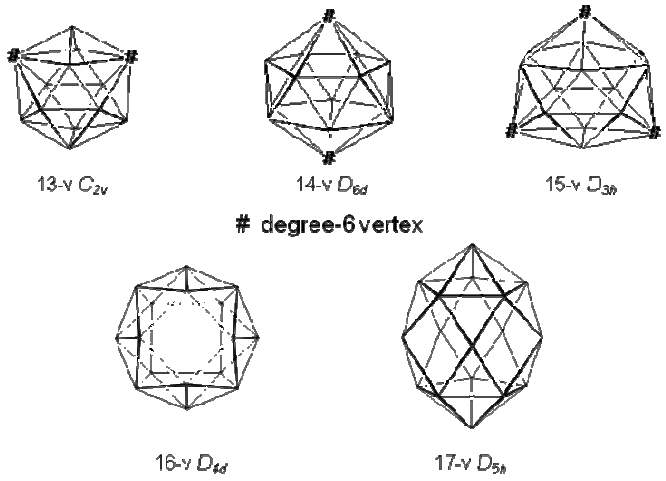

Figure 1.4.2 Predicted structures for $[B_nH_n]^{2-}$ (n = 13, 14, 15, 16 and 17) borane clusters. Degree-6 vertices highlighted.

It can be concluded from these structural/theoretical predictions that due to the great stability of (n=12) icosahedral species, the thermodynamically disfavoured 12- to 13-vertex pathway is a synthetic bottle-neck in the preparation of the, as yet unknown, supraicosahedral boranes.

1.5 Metallacarboranes.

1.5.1 Icosahedral metallacarboranes.

Metallacarboranes can be considered as metal-(carborane ligand) complexes or as carborane clusters in which a metal replaces a boron vertex. Hawthorne[37] first recognised the similarity between dicarbollide $[C_2B_9H_{11}]^{2-}$ and cyclopentadienide $[C_5H_5]^-$ anions (figure 1.5.1.1) and thus realised the potential for carborane dianions to be used as ligands in coordination chemistry. Icosahedral metallacarboranes are generally more stable than their metallocene analogues. Although cyclopentadienide and dicarbollide anions can be regarded as isolobal ligands, the frontier molecular orbitals in dicarbollide anions point towards the vacant site (figure 1.5.1.1), leading to a greater overlap with the bonding metal than with cyclopentadienide ligands and as a result, to more stable complexes.

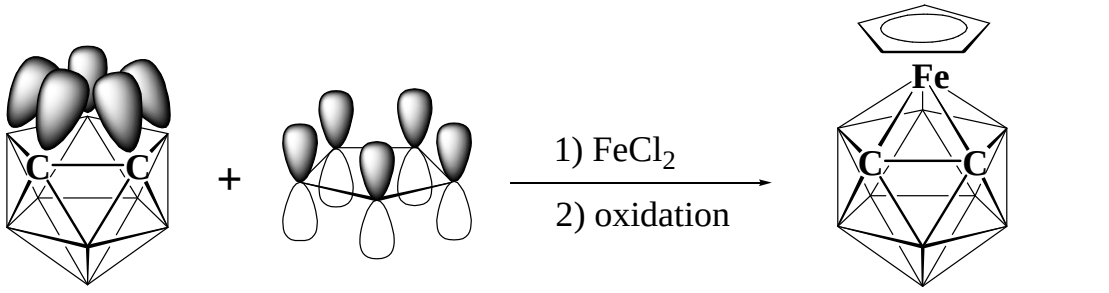

$[7,8\text{-}nido\text{-}C_2B_9H_{11}]^{2-}$ $[C_5H_5]^-$ 3-Cp-3,1,2-*closo*-$FeC_2B_9H_{11}$

Figure 1.5.1.1 Frontier molecular orbitals for dicarbollide and cyclopentadienide anions and preparation of the first metallacarborane, a half-sandwich ferracarborane.

Hundreds of icosahedral metallacarboranes have been synthesised after the first discovery by Hawthorne.[37b] The first reported compounds constitute rare examples of non-Wadian clusters, although in general, the structures of metallacarboranes can be explained according to Wade's rules.[9] The nomenclature of these compounds requires three numbers; the first one identifies the position of the metal and the other two indicate the vertices where the carbon atoms are located (figure 1.5.1.2). The nine isomeric examples of icosahedral metallacarboranes of the general type MC_2B_9 were summarised by Hughes[38] and are illustrated in figure 1.5.1.2.

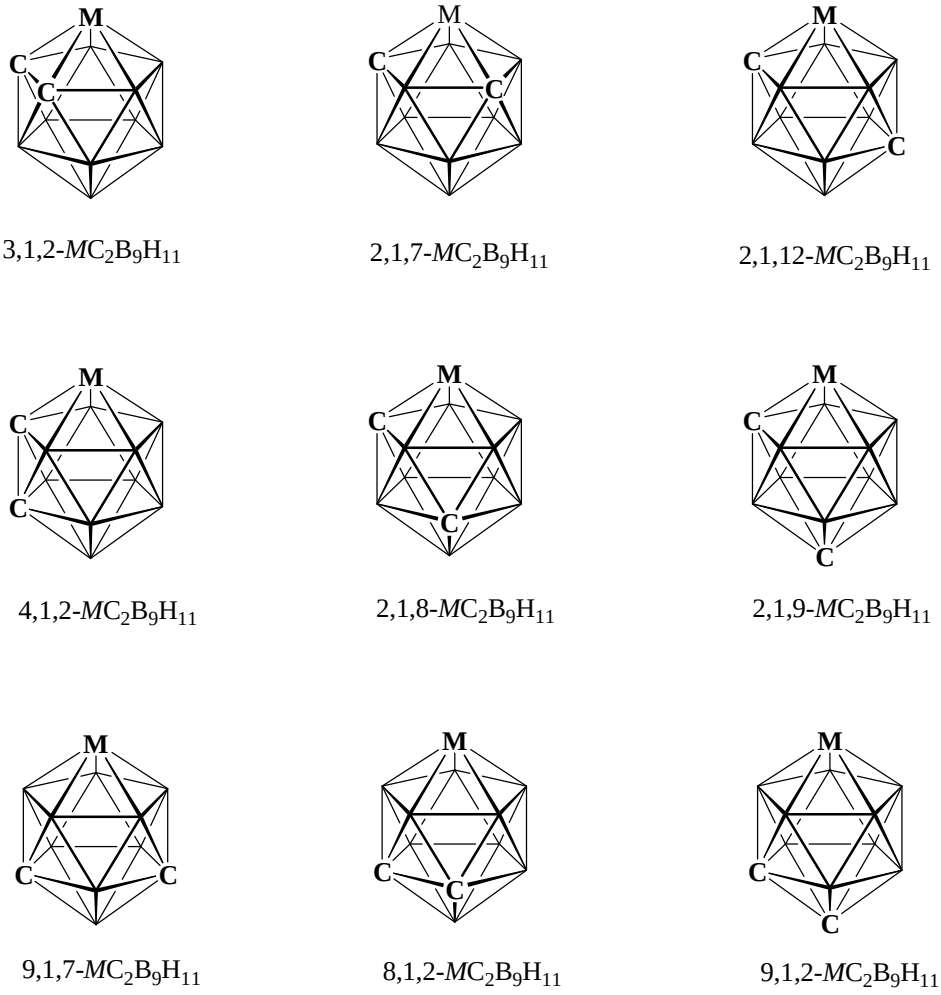

Figure 1.5.1.2 The nine isomeric structures of icosahedral MC_2B_9 metallacarboranes.

Among these nine metallacarboranes, the best known isomers are 3,1,2-[39] with 647 hits in the Cambridge Structural Database (CSD) at the time of writing up this chapter, followed by 2,1,7-[40] with 39 structures in the CSD. These two isomers along with 2,1,12-[38,40a] (1 hit) can be obtained by removal of the most positive boron vertex in *ortho*-, *meta*- and *para*-carborane respectively, followed by capitation with a suitable metal fragment. There are also known crystallographic examples of 2,1,8- (37 hits) and 4,1,2- (9 hits) isomers obtained by thermal isomerisation reactions.[41,42] However, almost fifty years after the synthesis of the first icosahedral metallacarborane, there are still no crystallographic-characterised examples of the remaining four isomers: 2,1,9-, 9,1,7-, 8,1,2- and 9,1,2-MC_2B_9. Despite this lack of structural characterisation, the syntheses of the nine isomeric forms, identified by spectroscopic means, are reported.[41]

Chapter 4 contains an expansion of the work of icosahedral metallacarboranes with the synthesis and characterisation of the first example of the 8,1,2-MC_2B_9 series.

1.5.2 Supraicosahedral metallacarboranes.

Research into supraicosahedral metallacarborane chemistry was first initiated by Hawthorne in 1971 with the synthesis and characterisation of the first supraicosahedral heteroborane, 4-Cp-4,1,6-*closo*-$CoC_2B_{10}H_{12}$.[43] Hawthorne and co-workers reduced 1,2-$C_2B_{10}H_{12}$ to generate the carbon atoms apart 7,9-*nido* dianion.[18] The six-atom open face of the reduced carborane was then treated with the {CpCo} fragment (which was generated in-situ by NaCp and $CoCl_2$) to introduce the 13th vertex in the cluster. This stepwise approach to supraicosahedral clusters is generally known as the polyhedral expansion method and consists of chemical reduction (Red) of a (n)-vertex closo carborane and its subsequent metallation (Met) with a suitable metal fragment to afford a (n+1)-vertex metallacarborane (figure 1.5.2.1).

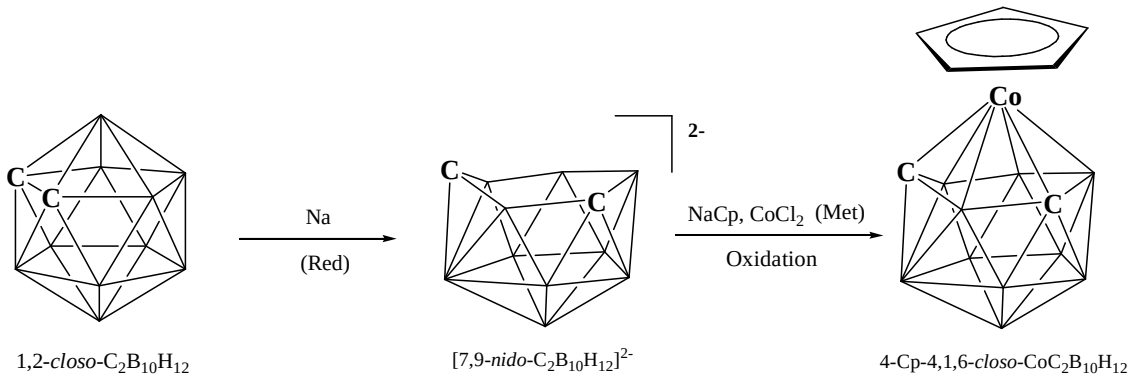

Figure 1.5.2.1 Synthesis of the first supraicosahedral metallacarborane by polyhedral expansion of *ortho*-carborane.

According to the isolobal principle[11], any metal fragment isolobal to {BH} would, in principle, be able to capitate the 12-vertex nido dianion and thus generate a stable 13-vertex metallacarborane. Metallation of 7,9-*nido*-C_2B_{10} dianions affords the 4,1,6-isomer which has the docosahedral structure predicted for 13-vertex polyhedral clusters.[44] The nomenclature of supraicosahedral carboranes follows the same rules

applied for smaller metallacarboranes: the first number indicates the position of the metal and the other two numbers identify the location of the carbon vertices in the docosahedron (figure 1.5.2.2).

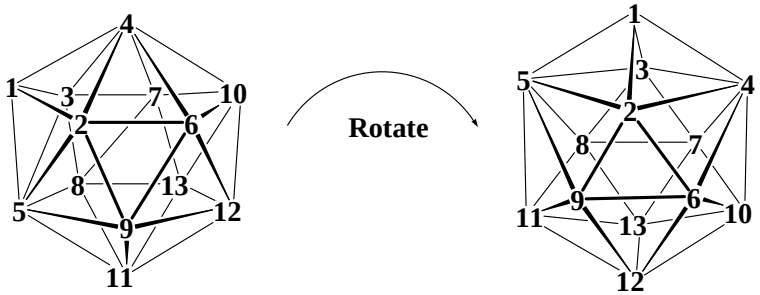

Figure 1.5.2.2 Two common views of a docosahedron and numbering scheme for docosahedral clusters.

The expansion of icosahedral carboranes to afford 13-vertex metallacarboranes has been extensively studied over the last decade. The reduction of 1,2-, 1,7- and 1,12-carboranes are known processes.[45] The first two are reduced to afford [7,9-*nido*-$C_2B_{10}]^{2-}$ species whereas reduction of *para*-carborane gives [7,10-*nido*-$C_2B_{10}]^{2-}$. It has been shown that metallation of these two dianions yields 4,1,6- and 4,1,10- 13-vertex metallacarboranes, respectively.[43,46]

The different kinetic MC_2B_{10} isomers obtained from metallation of 7,9- and 7,10-*nido* species can be thermally isomerised to the 4,1,12- isomer, the thermodynamically most stable isomer of 13-vertex metallacarboranes. The thermal rearrangement from 4,1,6- to 4,1,12- metallacarborane occurs in two steps through 4,1,8- species whereas the isomerisation from 4,1,10- to 4,1,12- is regarded as a single-step process.[47] The thermal conditions required for these isomerisations can change dramatically, from low to high temperatures, depending on the metal vertex and the functional groups attached to the cage carbon atoms. A summary of the major known cage expansions and isomerisations is shown in figure 1.5.2.3.

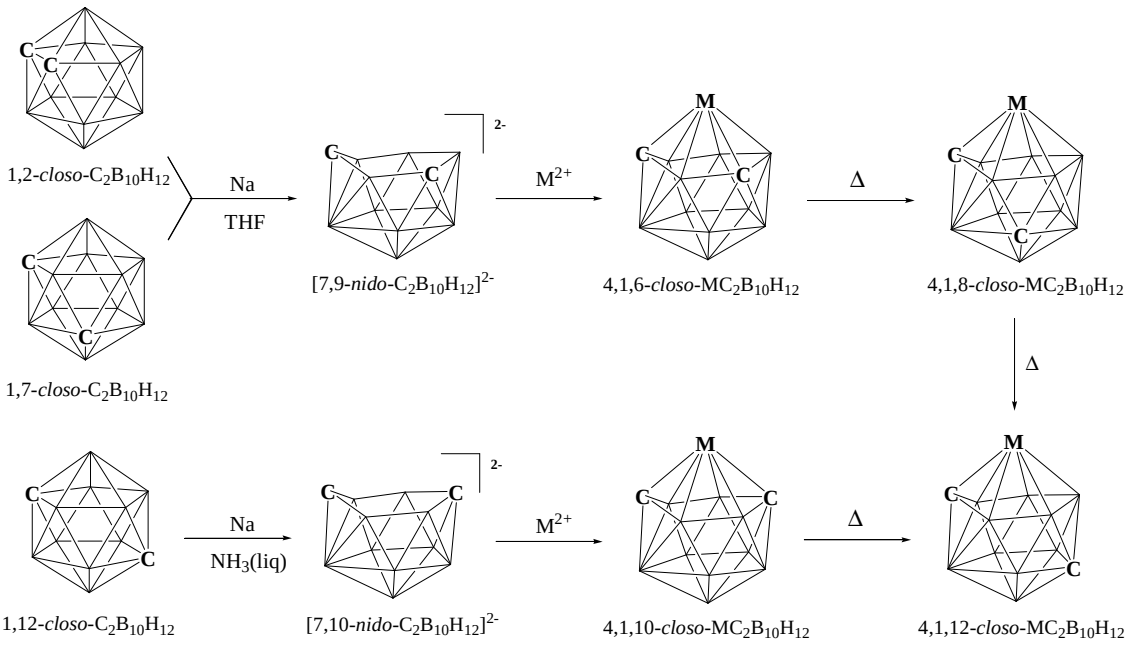

Figure 1.5.2.3 Reduction and metallation (Red/Met) of icosahedral carboranes and isomerisation of MC_2B_{10} species.

The docosahedral architecture of MC_2B_{10} metallacarboranes determines the preferred positions of metal and carbon vertices in the cluster. There are two six-connected vertices (4 and 5), ten five-connected vertices and only one four-connected vertex (1) in a docosahedron (figure 1.5.2.2). It has been established that metal fragments prefer highly connected vertices (degree 5 or 6) since their orbitals are larger and more diffuse.[48] On the other hand, carbon atoms have contracted orbitals since they are more electronegative than boron atoms, so they normally occupy the lowest connected sites (degree 4 or 5) of the docosahedron.[49] According to these principles, docosahedral MC_2B_{10} species will present preferred positions for the metal (position 4) and one of the carbon vertices (position 1), leaving only seven possible isomers of 4,1,X-MC_2B_{10} species (figure 1.5.2.4).

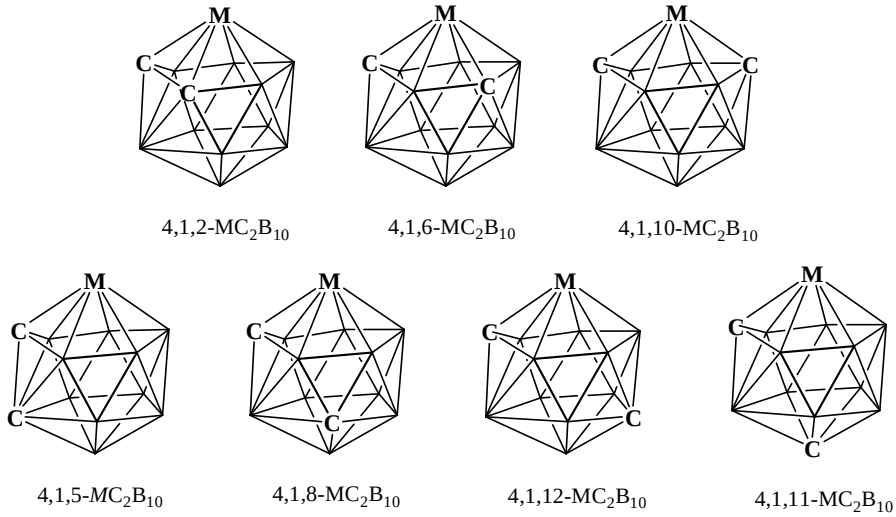

Figure 1.5.2.4 The seven possible isomers of 4,1,X-MC_2B_{10} metallacarboranes.

As has been described before, 4,1,6- and 4,1,10- isomers are the products from the expansion of icosahedral carboranes, whereas 4,1,8- and 4,1,12- can be obtained by thermal rearrangement of the former isomers. Metallacarboranes of the 4,1,2- architecture are synthesised by polyhedral expansion of C,C'-tethered *ortho*-carboranes, through $[7,8\text{-}nido\text{-}C_2B_{10}]^{2-}$ intermediates.[50] These compounds might adopt either docosahedral or henicosahedral structures depending on the metal fragment in position 4. Of the other two isomers, there is only one example of 4,1,11-MC_2B_{10} isolated as a minor product from the reduction and subsequent metallation of 1,12-Ph_2-*closo*-$C_2B_{10}H_{10}$.[51] The latter 4,1,5- isomer is unlikely to be synthesised as it requires a carbon atom to occupy a six-connected vertex.

The chemistry of 13-vertex metallacarboranes is not as developed as for their icosahedral analogues. Nevertheless, cage subrogations and expansions are possible for certain isomers. Hawthorne discovered that in the case of 4,1,8- and 4,1,12-MC_2B_{10} species the weakest bonded B5 can be removed by nucleophiles (KOH in ethanol, for example) to afford 12-vertex nido dianions. It was shown that the resulting dianions can be re-capitated with suitable metal fragments to afford 13-vertex bimetallacarboranes[52] (figure 1.5.2.5).

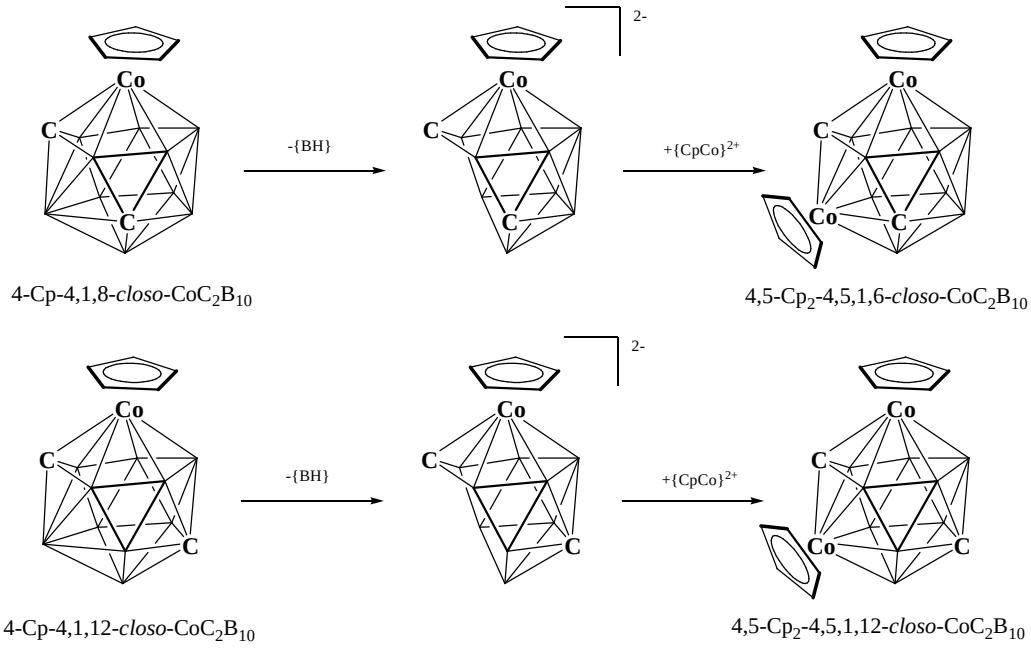

Figure 1.5.2.5 Synthesis of 13-vertex bimetallacarboranes by polyhedral subrogation.

The preparation of different isomers of 13-vertex bimetallacarboranes has also been reported either by polyhedral expansion of icosahedral metallacarboranes[53] or by electrophilic insertion.[54]

More interesting is the polyhedral expansion of 13-vertex MC_2B_{10} species to afford 14-vertex bimetallacarboranes. Following the previously described Red/Met procedures, certain 13-vertex metallacarboranes are reduced by Group 1 metals to give 13-vertex nido dianions, metallation of which yields 14-vertex bimetallacarboranes. In 1974, Hawthorne was the first to report the preparation of 14-vertex $M_2C_2B_{10}$ species although those compounds were only partially characterised.[55] In 2005, Welch and co-workers reported the synthesis and crystallographic characterisation of both hetero and homobimetallic 14-vertex $M_2C_2B_{10}$ species.[56] Welch confirmed that these species adopt a bicapped hexagonal antiprismatic geometry, the polyhedron predicted for 14-vertex heteroboranes[35,36] (figure 1.5.2.6). It has been argued that a carbon atom in the open face is required to stabilise the reduced nido species and thus encourage the second metallation. As a consequence, only those 13-vertex MC_2B_{10} precursors with a carbon atom in the lower belt of the docosahedron, 4,1,8- and 4,1,12-, have been successfully expanded to yield 14-vertex heteroborane clusters (figure 1.5.2.6).

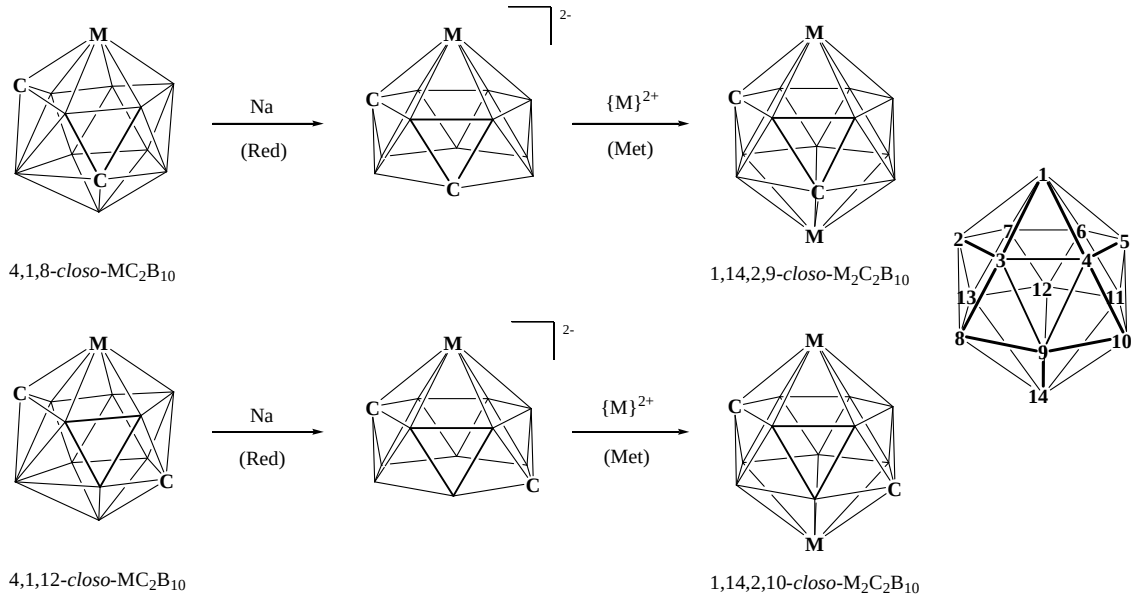

Figure 1.5.2.6 General procedure of Red/Met of selected 13-vertex MC_2B_{10} species to obtain 14-vertex $M_2C_2B_{10}$ bimetallacarboranes and numbering scheme for bicapped hexagonal antiprismatic geometries. ({M}= {CpCo}, {ArRu}, {Ni(dppe)})

As expected, the two metal fragments in 14-vertex bimetallacarboranes occupy the two high coordinated vertices, 1 and 14, of the polyhedron. The polyhedral expansion of $M_2C_2B_{10}$ species to generate 15-vertex trimetallacarborane clusters has been explored by our research group in recent years but $M_3C_2B_{10}$ clusters still remain as unknown species.

1.6 Supraicosahedral carboranes.

Despite their predicted stability, supraicosahedral boranes still remain as unknown species. On the other hand, the polyhedral expansion of icosahedral carboranes to afford 13- and 14-vertex metallacarboranes is now a well established procedure. It is accepted that the polyhedral expansion method cannot be applied to boranes of the $[B_nH_n]^{2-}$ series since the chemical reduction of such dianionic species is regarded as a disfavoured process whereas the reduction of neutral carboranes is possible. The field of supraicosahedral carboranes explores the reduction of icosahedral carboranes and subsequent capitation with boron fragments to prepare supraicosahedral carboranes. The main applications of borane clusters are due to their high boron content or their ability to delocalise electrons in an almost spherical structure. Therefore, there is considerable current interest in the expansion of carborane clusters by the addition of new boron vertices.

As has been described in previous sections, the reductions of the three isomers of carborane are known processes. The most logical procedure to obtain supraicosahedral carboranes would be the treatment of either 7,9- or 7,10-*nido*-$C_2B_{10}H_{12}$ dianions with suitable boron fragments in order to add the thirteenth vertex into the cage. However, boron insertion to those reduced carboranes does not occur. Instead, they undergo re-oxidation to 1,2- and 1,7-*closo*-$C_2B_{10}H_{12}$, respectively. After many attempts in different conditions, this problem was overcome in 2003 by Welch and co-workers.[57] Welch reported the capitation of the open face of a 7,8-*nido* dianion, generated after the reduction of a C,C'-tethered *ortho*-carborane,[58] with a {BPh} fragment allowing the preparation and characterisation of the first supraicosahedral carborane (figure 1.6.1).

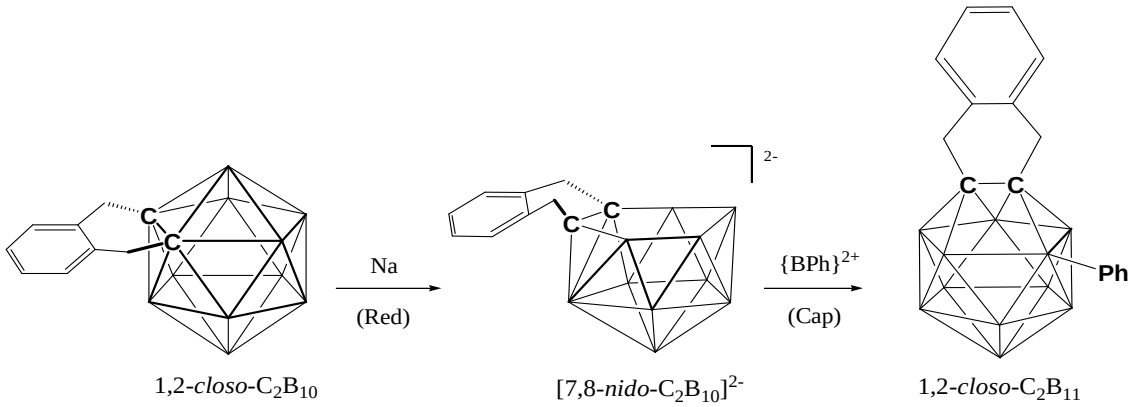

Figure 1.6.1 Synthesis of the first supraicosahedral carborane by Reduction/Capitation of a C,C'-tethered *ortho*-carborane.

Interestingly, the structure of the first supraicosahedral carborane was not the docosahedron predicted for $[B_{13}H_{13}]^{2-}$, but a henicosahedron featuring a trapezoidal C_2B_2 face. After this synthetic breakthrough the "ortho tethering" strategy has been reproduced to afford new examples of henicosahedral 13-vertex carboranes featuring different linkages and different groups on the thirteenth boron vertex. Following this strategy, all the examples of 13-vertex carboranes are the 5-R-1,2-C_2B_{11} isomer, obtained by capitation of carbon atoms adjacent 7,8-*nido* dianions by $\{BR\}^{2+}$ fragments (R = H, alkyl, allyl, aryl).[59]

The next step forward in supraicosahedral carborane chemistry occurred in 2005 with the synthesis of the first 14-vertex carborane. Xie and co-workers reported two different synthetic procedures to obtain the largest carborane known to date. The unique μ-2,8-$(CH_2)_3$-2,8-$C_2B_{12}H_{12}$ isomer can be prepared either by typical polyhedral expansion of 1,2-C_2B_{11} carboranes or, more surprisingly, by double capitation of a tetraanionic 12-vertex arachno carborane (figure 1.6.2).[60]

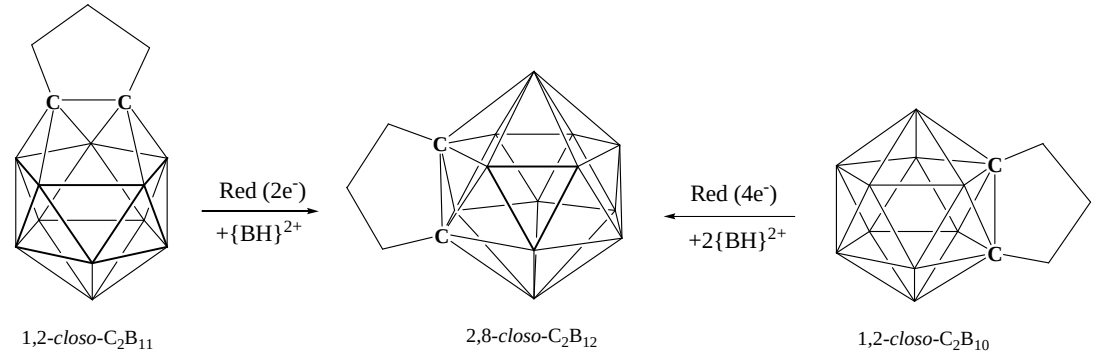

Figure 1.6.2 Syntheses of a 14-vertex carborane by polyhedral expansion of 13-vertex [13+1] or 12-vertex [12+2] carboranes.

Whereas the [13+1] expansion (figure 1.6.2 left) occurs as a result of the single capitation of a nido dianion, the [12+2] reaction (figure 1.6.2 right) proceeds via a tetraanionic arachno carborane, generated after a four electron reduction of 1,2-*closo*-C_2B_{10}. The tetraanionic intermediate is stabilised by the presence of a fixed C-C edge shared between two 5- and 6-atom open faces in its structure.[58] Such stabilisation of the arachno species allows the double capitation and consequent [12+2] expansion. The structure of the resulting supraicosahedral carborane is the bicapped hexagonal antiprism predicted for 14-vertex boranes.[35,36]

Although the polyhedral expansion method works well in the preparation of 13- and 14-vertex carboranes, it has been unsuccessful when applied to the synthesis of 15-vertex carboranes. However, although reduction and boron insertion methodologies have failed, the insertion of a metal fragment is possible. In fact, two examples of 15-vertex metallacarboranes have been reported. The first 15-vertex metallacarborane was reported by Welch and co-workers in 2006 and was obtained by thermolysis of a 14-vertex ruthenacarborane involving the adventitious capture of a {BH} fragment.[61] At the same time, Xie reported another isomer of the 15-vertex metallacarborane obtained by the polyhedral expansion of a 14-vertex carborane.[62] These two examples of 15-vertex ruthenacarboranes represent the largest *closo*-heteroborane clusters known thus far.

The use of a rigid tether to restrict the carbon atom movement during reduction has been the successful strategy utilised in the preparation of supraicosahedral carboranes. The first examples of 13- and 14-vertex carboranes and 15-vertex metallacarboranes have been prepared following this "*ortho*-tethering" strategy. As a result, all these supraicosahedral heteroboranes possess their carbon atoms in adjacent positions. In order to eliminate this restriction of movement, necessary for the capitation, Xie and co-workers reported the use of a silicon tether that can be removed after expansion procedures.[63] This strategy allowed the preparation of the first example of carbon atoms apart 13-vertex carborane. However, the "removable *ortho*-tethering" strategy has not been further developed in order to obtain larger carborane clusters.

Interestingly, after many years of research in the area, the use of the "*ortho*-tethering" strategy is still the only known approach for polyhedral expansion of carboranes. Boron insertion to the regular 7,9- or 7,10-*nido* dianions does not work, whereas the carbon atoms adjacent 7,8-*nido* intermediates can be expanded to larger closo carboranes. An explanation for the different chemistry of the three nido intermediates could lie in the stabilisation of the 7,8-*nido* dianion by the *exo*-tether. In the next section, the importance of the stabilisation of reduced intermediates in supraicosahedral carborane chemistry will be discussed.

1.7 Stabilisation of reduced carboranes.

The work presented in this thesis is focussed on the study and development of new strategies to stabilise dianionic nido carboranes. The synthesis of supraicosahedral carboranes requires synthetic techniques that favour boron insertion to 12-vertex nido dianions as opposed to their re-oxidation back to icosahedral clusters. There is indeed a competition between expansion and re-oxidation and thus far, only the "*ortho*-tethering" strategy has been successful. The work presented in following chapters is focussed on the stabilisation of 7,9-*nido* intermediates since those are the nido species obtained from the reduction of readily available *ortho*- and *meta*-carborane (figure 1.7.1).[64]

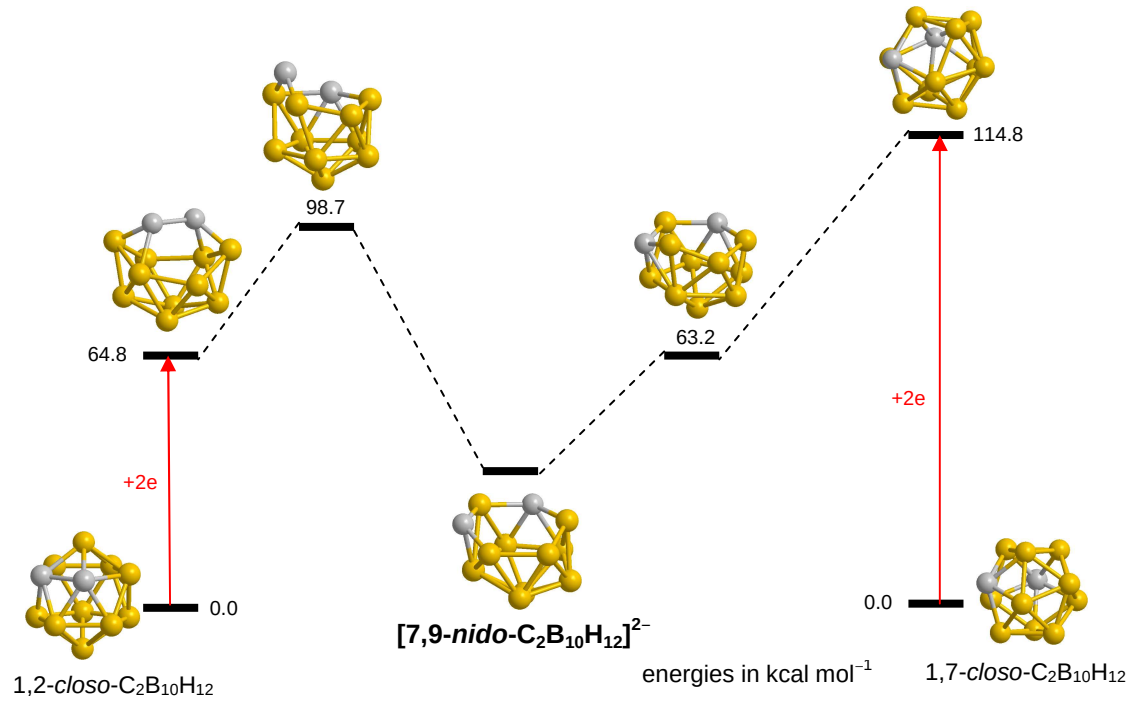

Figure 1.7.1 Energy profiles for the reduction of 1,2- and 1,7-*closo*-$C_2B_{10}H_{12}$ to the same 7,9-*nido* dianion.

Theoretical studies on the reduction of 1,2- and 1,7-*closo*-C_2B_{10} species to afford the same 7,9-*nido*-C_2B_{10} dianions are in good agreement with the experimental generation of 4,1,6-MC_2B_{10} supraicosahedral species after polyhedral expansion (Red/Met) of either 1,2- or 1,7-*closo* carboranes. On the other hand, the oxidation of 7,9-*nido* dianions back to icosahedral carboranes occurs to afford 1,2-*closo* carboranes

exclusively. Experimentally, 1,2-*closo*-C_2B_{10} species are the only products observed after reduction and subsequent oxidation of either 1,2- or 1,7-*closo*-carboranes. Computationally, oxidation of 7,9-*nido* dianions back to 1,2-*closo*-C_2B_{10} species is energetically more favoured than oxidation to 1,7-*closo* carboranes (figure 1.7.2).[64]

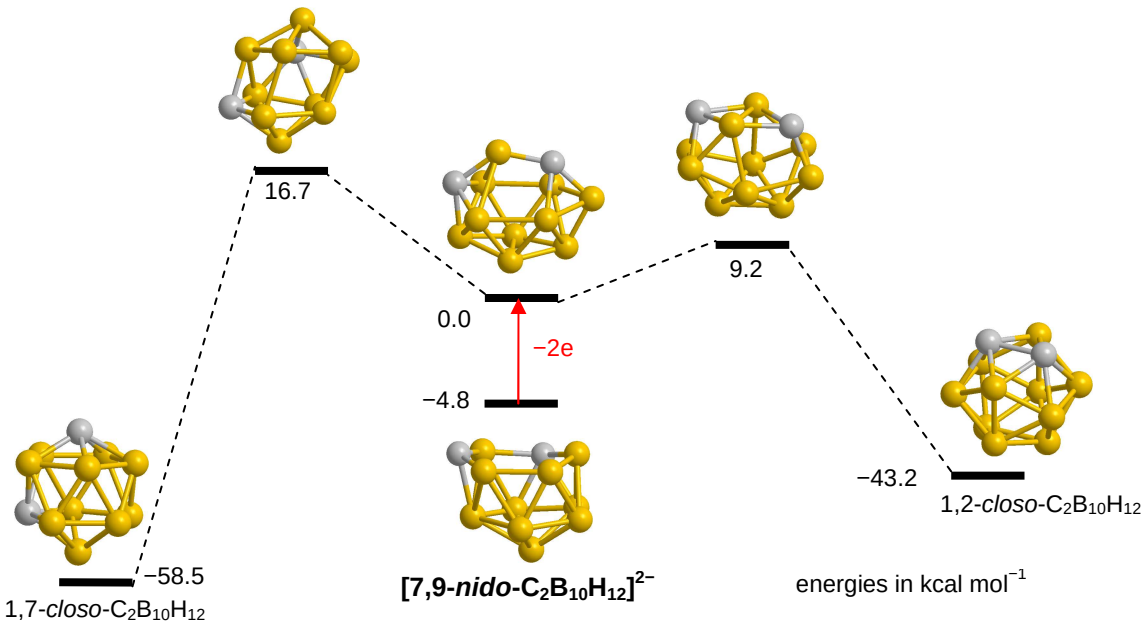

Figure 1.7.2 Energy profiles for the oxidation of [7,9-*nido*-$C_2B_{10}H_{12}$]$^{2-}$ to 1,2- and 1,7-*closo*-$C_2B_{10}H_{12}$.

The role of the *exo*-tether in "*ortho*-tethering" strategies is not completely understood, although computational studies have predicted that the oxidative closure of C,C'-linked 7,8-*nido* dianions is more difficult than for the carbon atoms apart 7,9-*nido* dianions. If re-oxidation becomes a difficult process, capitation should be relatively favoured. The computed relative energies for oxidation of tethered 7,8- and non-tethered 7,9-*nido*-C_2B_{10} dianions are shown in figure 1.7.3.[64]

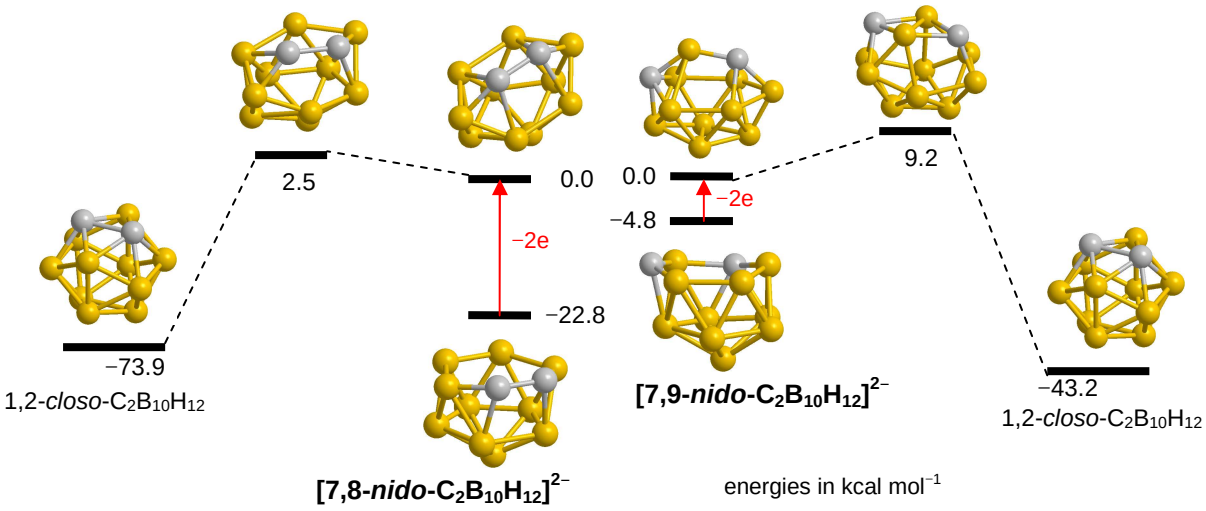

Figure 1.7.3 Comparison of the computed stability towards oxidation of tethered 7,8- and non-tethered 7,9-*nido* dianions.

The calculations shown in figure 1.7.3 suggest that the "*ortho*-tethering" strategy effectively disfavours the oxidation of reduced intermediates. The computed carbon atoms adjacent 7,8-*nido* dianion is 18 kcal mol^{-1} more stable towards oxidation than the carbon atoms apart 7,9-*nido* dianion. Following this principle, the more stable is the reduced dianion, the more difficult would be the re-oxidation, with capitation therefore becoming relatively favoured. New techniques able to stabilise reduced 7,9-*nido* dianions in a similar manner could led to new synthetic strategies for supraicosahedral heteroborane chemistry.

The work presented in this thesis is mainly focused in two different proposed techniques to stabilise 7,9-*nido* species:

i) The use of a rigid linker in order to control the carbon atoms movement in 7,9-*nido* species. Since control of carbon atoms movement appears to be the main benefit of "*ortho*-tethering" strategies, a similar tether designed to prevent the rearrangements required for the oxidation of 7,9-*nido* dianions to 1,2-*closo* carboranes is proposed.

ii) A study of the stabilising inductive effect of electron withdrawing groups attached to the cage carbon atoms. The stabilisation energy gained by the use of "*ortho*-tethering" strategies can be enhanced by the use of electron withdrawing groups. In order to obtain a better understanding of the importance of the stabilisation of nido dianions, the effect of selected electron withdrawing groups during polyhedral expansion procedures will be discussed.

1.8 References.

1.1 J. Daintith, *Dictionary of Chemistry 3rd Ed.*, Oxford University Press, 1996.

1.2 M. F. Hawthorne, *Angew. Chem. Int. Ed*., 1993, **32**, 950.

1.3 L. F. Tietze, U. Griesbach, U. Bothe, H. Nakamura and Y. Yamamoto, *ChemBioChem*, 2002, **3**, 219.

1.4 A. Stock, *Hydrides of Boron and Silicon*, Cornell University Press, Ithaca, New York, 1933.

1.5 H. C. Longuet-Higgins, *J. Chem. Phys.*, 1948, **16**, 894.

1.6 K. Hedberg and V. Schomaker, *J. Am. Chem. Soc*., 1951, **73**, 1482.

1.7 H. W. Smith and W. N. Lipscomb, *J. Chem. Phys*., 1965, **43**, 1060.

1.8 W. N. Lipscomb, *Boron Hydrides*, W. A. Benjamin, Inc., New York, 1963.

1.9 K. Wade, *J. Chem. Soc., Chem. Commun.*, 1971, 792.

1.10 D. M. P. Mingos and D. J. Wales, *Introduction to Cluster Chemistry*, Prentice Hall, Englewood Cliffs, 1990.

1.11 R. Hoffmann, *Angew. Chem. Int. Ed. Engl.*, 1982, **21**, 711 (Nobel lecture).

1.12 A. R. Pitochelli and M. F. Hawthorne, *J. Am. Chem. Soc*., 1960, **82**, 3228.

1.13 a) W. H. Knoth, *J. Am. Chem. Soc*., 1967, **89**, 1274; b) W. H. Knoth, *Inorg. Chem*. 1971, **10**, 598.

1.14 a) T. L. Heying, J. W. Ager, Jr., S. L. Clark, D. J. Mangold, H. L. Goldstein, M. Hillman, R. J. Polak and J. W. Szymanski, *Inorg. Chem.*, 1963, **2**, 1089; b) M. M. Fein, J. Bobinski, N. Mayes, N. Schwartz and M. S. Cohen, *Inorg. Chem*., 1963, **2**, 1111; c) L. I. Zakharkin, V. I. Stanko, V. A. Brattsev, Yu. A. Chapovsky and Yu. T. Struchkov, *Ivz. Akad. Nauk SSSR., Ser. Khim.,* 1963, 2069; d) L. I. Zakharkin, V. I. Stanko, V. A. Brattsev, Yu. A. Chapovsky and O. Yu. Okhlobystin, *Ivz. Akad. Nauk SSSR., Ser. Khim.,* 1963, 2238.

1.15 A. R. Siedle, *J. Organomet. Chem*., 1975, **90**, 249.

1.16 R. E. Williams, *Inorg. Chem*., 1971, **10**, 210.

1.17 R. N. Grimes, *Angew. Chem. Int. Ed.*, 2003, **43**, 1198.

1.18 D. Grafstein and J. Dvorak, *Inorg. Chem.*, 1963, **2**, 1128.

1.19 S. Papetti and T. L. Heying, *J. Am. Chem. Soc.*, 1964, **86**, 2295.

1.20 W. N. Lipscomb, *Science*, 1966, **153**, 373.

1.21 D. J. Wales, *J. Am. Chem. Soc.*, 1993, **115**, 1557.

1.22 H. D. Kaesz, R. Bau, H. A. Beall and W. N. Lipscomb, *J. Am. Chem. Soc.*, 1967, **89**, 4219.

1.23 C. A. Brown and M. L. McKee, *J. Mol. Model.*, 2006, **12**, 653.

1.24 D. McKay, unpublished work, *Heriot-Watt University*, 2010.

1.25 D. Grafstein, J. Bobinski, J. Dvorak, H. F. Smith, N. N. Schwartz, M. S. Cohen and M. M. Fein, *Inorg. Chem.*, 1963, **2**, 1089.

1.26 M. F. Hawthorne, *J. Organomet. Chem.*, 1975, **100**, 97.

1.27 R. Coult, M. A. Fox, W. R. Gill, P. L. Herbertson, J. A. H. MacBride and K. Wade, *J. Organomet. Chem.*, 1993, **462**, 19.

1.28 V. I. Bregadze, *Chem. Rev.*, 1992, **92**, 209 (and references therein).

1.29 R. A. Wiesboeck and M. F. Hawthorne, *J. Am. Chem. Soc.*, 1964, **86**, 1642.

1.30 a) J. S. Roscoe, S. Kongpricha and S. Papetti, *Inorg. Chem.*, 1970, **9**, 1561; b) M. F. Hawthorne and P. A. Wegner, *J. Am. Chem. Soc.*, 1968, **90**, 896.

1.31 G. Barberà, A. Vaca, F. Teixidor, R. Sillanpää, R. Kivekäs and C. Viñas, *Inorg. Chem.*, 2008, **47**, 7309.

1.32 a) M. F. Hawthorne, D. C. Young, T. D. Andrews, D. V. Howe, R. L. Pilling, A. D. Pitts, M. Reintjes, L. F. Warren and P. A. Wegner, *J. Am. Chem. Soc*., 1968, **90**, 879; b) D. C. Busby and M. F. Hawthorne, *Inorg. Chem.*, 1982, **21**, 4101.

1.33 Z. Zheng, W. Jiang, A. A. Zinn, C. B. Knobler and M. F. Hawthorne, *Inorg. Chem.*, 1995, **34**, 2095 (and references therein).

1.34 G. B. Dunks, R. J. Wiersema and M. F. Hawthorne, *J. Chem. Soc., Chem. Commun.*, 1972, 899.

1.35 L. D. Brown and W. N. Lipscomb, *Inorg. Chem.*, 1977, **16**, 2989.

1.36 P. v. R. Schleyer, K. Najafian and A. M. Mebel, *Inorg. Chem.*, 1998, **37**, 6765.

1.37 a) M. F. Hawthorne, D. C. Young and P. A. Wegner, *J. Am. Chem. Soc.*, 1965, **87**, 1818; b) M. F. Hawthorne and R. L. Pilling, *J. Am. Chem. Soc.*, 1965, **87**, 3988; c) M. F. Hawthorne and T. D. Andrews, *Chem. Commun*., 1965, 443.

1.38 A. S. Batsanov, P. A. Eva, M. A. Fox, J. A. K. Howard, A. K. Hughes, A. L. Johnson, A. M. Martin and K. Wade, *Dalton Trans.*, 2000, 3519.

1.39 For example: a) D. E. Smith and A. J. Welch, *Organometallics*, 1986, **5**, 760; b) L. Borodinsky, E. Sinn and R. N. Grimes, *J. Am. Chem. Soc.*, 1982, **21**, 1686.

1.40 For example: a) A. K. Hughes, *J. Organomet. Chem*., 2002, **657**, 9; b) C. Viñas, S. Gómez, J. Bertran, J. Barron, F. Teixidor, J. F. Dozol, H. Rouquette, R. Kivekäs and R. Sillanpää, *J. Organomet. Chem*., 1999, **581**, 188.

1.41 M. K. Kaloustian, R. J. Wiersema and M. F. Hawthorne, *J. Am. Chem. Soc*., 1972, **94**, 6679.

1.42 For example: a) L. F. Warren and M. F. Hawthorne, *J. Am. Chem. Soc*., 1970, **92**, 1157; b) R. M. Garrioch, P. Kuballa, K. S. Low, G. M. Rosair and A. J. Welch, *J. Organomet. Chem.*, 1999, **575**, 57.

1.43 G. B. Dunks, M. M. McKown and M. F. Hawthorne, *J. Am. Chem. Soc.*, 1971, **93**, 2541.

1.44 M. R. Churchill and B. G. DeBoer, *J. Chem. Soc., Chem. Commun*., 1972, 1326.

1.45 For example: a) G. B. Dunks, R. J. Wiersema and M. F. Hawthorne, *J. Am. Chem. Soc*., 1973, **95**, 3174; b) D. Ellis, M. E. Lopez, R. McIntosh, G. M. Rosair, A. J. Welch and R. Quenardelle, *Chem. Commun.*, 2005, 1348; c) L. I. Zakharkin, V. N. Kalinin and L. S. Podvisotskaya, *Bull. Acad. Sci. USSR, Div. Chem. Sci.*, 1966, 1444; d) V. I. Stanko, Yu. V. Gol'tyapin and V. A. Brattsev, *J. Gen. Chem. USSR*, 1969, 1142; e) L. I. Zakharkin, V. N. Kalinin, V. A. Antonovich and E. G. Rys, *Bull. Acad. Sci. USSR, Div. Chem. Sci.*, 1976, 1009.

1.46 For example: a) R. Khattar, C. B. Knobler and M. F. Hawthorne, *J. Am. Chem. Soc.*, 1990, **112**, 4962; b) K. Chui, H.-W. Li and Z. Xie, *Organometallics*, 2000, **19**, 7447; c) N. M. M. Wilson, D. Ellis, A. S. F. Boyd, B. T. Giles, S. A. Macgregor, G. M. Rosair and A. J. Welch, *Chem. Commun.*, 2002, 464; d) D. Ellis, M. E. Lopez, R. McIntosh, G. M. Rosair and A. J. Welch, *Chem. Commun*., 2005, 1917.

1.47 For example: a) D. F. Dustin, G. B. Dunks and M. F. Hawthorne, *J. Am. Chem Soc*., 1973, **95**, 1109; b) D. F. Dustin, G. B. Dunks and M. F. Hawthorne, *J. Am. Chem. Soc.*, 1974, **96**, 3085; c) A. Burke, R. McIntosh, D. Ellis, G. M. Rosair and A. J. Welch, *Collect. Czech. Chem. Commun.*, 2002, **67**, 991.

1.48 R. B. King, *J. Organomet. Chem.*, 2007, **692**, 1773.

1.49 R. E. Williams, *Chem. Rev.*, 1992, **92**, 177.

1.50 R. McIntosh, D. Ellis, J. Gil-Lostes, K. J. Dalby, G. M. Rosair and A. J. Welch, *Dalton Trans.*, 2005, 1842.

1.51 S. Zlatogorsky, M. J. Edie, D. Ellis, S. Erhardt, M. E. Lopez, S. A. Macgregor, G. M. Rosair and A. J. Welch, *Angew. Chem. Int. Ed.*, 2007, **46**, 6706.

1.52 D. F. Dustin and M. F. Hawthorne, *J. Am. Chem. Soc.*, 1974, **96**, 3462.

1.53 M. E. Lopez, M. J. Edie, D. Ellis, A. Horneber, S. A. Macgregor, G. M. Rosair and A. J. Welch, *Chem. Commun*., 2007, 2243.

1.54 A. R. Kudinov, D. S. Perekalin, S. S. Rynin, K. A. Lyssenko, G. V. Grintselev-Knyazev and P. V. Petrovskii, *Angew. Chem. Int. Ed.*, 2002, **41**, 4112.

1.55 W. J. Evans and M. F. Hawthorne, *J. Chem. Soc., Chem. Commun.*, 1974, 28.

1.56 D. Ellis, M. E. Lopez, R. McIntosh, G. M. Rosair and A. J. Welch, *Chem. Commun.*, 2005, 1917.

1.57 A. Burke, D. Ellis, B. T. Giles, B. E. Hodson, S. A. Macgregor, G. M. Rosair and A. J. Welch, *Angew. Chem. Int. Ed.*, 2003, **42**. 225.

1.58 G. Zi, H.-W. Li and Z. Xie, *Organometallics*, 2001, **20**, 3836.

1.59 L. Deng, H.-S. Chan and Z. Xie, *J. Am. Chem. Soc.*, 2006, **128**, 5218.

1.60 L. Deng, H.-S. Chan and Z. Xie, *Angew. Chem. Int. Ed.*, 2005, **44**, 2128.

1.61 R. McIntosh, D. Ellis, G. M. Rosair and A. J. Welch, *Angew. Chem. Int. Ed.*, 2006, **45**, 4313.

1.62 L. Deng, J. Zhang, H.-S. Chan and Z. Xie, *Angew. Chem. Int. Ed.*, 2006, **45**, 4309.

1.63 J. Zhang, L. Deng, H.-S. Chan and Z. Xie, *J. Am. Chem. Soc.*, 2007, **129**, 18.

1.64 D. McKay, PhD Thesis, *Heriot-Watt University*, 2010.

CHAPTER 2. Stabilisation by control of the carbon atoms movement in reduced carboranes.

2.1 Introduction.

The use of a tether in 1,2-*closo*-C_2B_{10} was the first successful strategy to prevent re-oxidation of *nido* dianions allowing the synthesis of supraicosahedral carboranes via polyhedral expansion.[1] The carbons adjacent [7,8-*nido*-C_2B_{10}]$^{2-}$ species generated after reduction of tethered ortho carboranes can be successfully capitated with suitable boron fragments to generate larger carboranes. The 13-vertex product has a henicosahedral geometry and the reaction proceeds with yields from poor to moderate depending on the tethering framework and the substituents on the haloboranes used for the capitation.[2]

However, this strategy presents a fundamental limitation. Direct capitation of carbons adjacent [7,8-*nido*-C_2B_{10}]$^{2-}$ species generates exclusively 1,2-*closo*-C_2B_{11} isomers. Computational studies on four of the possible isomers (1,2-, 1,6-, 1,10- and 1,12-) of 13-vertex C_2B_{11} carboranes (figure 2.1.1), taking the 1,2- isomer as reference, showed that the most thermodynamically stable isomer is 1,12-*closo*-C_2B_{11}. In fact, the 1,2-*closo*-C_2B_{11} isomer, which is the product from capitation of carbons adjacent [7,8-*nido*-C_2B_{10}]$^{2-}$ species, is the least stable isomer of the series (figure 2.1.1).

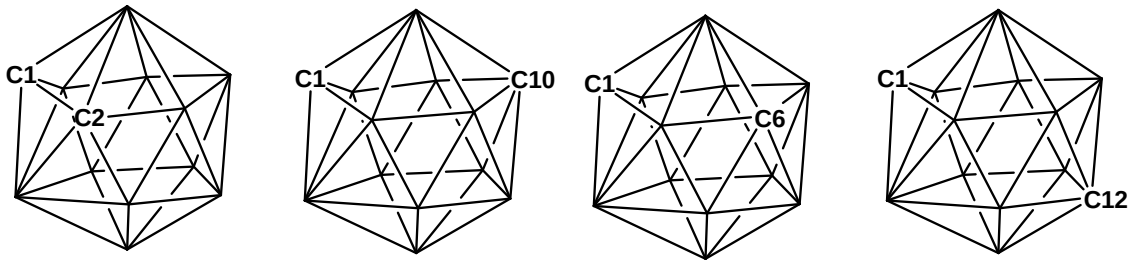

Figure 2.1.1 Relative energies of 13-vertex C_2B_{11} carboranes.[3] (N.B. Naked vertex = BH, C vertex = CH).

These computational predictions have been confirmed by Xie and co-workers using a removable tether in 1,2-*closo*-C_2B_{10} (figure 2.1.2).[4] In this experiment the tethered 1,2-*closo*-C_2B_{11} isomer afforded after capitation with a {BH} fragment was subject to a tether cleavage and then quantitatively isomerised without any decomposition to the thermodynamically more stable 1,6-*closo*-C_2B_{11} upon heating.

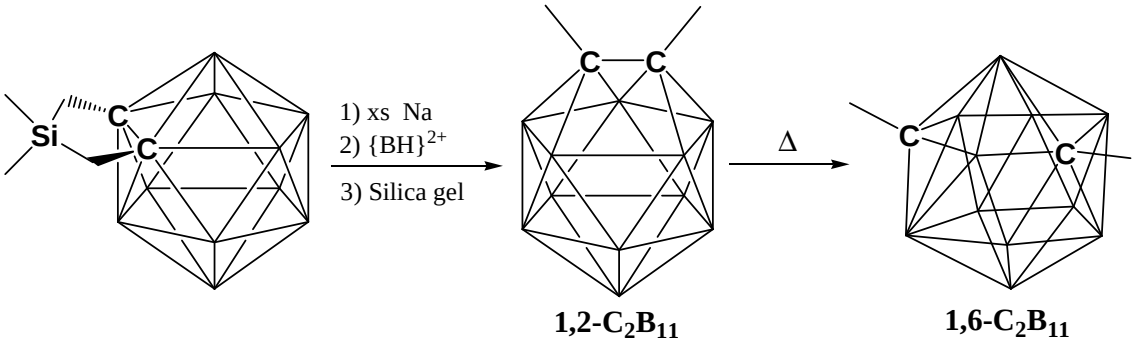

Figure 2.1.2 Synthesis of a carbon atoms apart 13-v carborane.[4]

This means that although tethering 1,2-*closo*-C_2B_{10} is a successful strategy to prevent the re-oxidation of the *nido* intermediate, the 1,2-*closo*-C_2B_{11} supraicosahedral carborane obtained is not the most stable one. *Ortho* tethering is a good method to obtain 13- [1] and 14- [5] carboranes and even 15-vertex [6] metallacarboranes, but unfortunately, this series of carbon-adjacent supraicosahedral carboranes are not thermodynamically stable enough to allow further expansions.

Summarising, the most thermodynamically stable isomer of the 13-v series is the 1,12- isomer but the 1,6- isomer is also much more stable than the 1,2-. A new strategy to prevent the re-oxidation of the *nido*-[7,9-C_2B_{10}]$^{2-}$ intermediate could be to keep the carbon atoms apart in the 12-v 1,7-*closo*-carborane via a suitable rigid *meta*-tether. This would represent a direct way to obtain more stable (1,6-) isomers of 13-v carboranes, which could be used as starting materials for further *Red-Cap* procedures.

The starting material for this strategy should be a *m*-carborane derivative in which a linkage joins the cage carbon atoms. The tether has to meet two basic requirements. First, it has to be rigid enough to keep the cage carbon atoms at the same distance.

Second, the linkage has to be inert towards sodium metal in order to allow the two electron reduction of the cage and consequently the generation of the 7,9-*nido* species.

There are only a few examples in the literature of tethered *m*-carboranes. The first reported compound was 1,7-μ-$(CH_2)_8$-1,7-*closo*-$C_2B_{10}H_{10}$ [7] in which a octamethylene tether links the cage carbon atoms. It is expected that such an aliphatic chain would not be rigid enough to prevent the cage carbon atoms movement during the oxidation of the *nido* dianion. Recent work from Mirkin and co-workers in carborane-based pincers has reported two new examples of tethered *m*-carboranes.[8] In these compounds the rigid linkage involves SBS Pd(II) and SeBSe Pd(II) complexes (figure 2.1.3). However those complexes do not meet the second requirement for the proposed strategy, due to their linkage involving several polarised bonds which could be broken by sodium metal reduction and also a boron vertex which could complicate the generation of the open face of 7,9-*nido* dianion.

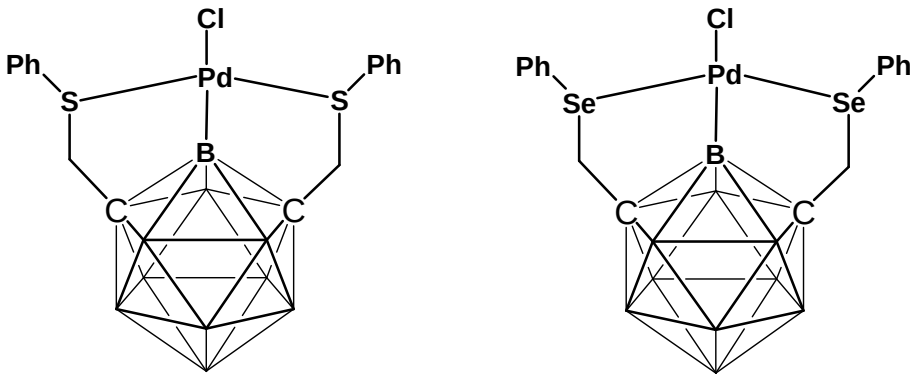

Figure 2.1.3 Reported tethered *m*-carboranes as carborane-based pincers.[8]

Since none of the reported tethered *m*-carboranes meets both requirements for our purposes, in this chapter are presented the design of a suitable tethered *m*-carborane, its synthesis and the attempt of its expansion in order to obtain 13-v species.

2.2 *meta*-Tether design.

Keeping carbon atoms apart in 1,7-*closo*-C_2B_{10} would prevent re-oxidation following reduction and could lead to a new tethered isomer of 13-vertex carborane which could be a suitable starting material for further Red/Cap procedures. To prevent the re-oxidation, the tether must be rigid enough to keep the both carbons apart and at the same distance in all the clusters formed during the Red/Cap process. These clusters are 1,7-*closo*-C_2B_{10}, *nido*-[7,9-C_2B_{10}]$^{2-}$ and 1,6-*closo*-C_2B_{11} (figure 2.2.1).

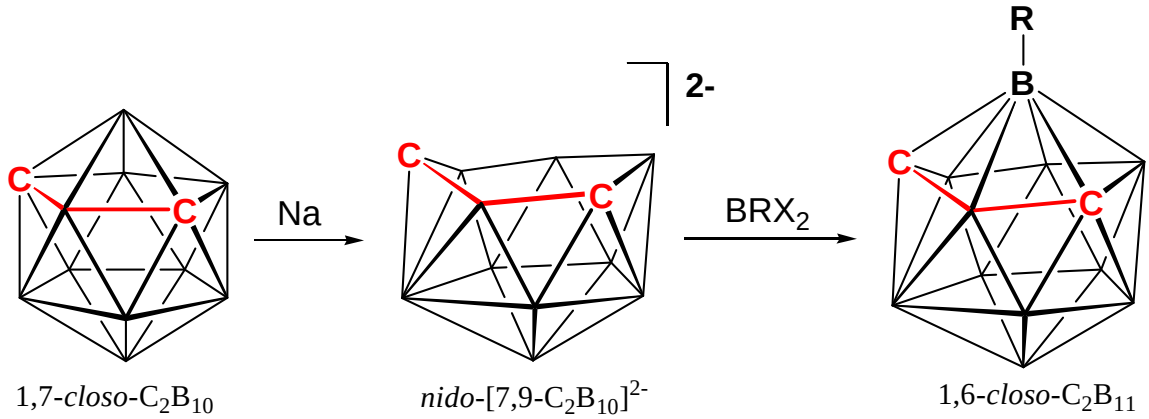

Figure 2.2.1 Cage carbon atoms separation during polyhedral expansion steps.

At this point the tether has to be designed. The design should be based on the C-C bite distance, the distance between the two groups directly bonded to the cage carbon atoms in either 1,7-R_2-1,7-*closo*-C_2B_{10} or in 1,6-R_2-1,6-*closo*-C_2B_{11} species. This bite distance has to be similar in both icosahedral and supraicosahedral clusters. This distance can be estimated by measurement of crystallographic structures. The bite distance for icosahedral species was measured in two different clusters with 1,7-R_2-1,7-*closo*-C_2B_{10} icosahedral architectures and was estimated to be 5.286 Å (average) (figure 2.2.2). In the case of supraicosahedral carboranes, there is only one example in the literature of the 1,6-R_2-1,6-*closo*-C_2B_{11} system but its solid state structure has not been determined. Therefore, the bite distance for supraicosahedral carboranes has to be estimated by measurement of the crystallographic structures of 13-v metallacarboranes of the 4-M-1,6-R_2-4,1,6-*closo*-MC_2B_{10} docosahedral architecture.

The estimation was the average of separate measurements in two different supraicosahedral clusters and is 5.170 Å (figure 2.2.3).

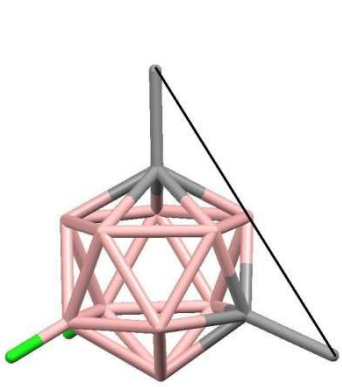

1,7-$(CH_3)_2$-9,10-Cl_2-1,7-*closo*-$C_2B_{10}H_8$ [9]

5.272 Å

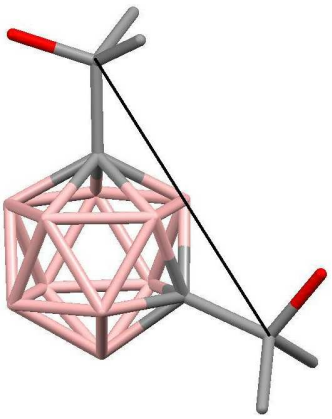

1,7-(CMe_2OH)-1,7-*closo*-$C_2B_{10}H_{10}$ [10]

5.300 Å

Figure 2.2.2 Bite distance measurements of icosahedral (1,7-R_2-1,7-*closo*-C_2B_{10}) carboranes. (Hydrogen atoms omitted for clarity).

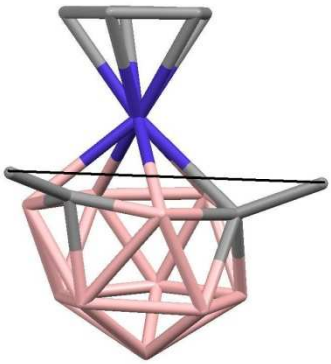

1,6-$(CH_3)_2$-4-Cp-4,1,6-*closo*-$CoC_2B_{10}H_{10}$ [11]

5.181 Å

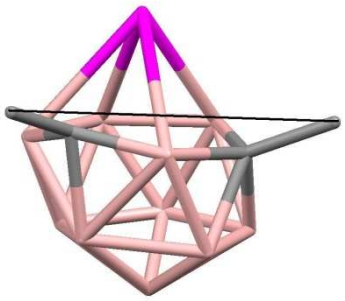

1,6-$(CH_3)_2$-4,1,6-*closo*-$SnC_2B_{10}H_{10}$ [12]

5.159 Å

Figure 2.2.3 Bite distance measurements of docosahedral (4-M-1,6-R_2-4,1,6-*closo*-MC_2B_{10}) carboranes. (Hydrogen atoms omitted for clarity).

Figures 2.2.2 and 2.2.3 show good agreement between the crystallographic bite distances in icosahedral and supraicosahedral species. Therefore a general estimation for the bite distance of a *meta*-tether could be established as 5.228 Å (average value from the four independent crystallographic measurements).

Moreover, the tether must be rigid enough to keep the carbons apart and must also be chemically inert in order to allow the sodium reduction.

Therefore finding a suitable molecule which has all the requirements above is mandatory. The most suitable structures, in terms of bite distance, rigidity and chemical stability are the 1,8-anthracene derivatives (figure 2.2.4).

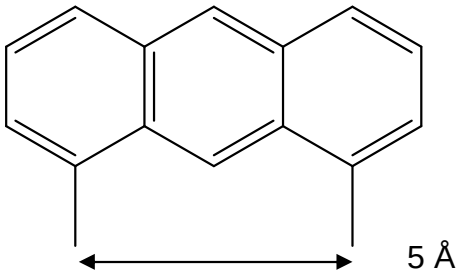

Figure 2.2.4 Bite distance in the anthracene tether.

However there is another point to consider in the design of a suitable *meta*-tether: the steric hindrance between the hydrogen atom bonded to C9 of the anthracene unit and the two hydrogen atoms bonded to B2 and B3 in the carborane cage, as shown in figure 2.2.5.

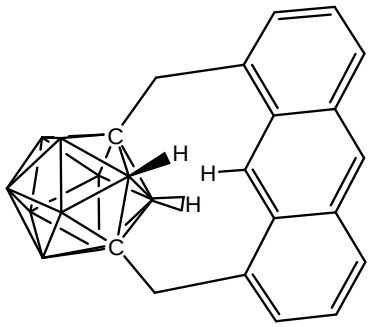

Figure 2.2.5 Predicted steric hindrance between the tether and the cage.

Therefore designs of *meta*-tethers have to consider the distance between the cage and the tether and incorporate a spacer between both frameworks. Due to the anthracene structure possessing all the requirements of rigidity, chemical stability and bite distance, a design of tether based on 1,8-disubstituted anthracene with ethynylmethylene groups as spacers was proposed in order to keep tether and cage sufficiently apart to allow the attachment. The resulting molecule following

attachment of this frame to *m*-carborane was computed to check its stability. The optimised structure and most important interatomic distances are given in table 2.2.1.

Tethering framework	**1,8-bis(methylethynyl)anthracene**
Optimized Structure	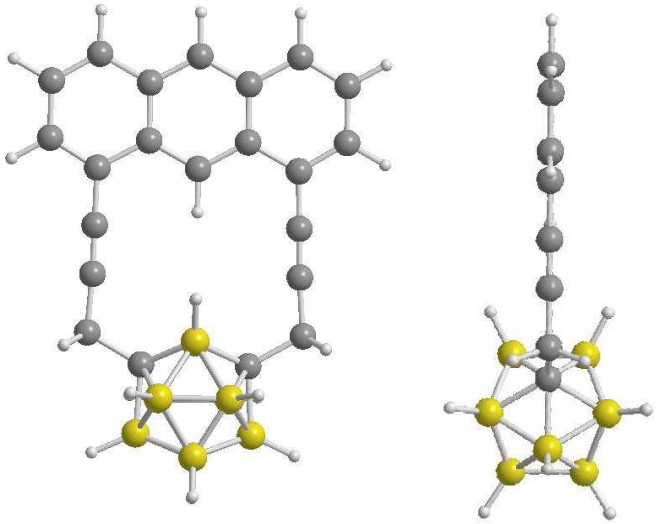
C···C Bite distance (Å)	5.328
H···H Distances (Å)	2.596, 2.597
Computational method	DFT (BP86/6-31G**) in Gaussian 03

Table 2.2.1 Optimised structure for the proposed tethered *m*-carborane.[13]

As table 2.2.1 shows, in the optimized structure the 1,8-diethynylanthracene tether lies perpendicularly between the two hydrogen atoms bonded to B2 and B3 in the carborane cage keeping the organic frame and the cage sufficiently apart, as the H···H distances show. Another interesting feature of this highly symmetric structure is the somewhat strained angles of 116º for the sp^3 hybridised carbon atoms of the linker. Overall, this optimised structure shows an extremely rigid tethered molecule which should effectively retain the cage carbon atoms distance during the proposed polyhedral expansion procedures.

2.3 Synthesis of the proposed tethering frame.

The project of tethering both carbon atoms in *m*-carborane starts with the synthesis of a suitable tethering frame. The proposed design (table 2.2.1) considers the avoidance of steric hindrance between the tether and the cage (figure 2.2.5) by addition of C≡C triple bonds between the anthracene ring and *m*-carborane. Two different approaches were considered to insert two triple bonds between the frames.

The addition of a C≡C triple bond in both 1 and 8 positions of the anthracene unit has been reported by Katz (figure 2.3.1).[14] The synthesis starts with the zinc reduction of 1,8-dichloroanthraquinone.[15] The resulting 1,8-dichloroanthracene **(A)** is the starting material for a nickel-catalyzed coupling with (trimethylsilyl)ethynyl-magnesium bromide affording 1,8-bis[(trimethylsilyl)ethynyl]-anthracene **(B)**. Trimethylsilyl groups are then easily removed[16] using KOH in MeOH to obtain 1,8-diethynylanthracene **(C)**.

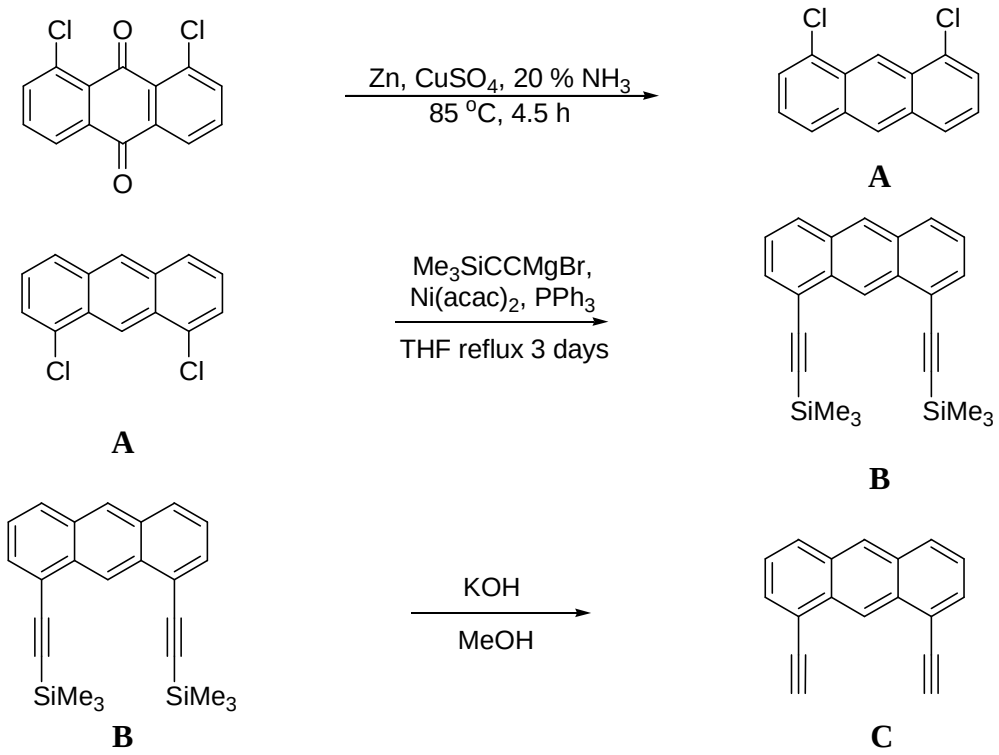

Figure 2.3.1 Synthesis of 1,8-diethynylanthracene (C) from 1,8-dichloroanthraquinone.

Since the addition of two C≡C triple bonds to the anthracene molecule is a reported process, at this point the next step is the formation of two C-C single bonds between the carborane cage and the acetylene. The chemistry of acetylenes is well known for nucleophilic substitutions. Acetylenic hydrogen atoms are acidic and can be easily removed with strong bases such alkyl lithium reagents to afford acetylenic carbanions. Due to their anionic properties acetylenic carbanions form C-C single bonds with electrophilic carbon atoms such alkyl halides and carbonyl groups. However, the chemistry of the carborane carbon atoms is also dominated by their acidic properties. Like acetylenes, cage carbon atoms can be deprotonated with base affording carbanions. Therefore to obtain a C-C bond, or in other words to join both molecules, one more carbon atom is required between both cage and acetylenic groups. These two new carbon atoms must be electrophilic to achieve the coupling with either the deprotonated acetylene or carborane. At this point two different approaches should be considered (figure 2.3.2).

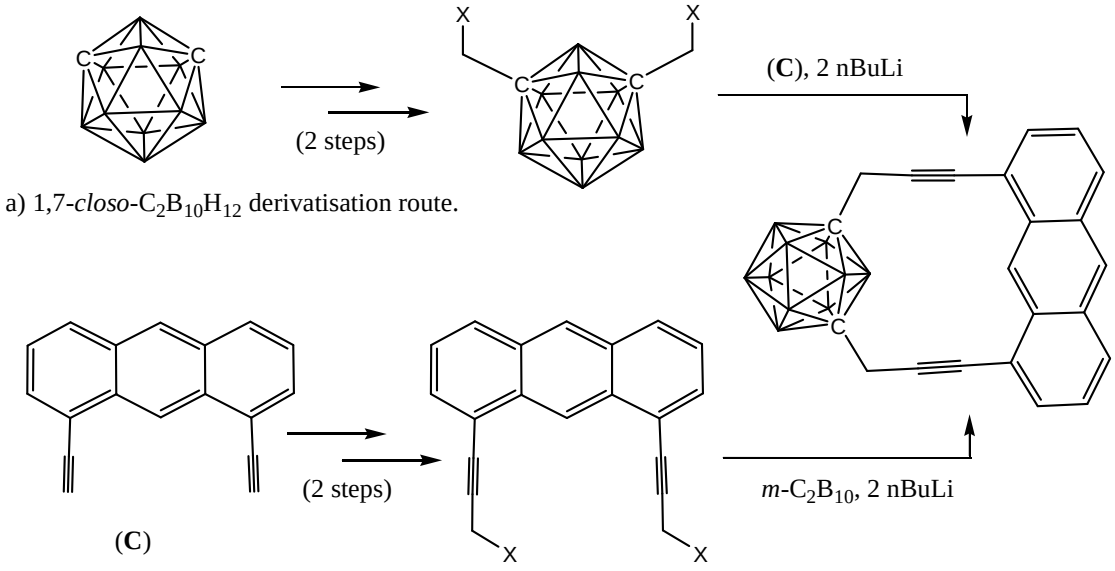

Figure 2.3.2 Two different synthetic routes to achieve the attachment.

One approach to attach ethynylanthracene to the cage is the incorporation of primary alkyl halides at both C1 and C7 positions of *m*-carborane (route “a” in figure 2.3.2). These functionalised carboranes could undergo nucleophilic substitution with

acetylenic carbanions of **C** leading to the tethered *m*-carborane. This first approach involves additional work on *m*-carborane to obtain electrophilic methylene groups directly bonded to the cage carbon atoms.

On the other hand (route "b" in figure 2.3.2), the electrophilic methylene groups necessary for the attachment could be introduced on the acetylenic positions of **C** to generate a 1,8-disubstituted ethynylanthracene which could be used directly as tether with deprotonated *m*-carborane. This second approach involves additional work on the anthracene framework to obtain electrophilic carbon atoms in the propargylic positions of **C**.

2.3.1 *m*-carborane derivatisation route.

In this approach several synthetic steps were carried out to prepare suitable functionalised *m*-carboranes. The aim of this approach is the synthesis of 1,7-$(CH_2OH)_2$-1,7-*closo*-$C_2B_{10}H_{10}$ **(D)** and then the transformation of the alcohol groups into better leaving groups such triflates (-OSO_2CF_3, -OTf) and iodides. These compounds would react with the acetylenic carbanions of deprotonated **C** leading to the tethered *m*-carborane.

The first step is the bonding of two additional carbon atoms to *m*-carborane. This was achieved by the reaction of deprotonated *m*-carborane and paraformaldehyde $(CH_2O)_n$ in ether followed by protonation. This process afforded **D** in good yield.

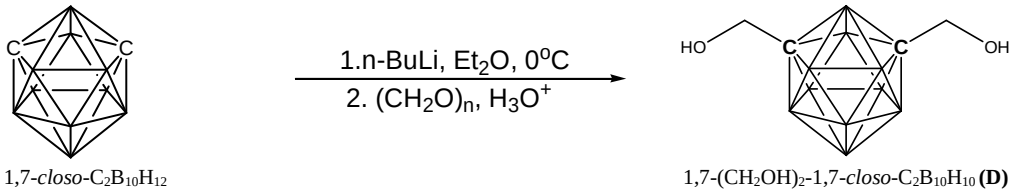

1,7-*closo*-$C_2B_{10}H_{12}$ 1,7-$(CH_2OH)_2$-1,7-*closo*-$C_2B_{10}H_{10}$ **(D)**

Figure 2.3.1.1 Synthesis of 1,7-$(CH_2OH)_2$-1,7-*closo*-$C_2B_{10}H_{10}$ (D).

Deprotonation of carborane was carried out following the usual procedure. Then excess of paraformaldehyde led to the production of **D** in 85% yield.

The next steps involve functionalization of the primary alcohol groups of **D**. The aim is the transformation of alcohols into better leaving groups such triflate (-OTf) or iodide (-I).

One reported process is the preparation of triflates (-OTf) from hydroxymethyl-*o*-carborane.[17] 1,2-$(CH_2OSO_2CF_3)_2$-1,2-*closo*-$C_2B_{10}H_{10}$ was reported by Kanilin *et al*. as a white solid in excellent yields. The same procedure as published was carried out using **D** as starting material to afford 1,7-$(CH_2OSO_2CF_3)_2$-1,7-*closo*-$C_2B_{10}H_{10}$ **(1)**.

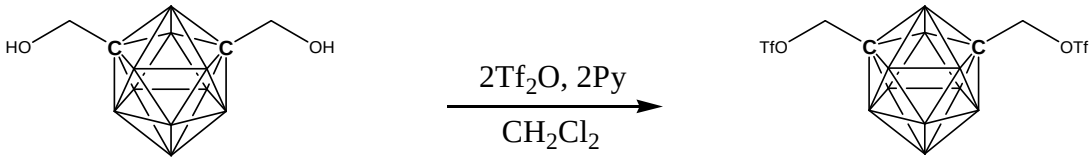

1,7-$(CH_2OH)_2$-1,7-*closo*-$C_2B_{10}H_{10}$ **(D)**

1,7-$(CH_2OSO_2CF_3)_2$-1,7-*closo*-$C_2B_{10}H_{10}$ **(1)**

Figure 2.3.1.3 Synthesis of 1,7-$(CH_2OSO_2CF_3)_2$-1,7-*closo*-$C_2B_{10}H_{10}$ (1).

Despite the fact that the *ortho*-isomer of **1** has been reported to be a white solid, the *meta*-isomer, although isolated in better yield (95%), was a colourless oil.

Compound **1** could be a suitable partner in the coupling with 1,8-diethynylanthracene **(C)**. The attachment must be a strictly stoichiometric reaction to avoid polymerization processes. However crystal structures of functionalized carboranes are interesting in order to calculate the exact bite distance between two *exo*-carbon atoms. Therefore the synthesis of derivatives of **1** was carried out in order to find a suitable and solid di-functionalised *m*-carborane.

Since **1** possesses two triflate groups, excellent leaving groups for nucleophilic substitutions, that reaction was carried out with iodide as nucleophile. The reaction of **1** and sodium iodide as nucleophile source afforded 1,7-$(CH_2I)_2$-1,7-*closo*-$C_2B_{10}H_{10}$ **(2)**. To achieve the nucleophilic substitution the mixture in THF had to be heated to reflux. This process afforded mixtures of ca. 50/50 of starting material/product. Extensive treatment of these mixtures with sodium iodide finally yielded quantitative transformations of **1** into **2** (figure 2.3.1.4).

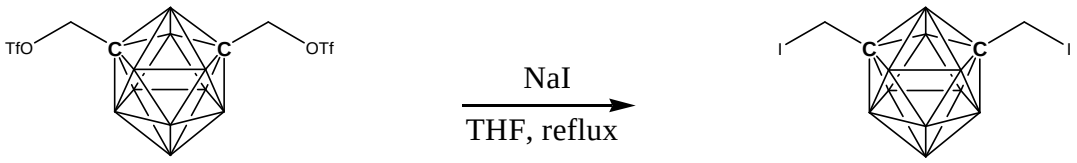

1,7-$(CH_2OSO_2CF_3)_2$-1,7-*closo*-$C_2B_{10}H_{10}$ **(1)**

1,7-$(CH_2I)_2$-1,7-*closo*-$C_2B_{10}H_{10}$ **(2)**

Figure 2.3.1.4 Synthesis of 1,7-$(CH_2I)_2$-1,7-*closo*-$C_2B_{10}H_{10}$ (2).

The new functionalized *m*-carborane was isolated again as colourless oil, however this sample could be crystallized from methanol at -30ºC. Unfortunately, although crystals of **2** were produced they were not of suitable quality for *X*-ray diffraction.

Following the last synthesis two different functionalised *m*-carboranes **1** and **2** have been prepared as suitable coupling partners for the attachment with 1,8-diethynylanthracene **(C)**.

2.3.2 1,8-diethynylanthracene derivatisation route.

The second approach to attach *m*-carborane and anthracene consists of the addition of two electrophilic carbon atoms such alkyl halides to both alkyne units of **C**. Since the reaction of deprotonated carboranes with alkyl halides follows a S_N2 mechanism, this process will be favoured in the preparation of primary alkyl halides. Therefore a suitable synthetic approach would start with the addition of primary alcohols to both acetylenic units of **C**. These primary alcohols can be later transformed into better leaving groups such as halides or triflates leading to a 1,8-difunctionalised anthracene that could be used directly as a *meta*-tether.

In order to obtain propargyl alcohols from alkynes the most logical reaction is that of deprotonated alkynes with carbonyl groups such as aldehydes and ketones. However the scope of carbonyl molecules is reduced to formaldehyde in order to obtain primary propargyl alcohols. Following reported procedures,[18] paraformaldehyde was used as the source of formaldehyde.

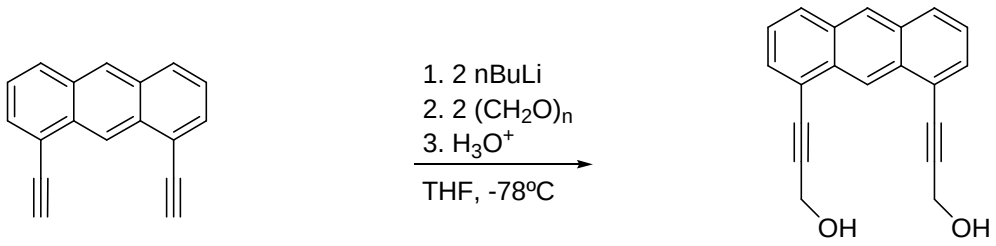

C **3**

Figure 2.3.2.1 Synthesis of 1,8-bis[(hydroxymethyl)ethynyl]-anthracene (3).

The reported procedures considered in the synthesis of **3** are examples of aldehyde-alkyne couplings in molecules which contain only one alkyne group. However despite the reported information about this process, the last reaction failed to afford **3** in better yields than 40%. Another problem found in this synthesis was the isolation of **3** from a crude mixture containing the mono-hydroxylated species as main product. Chromatographic techniques in silica were not really successful due to the fact that both mono- and di-hydroxylated compounds adsorb strongly on silica, with the consequent broadening and overlapping of the chromatographic bands.

After the synthesis of **3** the next step was the transformation of the terminal alcohols into better leaving groups suitable for undergoing a nucleophilic substitution process with deprotonated *m*-carborane. The transformation of primary alcohols (propargylic alcohols in this case) into alkyl halides can be performed in different ways. Bromination by PBr_3 was chosen as a convenient procedure. The mixture of mono- and di-alcohol obtained from the last synthetic step was used as starting material in this reaction.

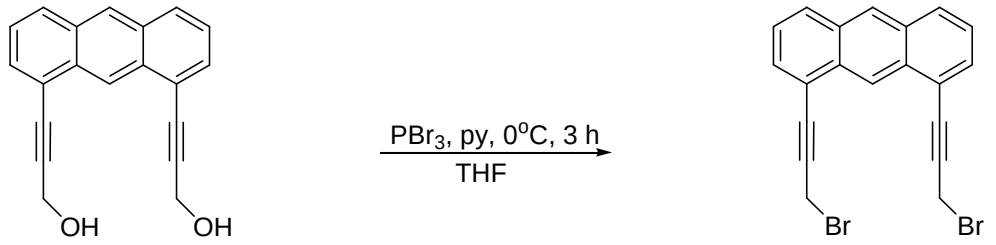

3 **4**

Figure 2.3.2.2 Synthesis of 1,8-bis[(bromomethyl)ethynyl]-anthracene (4).

Avoiding the purification of **3** was found to give an improvement in the overall yield of **4** because the resulting mono- and di-brominated molecules were easier to separate than the corresponding alcoholic compounds. However the overall calculated yield of **4** from **C** was 20% and less than 10% starting from 1,8-dichloroanthraquinone.

The synthesis of a suitable tether for *m*-carborane was achieved. This new compound crystallises easily as yellow needles but has to be kept under inert atmosphere because after prolonged exposure to air it decomposes forming an insoluble brown solid. An *X*-ray diffraction study of **4** revealed the bite distance between electrophilic carbon atoms in the molecule. See figure 2.3.2.3.

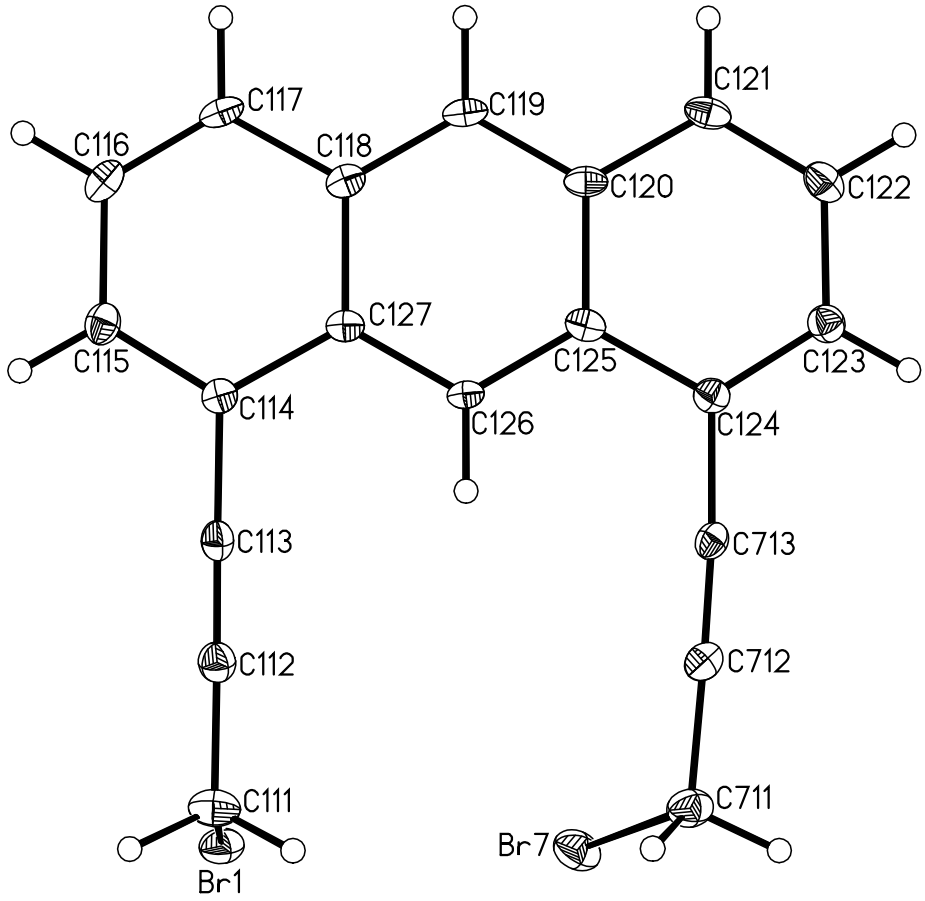

Figure 2.3.2.3 Perspective view of 1,8-bis[(bromomethyl)ethynyl]-anthracene (4). Displacement ellipsoids are drawn at the 50% probability level except for H atoms.

The bite distance was found to be ca. 4.8 Å which is reasonable compared to the bite distance considered in the design (figures 2.2.2 and 2.2.3). The next step is the reaction between the new tether and carborane.

2.4 Attempted coupling between functionalized cage and 1,8-diethynylanthracene (C).

In section 2.3.1 the synthesis of two 1,7-difunctionlized *m*-carboranes has been described with the aim of obtaining suitable partners for a successful alkynylation coupling with 1,8-diethynylanthracene **(C)**.

The coupling between a terminal alkyne and an electrophilic carbon atom such as an organic halide can be achieved following different procedures. The simplest one is deprotonation of the terminal alkyne with strong base such an alkyl lithium reagent or metal hydride. However the scope of these alkynylation couplings has been developed during the last years, including high efficient catalytic alkynylations of a wide range of organic electrophiles. The most reported catalytic-alkynylation procedures can be summarised in three main reactions as figure 2.4.1 shows:

Castro-Stephens reaction:[19]

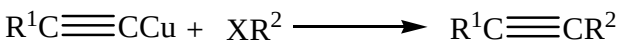

Heck alkynylation reaction:[20]

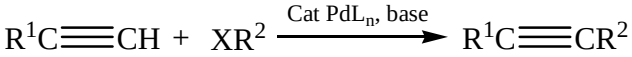

Sonogashira alkynylation reaction:[21]

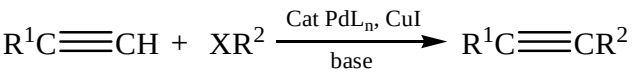

Figure 2.4.1- Catalytic alkynylation reactions.[22]

Research in catalyzed alkynylation procedures, especially using palladium catalysts, has magnified the yields and the scope of organic electrophiles that can be alkynylated.[22] However, alkyl electrophiles lacking a β-γ-unsaturated bond are the only subclass of organic electrophiles that do not undergo synthetically useful oxidative addition with Pd. This problem can be solved by the use of carbene ligands in the palladium catalyst allowing the Sonogashira cross-coupling of unactivated alkyl

halides as has been recently reported.[23] However the scope of this work is limited to a few examples of alkyl iodides and bromides using expensive catalysts that cannot be easily recovered at the end of the reaction. Therefore alkynylation of the functionalized *m*-carborane in order to attach both carbon atoms to the tether has to be limited to non-catalyzed alkynylation methods.

The first step in the coupling reaction between **C** and functionalized *m*-carborane **2** is the deprotonation of the alkyne acidic hydrogen atoms to obtain alkyne carbanions suitable to act as nucleophiles for substitution of the iodide groups in **2**. The use of alkyl lithium reagents such nBuLi has been widely reported [24] as a successful method to remove acetylenic hydrogens in molecules which contains an alkyne group. However this strong base can react with the anthracene removing the hydrogens at 9 and 10 positions [25] leading to side reactions. According to the pK_a values of aromatic ($pK_a \approx 40$) and acetylenic ($pK_a \approx 25$) hydrogen atoms, use of stoichiometric amounts of base and **C** should be sufficient precaution to avoid these side reactions in the anthracene, due to alkyne hydrogen atoms being more acidic than the aromatic ones. On the other hand, the main examples in the literature of alkyl halide alkynylations are focused on molecules which contain only one alkyne group. The examples of double alkynylations are limited to few examples with low yields (10-25%).[14,24] Previous experiments in coupling reactions between **C** and ethylbromide (EtBr) as alkyl halide showed a single coupling in only one of the alkyne positions of **C**. Even using a slightly excess of base, the double coupling was never achieved in synthetically useful yields. Experimental results showed that double deprotonation and consequently double alkynylation can be carried out only at low temperature (-78ºC) for several hours.

After different experiments with EtBr, the process was optimised with ca. 30% yield. The same conditions were used in the reaction of 1,8-diethynylanthracene **(C)** and 1,7-$(CH_2I)_2$-1,7-*closo*-$C_2B_{10}H_{10}$ **(2)**. Unfortunately, after several attempts this coupling reaction never worked. The same procedure was carried out using **1** as a coupling partner without success.

Many reasons can be considered to explain this failure. Since the optimized reaction of **C** with EtBr was in low yield, it is expected to be even lower with **2** due to the

steric hindrance between molecules. Another important factor could be the temperature since deprotonation of **C** requires low temperature but higher temperature may be necessary to achieve a successful approach of both molecules for the double S_N2 process.

2.5 Attachment reaction of tether (4) and *m*-carborane.

After the synthesis of a suitable tethering molecule (**4**), the next step is the reaction of this framework with deprotonated *m*-carborane in order to obtain the desired tethered carborane. This process should not be so difficult since the reaction of lithiated carborane and primary halides is well known. The logical procedure should be the same as that used to tether *o*-carborane with an *o*-xylene bridge.[1] In this procedure deprotonated carborane at 0ºC in diethyl ether is added to a solution of the dihalogenated ligand. After gentle reflux the reaction affords tethered *o*-carborane in good yield.

However this procedure did not work with **4** and deprotonated *m*-carborane. After two hours in refluxing diethyl ether only starting materials were recovered from the reaction mixture. Computational studies (table 2.2.1) showed the stability of the tethered *m*-carborane. Therefore, the failure of these preliminary attachment attempts should lie in the conditions in which the reaction was carried out. The attachment process involves two steps: deprotonation of carborane and nucleophilic substitution between cage carbanions and tether halide groups. In order to optimise both processes several experiments considering solvents, temperature and use of a phase transfer catalyst (PTC) were carried out. To find the appropriate reaction conditions another molecule instead of **4** was used for the optimisation experiments. Since the synthesis of **4** is a long and complicated process (ca. 10% overall yield after 5 synthetic steps) the compound utilised to optimise the coupling reaction was 1-(3-bromoprop-1-ynyl)benzene (figure 2.5.1). This compound possesses the same chemical properties as **4** and can be readily obtained in only two steps from phenylacetylene.

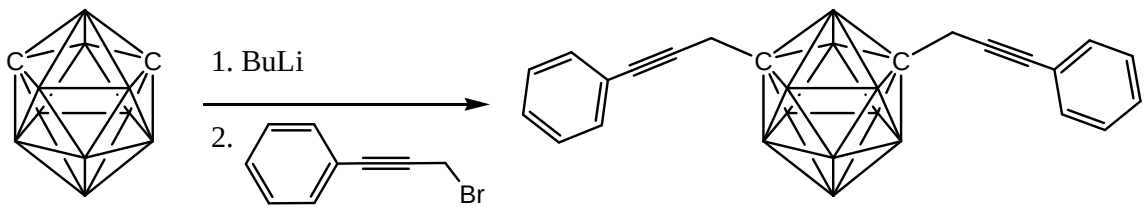

Figure 2.5.1 Optimisation experiments with 1-(3-bromoprop-1-ynyl)benzene.

The scope of suitable solvents for this reaction is limited to aprotic ones due to the use of alkyl lithium reagents. Therefore only THF and diethylether were utilized during the optimization experiments. Coupling temperature was also considered. Additions of the bromide to deprotonated carborane at either 0ºC or -78ºC were carried out. The effect of a phase transfer catalyst (PTC) was studied in order to improve the solubility of the dilithiated carborane produced during the deprotonation step. 12-crown-4 was chosen due to its selectivity for lithium cations. The stoichiometry of the process was also studied in one experiment using four equivalents of 1-(3-bromoprop-1-ynyl)benzene. In total six cross-linking experiments were performed (table 2.5.1) to determine the best reaction conditions. (NB. The percentage of conversion was estimated by comparison of ^{1}H-NMR relative peak intensities).

Exp.	Solvent	Temp.	Stoichiometry	PTC	%
1	Et_2O	0ºC	2 eqs $PhC{\equiv}CCH_2Br$	no	71.4
2	Et_2O	-78ºC	2 eqs $PhC{\equiv}CCH_2Br$	no	81.6
3	THF	0ºC	2 eqs $PhC{\equiv}CCH_2Br$	12-crown-4	75.7
4	Et_2O	0ºC	4 eqs $PhC{\equiv}CCH_2Br$	no	72.1
5	Et_2O	-78ºC	2 eqs $PhC{\equiv}CCH_2Br$	12-crown-4	82.3
6	THF	-78ºC	2 eqs $PhC{\equiv}CCH_2Br$	no	88.5

Table 2.5.1 Cross-linking experiments to optimise the attachment reaction conditions.

After optimisation experiments THF as solvent and low temperature (-78ºC) were found to be the best conditions for the attachment. An excess of 1-(3-bromoprop-1-ynyl)benzene and the use of 12-crown-4 as PTC were found to be irrelevant in these experiments.

Once the best conditions were found the coupling reaction between **4** and *m*-carborane was carried out (figure 2.5.2). 1,7-*closo*-$C_2B_{10}H_{12}$ was deprotonated with two equivalents of n-BuLi in THF. Then the mixture was cooled with a dry ice/acetone bath and a solution of one equivalent of **4** in THF was added by syringe. The mixture was stirred for two hours at low temperature and then another two hours at room temperature. The solvent was removed under vacuum affording an orange solid

residue. Mass spectrometry of this residue showed intense peaks at m/z 394 which corresponds with the mass of the desired tethered *m*-carborane but also at m/z 412 which corresponds with the unreacted tether and at m/z 178, which matches with anthracene's molecular weight.

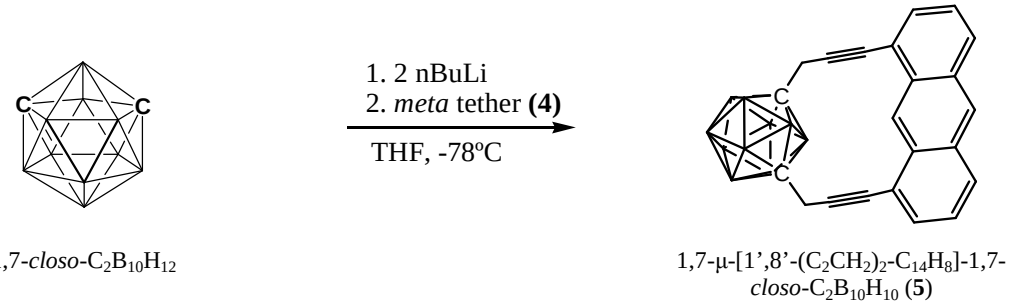

1,7-*closo*-$C_2B_{10}H_{12}$

1,7-μ-[1',8'-$(C_2CH_2)_2$-$C_{14}H_8$]-1,7-*closo*-$C_2B_{10}H_{10}$ (**5**)

Figure 2.5.2 Coupling of tether and *m*-carborane cage under optimized reaction conditions to afford 1,7-μ-[1',8'-$(C_2CH_2)_2$-$C_{14}H_8$]-1,7-*closo*-$C_2B_{10}H_{10}$ (5).

Extensive chromatography of the reaction mixture led to the isolation of **5** in low but enough yield to prove the success of the coupling. One interesting sub-product of the reaction showed in figure 2.5.2 was anthracene. This aromatic compound was isolated in better yield than **5**. Since **4** has shown good stability even after hours of reflux in THF, a reasonable mechanism for anthracene formation is the cleavage of **5**. This cleavage could be favoured due to the strained structure of **5**, as computational studies predicted (table 2.2.3).

Another sub-product of this reaction was an orange insoluble solid. This compound may be a polymer consisting of *m*-carborane cages bridged by **4** although its structure was not characterised.

Single crystals of **5** were obtained after slow evaporation of a concentrated solution in DCM. An *X*-ray diffraction study revealed the structure of the first tethered *m*-carborane in which a rigid organic frame keeps the cage carbon atoms apart (figure 2.5.3).

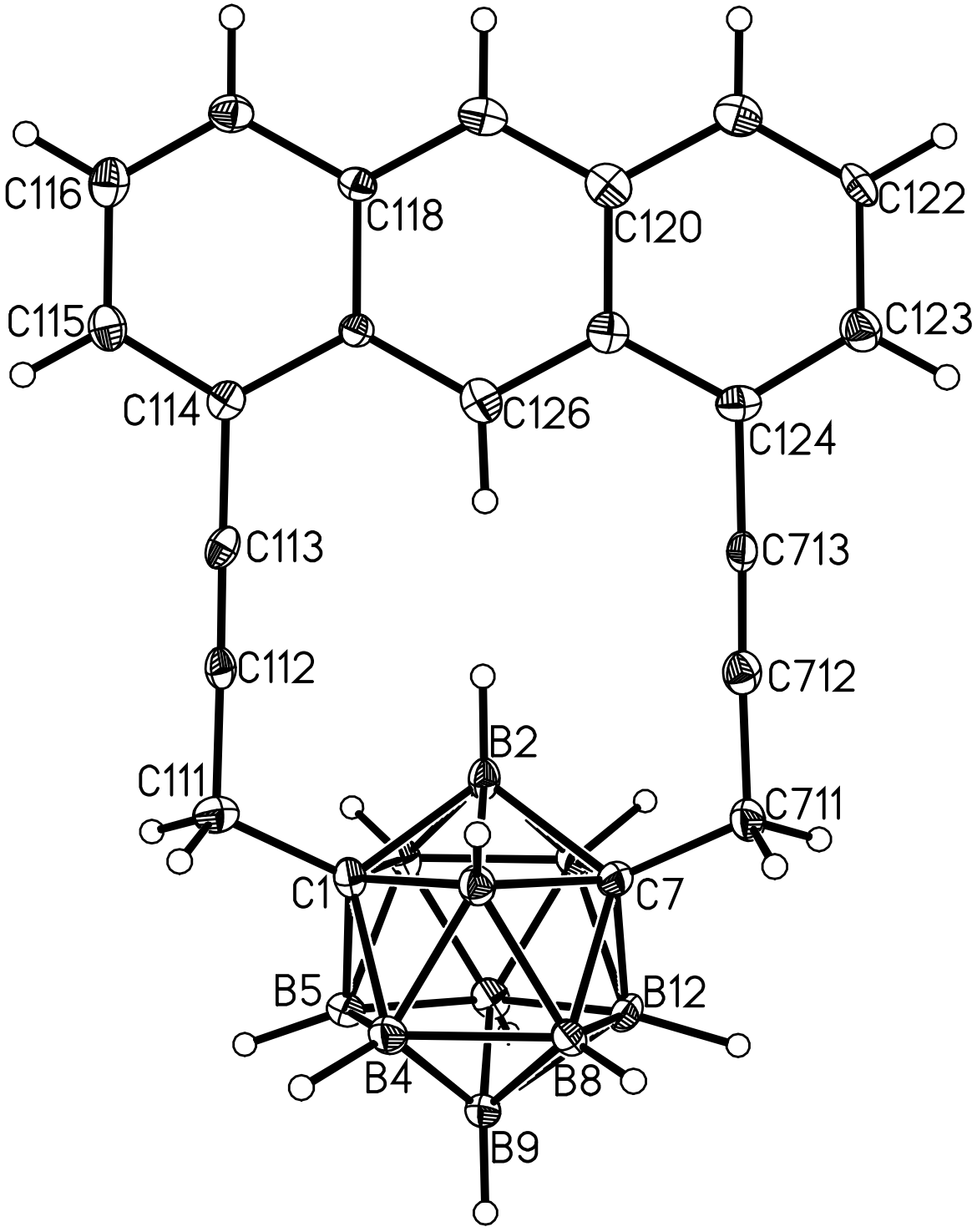

Figure 2.5.3 Perspective view of 1,7-μ-[1',8'-$(C_2CH_2)_2$-$C_{14}H_8$]-1,7-*closo*-$C_2B_{10}H_{10}$ (5). Displacement ellipsoids are drawn at the 50% probability level except for H atoms.

Following the determination of the solid state structure of **5**, its most interesting bond distances and angles can be compared to those of the molecular structure predicted by computational studies during its design (table 2.5.2).

Structure	Predicted (table 2.2.1)	*X*-ray (**5**)
	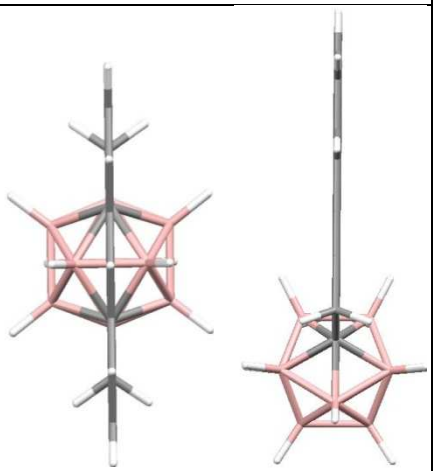	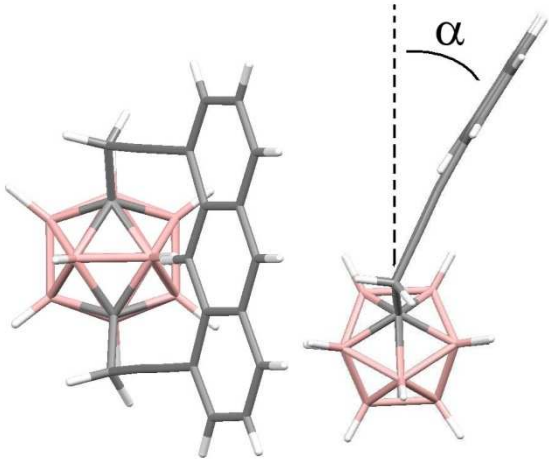
C···C Bite distance	5.328 Å	5.229 Å
α	0º	33.14º

Table 2.5.2 Comparison between solid state structure of 5 and its computationally predicted structure.

The most interesting feature of the molecular structure of **5** is the disposition of the anthracene unit relative to the carborane cage. Whereas in the predicted structure the aromatic ring lies in a perpendicular orientation to the B2-B3 bond, in the solid state structure determined by *X*-ray diffraction the anthracene lies at an angle of 33.14º with the plane that contains C1, C2, B5 and B12. This crystallographic information suggests that rotation about the C_{cage}-C_{sp2} bonds allows the tether in solution to flip over an angle of at least 66.28º. This flexibility could favour the capitation of the hypothetical tethered 7,9-*nido* dianion generated after two electron reduction of **5** by reducing the expected steric hindrance between the anthracene ring and the six-membered open face of the reduced *nido* species.

In conclusion the synthesis of a tethered *m*-carborane has been achieved. This molecule may afford a tethered *nido*-[7,9-C_2B_{10}]$^{2-}$ dianion after 2e sodium reduction which could be capitated with a suitable boron fragment leading to the first tethered 1,6-C_2B_{11} carborane. However due to cleavage of **5** to afford anthracene and the polymer formation, the yield in the attachment reaction was not very good.

2.6 Attempted polyhedral expansion of 5.

Once the tethered *m*-carborane had been synthesised, isolated and characterised, the polyhedral expansion of this cluster was attempted. Direct attempt of capitation with a boron fragment was performed with the aim of generating a tethered 13-v 1,6-*closo*-C_2B_{11} carborane (figure 2.6.1).

One equivalent of 1,7-μ-[1',8'-$(C_2CH_2)_2$-$C_{14}H_8$]-1,7-*closo*-$C_2B_{10}H_{10}$ (**5**) was dissolved in THF under a dinitrogen atmosphere and stirred with an excess of finely cut sodium metal for three days. The resulting dark brown solution was transferred by cannula to another Schlenk tube. Then the solvent was removed under reduced pressure and the residue dissolved in degassed toluene and cooled with a dry ice/acetone bath. To this solution were added two equivalents of $HBBr_2$•SMe_2 and, as a result, the solution slowly turned back to the original pale yellow colour. Volatiles were removed under vacuum and a pale yellow residue was left. Its mass spectrometric analysis revealed no evidence of 13-v species formation. The two main peaks in the spectrum were due to anthracene and carborane. No peak for the starting material **5** was found.

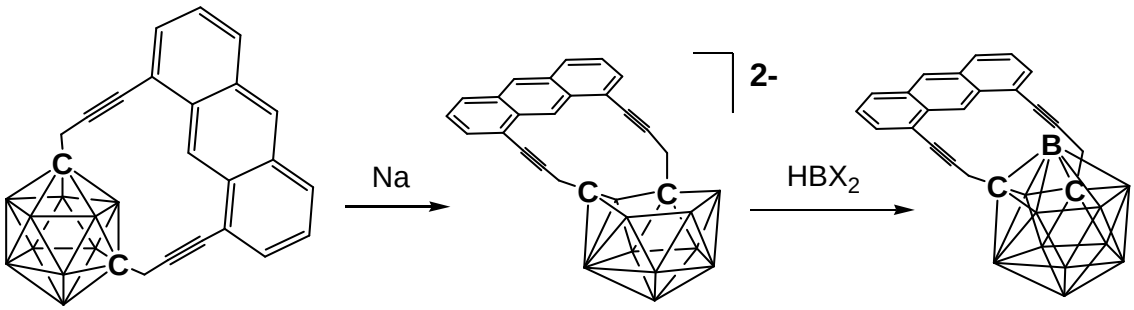

Figure 2.6.1 Attempted polyhedral expansion of 5.

Chromatographic purification of the pale yellow residue led to isolation of *m*-carborane and anthracene in high yields.

2.7 Discussion.

Although the synthesis of a tethered *m*-carborane was achieved, its attempted polyhedral expansion to a 13-vertex carborane was not successful. The failure of this reaction could lie in either the reduction or capitation processes. The two main products of the reaction shown in figure 2.6.1 were anthracene and *m*-carborane. A third product isolated in low yield was anthraquinone. The identities of these three compounds, recovered after the attempted expansion, suggest three different preliminary conclusions:

1- The carborane cage was never reduced since the carborane isolated after the reaction was the 1,7 isomer according to the NMR signals.
2- The tethering frame was not inert towards sodium reduction, leading to its cleavage according to the pure anthracene recovered.
3- The cleavage mechanism begins with the reduction of the central ring of anthracene in **5**, suggested by the isolated anthraquinone.

In conclusion, the anthracene ring in **5** was reduced by sodium leading to a tether cleavage process rather than to the reduction of the carborane cage. In hindsight this result was not completely surprising. In fact, reduction of the aromatic ring was expected since conjugated π systems are relatively easy to reduce. Nevertheless, it was also expected that once the anthracene unit is reduced, it would transfer the unpaired electron from its SOMO to the LUMO of the *m*-carborane cage and recover the aromaticity. Following this principle, the anthracene-based tether would act as an electron shuttle, catalysing the reduction as naphthalene normally does.

However, in the conjugated system of **5** electron transfer did not occur. The reason could lie in the energy gain of the electron transfer, i.e. the energy difference between the SOMO of the reduced conjugated system and the LUMO of *m*-carborane. A comparison between the energies of the SOMO of different conjugated systems (naphthalene, anthracene and 1,8-dialkynylanthracene) and the LUMO of *m*-carborane (figure 2.7.1) could explain why the electron transfer occurs from naphthalenide but not from anthracenide.

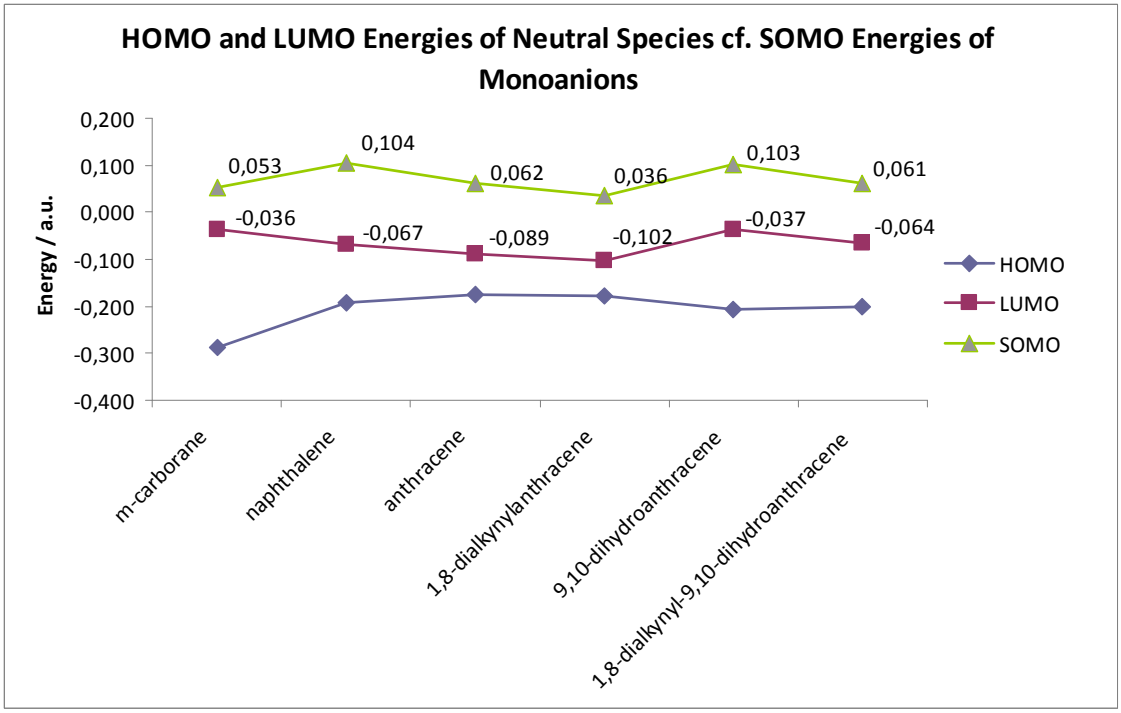

Figure 2.7.1 Energy gaps for electron transfer processes.[26]

When naphthalene is used as a catalyst in the reduction of *m*-carborane, the energy gain of the electron transfer is higher than when using anthracene (figure 2.7.1). In fact it could be established that the energy gain of the process decreases when the conjugation of the series (naphthalene, anthracene, 1,8-dialkynylanthracene) increases. The conjugation stabilises the SOMO and therefore the greater is the conjugation in the π system, the more difficult is the electron transfer.

According to the energies in figure 2.7.1, the electron transfer from anthracenide in **5** to *m*-carborane would not be a very favoured process. This could explain the failure in the reduction of the carborane cage in **5** during the attempted expansion (figure 2.6.1.). It could also explain the formation of anthraquinone by aerial oxidation of the reduced central ring of anthracene.

In conclusion, the reported tethered *m*-carborane (**5**) does not meet one of the basic requirements for this project: it is not stable towards sodium reduction. Although the reduction of the central ring of anthracene was expected, experimental and computational results have shown the failure of the electron transfer that would have allowed the reduction of the *m*-carborane cage.

Since the extended π conjugation disfavours the electron transfer, a similar design of *meta*-tether in which the central ring of anthracene has been selectively hydrogenated in order to break the conjugation could be a solution to this problem. The new tether would be 1,8-dialkynyl-9,10-dihydroanthracene. As figure 2.7.1 shows, reducing the conjugation of the tethering frame would destabilise the SOMO of the tether and therefore would favour the electron transfer to the LUMO of *m*-carborane by increasing the energy gain of the process.

The calculations shown in figure 2.7.1 suggest that the new proposed tethering unit would be better transferring the electrons to the carborane cage than **5**. However, the energy gain improvement in the electron transfer for the new design (0.097 a.u.), although higher than when compared to **5** (0.072 a.u.), is still not as great as that of naphthalene (0.104 a.u) (figure 2.7.1). Moreover, this new design would require additional synthetic steps to the six-step low yielding route necessary to prepare **5**. Icosahedral precursors for polyhedral expansions should ideally be obtained by simple procedures and in good yields. Therefore new designs of *meta*-tethers will not be considered in this thesis. Instead, the following chapters will present different techniques to stabilise the 7,9-*nido* species by simpler means.

2.8 References.

2.1 A. Burke, D. Ellis, B. T. Giles, B. E. Hodson, S. A. Macgregor, G. M. Rosair and A. J. Welch, *Angew. Chem. Int. Ed.*, 2003, **42**, 225.

2.2 L. Deng and Z. Xie, *Organometallics*, 2007, **26**, 1832.

2.3 B. T. Giles, PhD Thesis, *Heriot-Watt University*, 2003.

2.4 J. Zhang, L. Deng, H. S. Chang and Z. Xie, *J. Am. Chem. Soc.*, 2007, **129**, 18.

2.5 L. Deng, H. S. Chan and Z. Xie, *Angew. Chem. Int. Ed.*, 2005, **44**, 2128.

2.6 R. D. McIntosh, D. Ellis, G. M. Rosair and A. J. Welch, *Angew. Chem. Int. Ed.*, 2006, **45**, 4313.

2.7 L. Barnett-Thamattoor, J. J. Wu, D. M. Ho and M. Jones Jr., *Tetrahedron Lett.*, 1996, **37**, 7221.

2.8 A. M. Spokoyny, M. G. Reuter, C. L. Stern, M. A. Ratner, T. Seideman and C. A. Mirkin, *J. Am. Chem. Soc.*, 2009, **131**, 9482.

2.9 H. V. Hart and W. N. Lipscomb, *Inorg. Chem.*, 1973, **12**, 2644.

2.10 B. W. Hutton, Unpublished results, *Heriot-Watt University*, 2007.

2.11 A. McAnaw, Unpublished results, *Heriot-Watt University*, 2008.

2.12 N. M. M. Wilson, D. Ellis, A. S. F. Boyd, B. T. Giles, S. A. Macgregor, G. M. Rosair and A. J. Welch, *Chem. Commun.*, 2002, 464.

2.13 S. Erhardt, Unpublished results, *Heriot-Watt University*, 2008.

2.14 H. E. Katz, *J. Org. Chem.*, 1989, **54**, 2179.

2.15 R. Guilard, M. A. Lopez, A. Tabard, P. Richard, C. Lecomte, S. Brandes, J. E. Hutchison and J. P. Collman, *J. Am. Chem. Soc.*, 1992, **114**, 9877.

2.16 F. Le-Strat and J. Maddaluno, *J. Org. Lett.*, 2002, **4**, 2791.

2.17 V. N. Kalinin, E. G. Rys, A. A. Tyutyunov, Z. A. Starikova, A. A. Korlyukov, V. A. Ol´shevskaya, D. D. Sung, A. B. Ponomaryov, P. V. Petrovskii and E. Hey-Hawkins, *Dalton Trans.*, 2005, 903.

2.18 Y. Yuasa and Y. Kato, *Org. Process Res. Dev.*, 2005, **9**, 825.

2.19 C. E. Castro and R. D. Stephens, *J. Org. Chem.*, 1963, **28**, 2163.

2.20 H. A. Dieck and F. R. Heck, *J. Organomet. Chem.*, 1975, **93**, 259.

2.21 K. Sonogashira, Y. Tohda and N. Hagihara, *Tetrahedron Lett.*, 1975, 4467.

2.22 E. Negishi and L. Anastasia, *Chem. Rev.*, 2003, **103**, 1979.

2.23 M. Eckhardt and G. C. Fu, *J. Am. Chem. Soc.*, 2003, **125**, 13642.

2.24 M. Ramming and R. Gleiter, *J. Org. Chem.*, 1997, **62**, 5821.

2.25 G. M. Harvey and C. C. Davis, *J. Org. Chem.*, 1969, **34**, 3607.

2.26 D. McKay, Unpublished results, *Heriot-Watt University*, 2008.

CHAPTER 3. Stabilisation of reduced carboranes by inductive effect

3.1 Introduction.

The success of the "*ortho*-tethering" strategy in supraicosahedral heteroborane chemistry is attributed to the stabilising effect of the *exo*-tether on 7,8-*nido* reduced dianions (figure 1.7.3). Stabilisation towards re-oxidation relatively favours boron insertion and allows the preparation of supraicosahedral carboranes. A new approach to stabilise reduced carborane dianions could lie in the inductive effect of selected functional groups bonded to the cage.

There are only a few reported examples of the polyhedral expansion of functionalised carboranes but, in general, expansions of C-alkyl and C-aryl carboranes occur in similar manner as for unmodified $C_2B_{10}H_{12}$ carboranes. Reduction and subsequent metallation of C,C'-disubstituted 1,2- and 1,7-*closo*-C_2B_{10} species affords 4,1,6-MC_2B_{10} species and the same process applied to disubstituted 1,12-*closo*-C_2B_{10} yields 4,1,10- 13-vertex metallacarboranes.[1] As has been described in the introduction chapter, the scope of substituents that can be attached to carborane cages is broad. Reduction of the resulting modified carboranes might afford more stable 7,9-*nido* species.

The stabilising effect of different functional groups towards the oxidation of reduced carborane dianions can be predicted by computational methods. Focussing on the stabilisation energy, ΔE, between substituted 7,9-*nido* species over their first oxidation intermediate, the predicted stabilisation effect towards oxidation of different *exo*-groups can be quantified. Computational studies on C,C'-disubstituted species revealed that stabilisation improves when the electron withdrawing character of the substituent increases (figure 3.1.1).[2]

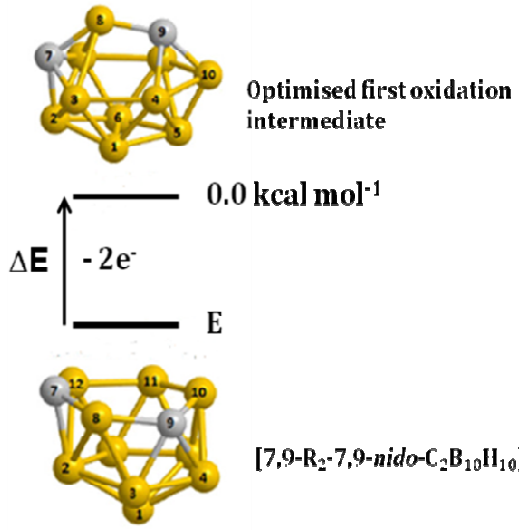

R Group	ΔE / kcal mol^{-1}
-H	4.8
-Me	6.5
-^{t}Bu	12.4
-Ph	29.8
-F	30.7
-COOH	43.6

Figure 3.1.1 DFT-optimised (B3LYP/6-31G*) ΔE values between [7,9-R_2-7,9-*nido*-$C_2B_{10}H_{10}$]$^{2-}$ species and their first oxidation intermediates for different R groups.

Unsurprisingly, the stability of carborane dianions is greater for those bearing electron withdrawing groups (EWG) able to remove electron density from the reduced cluster. However, the energy values shown in figure 3.1.1 could only be useful if the chemical reduction of the closo starting materials to the nido dianions is possible. As an example, carboxylic groups are the most stabilising groups shown in figure 3.1.1, although those groups could never be utilised for polyhedral expansions because they are not inert towards the sodium metal conditions necessary for the reduction process. The first step, then, is the selection of adequate stabilising groups for 7,9-*nido*-C_2B_{10} dianions. In the selection of these groups, two main concepts are considered: electron withdrawing character and chemical stability towards reduction.

3.2 Electron withdrawing fluorinated groups.

The substitution of fluorine for hydrogen in organic functional groups increases their electron withdrawing character due to the small size and high electronegativity of fluorine atoms. The resulting C-F bonds are covalent and in general very stable, as in fluorocarbons such as poly(tetrafluoroethylene) (PTFE). These two facts make organofluorine compounds attractive candidates as stabilising groups for supraicosahedral carborane chemistry. The computationally-predicted stabilisation energies [2] (ΔE in figure 3.1.1) gained by the substitution of fluorine for hydrogen atoms in common organic groups are shown in figure 3.2.1.

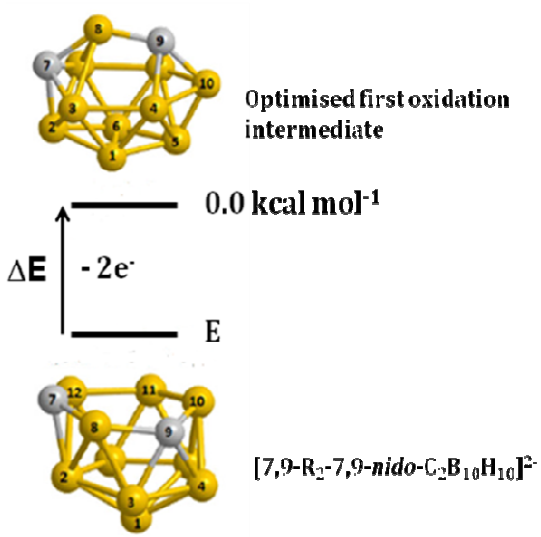

R Group	ΔE / kcal mol^{-1}
-H	4.8
-F	30.7
-CH_3	6.5
-CF_3	45.8
-C_6H_5	29.8
-C_6F_5	49.3

Figure 3.2.1 DFT-optimised (B3LYP/6-31G*) ΔE values between [7,9-R_2-7,9-*nido*-$C_2B_{10}H_{10}$]$^{2-}$ species and their first oxidation intermediates for common organic and organofluorine substituents.

The gain in stabilisation energy for reduced nido species caused by the use of organofluorine substituents is predicted to be significant. However, the polyhedral expansion of carborane cages bearing organofluorine compounds has never been reported. In fact, there are few examples of carborane with organofluorine substituents in the literature.

In the early years of polyhedral borane chemistry, the exhaustive halogenation of borane and carborane clusters was studied in detail. That work led to the synthesis and characterisation of perfluorinated species such as $[B_{12}F_{12}]^{2-}$,[3] 1,2-$(H)_2$-1,2-$C_2B_{10}F_{10}$,[4]

1,7-$C_2B_{10}F_{12}$,[4,5] and 1,12-$(H)_2$-1,12-$C_2B_{10}F_{10}$.[4] More recently, the synthesis of perfluoromethylated carboranes such as $[CB_{11}(CF_3)_{12}]^-$ and 1,12-$(F)_2$-1,12-$C_2B_{10}(CF_3)_{10}$ has also been reported.[6] However, there are some reasons that discourage the use of those species for polyhedral expansion procedures; the first class of B-fluorinated compounds were reported to be, in general, unstable to moist air, hydrolysing to form boric acid as the final product[4] and, on the other hand, some perfluoromethylated carboranes are reported to be unsafe explosive compounds.[6a] In addition, perfluorination of carboranes can only be achieved by fluorine gas in high pressure reactors affording complex mixtures of products. In accord with the above, perfluorinated (methyl)carboranes were discarded for the purposes of this work due to their instability and complex synthesis.

The attachment of fluorinated alkyl substituents to the cage carbon atoms is a rather complicated process. Generally, the alkylation of carboranes occurs via carbon atom deprotonation of the parent carborane and reaction with a suitable electrophile, following a S_N2 mechanism. However, due to the high electronegativity of fluorine atoms, fluorinated alkyl groups behave as nucleophiles rather than electrophiles and do no undergo such substitution. In fact, reaction of pentafluoroethyl iodide (CF_3CF_2I) with deprotonated *ortho*-carborane affords 1,2-I_2-1,2-*closo*-$C_2B_{10}H_{10}$ as the only product.

Perfluoroaromatic rings are predicted to afford a higher stabilisation of reduced carboranes than fluorinated alkyl groups (figure 3.2.1). The attachment of perfluoroaryl substituents to carborane cages was first reported by Zakharkin and Lebedev in 1970.[7] They reported the reactions of C-lithiocarboranes with hexafluorobenzene (C_6F_6) although some of the products were not conclusively identified. This work was further developed by Welch in 1996 and more recently by Wade and co-workers to finally establish the reactivity of deprotonated carboranes with perfluoroaromatic molecules.[8] These reactions proceed through a S_NAr mechanism and the replacement of a fluorine atom by a carboranyl group leads to a strong activation of the fluorine atom in the para position of the ring. In the presence of nucleophiles, the second fluorine atom is readily substituted leading to 1,4-nucleophilic aromatic disubstitutions. Therefore, the reaction of $Li_2C_2B_{10}H_{10}$ with C_6F_6 affords oligomeric products of carborane cages bridged by C_6F_4 rings.

Nevertheless, the oligomerisation process can be prevented by the use of C-monosubstituted carboranes to obtain bis(cage) species, as figure 3.2.2 shows.

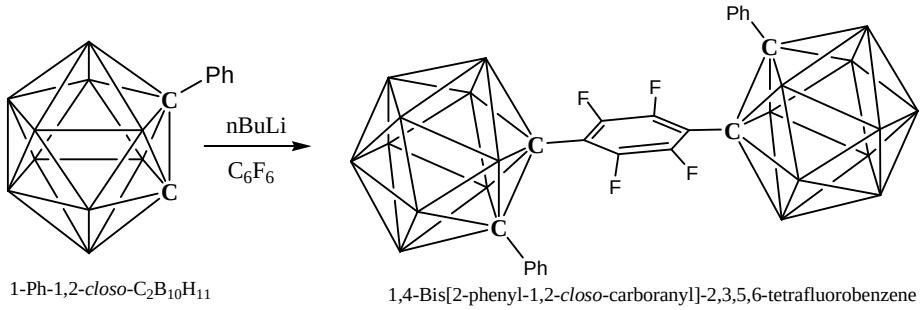

Figure 3.2.2 Double S_NAr of hexafluorobenzene by C-monosubstituted carboranes. (N.B. Naked vertex = BH, C vertex = CH).

Although the introduction of C_6F_5 substituents onto the cage carbon atoms via C_6F_6 is disfavoured by the formation of oligomers due to double nucleophilic substitutions, different approaches such as the use of analogues of hexafluorobenzene, protection of activated C-F bonds or the insertion of fluorinated arylethynes into decaborane should afford discrete carborane molecules bearing the desired perfluoroaryl groups (Ar_F).

The work presented in this chapter is focused on the structural and electronic effects of different fluorinated aryl groups on icosahedral carboranes. As a preliminary investigation, phenyl groups are used as a reference for comparison with the fluorinated aryl groups.

3.3 Fluorinated aryl group (Ar_F)– phenyl series.

In order to compare the structural and electronic effect of different fluorinated aryl (Ar_F) groups on carboranes, a series of 1-Ar_F-2-Ph-1,2-*closo*-$C_2B_{10}H_{10}$ species were synthesised. The phenyl group in the C2 position helps to resolve possible CH/BH disorder problems,[9] contributes to the stabilising effect (figure 3.1.1) and also provides an internal structural and spectroscopic reference.

3.3.1 Synthesis of 1-C_6F_5-2-Ph-1,2-*closo*-$C_2B_{10}H_{10}$ (6).

Pentafluorophenyl (C_6F_5) was the first fluorinated aryl substituent considered. The target compound was 1-C_6F_5-2-Ph-1,2-*closo*-$C_2B_{10}H_{10}$ (**6**) and, although this compound has never been isolated or characterised, it has been reported[8b] to be an intermediate in the synthesis of the bis(cage) species shown in figure 3.2.2. Compound **6** was prepared by the insertion of pentafluorophenylethynylbenzene (**E**) ($C_6F_5C{\equiv}CPh$) into decaborane mediated by Lewis base (figure 3.3.1.1).

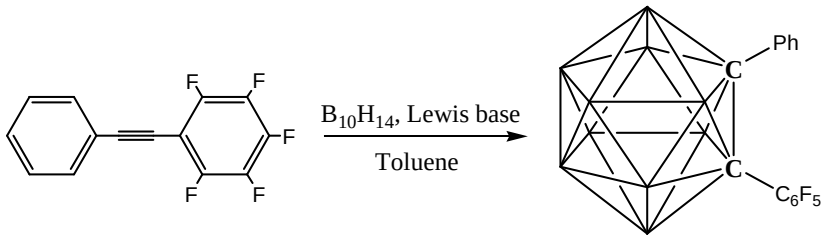

pentafluorophenylethynylbenzene (**E**) 1-C_6F_5-2-Ph-1,2-*closo*-$C_2B_{10}H_{10}$ (**6**)

Figure 3.3.1.1 Synthesis of 1-C_6F_5-2-Ph-1,2-*closo*-$C_2B_{10}H_{10}$ (6) by alkyne insertion of E into decaborane.

Pentafluorophenylethynylbenzene[10] (**E**) was prepared from the Sonogashira cross coupling reaction of iodopentafluorobenzene with phenylacetylene and inserted into decaborane to afford **6** as a white crystalline solid in ca. 60% yield.

The resulting white solid was first analysed by mass spectrometry and elemental analysis. Elemental analysis showed good agreement between expected and measured values and mass spectrometry confirmed the presence of the molecular ion at m/z 386.

Compound **6** was also characterised by multinuclear NMR spectroscopy. The ^{1}H-NMR spectrum indicated the presence of the phenyl ring with two multiplets in the aromatic region of the spectrum. The ^{11}B-NMR spectrum showed only three resonances in a 1:1:8 ratio (high frequency to low frequency). This pattern must involve some signal coincidences, since the molecule can have only C_s symmetry. Interestingly, the peaks in the ^{11}B-NMR spectrum of **6** were shifted downfield, compared to the reported values for diphenylcarborane, confirming the expected electron withdrawing effect of the fluorinated substituent. Finally, ^{19}F-NMR spectroscopy confirmed the presence of three (ortho, meta and para) distinct fluorine environments. Compound **6** was ultimately characterised by an *X*-ray diffraction study, allowing the determination of its solid state molecular structure (figure 3.3.1.2).

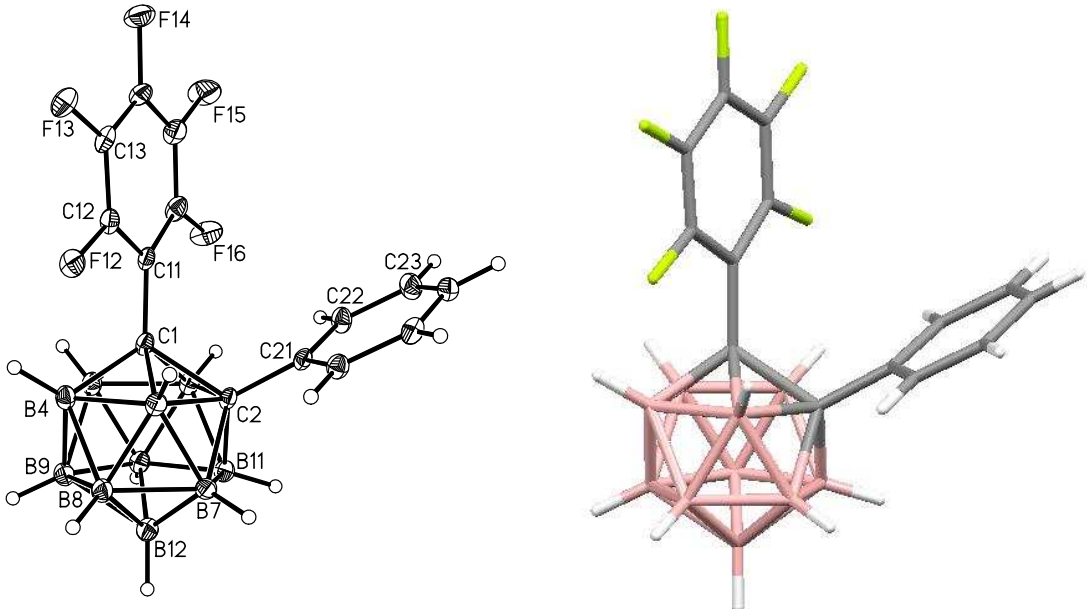

Figure 3.3.1.2 Perspective views of 1-C_6F_5-2-Ph-1,2-*closo*-$C_2B_{10}H_{10}$ (6). Displacement ellipsoids are drawn at the 50% probability level except for H atoms.

Although the synthesis of **6** was successfully achieved, its use as starting material for polyhedral expansions was discouraged by the possibility of undesired side reactions. The para fluorine atom (F14) in **6** has been reported to be very activated towards nucleophilic substitutions. One approach to prevent side reactions might lie in the protection of the para position of the fluorinated ring. Different groups, less vulnerable to undergo S_NAr processes, could occupy the para position of the fluorinated ring leading to more stable analogues of **6**.

3.3.2 Synthesis of 1-(4'-$H_3CC_6F_4$)-2-Ph-1,2-*closo*-$C_2B_{10}H_{10}$ (7).

The first considered approach to stabilise **6** towards undesired S_NAr reactions was the substitution of the para fluorine atom by a methyl group. This reaction should afford the more stable 1-(4'-$H_3CC_6F_4$)-2-Ph-1,2-*closo*-$C_2B_{10}H_{10}$ (**7**), although the substitution of a strong electron withdrawing para fluorine atom by an electron donating methyl group might decrease the inductive effect of the fluorinated ring. Wade and co-workers reported the reaction of the *meta*-analogue of **6** with BuLi to substitute the para fluorine by a butyl group.[8b] The same procedure involving reaction of **6** with MeLi was successfully applied to prepare **7** (figure 3.3.2.1).

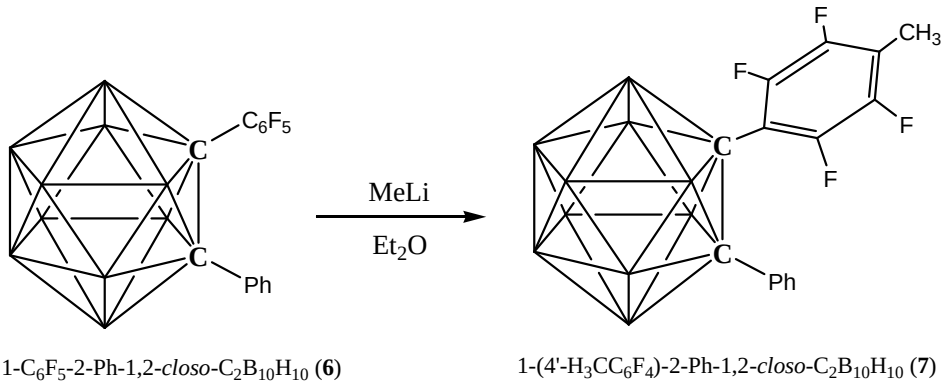

1-C_6F_5-2-Ph-1,2-*closo*-$C_2B_{10}H_{10}$ (**6**) 1-(4'-$H_3CC_6F_4$)-2-Ph-1,2-*closo*-$C_2B_{10}H_{10}$ (**7**)

Figure 3.3.2.1 Synthesis of 1-(4'-$H_3CC_6F_4$)-2-Ph-1,2-*closo*-$C_2B_{10}H_{10}$ (7) by nucleophilic aromatic substitution of fluoride by methyl anion.

Compound **7** was isolated after aqueous work-up as a white crystalline solid in ca. 85% yield. Mass spectrometry showed the parent molecular ion at m/z 382 and elemental analysis results were concordant with expected values.

The identity of **7** was also confirmed by multinuclear NMR studies. Although the ^{11}B-NMR spectrum showed a similar pattern as **6**, the three peaks were slightly shifted upfield as a consequence of the electron donating effect of the methyl group. ^{1}H-NMR studies revealed the presence of the methyl group as a singlet at δ 2.18 as well as the presence of the phenyl group as two multiplets in the aromatic range of the spectrum. The ^{19}F-NMR spectrum of **7** consisted of just two signals corresponding to the two ortho and two meta fluorine atoms in the ring.

Although all the analytical techniques confirmed the identity of **7**, a block crystal suitable for *X*-ray diffraction studies was selected in order to obtain the solid state structure of **7** (figure 3.3.2.2).

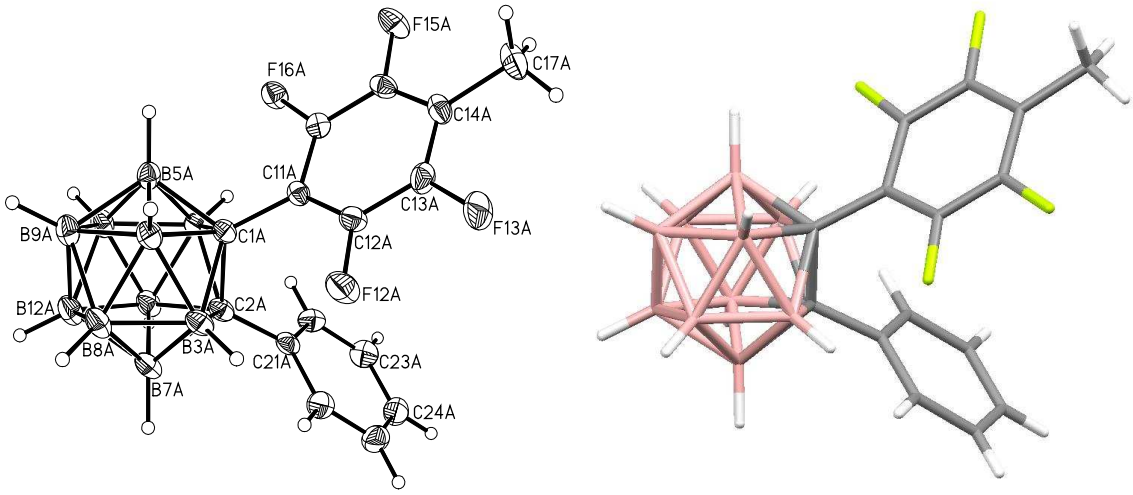

Figure 3.3.2.2 Perspective views of 1-(4'-$H_3CC_6F_4$)-2-Ph-1,2-*closo*-$C_2B_{10}H_{10}$ (7) (one of the two crystallographic independent molecules). Displacement ellipsoids are drawn at the 50% probability level except for H atoms.

Single crystal *X*-ray diffraction studies ultimately confirmed the molecular structure of **7**. Protection of the para position in the fluorinated ring has been achieved; however, ^{11}B-NMR studies implied that the presence of a methyl group decreases the electron withdrawing effect of the fluorinated ring on the carborane cage.

In order to protect the para position in the fluorinated ring and, at the same time, increase the electron withdrawing effect of the group, the electron donating methyl group could be replaced by strong electron withdrawing fluoroalkyl substituents.

3.3.3 Synthesis of 1-(4'-$F_3CC_6F_4$)-2-Ph-1,2-*closo*-$C_2B_{10}H_{10}$ (8).

The presence of a fluorinated alkyl substituent in the para position of the ring is expected to increase the stabilising effect of the group as well as prevent undesired nucleophilic substitution. The simplest fluorinated alkyl group is the trifluoromethyl substituent; however, this substituent cannot be directly attached at the para position of the C_6F_5 ring since that would involve the use of unavailable trifluoromethyl

lithium. A different approach to attach a perfluorotolyl (4-$F_3CC_6F_4$, C_7F_7) group to the carborane cage had to be considered. Because of the strong electron withdrawing nature of CF_3 groups, perfluorotoluene (C_7F_8) is even more susceptible to nucleophilic attack than C_6F_6. In addition, the nucleophilic substitution occurs regioselectively at the carbon atom in the para position to the trifluoromethyl group, preventing additional S_NAr reactions.[11] Therefore, the direct reaction of deprotonated monophenylcarborane with C_7F_8 was performed in order to synthesise 1-(4'-$F_3CC_6F_4$)-2-Ph-1,2-*closo*-$C_2B_{10}H_{10}$ (**8**) (figure 3.3.3.1).

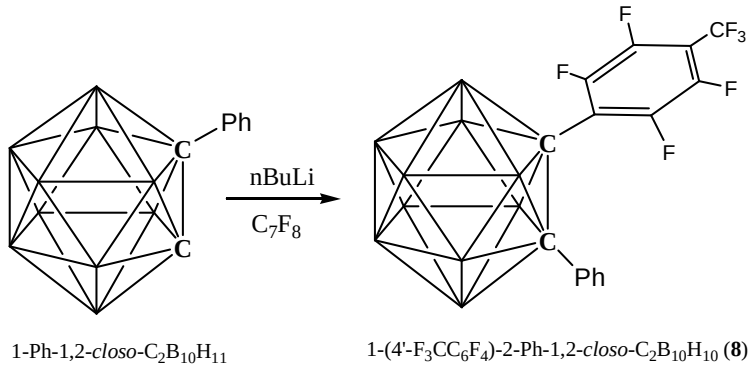

1-Ph-1,2-*closo*-$C_2B_{10}H_{11}$ 1-(4'-$F_3CC_6F_4$)-2-Ph-1,2-*closo*-$C_2B_{10}H_{10}$ (**8**)

Figure 3.3.3.1 Synthesis of 1-(4'-$F_3CC_6F_4$)-2-Ph-1,2-*closo*-$C_2B_{10}H_{10}$ (8) by direct reaction of deprotonated monophenyl carborane with perfluorotoluene.

Monophenylcarborane[12] in diethyl ether solution was deprotonated with one equivalent of n-BuLi and treated with C_7F_8 to afford **8** in 85% yield after aqueous work-up. Compound **8** was isolated as a colourless oil that slowly crystallised at room temperature to afford a white solid. The identity of **8** was confirmed by the presence of the molecular ion at m/z 436 in the mass spectrum and the purity by good agreement with theory of the results of the elemental analysis.

The ^{11}B-NMR spectrum of **8** showed the same 1:1:8 pattern as **6** and **7**, although the signals of **8** were shifted to higher frequencies due to the stronger electron withdrawing character of the perfluorotolyl group. An ^{1}H-NMR experiment indicate the presence of the phenyl group and the three peaks at $\delta -56.9$, $\delta -137.9$ and $\delta -128.0$ in the ^{19}F-NMR spectrum confirmed the presence of the CF_3 group and the two sets of aromatic fluorine atoms, respectively.

The solid-state molecular structure of **8** was revealed by *X*-ray diffraction study of a single crystal and is shown in figure 3.3.3.2.

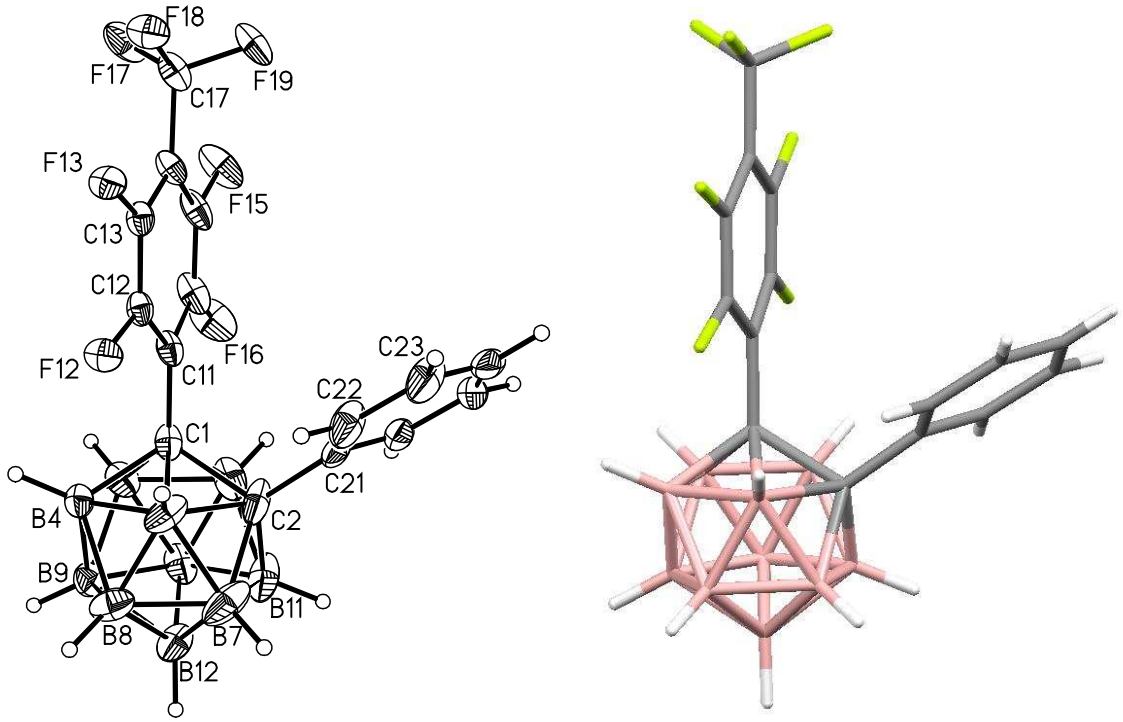

Figure 3.3.3.2 Perspective views of 1-(4'-$F_3CC_6F_4$)-2-Ph-1,2-*closo*-$C_2B_{10}H_{10}$ (8). Displacement ellipsoids are drawn at the 50% probability level except for H atoms.

The solid-state structure of **8** was found to present minor crystallographic disorder in both phenyl and trifluoromethyl positions (which have been omitted in figure 3.3.3.2). Nevertheless, the identity of **8** was undoubtedly confirmed. According to the spectroscopic analysis of **8** (which will be discussed in detail in following sections), the presence of a trifluoromethyl moiety at the para position of the aromatic ring enhances the electron withdrawing effect of the fluorinated substituent. In addition, trifluoromethyl groups are more stable towards undesired S_NAr processes than $C_{(sp2)}$-F containing substituents. Therefore, a substituent consisting of a phenyl ring bearing a trifluoromethyl group at the para position could be an interesting alternative to the use of fluoroaryl groups.

3.3.4 Synthesis of 1-(4'-$F_3CC_6H_4$)-2-Ph-1,2-*closo*-$C_2B_{10}H_{10}$ (9).

In order to introduce a *para*-trifluoromethylphenyl (4-$F_3CC_6H_4$) unit into monophenylcarborane, several synthetic approaches were considered. An Ullman type coupling via C-copper derivatives was discarded since it cannot afford C-disubstituted ortho carboranes.[13] On the other hand, direct reaction of deprotonated monophenylcarborane with 4-fluorobenzotrifluoride via an S_NAr reaction failed even in the DMF conditions reported by Endo and co-workers.[14] Therefore preparation of the corresponding fluorinated phenylacetylene and insertion into decaborane was the chosen synthetic strategy (figure 3.3.4.1).

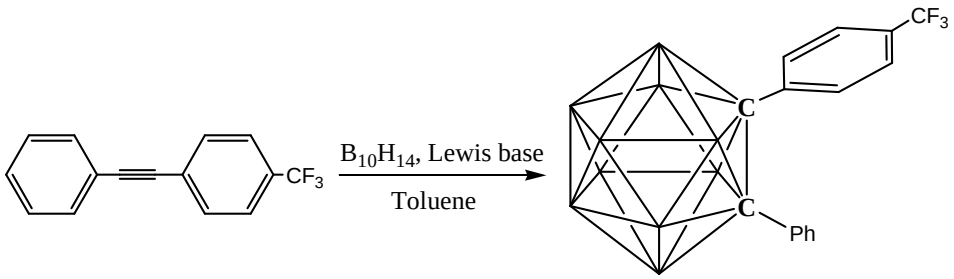

paratrifluorobenzylethynylbenzene (**F**) 1-(4'-$F_3CC_6H_4$)-2-Ph-1,2-*closo*-$C_2B_{10}H_{10}$ (**9**)

Figure 3.3.4.1 Synthesis of 1-(4'-$F_3CC_6H_4$)-2-Ph-1,2-*closo*-$C_2B_{10}H_{10}$ (9) by insertion of F into decaborane.

para-trifluorobenzylethynylbenzene[15] (**F**) was prepared in good yield by a Sonogashira cross coupling reaction of phenylacetylene and 4-iodobenzotrifluoride. The reaction of **F** with decaborane, mediated by Lewis base, afforded 1-(4'-$F_3CC_6H_4$)-2-Ph-1,2-*closo*-$C_2B_{10}H_{10}$ (**9**) as a white solid in ca. 60% yield.

Elemental analysis of **9** was concordant with expected values and mass spectrometry showed the molecular ion at m/z 364. The ^{1}H-NMR spectrum of **9** is complex with several multiplets in the aromatic area δ 7.6-7.1 corresponding to the nine aromatic hydrogen atoms in five different chemical environments. The pattern obtained in the ^{11}B-NMR spectrum of **9** is 2:2:4:2, more appropiate for the "*pseudo* C_{2v}" cage symmetry, rather than the 1:1:8 ratios obtained for **6**, **7** and **8**. The ^{19}F-NMR spectrum showed only one signal, indicating the presence of a CF_3 group in the molecule. To complete the structural characterisation of the series, a single block crystal was

selected and subjected to *X*-ray diffraction to obtain the molecular structure of **9** (figure 3.3.4.2).

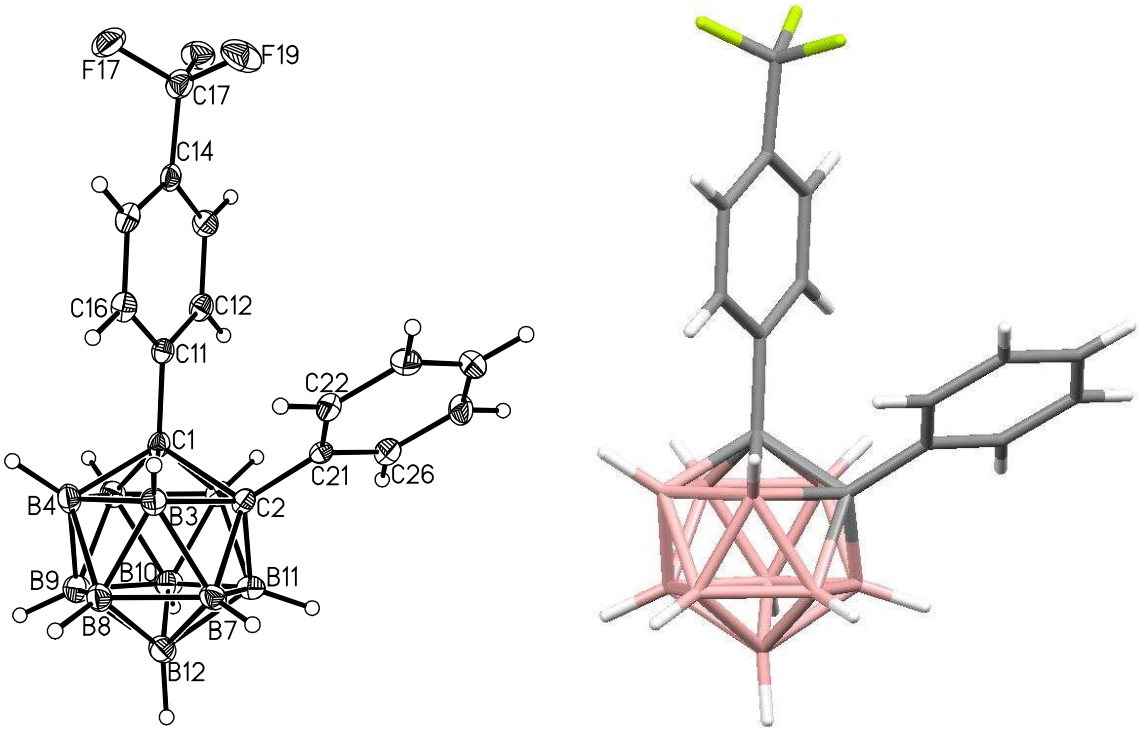

Figure 3.3.4.2 Perspective views of 1-(4'-$F_3CC_6H_4$)-2-Ph-1,2-*closo*-$C_2B_{10}H_{10}$ (9). Displacement ellipsoids are drawn at the 50% probability level except for H atoms.

In summary, four different fluorinated aryl groups (Ar_F) have been attached to monophenylcarborane leading to four new carboranes of the 1-Ar_F-2-Ph-1,2-*closo*-$C_2B_{10}H_{10}$ series.

3.3.5 Discussion.

The introduction of different fluorinated aromatic (Ar_F) groups to phenylcarborane has been accomplished. The effect of these groups towards the stabilisation of reduced carborane dianions will be discussed in terms of computational, spectroscopic and electrochemical studies of the 1-Ar_F-2-Ph-1,2-*closo*-$C_2B_{10}H_{10}$ series (compounds **6**, **7**, **8** and **9**). Since supraicosahedral (hetero)carboranes bearing phenyl groups on cage carbon atoms are known, it is appropriate to include 1,2-Ph_2-1,2-*closo*-$C_2B_{10}H_{10}$ (**G**)[16] as a reference compound for the Ar_F classification. The four different electron

withdrawing fluorinated (EWF) groups pentafluorophenyl (C_6F_5), *para*-methyltetrafluorophenyl (4-$H_3CC_6F_4$), perfluorotolyl (4-$F_3CC_6F_4$) and *para*-trifluoromethylphenyl (4-$F_3CC_6H_4$) along with the phenyl group (figure 3.3.5.1) will be compared in order to select the best candidate for polyhedral expansion purposes.

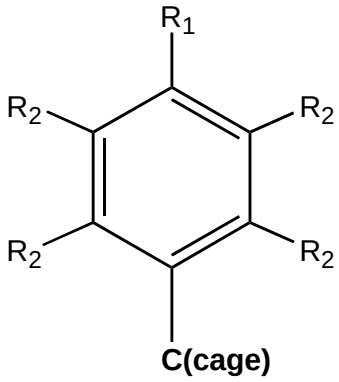

Substituents	**R_1/R_2**
pentafluorophenyl, (C_6F_5)	R_1=R_2=F
para-methyltetrafluorophenyl, (4-$H_3CC_6F_4$)	R_1=CH_3, R_2=F
perfluorotolyl, (4-$F_3CC_6F_4$)	R_1=CF_3, R_2=F
para-trifluoromethylphenyl, (4-$F_3CC_6H_4$)	R_1=CF_3, R_2=H
phenyl, (C_6H_5)	R_1=R_2=H

Figure 3.3.5.1 Summary of the four fluorinated electron withdrawing groups studied.

3.3.5.1 Computational predictions.

The stabilising effect of the selected Ar_F groups towards the oxidation of reduced carboranes can be predicted by DFT calculations. As has been described at the beginning of the chapter, the degree of stabilisation generated by the R substituents in 7,9-R_2-7,9-*nido*-C_2B_{10} dianions can be computationally quantified by the energy difference between the reduced species and their first oxidation intermediates (figure 3.3.5.1.1). In order to compare the four Ar_F substituents studied, the nido dianionic structures generated after reduction of compounds **6**, **7**, **8** and **9** and their corresponding first oxidation intermediates were computationally optimised and the predicted stabilisation energies (ΔE) calculated (figure 3.3.5.1.1).[2]

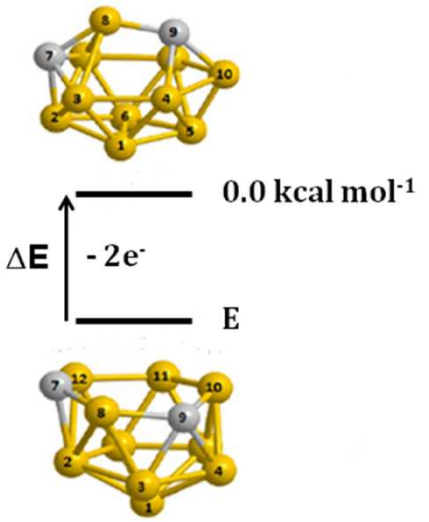

R_1 Groups	ΔE(kcal mol^{-1})
R_1= C_6F_5 (**6**)	39.4
R_1= 4-$H_3CC_6F_4$ (**7**)	35.2
R_1= 4-$F_3CC_6F_4$ (**8**)	45.5
R_1= 4-$F_3CC_6H_4$ (**9**)	40.3
R_1= C_6H_5 (**G**)	29.8

Figure 3.3.5.1.1 DFT-optimised (B3LYP/6-31G*) ΔE values between [7-R_1-9-Ph-7,9-*nido*-$C_2B_{10}H_{10}]^{2-}$ species and their first oxidation intermediates for compounds 6, 7, 8, 9 and G.

According to the calculations, the four Ar_F groups in compounds **6**-**9** are all expected to stabilise 7,9-*nido* dianions to a greater degree than a phenyl group (**G**) (figure 3.3.5.1.1). Interestingly, the nature of the group at the para postion of the aryl ring affects the predicted stabilisation effect. The electron withdrawing character of trifluoromethyl groups enhances the stabilisation energy of the substituent (compare ΔE values for compounds **9** and **G** as a pair, and **8** and **6** as a pair, figure 3.3.5.1.1) whereas the presence of an electron donating methyl group decreases that stabilisation effect (compare ΔE values for compounds **6** and **7** as a pair, figure 3.3.5.1.1). The predicted stabilisation caused by the *para*-trifluoromethylphenyl (4-$F_3CC_6H_4$) group in compound **9** is really fascinating, taking into account that this aryl substituent does not involve any aromatic fluorine atoms. Nevertheless, it can be concluded that according to DFT calculations the most stabilising substituent is the *para*-perfluorotolyl (4-$F_3CC_6F_4$) group.

3.3.5.2 Spectroscopic studies.

The inductive effect of the various Ar_F groups on carborane cages in compounds **6**-**9** can be conveniently studied by NMR spectroscopic techniques. The electron withdrawing nature of the four different groups causes a relative deshielding of the C1 nuclei and, due to electron delocalisation, of the whole cluster. ^{11}B nuclei were

selected over ^{1}H, ^{13}C and ^{19}F since spectroscopic study of the boron atoms is directly related to the electronic influence of Ar_F groups on the cage. In general, the electronic influence of the substituents attached to the cage carbon atoms is greater in the antipodal boron positions of the carborane cluster. For the 1-Ar_F-2-Ph-1,2-C_2B_{10} series (**6**, **7**, **8** and **9**), the boron atom B12, antipodal to C1, is the most influenced, although in compound **9** the observed $\delta^{11}B_{(antipod)}$ corresponds to $\delta^{11}B12$ and $\delta^{11}B9$ due to signal coincidences. Nevertheless, the overall NMR shift caused by Ar_F groups can be discussed in terms of the averaged ^{11}B chemical shift, $<\delta^{11}B>$, in order to estimate the influence of the group on the whole carborane cage. With the aim of comparing the four selected Ar_F groups, the values of $\delta^{11}B12$ and $<\delta^{11}B>$ for compounds **6**-**9**, along with those for **G**, are summarised in table 3.3.5.3.1.

	^{11}B-NMR pattern	$\delta^{11}B_{(antipod)}$	$<\delta^{11}B>$
1-(C_6F_5)-2-Ph-1,2-*closo*-$C_2B_{10}H_{10}$ (**6**)	1:1:8	0.61	-7.76
1-(4'-$H_3CC_6F_4$)-2-Ph-1,2-*closo*-$C_2B_{10}H_{10}$ (**7**)	1:1:8	0.27	-7.93
1-(4'-$F_3CC_6F_4$)-2-Ph-1,2-*closo*-$C_2B_{10}H_{10}$ (**8**)	1:1:8	1.19	-7.53
1-(4'-$F_3CC_6H_4$)-2-Ph-1,2-*closo*-$C_2B_{10}H_{10}$ (**9**)	2:2:4:2	-2.48	-8.81
1,2-Ph_2-1,2-*closo*-$C_2B_{10}H_{10}$ (**G**)	2:2:4:2	-2.65	-8.98

Table 3.3.5.2.1 Most relevant ^{11}B-NMR spectroscopic features of compounds 6, 7, 8, 9 and G. $\delta^{11}B_{(antipod)}$ refers to B12 in compounds 6-8 and to B12/B9 in compounds 9 and G. It is assumed that the least negative ^{11}B resonance is attributed to $B_{(antipod)}$ by analogy with 1,2-*closo*-$C_2B_{10}H_{12}$.[18]

The ^{11}B resonances for compounds **6**-**9** are all shifted downfield compared to **G**, due to the greater inductive effect of the electron withdrawing Ar_F groups. According to these spectroscopic studies, the influence of the group in the para position of the aromatic ring is not as important as the DFT calculations predict (figure 3.3.5.1.1). This can be illustrated with the $<\delta^{11}B>$ values for the pairs of compounds **6** and **7** and **9** and **G** (table 3.3.5.2.1). Substitution of a fluorine atom by a methyl group at the para position of the ring (**6**→**7**) decreases the influence of the Ar_F group, although only to a minor degree. Equally, the presence of a trifluoromethyl group in the phenyl ring (**G**→**9**) also does not affect much the ^{11}B chemical shift. Therefore, the greater electronic effect is not due to the nature of group at the para position of the ring but due to the presence of aromatic fluorine atoms. Substitution of hydrogen atoms by fluorine atoms in a phenyl ring (**G**→**6**) leads to a greater shift of the ^{11}B resonances and in general, fluoroaryl compounds have been found to display a positive value for

$\delta^{11}B_{(antipod)}$ and a distinctive NMR pattern of signal ratios (compare spectroscopic values for fluoroaryl compounds **6**, **7** and **8**, and non-fluoroaryl compounds **9** and **G**, table 3.3.5.2.1).

It can be concluded that the presence of aromatic fluorine atoms is more relevant in ^{11}B-NMR than the influence of the group at the para position of the ring. Nevertheless, the combination of both factors leads to the greatest deshielding effect, as has been found for the perfluorotolyl group (4-$F_3CC_6F_4$) in compound **8**, which was also the most stabilising group according to the computational studies.

3.3.5.3 Electrochemical studies.

Thus far, the direct effect of the selected Ar_F groups on nido carborane dianions has been only discussed in terms of DFT calculations. In order to investigate the effect of these groups on carborane reduction, compounds **6**-**9** were subjected to electrochemical studies. Cyclic voltammetry was selected as the most appropriate technique to study the reduction/oxidation processes of the four compounds. In theory, compounds **6**-**9** should undergo two separate one-electron reductions to afford 7,9-*nido* dianions in a reversible manner, yielding the starting material after re-oxidation. A reversible wave in the cyclic voltammogram would confirm the stability of the Ar_F groups towards reduction. In addition, the electron withdrawing character and the consequent stabilisation effect of the four Ar_F groups could be classified according to the reduction potentials of compounds **6**-**9**. The cyclic voltammograms for compounds **6**-**9** including the most relevant electrochemical data are shown in figure 3.3.5.3.1.

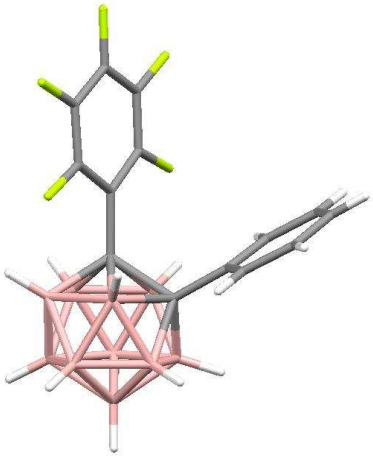	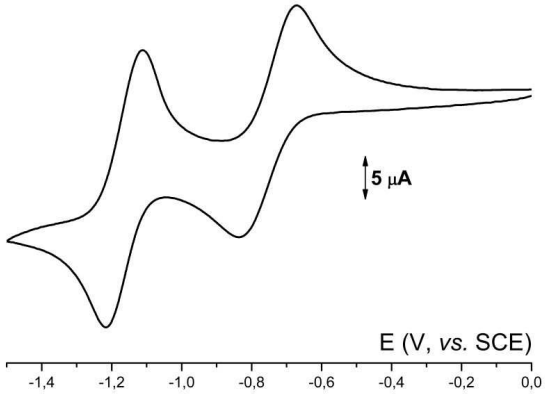		
1-C_6F_5-2-Ph-1,2-*closo*-$C_2B_{10}H_{10}$ (**6**)	$E_1°$= –0.77	$E_2°$= –1.17	$\Delta E°$= 0.40
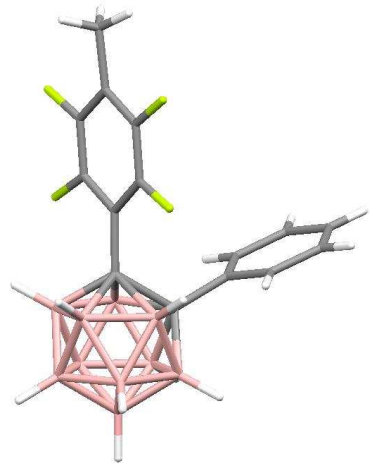	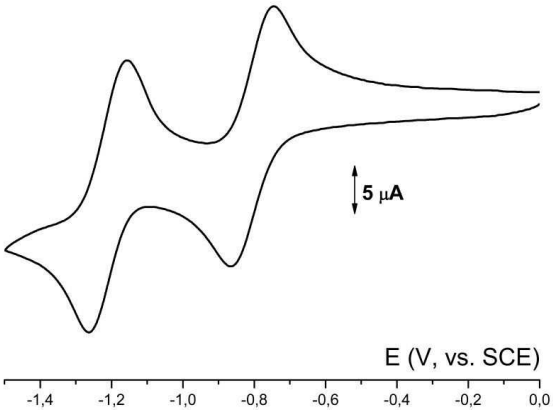		
1-(4'-$H_3CC_6F_4$)-2-Ph-1,2-*closo*-$C_2B_{10}H_{10}$ (**7**)	$E_1°$= –0.81	$E_2°$= –1.21	$\Delta E°$= 0.40
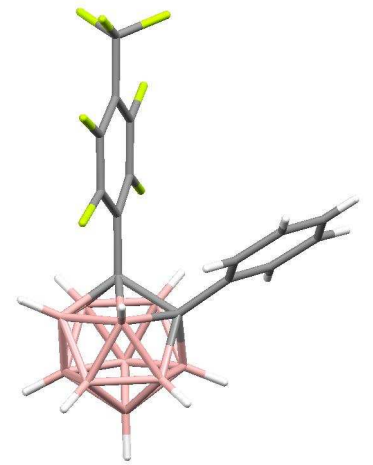	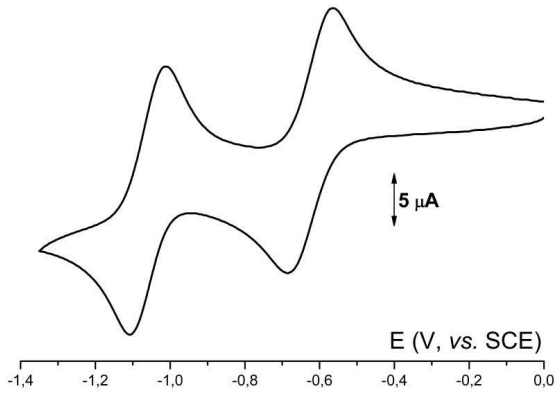		
1-(4'-$F_3CC_6F_4$)-2-Ph-1,2-*closo*-$C_2B_{10}H_{10}$ (**8**)	$E_1°$= –0.65	$E_2°$= –1.06	$\Delta E°$= 0.41

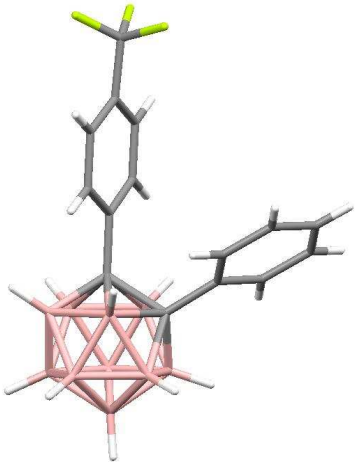	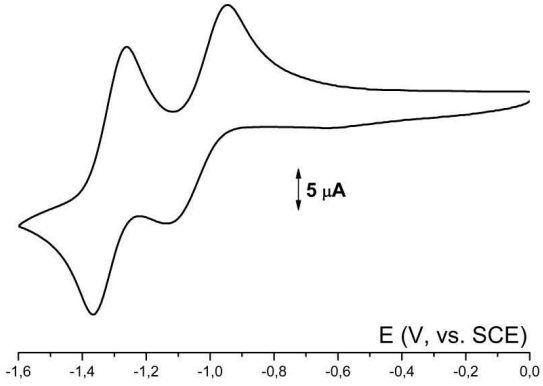		
1-(4'-$F_3CC_6H_4$)-2-Ph-1,2-*closo*-$C_2B_{10}H_{10}$ (**9**)	$E_1°$= –1.04	$E_2°$= –1.32	$\Delta E°$= 0.28

Figure 3.3.5.3.1 Cyclic voltammograms recorded at a gold electrode in THF solution of 6, 7, 8 and 9 (scan rate 0.05 Vs^{-1}), $[NBu_4][PF_6]$ supporting electrolyte (0.2 M), T = 293 K, Reduction potentials for first reduction ($E_1°$), second reduction ($E_2°$) and peak separation ($\Delta E°$).

According to the cyclic voltammograms shown in figure 3.3.5.3.1, compounds **6-9** display two sequential chemically reversible and electrochemical quasi-reversible one-electron reduction waves. The stability of Ar_F groups towards carborane reduction has been confirmed since every electrochemical reduction peak has a directly associated re-oxidation peak. In addition, the effect caused by the Ar_F groups on the reduction potentials has been demonstrated. The reduction potentials of compounds **6-9** are affected by the degree of fluorination in the aryl groups. As expected, less negative potentials are required when the electron withdrawing character of the group, or in other words, the fluorination degree, increases. The presence of aromatic fluorine atoms facilitates the reduction and, as a consequence, perfluorotolyl substituted compound **8** exhibits the least negative potentials, followed by compounds **6** and **7**. In contrast, the lack of aromatic fluorine atoms in compound **9** leads to the most negative potentials of the series.

The peak-to-peak separation ($\Delta E°$) also depends on the fluorination degree of the group. This potential separation of E_1 and E_2 gives a measure of the stability of monoanionic carborane radical anions with respect to disproportionation. The electron withdrawing nature of the four Ar_F groups determines the peak-to-peak separation values in the cyclic voltammograms of compounds **6-9** and predictably, the $\Delta E°$

values obtained for compounds **6-9** are, in the four cases, higher than those reported for **G**.[18]

3.3.5.4 Preliminary tendencies and conclusions.

All the computational, spectroscopic and electrochemical results have been compiled in the three different plots shown in figure 3.3.5.4.1, summarising the formerly mentioned tendencies. Perfluorotolyl groups in compound **8** are the most stabilising carborane substituents according to the spectroscopic and electrochemical studies (figure 3.3.5.4.1). These experimental conclusions are also in good agreement with the stabilising energy values obtained by DFT calculations, confirming compound **8** as the most appropriate precursor for polyhedral expansions.

The second best stabilising group is pentafluorophenyl, although the possibility of undesired S_NAr reactions discourages its use. Since the protection of pentafluorophenyl by transformation into *para*-methyltetrafluorophenyl groups decreases the stabilising effect, as confirmed by spectroscopic and electrochemical investigations, compounds **6** and **7** were discarded for further studies. The *para*-trifluoromethylphenyl group of compound **9** might not be as attractive as the rest, as spectroscopic and electrochemical studies revealed; however, it afforded the second best stabilisation energy (ΔE) of the series (figure 3.3.5.4.1). In addition, compound **9** is the only one that does not involve aromatic fluorine atoms and therefore could prevent undesired side reactions.

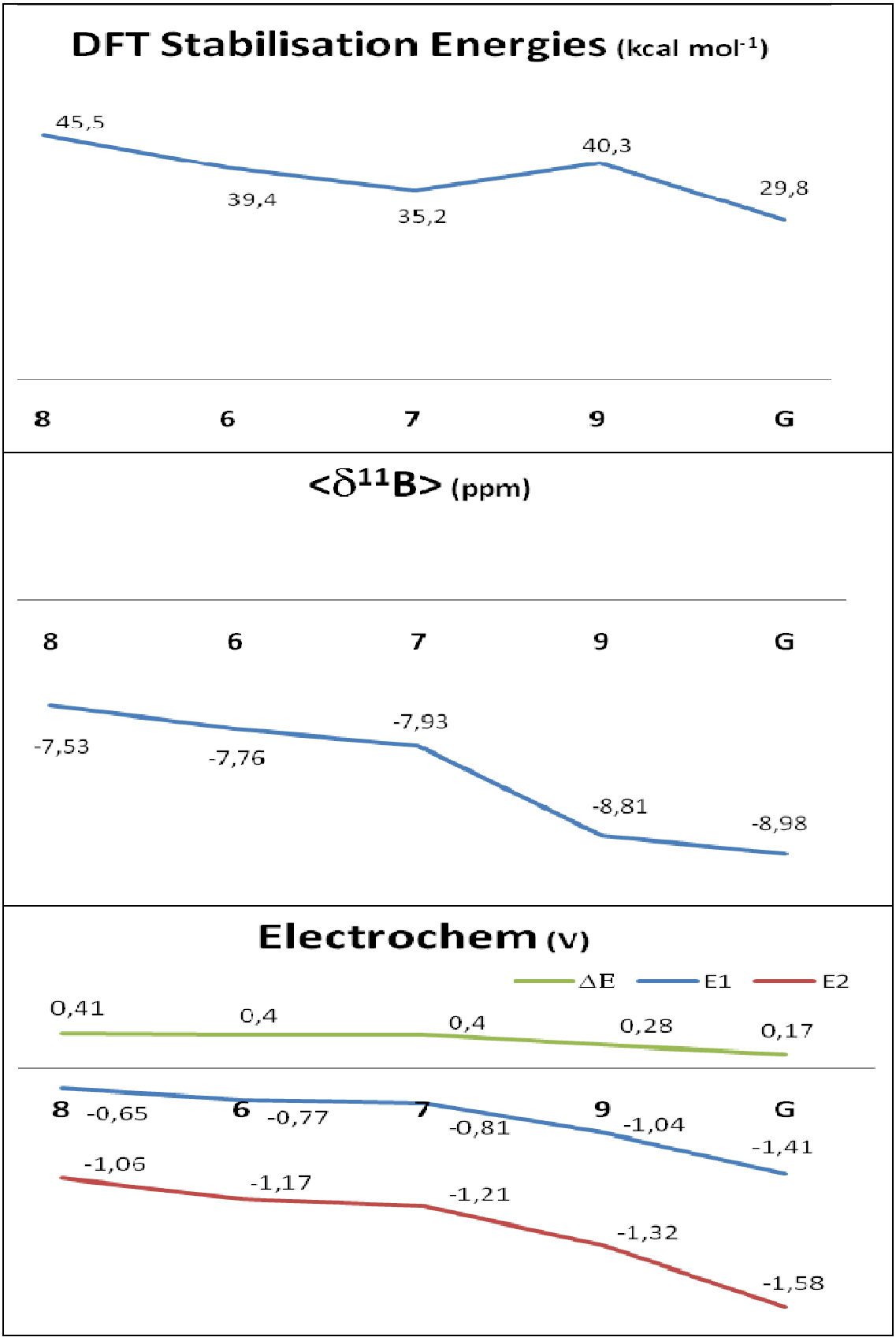

Figure 3.3.5.4.1 Computational (ΔE, kcal mol^{-1}), spectroscopic (<δ^{11}B>, ppm) and electrochemical (E^{o}_{1}, E^{o}_{2}, ΔE^{o}, V) tendencies for compounds 6, 7, 8, 9 and G according to the values reported in the former section.

Therefore, perfluorotolyl (4-$F_3CC_6F_4$) and *para*-trifluoromethylphenyl (4-$F_3CC_6H_4$) groups are proposed as the most suitable substituents for the stabilisation of reduced [7,9-*nido*-C_2B_{10}]$^{2-}$ species. Nevertheless, all these preliminary conclusions are the result of the study on 1-Ar_F-2-Ph-1,2-$C_2B_{10}H_{10}$ compounds (**6**-**9**). The electronic features of compounds **8** and **9** might be improved by their disubstituted analogues. The next section is focussed on the preparation and study of bis(perfluorotolyl) and bis(*para*-trifluoromethylphenyl) carboranes.

3.4 Disubstituted 1,2-$(Ar_F)_2$-1,2-*closo*-$C_2B_{10}H_{10}$ species.

After the study of the 1-Ar_F-2-Ph-1,2-*closo*-$C_2B_{10}H_{10}$ series (**6**-**9**), the scope of the project has been reduced to perfluorotolyl (4-$F_3CC_6F_4$) and *para*-trifluoromethylphenyl (4-$F_3CC_6H_4$) groups. The work presented in this section is focussed on the preparation of disubstituted 1,2-$(Ar_F)_2$-1,2-*closo*-$C_2B_{10}H_{10}$ and, for comparison, monosubstituted 1-Ar_F-1,2-*closo*-$C_2B_{10}H_{11}$ analogues of compounds **8** and **9**.

3.4.1 Synthesis of 1,2-(4'-$F_3CC_6F_4)_2$-1,2-*closo*-$C_2B_{10}H_{10}$ (10) and 1-(4'-$F_3CC_6F_4$)-1,2-*closo*-$C_2B_{10}H_{11}$ (11).

In order to attach two perfluorotolyl groups on an *ortho*-carborane cage, reaction of the deprotonated carborane with two equivalents of octafluorotoluene was performed leading to the synthesis and characterisation of two new compounds: 1,2-(4'-$F_3CC_6F_4)_2$-1,2-*closo*-$C_2B_{10}H_{10}$ (**10**) and 1-(4'-$F_3CC_6F_4$)-1,2-*closo*-$C_2B_{10}H_{11}$ (**11**) (figure 3.4.1.1).

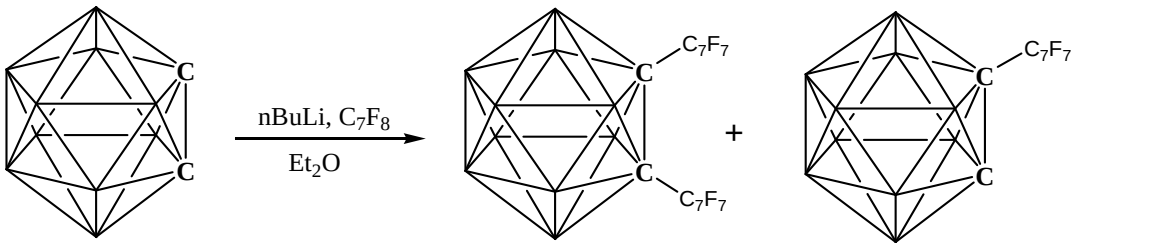

1,2-*closo*-$C_2B_{10}H_{12}$ 1,2-(4'-$F_3CC_6F_4)_2$-1,2-*closo*-$C_2B_{10}H_{10}$ (**10**) 1-(4'-$F_3CC_6F_4$)-1,2-*closo*-$C_2B_{10}H_{11}$ (**11**)

Figure 3.4.1.1 Synthesis of 1,2-(4'-$F_3CC_6F_4)_2$-1,2-*closo*-$C_2B_{10}H_{10}$ (10) and 1-(4'-$F_3CC_6F_4$)-1,2-*closo*-$C_2B_{10}H_{11}$ (11).

Although many attempts under different conditions were performed, bis(perfluorotolyl) compound **10** was always isolated in lower yields than 40%. Surprisingly, the monosubstituted analogue **11** was always isolated from the synthesis of **10** but only in trace amounts, although it can be deliberately prepared in almost 70% yield using only one equivalent of BuLi and C_7F_8. Chromatographic techniques

were necessary to separate the mono- and di-substituted compounds that were isolated as colourless oils that crystallised at room temperature after a few hours.

The purity and identity of compounds **10** and **11** were first confirmed by mass spectrometry and elemental analysis. Compounds **10** and **11** were also characterised by multinuclear NMR spectroscopy. Whereas ^{19}F-NMR spectra of both compounds were not conclusive, displaying in both cases three peaks corresponding to the perfluorotolyl groups, ^{1}H- and ^{11}B-NMR spectroscopies proved the identities of **10** and **11**. The most relevant data were the presence of the acidic $C_{(cage)}$-H signal at δ 4.87 in the ^{1}H-NMR spectrum of **11** and the difference in the signal ratio patterns in their ^{11}B-NMR spectra, 2:4:4 for **10** and 1:1:2:2:2:2 for **11**, which is in good agreement with the cage symmetries of both compounds.

Although the identity of compounds **10** and **11** had been confirmed by spectroscopic studies, the solid state molecular structure of **10** is interesting for further studies and comparisons. Therefore, a single crystal was grown by slow evaporation of a concentrated solution of **10** in hexane and *X*-ray diffraction studies were performed on the crystal in order to obtain the molecular structure (figure 3.4.1.2).

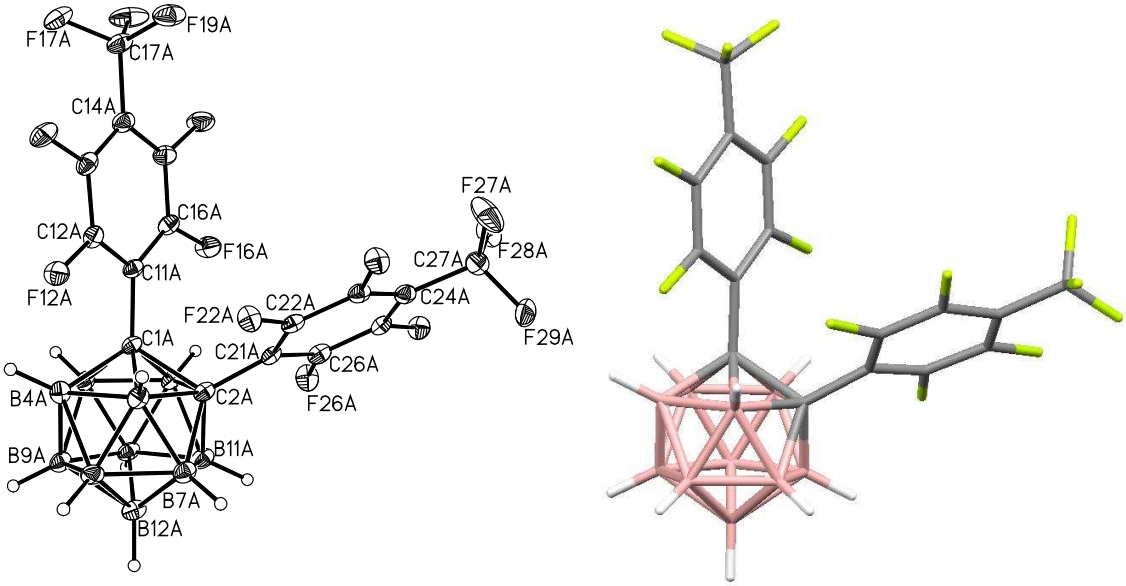

Figure 3.4.1.2 Perspective views of 1,2-(4'-$F_3CC_6F_4)_2$-1,2-*closo*-$C_2B_{10}H_{10}$ (10) (one of the two crystallographic independent molecules). Displacement ellipsoids are drawn at the 50% probability level except for H atoms.

3.4.2 Synthesis of 1-(4'-$F_3CC_6H_4$)-1,2-*closo*-$C_2B_{10}H_{11}$ (12) and 1,2-(4'-$F_3CC_6H_4)_2$-1,2-*closo*-$C_2B_{10}H_{10}$ (13).

The double introduction of *para*-trifluoromethylphenyl groups into *ortho*-carborane appeared to be more complicated than the attachment of the perfluorotolyl units. The first approach considered involved the coupling of C,C'-dicopper *ortho*-carborane with 4-iodobenzotrifluoride, mediated by pyridine. This Ullmann type coupling of carboranes with aryl halides is generally limited to monosubstitution in the case of 1,2-C_2B_{10} species. Nevertheless, the copper (I) mediated coupling of *ortho*-carborane with 4-iodobenzotrifluoride had never been reported before, thus it was attempted in order to obtain disubstituted species. Unfortunately this reaction afforded 1-(4'-$F_3CC_6H_4$)-1,2-*closo*-$C_2B_{10}H_{11}$ (**12**) as the single product of the reaction (figure 3.4.2.1).

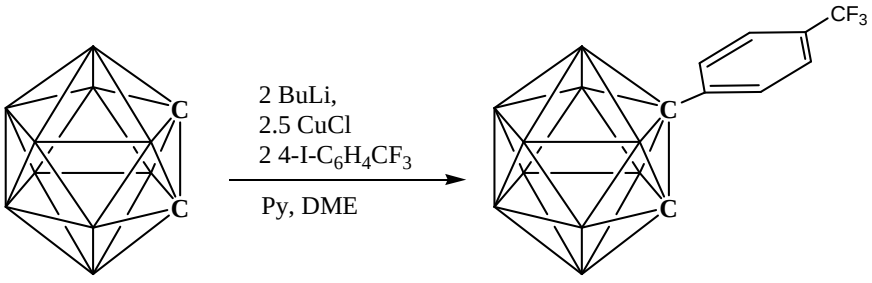

Figure 3.4.2.1 Synthesis of 1-(4'-$F_3CC_6H_4$)-1,2-*closo*-$C_2B_{10}H_{11}$ (12) by carborane-aryl copper coupling. (N.B. naked vertex = BH, C vertex = CH).

Although **12** was not the desired compound, it was isolated in 65% yield and fully characterised by mass spectrometry, by ^{1}H, ^{11}B and ^{19}F-NMR spectroscopies and by elemental analysis. The molecular ion at m/z 288 was present in the mass spectrum and the elemental results were concordant with the expected values. The ^{1}H-NMR spectrum indicated the presence of four aromatic hydrogen atoms and more interestingly, the presence of the $C_{(cage)}$-H signal at δ 3.97. This resonance is shifted to higher frequencies compared to the typical $C_{(cage)}$-H resonance observed at δ 3.58 for 1-Me-1,2-*closo*-$C_2B_{10}H_{11}$, due to the electron withdrawing effect of the substituent attached to C1. The ^{11}B-NMR spectrum showed pattern of signals typical for a monosubstituted aryl carborane and ^{19}F-NMR spectroscopy confirmed the presence of

the CF_3 group showing a single peak at δ −63.1. All the analytical data confirmed the structure of monosubstituted compound **12** and one single crystal of the white solid obtained was subjected to *X*-ray diffraction to reveal the solid state molecular structure, shown in figure 3.4.2.2.

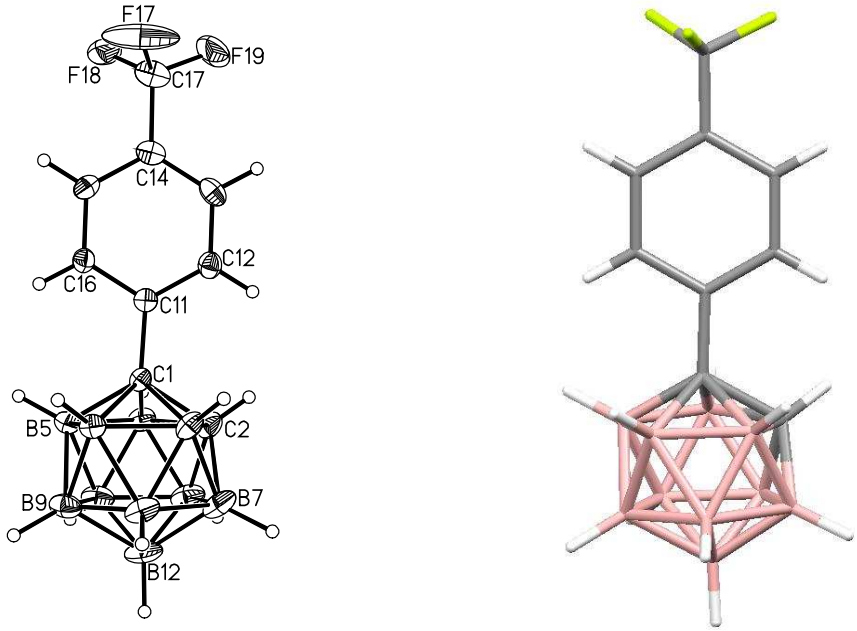

Figure 3.4.2.2 Perspective views of 1-(4'-$F_3CC_6H_4$)-1,2-*closo*-$C_2B_{10}H_{11}$ (12). Displacement ellipsoids are drawn at the 50% probability level except for H atoms.

After the failure of copper coupling procedures to prepare bis(*para*-trifluoromethylphenyl) *ortho*-carboranes, alkyne insertion into decaborane was considered. Bis(*para*-trifluoromethylphenyl)acetylene[19] (**H**) was prepared by two sequential Sonogashira couplings between 4-iodobenzotrifluoride and trimethylsilylacetylene, and reacted with decaborane in presence of Lewis base to afford 1,2-(4'-$F_3CC_6H_4)_2$-1,2-*closo*-$C_2B_{10}H_{10}$ (**13**) (figure 3.4.2.3).

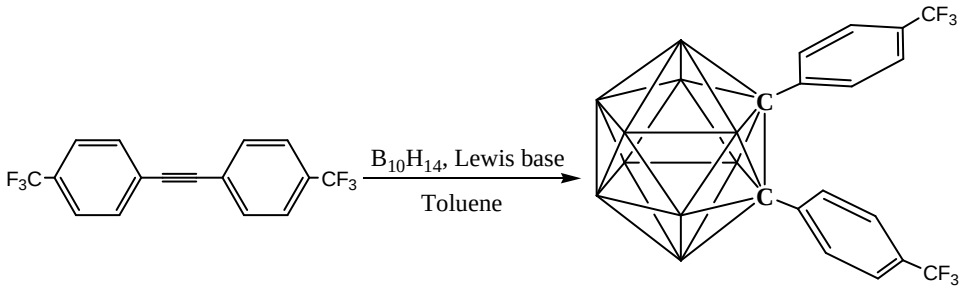

bis-*para*-trifluoromethylphenylacetylene (**H**) 1,2-(4'-$F_3CC_6H_4)_2$-1,2-*closo*-$C_2B_{10}H_{10}$ (**13**)

Figure 3.4.2.3 Synthesis of 1,2-(4'-$F_3CC_6H_4)_2$-1,2-*closo*-$C_2B_{10}H_{10}$ (13) by insertion of H into decaborane.

Although four steps were necessary, the synthesis of C,C'- bis(*para*-trifluoromethylphenyl) *ortho*-carborane was accomplished. The four reactions (first Sonogashira coupling, deprotection of trimethylsilyl group, second Sonogashira coupling and insertion into decaborane) were performed in moderate to good yields. However, due to the number of steps involved, the overall yield for the preparation of **13** was lower than 30%. Mass spectrometric analysis of the white powder obtained after chromatographic purification indicated the presence of the molecular ion of **13** at m/z 432 and the purity of this compound was confirmed by elemental analysis. Compound **13** was also characterised by multinuclear NMR spectroscopy. Only aromatic hydrogen atoms were observed in the ^{1}H-NMR spectrum of **13**, whilst ^{11}B-NMR spectroscopy revealed the presence of a symmetric structure whose spectrum resembled that of diphenyl *ortho*-carborane (**G**), although the resonances were slightly shifted downfield. The ^{19}F-NMR spectrum of **13** indicated only one signal due to the presence of CF_3 groups as the only source of fluorine atoms in the molecule. The molecular structure of **13** was ultimately confirmed by single crystal *X*-ray diffraction and it is shown in figure 3.4.2.4.

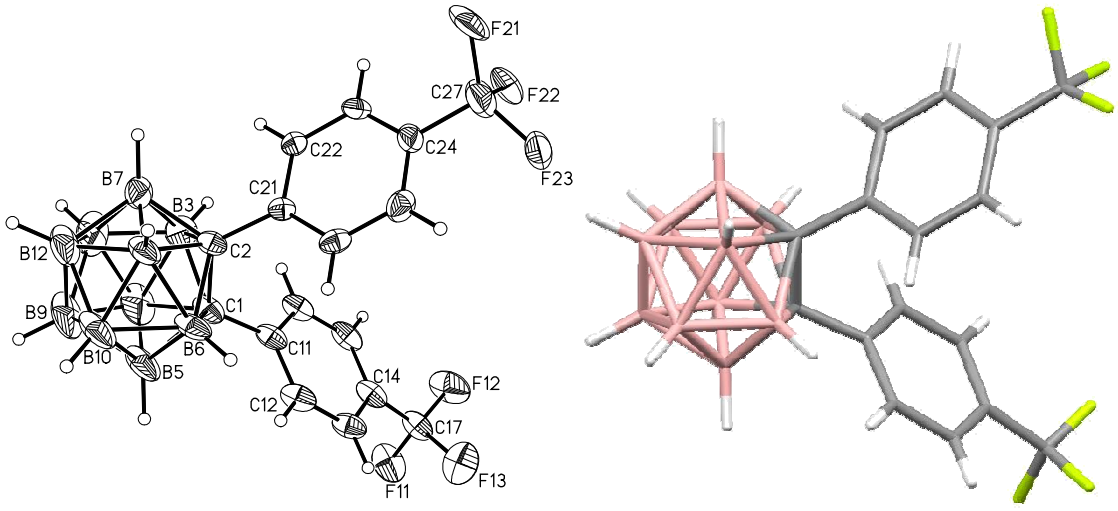

Figure 3.4.2.4 Perspective views of 1,2-(4'-$F_3CC_6H_4)_2$-1,2-*closo*-$C_2B_{10}H_{10}$ (13). Displacement ellipsoids are drawn at the 50% probability level except for H atoms.

With the synthesis and characterisation of **13**, the preparation of C,C'-disubstituted bis(perfluorotolyl) and bis(*para*-trifluoromethylphenyl) ortho carboranes was accomplished. Compounds **10** and **13** are expected to be more convenient candidates

for polyhedral expansion procedures than their phenylated analogues **8** and **9** due to the cumulative effect of both Ar_F groups in these disubstituted compounds.

3.4.3 Discussion.

The preparation of C,C'-disubstituted perfluorotolyl (4-$F_3CC_6F_4$) and *para*-trifluoromethylphenyl (4-$F_3CC_6H_4$) ortho carboranes has been described. The effect of these groups on the stabilisation of reduced carborane dianions will be discussed in terms of computational, spectroscopic and electrochemical studies of the 1,2-$(Ar_F)_2$-1,2-*closo*-$C_2B_{10}H_{10}$ compounds (**10** and **13**). Since there are two different Ar_F groups to be compared, it is appropriate to include in the discussion their phenylated analogues (**8** and **9**) in order to evaluate the effect of the double substitution.

3.4.3.1 Computational predictions.

As has been described for the phenyl series (**6**-**9**), the degree of stabilisation provided by the R substituents in 7,9-R_2-7,9-*nido*-C_2B_{10} dianions can be predicted from the energy difference between the reduced species and their first oxidation intermediates (figure 3.4.3.1.1). In order to evaluate the effect of double substitution with perfluorotolyl and *para*-trifluoromethylphenyl groups in carborane, the nido dianionic structures generated after reduction of compounds **8**, **9**, **10** and **13** and their first oxidation intermediates were optimised and the predicted stabilisation energies (ΔE) calculated (figure 3.4.3.1.1).[2]

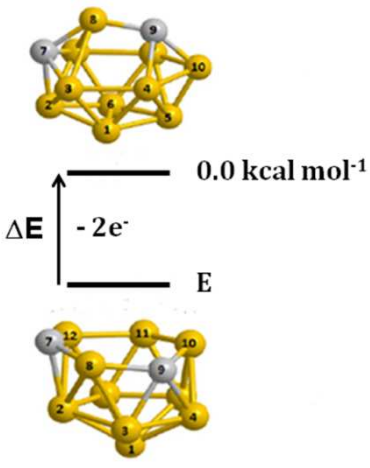

R Groups	ΔE(kcal mol^{-1})
R_1= 4-$F_3CC_6F_4$, R_2= Ph (**8**)	45.5
R_1= 4-$F_3CC_6H_4$, R_2= Ph (**9**)	40.3
R_1= R_2= 4-$F_3CC_6F_4$ (**10**)	60.8
R_1= R_2= 4-$F_3CC_6H_4$ (**13**)	50.1

Figure 3.4.3.1.1 DFT-optimised (B3LYP/6-31G*) ΔE values between [7-R_1-9-R_2-7,9-*nido*-$C_2B_{10}H_{10}$]$^{2-}$ species and their first oxidation intermediates for compounds 8, 9, 10 and 13.

According to the computational study, 7,9-*nido* dianions of disubstituted compounds **10** and **13** are expected to be stabilised towards re-oxidation to a greater extent than their phenylated analogues (figure 3.4.3.1.1). The predicted improvement on the stabilisation energy is higher for perfluorotolyl groups than for *para*-trifluoromethylphenyl substituents thus bis(perfluorotolyl) carborane **10** appears to be the best candidate for polyhedral expansion.

3.4.3.2 Spectroscopic studies.

Double C,C'-substitution with strong electron withdrawing Ar_F groups increases the nuclear deshielding of the two directly bonded cage carbon atoms and consequently shifts the magnetic resonances of the whole cluster. This electronic influence can be investigated by ^{11}B-NMR spectroscopy, as has been discussed in section 3.3.5.2. The inductive effect of the selected Ar_F groups in compounds **10** and **13** can be conveniently monitored by the ^{11}B-NMR chemical shift of the most influenced antipodal vertices $\delta^{11}B_{(antipod)}$ and the averaged ^{11}B chemical shift $<\delta^{11}B>$ to estimate the overall electronic influence of the two groups on the carborane cages.

Another spectroscopic approach to compare the inductive effect of perfluorotolyl and *para*-trifluoromethylphenyl groups in *ortho*-carborane cages lies in the ^{1}H-NMR chemical shift of the hydrogen atom directly bonded to C2 cage carbon atom, $\delta\,^1H_{C(cage)}$ for the monosubstituted compounds **11** and **12**. In order to evaluate the inductive effect caused by the cumulative addition of perfluorotolyl and *para*-trifluoromethylphenyl groups, the values of $\delta^1H_{C(cage)}$, $\delta^{11}B_{(antipod)}$ and $<\delta^{11}B>$ for compounds **8**, **9**, **10**, **11**, **12** and **13** are summarised in table 3.4.3.3.1.

	^{11}B pattern	$\delta^{11}B_{(antipod)}$	$<\delta^{11}B>$	$\delta^{1}H_{C(cage)}$
1-(4'-$F_3CC_6F_4$)-1,2-*closo*-$C_2B_{10}H_{11}$ (**11**)	1:1:2:2:2:2	-0.60	-8.81	4.87
1-(4'-$F_3CC_6H_4$)-1,2-*closo*-$C_2B_{10}H_{11}$ (**12**)	1:1:2:2:2:2	-2.03	-9.92	3.97
1-(4'-$F_3CC_6F_4$)-2-Ph-1,2-*closo*-$C_2B_{10}H_{10}$ (**8**)	1:1:8	1.19	-7.53	
1-(4'-$F_3CC_6H_4$)-2-Ph-1,2-*closo*-$C_2B_{10}H_{10}$ (**9**)	2:2:4:2	-2.48	-8.81	
1,2-(4'-$F_3CC_6F_4)_2$-1,2-*closo*-$C_2B_{10}H_{10}$ (**10**)	2:4:4	0.39	-6.34	
1,2-(4'-$F_3CC_6H_4)_2$-1,2-*closo*-$C_2B_{10}H_{10}$ (**13**)	2:2:4:2	-1.93	-8.54	

Table 3.4.3.3.1 Most relevant NMR spectroscopic features of compounds 8, 9, 10, 11, 12 and 13. $\delta^{11}B_{(antipod)}$ refers to B12 in compounds 8, 11 and 12 and to B12/B9 in compounds 9, 10 and 13. It is assumed that the least negative ^{11}B resonance is attributed to $B_{(antipod)}$ by analogy with 1,2-*closo*-$C_2B_{10}H_{12}$.

Examination of the spectroscopic data in table 3.4.3.3.1 reveals some interesting information. It can be concluded that the presence of perfluorotolyl groups affects the NMR signals of carborane cages to a much greater degree than *para*-trifluoromethylphenyl substituents, since the remaining proton attached to the cage carbon atom in compound **11** becomes much more acidic than the $C_{(cage)}$-H proton of **12**. In addition, in all cases perfluorotolyl substituted carboranes result in higher values of $\delta^{11}B_{(antipod)}$ and $<\delta^{11}B>$ than their *para*-trifluoromethylphenyl substituted analogues. Since both spectroscopic parameters are related, it was expected that the same compound would present the highest value of $\delta B_{(antipod)}$ and the least negative $<\delta^{11}B>$. However, due to the symmetry differences between mono and disubstituted species, compound **8** presents the most positive ^{11}B chemical shift at the boron vertex antipodal to C1, whereas disubstituted compound **10** presents the highest averaged ^{11}B chemical shift.

3.4.3.3 Electrochemical studies.

The effect of Ar_F groups towards the reduction of disubstituted compounds **10** and **13** was also analysed by electrochemical studies. Cyclic voltammograms were recorded to reveal the two sequential and reversible one-electron reductions of compounds **10** and **13**, as figure 3.4.3.3.1 shows.

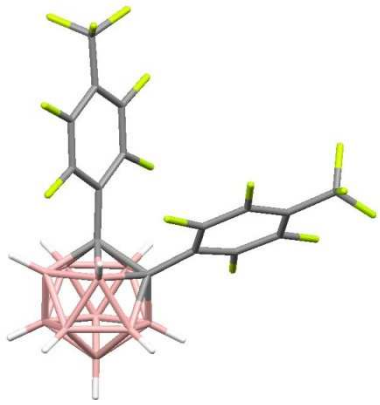	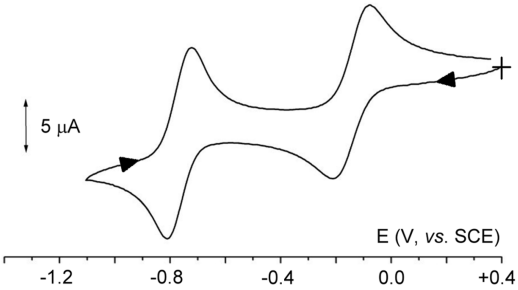		
1,2-(4'-$F_3CC_6F_4)_2$-1,2-*closo*-$C_2B_{10}H_{10}$ (**10**)	$E_1°$= –0.15	$E_2°$= –0.76	$\Delta E°$= 0.61
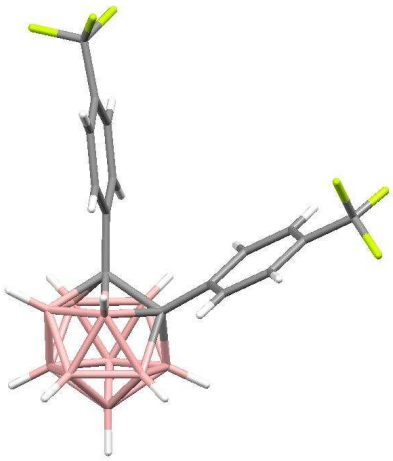	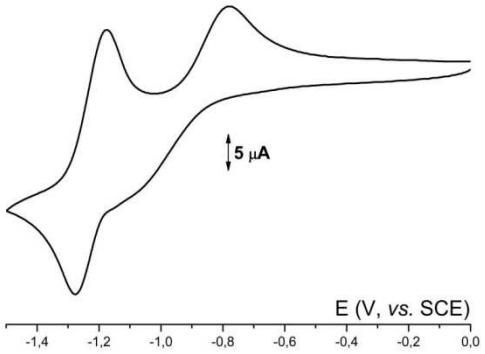		
1,2-(4'-$F_3CC_6H_4)_2$-1,2-*closo*-$C_2B_{10}H_{10}$ (**13**)	$E_1°$= –0.97	$E_2°$= –1.23	$\Delta E°$= 0.26

Figure 3.4.3.3.1 Cyclic voltammograms recorded at a gold electrode in THF solution of 10 and 13 (scan rate 0.05 Vs^{-1}), $[NBu_4][PF_6]$ supporting electrolyte (0.2 M), T = 293 K, Reduction potentials for first reduction ($E_1°$), second reduction ($E_2°$) and peak separation ($\Delta E°$).

Double substitution with Ar_F groups shifts the reduction potentials to even less negative values, facilitating the two-electron reduction and stabilising the resulting 7,9-*nido* dianion. This can be illustrated by comparison of the potential values of compounds **8** and **9** (figure 3.3.5.3.1) with those of their disubstituted analogues **10** and **13** (figure 3.4.3.3.1). Although in both cases the double substitution has a positive effect in the reduction potentials, the greater electron withdrawing effect of perfluorotolyl over *para*-trifluoromethylphenyl groups is clear from the electrochemical results. In fact, the reduction potentials of phenylated compound **8** are less negative than those of disubstituted compound **13**, thus a greater stability of the reduced dianion of **8** over that of **13** is expected.

Interestingly, the peak-to-peak separation (ΔE°) increases as the reduction potentials are shifted to less negative values, thus the most positive values together with the greatest peak-to-peak separation are exhibited for compound **10**, confirming the predicted stability of radical monoanionic species derived from perfluorotolyl carboranes. For all the abovementioned reasons, bis(perfluorotolyl) compound **10** is expected to be the best precursor of stabilised reduced dianions.

3.4.3.4 General tendencies and conclusions.

From the studies on the phenyl series (**6**-**9**) discussed in section 3.3, perfluorotolyl and para-trifluoromethylphenyl groups were selected as the most appropriate stabilising substituents for 7,9-*nido* dianions. In this section, the C,C'-disubstituted *ortho*-carboranes **10** and **13** have been studied by the same computational, spectroscopic and electrochemical means. In addition, compounds **6**, **7**, **8**, **9**, **10** and **13** were structurally characterised by single crystal *X*-ray diffraction studies. In contrast to other reported aryl-substituted carboranes,[20] only one molecule was found in the asymmetric fraction of the unit cell for all cases except for **7** and **10**, whose asymmetric units contained two independent molecules. All the molecular structures of the studied compounds resemble that of diphenylcarborane (**G**), in which both phenyl rings are orientated roughly perpendicular to the symmetry plane that contains C1, C2, B9 and B19 cage vertices.

This preferred orientation is believed to minimise the steric hindrance between aryl groups.[12] The aryl groups orientation is important because the $C1_{(cage)}$-$C2_{(cage)}$ distance is sensitive to it.[21] Generally, the C1-C2 bond length is longest when the aromatic rings are orientated totally perpendicular to the plane of symmetry containing $C_{(cage)}$ atoms in *ortho*-carborane cages. In addition, the length of C1-C2 bonds in aryl-substituted 1,2-*closo* carboranes also depends on the electronic character of the substituents. In general, strongly electron donating groups bonded to the cage carbon atoms tend to increase C1-C2 bond lengths,[19a,22] although the structural variations in response to aryl substituents are small compared to the changes when atoms different to carbon are directly bonded to the cage carbon atoms.

The Ar_F groups of compounds **6**, **7**, **8**, **9**, **10** and **13** are expected to have strong electron withdrawing character, however, the C1-C2 bond lengths of these compounds appear to be insensitive to both the orientation and the electronic effect of the substituents being 1.727 Å as average, which is comparable to the 1.733(4) and 1.720(4) Å distances reported for 1,2-Ph_2-1,2-*closo*-$C_2B_{10}H_{10}$ (**G**).[16] The C1-C2 bond lengths for compounds **6**, **7**, **8**, **9**, **10** and **13** are summarised in table 3.4.3.4.1.

Compound	**C1-C2 (Å)**
R=C_6F_5, R'= Ph (**6**)	1.748(3)
R=4-$H_3CC_6F_4$, R'= Ph (**7**)	
7A	1.746(3)
7B	1.738(3)
R=4-$F_3CC_6F_4$, R'= Ph (**8**)	1.721(4)
R=4-$F_3CC_6H_4$, R'= Ph (**9**)	1.715(3)
R=R'=4-$F_3CC_6F_4$ (**10**)	
10A	1.713(6)
10B	1.723(6)
R=R'=4-$F_3CC_6H_4$ (**13**)	1.713(5)

Table 3.4.3.4.1 Interatomic C1-C2 distances in the molecular structures of compounds 6, 7, 8, 9, 10 and 13. Two different rows are shown for the two independent molecules of 7 and 10.

In conclusion, the presence of fluorinated aryl groups attached to the cage carbon atoms in ortho carboranes does not have any significant effect on the icosahedral structure (for detailed information about interatomic distances and angles of all the structures see appendix 2). Since there are no structural distortions found for the compounds described, all the properties and trends revealed by computational, spectroscopic and electrochemical studies are solely due to the electronic inductive effect of the Ar_F groups.

It has been found that all the properties of phenylated compounds **8** and **9** which are important in the stabilisation of reduced forms are enhanced by their disubstituted analogues **10** and **13**. However, the supremacy of perfluorotolyl substituted carboranes (**8** and **10**) over *para*-trifluoromethylphenyl compounds (**9** and **13**) has

also been demonstrated. Following these extensive studies on fluoroaryl carboranes, the six C,C'-disubstituted carboranes (**6**, **7**, **8**, **9**, **10** and **13**) can be ranked revealing that the predicted stabilisation of the respective 7,9-*nido* dianions depends on the fluorination degree of their aryl substituents. Therefore, the six compounds can be classified in decreasing stabilisation order as **10** > **8** > **6** > **7** > **13** > **9**, according to the general trends obtained from the computational, spectroscopic and electrochemical results (figure 3.4.3.4.1).

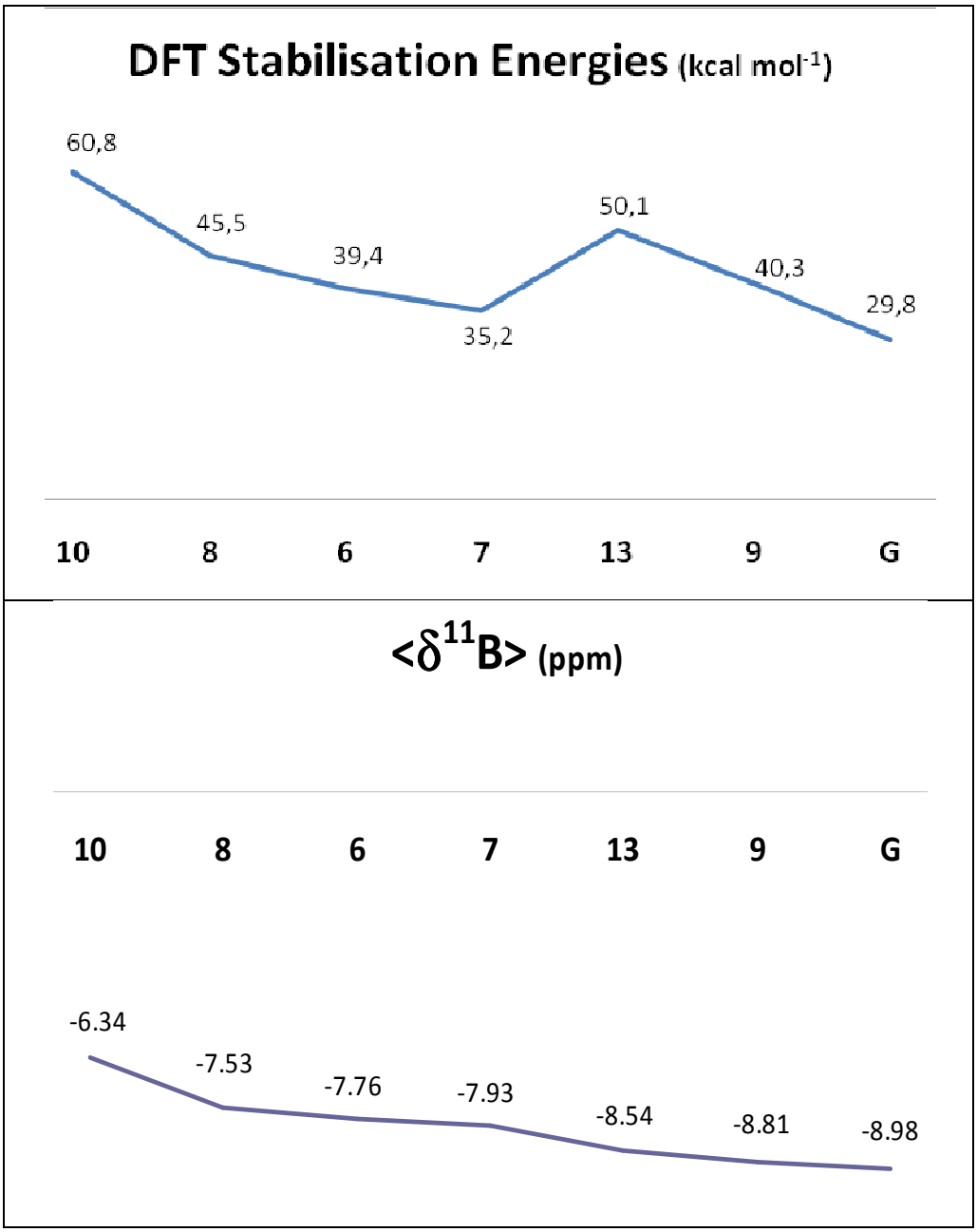

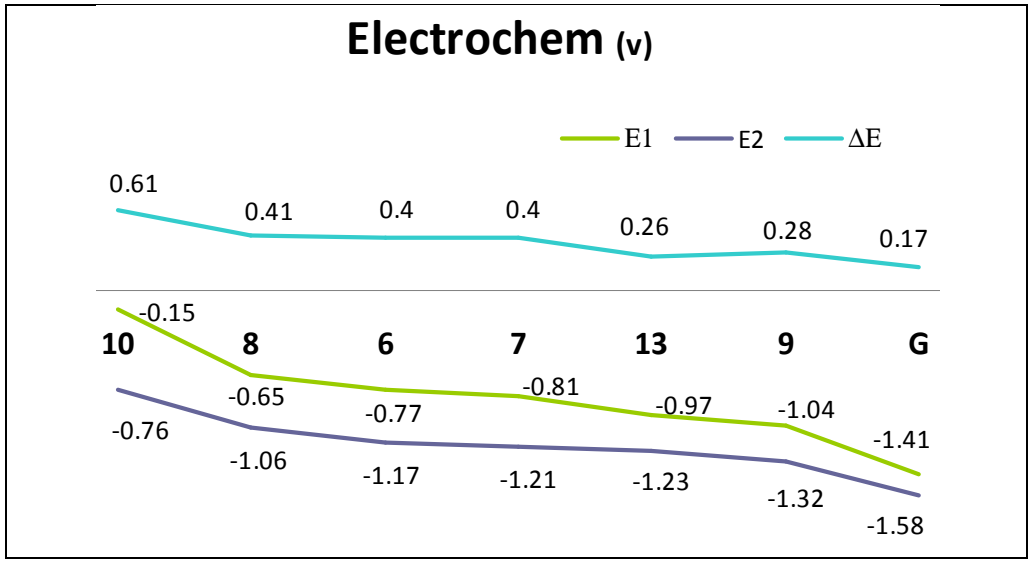

Figure 3.4.3.4.1 Computational (ΔE, kcal mol^{-1}), spectroscopic (<δ^{11}B>, ppm) and electrochemical (E^{o}_{1}, E^{o}_{2}, ΔE^{o}, v) tendencies for compounds 6, 7, 8, 9, 10, 13 and G.

The classification described (**10** > **8** > **6** > **7** > **13** > **9**) is in perfect agreement with the spectroscopic and the electrochemical studies. In fact, the cyclic voltammograms for the six compounds can be displayed on the same figure to confirm that trend (figure 3.4.3.4.2).

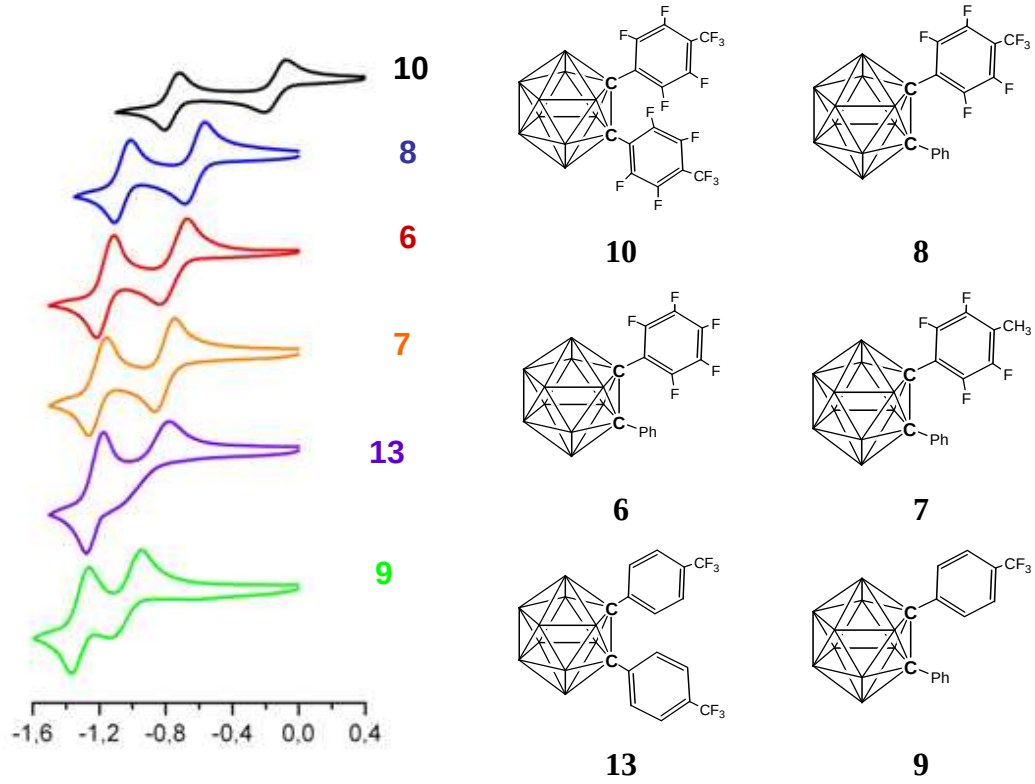

Figure 3.4.3.4.2 Electrochemical classification of compounds 6, 7, 8, 9, 10 and 13 [E (V vs. SCE)]. Reduction potentials recorded at a gold electrode in THF solution (scan rate 0.05 Vs^{-1}). [NBu_4][PF_6] supporting electrolyte (0.2 M). T = 293 K.

On the other hand, the DFT predicted stabilisation energies for 7,9-*nido* dianions appear to follow two different trends depending on the presence of aromatic fluorine atoms in the aryl group. Bis(perfluorotolyl) compound **10** presents the highest stabilisation energy of the entire series, followed by **13**, which is the first member of the second trend (figure 3.4.3.4.1).

In conclusion, perfluorotolyl (4-$F_3CC_6F_4$) groups are selected as the most appropriate groups to stabilise reduced carborane dianions. As a result, only compounds **8** and **10** are selected for polyhedral expansion experiments. Compound **10** is expected to be the most suitable precursor of stabilised 7,9-*nido* dianions in the whole series (**6**-**13**) (figures 3.4.3.5.1 and 3.4.3.5.2), although it has an important disadvantage: **10** can be only prepared in low yield. On the other hand, in spite of the slightly lower stabilisation effect, compound **8**, the second best in the classification, can be prepared in excellent yield from the readily available monophenylcarborane.

3.5 *ortho*-, *meta*- and *para*-Bis(perfluorotolyl) carboranes.

Perfluorotolyl groups have been selected as the most stabilising substituents for reduced carborane dianions. In addition, C,C'-disubstitution has been found to enhance the electron withdrawing effect and, as a result, 1,2-(4'-$F_3CC_6F_4)_2$-1,2-*closo*-$C_2B_{10}H_{10}$ (**10**) is the most appropiate candidate for polyhedral expansions. In order to investigate the effect of perfluorotolyl substituents towards reduction of icosahedral carboranes, the three isomeric *ortho*-, *meta*- and *para*-bis(perfluorotolyl) carboranes were prepared. Furthermore, it would be interesting to compare the well established reduction chemistry of the three icosahedral $C_2B_{10}H_{12}$ species with their perfluorotolyl analogues.

3.5.1 Synthesis of 1,7-(4'-$F_3CC_6F_4)_2$-*closo*-1,7-$C_2B_{10}H_{10}$ (14) and 1,12-(4'-$F_3CC_6F_4)_2$-*closo*-1,12-$C_2B_{10}H_{10}$ (15).

Since reduction of ortho and meta carboranes affords the same 7,9-*nido* dianion, a different approach to obtain [7,9-(4'-$F_3CC_6F_4)_2$-7,9-*nido*-$C_2B_{10}H_{10}]^{2-}$ for polyhedral expansions might start with the synthesis of the meta analogue of **10**. This synthesis is expected to afford better yields due to the lower steric hindrance between perfluorotolyl groups. Following the same procedure employed in the synthesis of **10**, 1,7-*closo*-$C_2B_{10}H_{12}$ was deprotonated with two equivalents of BuLi and treated with perfluorotoluene (C_7F_8) to afford 1,7-(4'-$F_3CC_6F_4)_2$-*closo*-1,7-$C_2B_{10}H_{10}$ (**14**) in 82% yield after aqueous work up (figure 3.5.1.1).

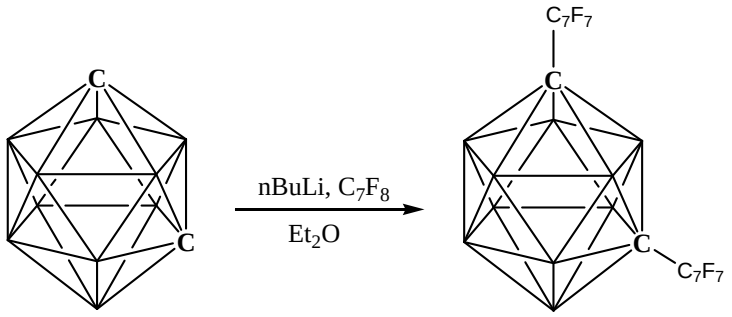

1,7-*closo*-$C_2B_{10}H_{12}$ 1,7-(4'-$F_3CC_6F_4)_2$-1,7-*closo*-$C_2B_{10}H_{10}$ (**14**)

Figure 3.5.1.1 Synthesis of 1,7-(4'-$F_3CC_6F_4)_2$-*closo*-1,7-$C_2B_{10}H_{10}$ (14) by reaction of deprotonated *meta*-carborane with perfluorotoluene. (N.B. naked vertex = BH, C vertex = CH).

Compound **14** was isolated as a colourless oil that slowly crystallised at room temperature after a few days to afford a white solid. As was expected, the preparation of **14** occurred in higher yield than that for the ortho analogue (**10**). The identity and purity of compound **14** was first confirmed by mass spectrometry and elemental analysis. The structure of the meta analogue of **10** was established by multinuclear NMR spectroscopy. Whilst the ^{19}F-NMR spectrum of **14** indicated the presence of perfluorotolyl groups, the ^{11}B-NMR spectrum confirmed the nuclear deshielding effect of the electron withdrawing substituents on the *meta*-carborane cage. Interestingly, the B5 and B12 antipodal vertices in **14** appear to be less influenced by the Ar_F groups than B9 and B12 in **10**, according to $\delta^{11}B_{(antipod)}$ values (table 3.5.1.1). The molecular structure of **14** was ultimately revealed by *X*-ray diffraction study of a block crystal and is shown in figure 3.5.1.2.

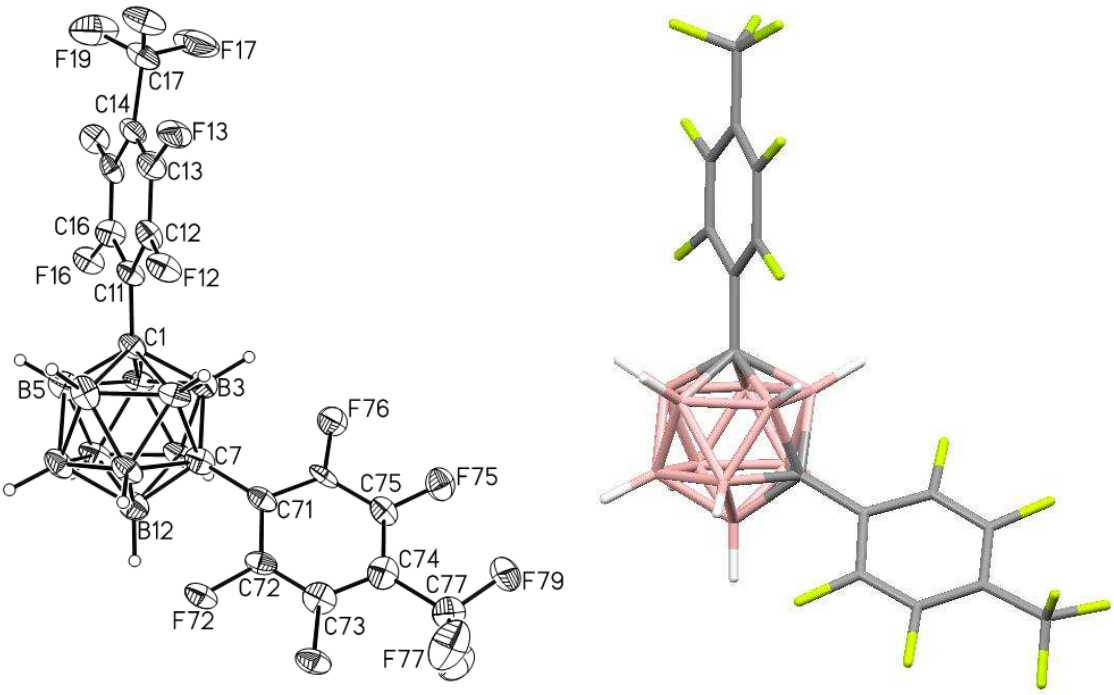

Figure 3.5.1.2 Perspective views of 1,7-(4'-$F_3CC_6F_4)_2$-1,7-*closo*-$C_2B_{10}H_{10}$ (14). Displacement ellipsoids are drawn at the 50% probability level except for H atoms.

Thus compound **14** was successfully prepared and characterised. It could be concluded that the low yield obtained in the preparation of **10** (lower than 40%) is due to steric reasons and is thus enhanced by increasing the separation of the cage carbon atoms. Following this principle, reaction of deprotonated *para*-carborane with

perfluorotoluene was performed to afford 1,12-(4'-$F_3CC_6F_4)_2$-1,12-*closo*-$C_2B_{10}H_{10}$ (**15**) in ca. 90% yield. The white crystalline solid obtained after the purification of **15** was also characterised by mass spectrometry, elemental analysis and by multinuclear NMR spectroscopy (table 3.5.1.1). A single crystal of **15** was subjected to *X*-ray diffraction to obtain the solid state molecular structure of the new compound (figure 3.5.1.3).

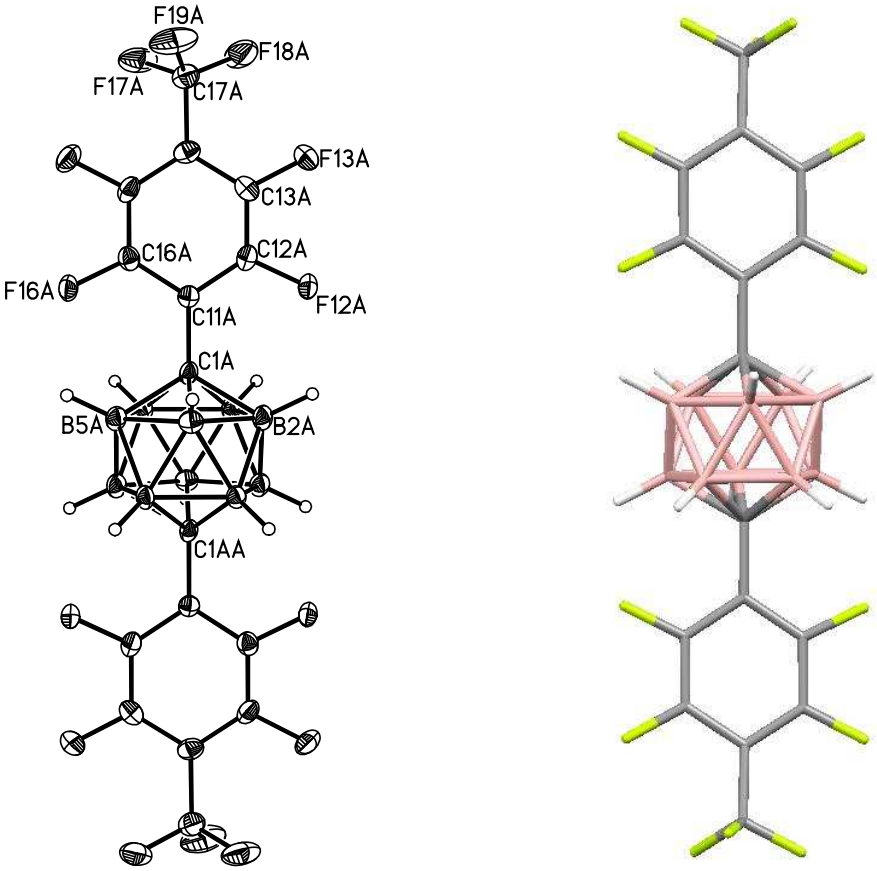

Figure 3.5.1.3 Perspective views of 1,12-(4'-$F_3CC_6F_4)_2$-1,12-*closo*-$C_2B_{10}H_{10}$ (15) (one of the two half-molecules in the asymmetric unit lying on centres of inversion; atoms with the suffix AA are generated with the symmetry operation -x,-y+1,-z+1). Displacement ellipsoids are drawn at the 50% probability level except for H atoms.

As revealed by multinuclear NMR studies on bis(perfluorotolyl) carboranes (**10**, **14** and **15**), the nuclear deshielding effect caused by Ar_F groups on the carborane cage decreases when the distance between the cage carbon atoms increases. The highest average ^{11}B chemical shift $<\delta^{11}B>$ is for carbon atoms adjacent **10**, whilst the lowest shift is for the para cage in **15** (table 3.5.1.1). Interestingly, the ^{19}F-NMR resonances corresponding to aromatic fluorine atoms in the perfluorotolyl groups of compounds

10, **14** and **15** were found to follow different trends depending on the nature of the cage vertex antipodal to the perfluorotolyl group. In compounds **10** and **14**, perfluorotolyl groups are antipodal to cage boron vertices (B9 and B12 for **10**, B5 and B12 for **14**) and the δ ^{19}F of aromatic fluorine atoms were found at approximately the same frequency. On the other hand, perfluorotolyl groups in compound **15** are antipodal to each other and, as a result, the δ ^{19}F corresponding to aromatic fluorine atoms were found shifted to lower frequencies. However, the nature of the cage do not affect the δ ^{19}F corresponding to CF_3 groups, since they were found at approximately δ –56.8 for the three compounds. The most relevant spectroscopic features of *ortho*-, *meta*- and *para*-bis(perfluorotolyl) carboranes (**10**, **14** and **15**) are summarised in table 3.5.1.1.

	1,2-(4'-$F_3CC_6F_4)_2$-1,2-*closo*-$C_2B_{10}H_{10}$ (**10**)	1,7-(4'-$F_3CC_6F_4)_2$-1,7-*closo*-$C_2B_{10}H_{10}$ (**14**)	1,12-(4'-$F_3CC_6F_4)_2$-1,12-*closo*-$C_2B_{10}H_{10}$ (**15**)
$\delta^{11}B_{(antipod)}$	0.40	-1.77	n.a.
$<\delta^{11}B>$	-6.34	-8.71	-11.90
$\delta^{19}F_{(ortho)}$	-127.8	-127.9	-131.2
$\delta^{19}F_{(meta)}$	-136.3	-136.4	-139.1
$\delta^{19}F_{(CF_3)}$	-56.9	-56.9	-56.8

Table 3.5.1.1 Boron and Fluorine NMR spectroscopic features of bis(perfluorotolyl) carboranes (10, 14 and 15). $\delta^{11}B_{(antipod)}$ refers to B12/B9 in compound 10 and to B9/B10 in compound 14. It is assumed that the least negative ^{11}B resonance is attributed to $B_{(antipodal)}$ by analogy with 1,2-*closo*-$C_2B_{10}H_{12}$.

3.5.2 Experimental reduction of bis(perfluorotolyl) carboranes.

Once the syntheses of the three isomeric forms of bis(perfluorotolyl) carborane had been accomplished, a study of their reduction chemistry was performed. Ideally, perfluorotolyl groups should allow the two-electron reductive opening of the closo cages to afford 7,9-*nido* dianions in the case of **10** and **14**, and the 7,10-*nido* species in the case of **15**. Nevertheless, reduction of Ar_F groups is expected to occur as the first step, although it is also expected that once the perfluorotolyl unit is reduced, it would transfer the unpaired electron to the carborane cage and recover its aromaticity.

The chemical stability of Ar_F groups in bis(perfluorotolyl) compounds **10**, **14** and **15** was tested by reduction/oxidation experiments. These compounds were treated with an excess of sodium metal in THF solution under a dinitrogen atmosphere, followed by an aerial oxidation back to neutral species. The importance of these experiments lies in the *para→meta* and *meta→ortho* red/ox isomerisations that icosahedral carboranes undergo. According to the well known reduction/oxidation chemistry of icosahedral $C_2B_{10}H_{12}$ species,[23] reduction and subsequent oxidation of **15** should afford **14** via a 7,10-*nido* species, and the same process applied to **14** should afford compound **10** through a 7,9-*nido* intermediate. The success in the chemical reduction of compounds **14** and **15** can be conveniently confirmed by ^{11}B-NMR analysis of the re-oxidised products. On the other hand, the ^{19}F-NMR analysis of the re-oxidised products would confirm the stability of aromatic fluorine atoms of the perfluorotolyl groups upon reduction. The experimental observations during the chemical reduction of the three isomeric compounds and the spectroscopic analysis of the products obtained after the oxidation are summarised in table 3.5.2.1.

Experiment	Observations	^{11}B-NMR analysis	^{19}F-NMR analysis
10 + (xs)Na, THF	Solution turns red, exothermic.	No change observed.	Several new signals arise.
14 + (xs)Na, THF	Solution turns brown, exothermic.	No change observed.	Several new signals arise.
15 + (xs)Na, THF	Solution turns black, exothermic.	No change observed.	Several new signals arise.

Table 3.5.2.1 Summary of the observations during reduction/oxidation experiments on bis(perfluorotolyl) carboranes.

Compound **10** reacts with sodium metal to give a dark red solution in an exothermic process. The solution colour is similar to that observed during the sodium reduction of aryl carboranes. However, re-oxidation of the red solution to afford neutral species is a difficult process. In fact, the red solution of reduced **10** can be stirred in the open laboratory for days without decolouration. Only the addition of an oxidising agent

such as permanganate or the continuous bubbling of air through the red solution afforded a pale yellow residue typical of re-oxidised products. NMR analysis of that residue indicated the presence of an *ortho*-carborane cage (^{11}B-NMR evidence), although partial decomposition due to C-F activation was also revealed (^{19}F-NMR evidence). Despite the spectroscopic studies, the experiments on compound **10** were inconclusive: there was some confirmation of the stability of reduced species but there was no evidence of reductive cage opening to nido species.

From the red/ox experiments on **14** and **15**, it can be concluded that the reduction chemistry was only located on the fluorinated aryl rings. Despite the exothermic electron uptake, the observed colours during the experiments (brown for **14**, black for **15**) have, to our knowledge, never been observed before in aryl-carborane reduction chemistry. Furthermore, ^{11}B-NMR analysis of the residues obtained after re-oxidation revealed that the carborane cages were not reduced and the new signals arising in the ^{19}F-NMR spectra supported that the sodium reduction led to C-F activation in the perfluorotolyl units with the consequent undesired side reactions.

3.5.3 Computational study of the reduction of bis(perfluorotolyl) carboranes.

The reduction/oxidation experiments on bis(perfluorotolyl) carboranes (**10**, **14** and **15**) were not completely satisfactory. The chemical reduction of **10** affords the expected dark red solution although spectroscopic analysis of the re-oxidation products cannot confirm the reductive opening to afford 7,9-*nido* species. On the other hand, the experiments on **14** and **15** proved the failure of their cage reduction since the expected 1,12→1,7 and 1,7→1,2 isomerisations did not occur, according to the ^{11}B-NMR spectra of the re-oxidised products. In order to explore whether the reduction processes are centred on the Ar_F rings or in the carborane cage, the LUMOs of the optimised isomeric compounds **10**, **14** and **15** were computed by DFT calculations and are shown in figure 3.5.3.1.[2]

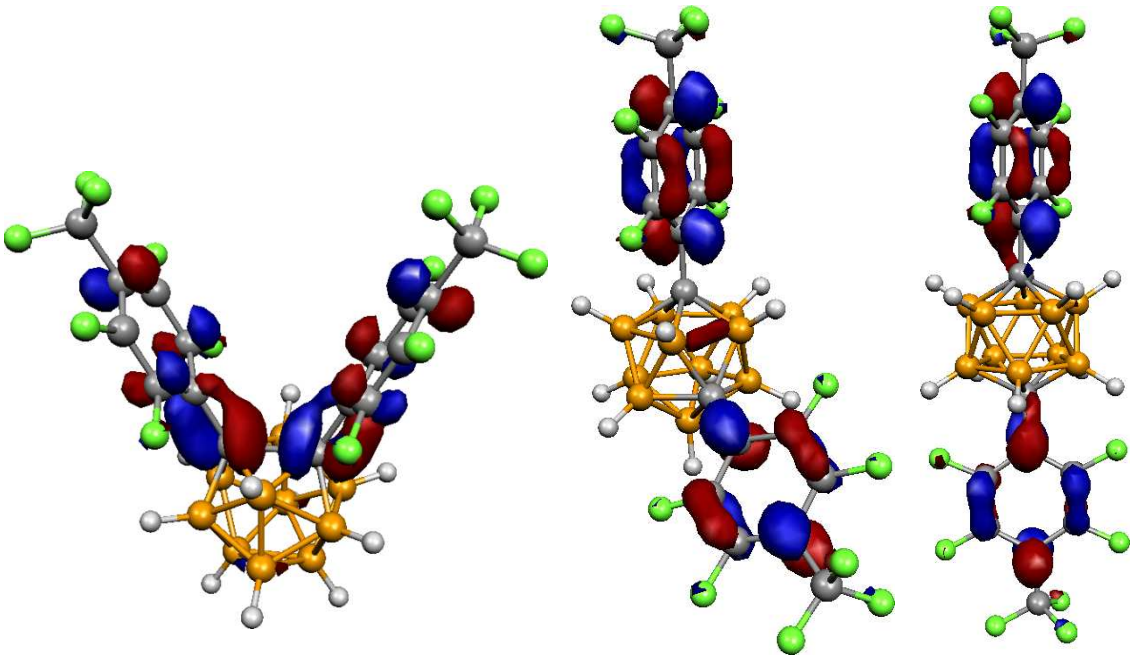

10 **14** **15**

Figure 3.5.3.1 LUMOs of DFT-optimised (B3LYP/6-31G*) compounds 10, 14 and 15.

From the DFT calculations it can be concluded that the electron uptake during reduction of the three bis(perfluorotolyl) carboranes is centred on the perfluorotolyl units, where the LUMOs of compounds **10**, **14** and **15** are mainly located. However, there are some differences between these. Whereas the LUMO of **15** is exclusively located on the perfluorotolyl rings, the LUMOs of compounds **10** and **14** have some contribution from the carborane cage. Although the cage contribution to the LUMO is rather small for the meta analogue **14**, the LUMO of **10** has a strong antibonding contribution from the C1-C2 connectivity of the ortho isomer (figure 3.5.3.1). It seems that whilst the electron uptake of *meta*- and *para*-bis(perfluorotolyl) carboranes (**14** and **15**) only results in the reduction of the Ar_F groups, the reduction of **10** effectively breaks the C1-C2 cage connectivity, which is regarded as the first step during the reductive opening to afford nido species.

In accord with the DFT calculated LUMOs shown in figure 3.5.3.1, the reduction of compounds **15** and **14** to generate nido species is very complicated. It appears that

ortho-bis(perfluorotolyl) carborane **10** is the only one of the three isomers susceptible of cage reduction processes.

3.5.4 Electrochemical reduction of bis(perfluorotolyl) carboranes (10, 14 and 15).

Another approach to investigate the chemical stability of bis(perfluorotolyl) carboranes towards reduction/oxidation processes would be their analysis by cyclic voltammetry. Generally, a reversible wave in the cyclic voltammogram gives evidence about the chemical stability of aryl *ortho*-carboranes upon reduction/oxidation processes. However, the reduction/oxidation processes of non-ortho compounds **14** and **15** are expected to be irreversible processes, due to the isomerisations described previously and, as a consequence, electrochemical analysis of these compounds should not afford reversible cyclic voltammograms. Nevertheless, the electrochemical study of compounds **14** and **15** might afford interesting information about their reduction behaviour. The cyclic voltammogram of compound **10**, which has already been shown in figure 3.4.3.4.1, confirmed the chemical reversibility of the reduction and the consequent stability of perfluorotolyl units during the process. The same electrochemical analysis applied to compounds **14** and **15** afforded the cyclic voltammograms shown in figure 3.5.4.1.

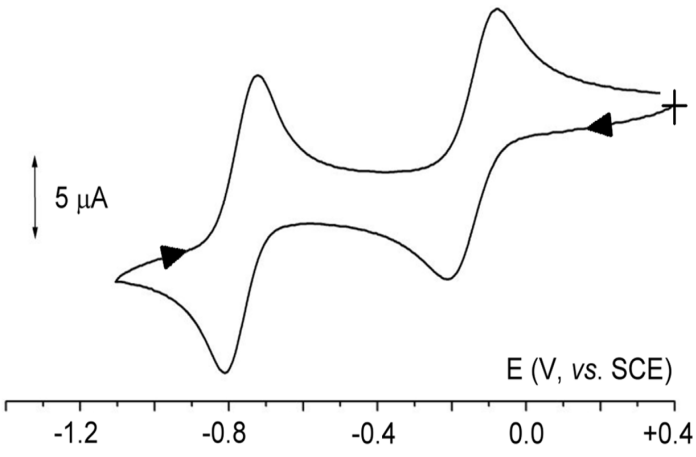

1,2-(4'-$F_3CC_6F_4)_2$-1,2-*closo*-$C_2B_{10}H_{10}$ (**10**)

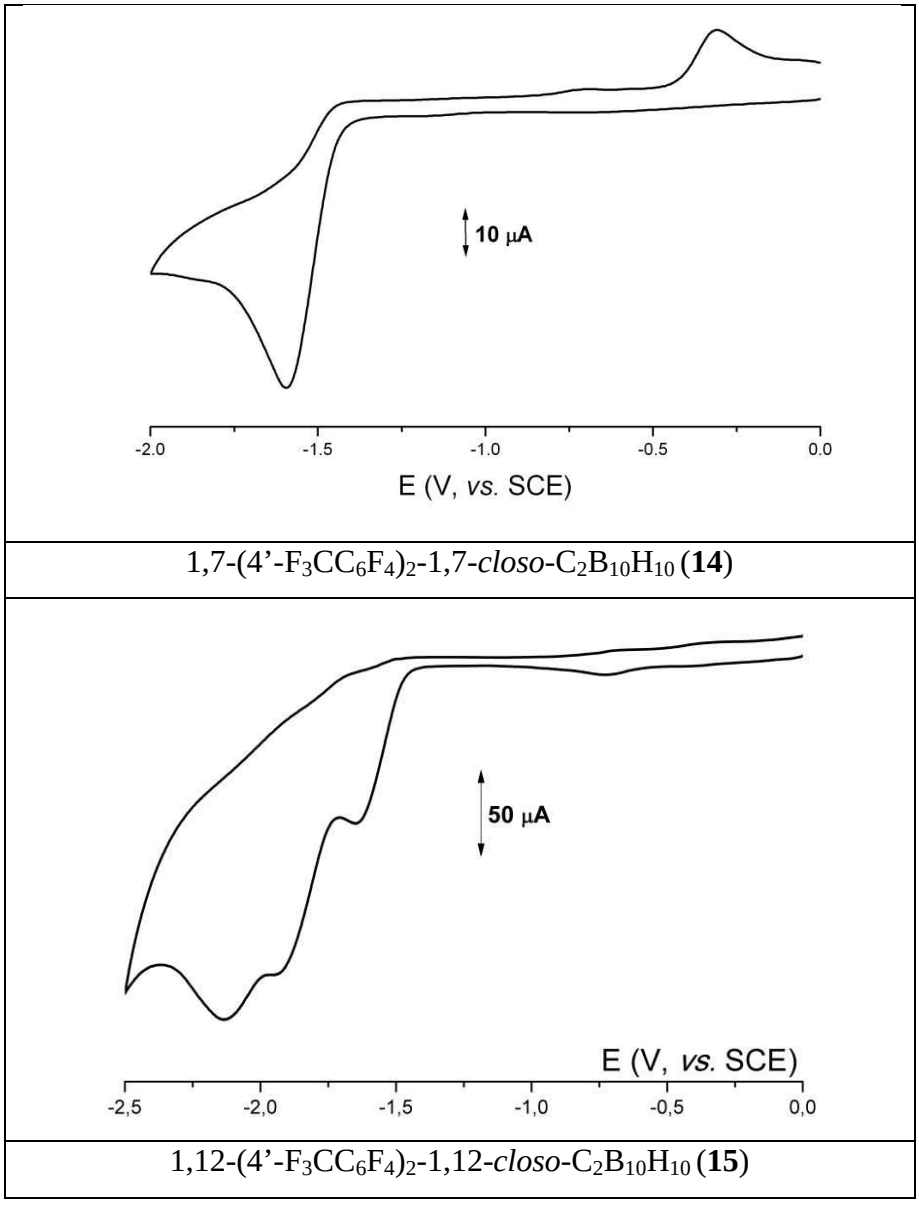

1,7-(4'-$F_3CC_6F_4)_2$-1,7-*closo*-$C_2B_{10}H_{10}$ (**14**)

1,12-(4'-$F_3CC_6F_4)_2$-1,12-*closo*-$C_2B_{10}H_{10}$ (**15**)

Figure 3.5.4.1 Cyclic voltammograms recorded at a gold electrode in THF solution of 10, 14 and 15 (scan rate 0.05 Vs^{-1} for 10, 0.2 Vs^{-1} for 14 and 15). $[NBu_4][PF_6]$ supporting electrolyte (0.2 M). T = 293 K.

The cyclic voltammogram of compound **14** indicates an irreversible reduction (E° = −1.60 V), which does not display any directly associated re-oxidation peak even at high scan rates. The spurious re-oxidation peak at −0.27 V in the cyclic voltammogram confirms that reduction of **14** causes decomposition of the original species to unidentified byproducts. The cyclic voltammogram of **15** presents similar features. It reveals an irreversible reduction (E° = −1.60 V), followed by several more reductions but no re-oxidation peak for any of these.

From the cyclic voltammograms shown in figure 3.5.4.1, it appears that reduction of compounds **14** and **15** leads to chemical decomposition to unknown species, which is in good agreement with the computational predictions for the reduction of bis(perfluorotolyl) carboranes described in the previous section. Whereas reduction of carbon atoms adjacent **10** to afford nido dianions is possible, reduction of **14** and **15** is centred in the perfluorotolyl units leading to decomposition instead of reductive cage opening. Although the suspected decomposition products were never isolated, this hypothesis about the reduction of compounds **14** and **15** is supported by the appearance of the first reduction peak at –1.60 V, in both cases, which could be a good indication of reduction of the perfluorotolyl unit.

In conclusion, only the *ortho*-bis(perfluorotolyl) carborane **10** allows the reductive cage opening necessary for polyhedral expansion procedures. The strong electron withdrawing effect of perfluorotolyl substituents facilitates the chemical reduction of the ortho cage due to the anti-bonding contribution to the LUMO from the C1-C2 bond, however, when the cage carbon atoms separation increases, the contribution to the LUMO from the cage disappears and, as a consequence, the cage reduction of meta and para bis(perfluorotolyl) species is not seen. Nevertheless, the experimental reduction of *ortho*-bis(perfluorotolyl) carborane **10** with excess Na always indicates C-F activation, thus exclusively stoichiometric two-electron reduction conditions must be used to minimise decomposition.

3.6 B-functionalisation of selected species.

Thus far, the work presented in this chapter has been focussed on C-functionalisation of carboranes because, according to DFT calculations,[2] the inductive effect of the *exo*-substituents in the cage is higher for C-substitution. Besides, the experimental attachment of functional groups to boron vertices is more complicated than their addition to cage carbon atoms. However, despite the great stabilisation attributed to C-functionalisation with Ar_F groups, it has been found that in the case of *meta*- and *para*-carborane, attachment of perfluorotolyl (4-$F_3CC_6F_4$) groups leads to compounds that do not allow the two-electron reductive opening required to afford nido dianions.

From the conclusions reached in former sections, 1,2-(4'-$F_3CC_6F_4)_2$-*closo*-1,2-$C_2B_{10}H_{10}$ (**10**) has been selected as the best precursor for polyhedral expansions. This compound only presents one weakness: its low yielding synthesis. As has also been previously discussed, the low yielding problem would be overcome by the use of its meta analogue **14** if its reduction afforded 7,9-*nido* species. Unfortunately, reduction of **14** leads to decomposition due to perfluorotolyl reduction, as the computational studies suggested (figure 3.5.3.1) and the electrochemical analysis confirmed (figure 3.5.4.1).

A plausible solution to afford the cage reduction of compound **14** could lie in its B-functionalisation. Since the LUMO of **14** is partially located in the *meta*-carborane cage (figure 3.5.3.1), the attachment of electron withdrawing groups to the boron vertices might increase the contribution of the cage to the LUMO in **14** and perhaps allow the reductive cage opening.

3.6.1 Synthesis of 1,7-(4'-$F_3CC_6F_4)_2$-9,10-Ph_2-1,7-*closo*-$C_2B_{10}H_8$ (16).

The attachment of phenyl rings to selected boron vertices in the carborane cage is a well known process, although their electron withdrawing character is rather small

compared to perfluoroaryl substituents. Nevertheless, phenylation of boron vertices might well increase the contribution of the cage to the LUMO and consequently allow the chemical reduction of the meta cluster. 9,10-Ph_2-1,7-*closo*-$C_2B_{10}H_{10}$ was prepared according reported procedures,[24] deprotonated with BuLi and treated with octafluorotoluene (C_7F_8) to afford 1,7-(4'-$F_3CC_6F_4)_2$-9,10-Ph_2-1,7-*closo*-$C_2B_{10}H_8$ (**16**) in good yield after aqueous work up (figure 3.6.1.1).

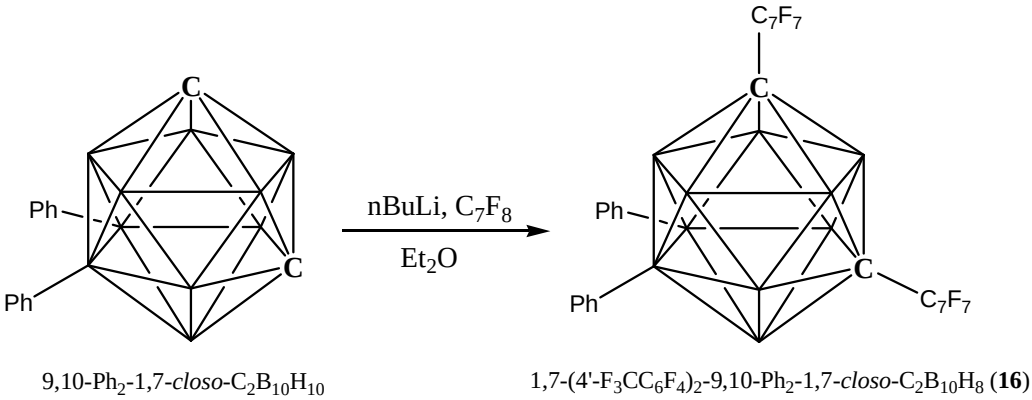

9,10-Ph_2-1,7-*closo*-$C_2B_{10}H_{10}$ 1,7-(4'-$F_3CC_6F_4)_2$-9,10-Ph_2-1,7-*closo*-$C_2B_{10}H_8$ (**16**)

Figure 3.6.1.1 Synthesis of 1,7-(4'-$F_3CC_6F_4)_2$-9,10-Ph_2-1,7-*closo*-$C_2B_{10}H_8$ (16) by reaction of [9,10-Ph_2-1,7-*closo*-$C_2B_{10}H_8$]Li_2 with perfluorotoluene. (N.B. naked vertex = BH, C vertex = CH).

Compound **16** was isolated as a white crystalline solid after chromatographic purification. It was obtained in slightly lower yield than **14** but in much higher yield than **10**. The identity of the new compound was confirmed by elemental analysis and by the presence of its molecular ion at m/z 728 in the mass spectrum. Compound **16** was also characterised by multinuclear NMR spectroscopy. Whilst the ^{1}H-NMR spectrum confirmed the existence of the phenyl rings, ^{19}F-NMR proved the presence of the perfluorotolyl units and the ^{11}B-NMR spectrum revealed the existence of two decoupled boron vertices in a highly symmetric *meta*-carborane cage. The molecular structure of this B-functionalised carborane was ultimately confirmed by *X*-ray diffraction study of a single block crystal of **16** and is shown in figure 3.6.1.2.

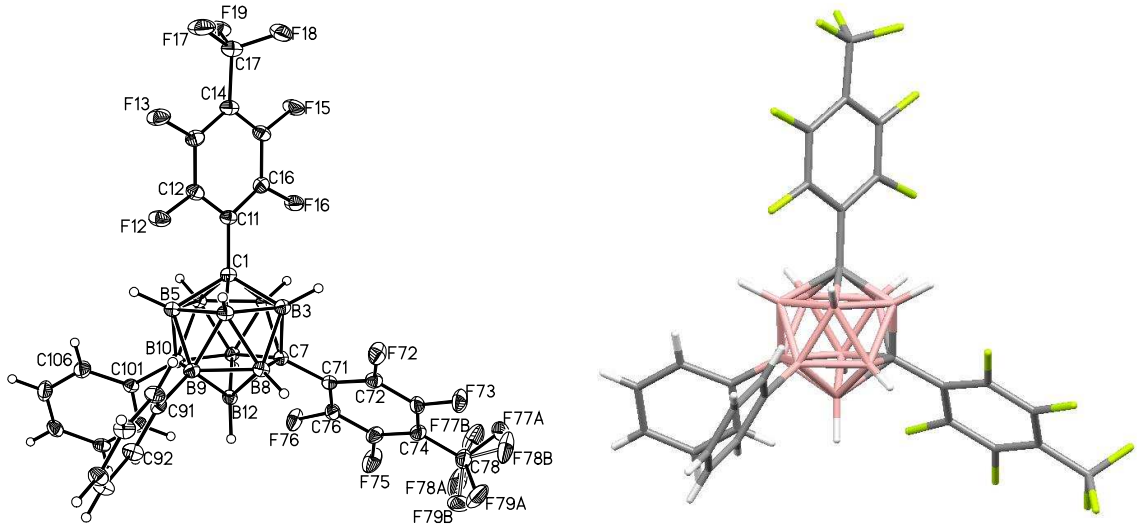

Figure 3.6.1.2 Perspective views of 1,7-(4'-$F_3CC_6F_4)_2$-9,10-Ph_2-1,7-*closo*-$C_2B_{10}H_8$ (16). Displacement ellipsoids are drawn at the 50% probability level except for H atoms.

3.6.2 Experimental reduction of the B-substituted compound.

The introduction of two phenyl rings on the B9 and B10 vertices in the structure of **14** has been accomplished affording the tetrasubstituted compound **16**. The new compound has been designed to favour the two-electron reduction of the *meta*-carborane cage required to obtain a 7,9-*nido* dianion. The success of this strategy could be confirmed by ^{11}B-NMR analysis of reduction/oxidation experiments since in general, *meta*-carborane cages are reduced to afford 7,9-*nido* species, which on re-oxidation yield exclusively ortho cages.

Compound **16** was stirred with excess of finely cut sodium metal in THF under a dinitrogen atmosphere to afford a brown/yellow solution. Aerial oxidation of this solution afforded an oily brown residue that contained exclusively *meta*-carborane cages according to ^{11}B-NMR analysis, indicating failure of the reductive opening of **16**. ^{19}F-NMR analysis of the re-oxidised products revealed new peaks which once again supported the suspected perfluorotolyl reduction.

3.6.3 Computational studies.

In order to understand the difficulty in the cage reduction of compound **16**, the two-electron reduction of this compound was studied by DFT calculations.[2] This showed that reduction of **16** should afford [5,6-Ph_2-7,9-(4'-$F_3CC_6F_4)_2$-7,9-*nido*-$C_2B_{10}H_8$]$^{2-}$, which would also be the reduction product of the ortho analogue: 1,2-(4'-$F_3CC_6F_4)_2$-9,12-Ph_2-*closo*-1,2-$C_2B_{10}H_8$ (figure 3.6.2.1).

The predicted stabilisation energy towards oxidation (ΔE), defined before by the energy difference between this nido species and its first optimised oxidation intermediate, was also obtained computationally and is shown in figure 3.6.3.1.[2]

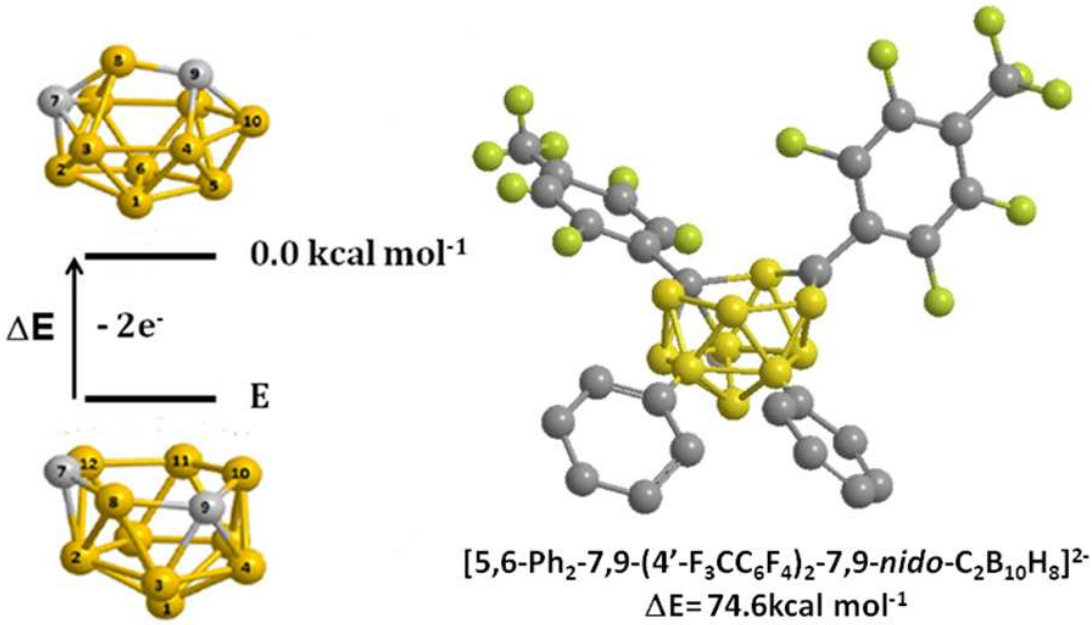

Figure 3.6.3.1 DFT-optimised (B3LYP/6-31G*) ΔE value between the predicted nido structure for the reduction of 16 and its first oxidation intermediate. Hydrogen atoms omitted for clarity.

The optimised nido species shown in figure 3.6.3.1 is expected to be extremely stable towards oxidation, giving the greatest ΔE (74.6 kcal mol^{-1}) of the whole series of carboranes studied in this chapter. However, in spite of the DFT predictions, reduction of **16** to afford that optimised nido species did not occur.

Since the reason of this failure might lie again in the nature of the molecular orbitals of **16**, the localisation and nature of the LUMO of **16** was computed and it is compared to its non phenylated analogue **14** in figure 3.6.3.2.

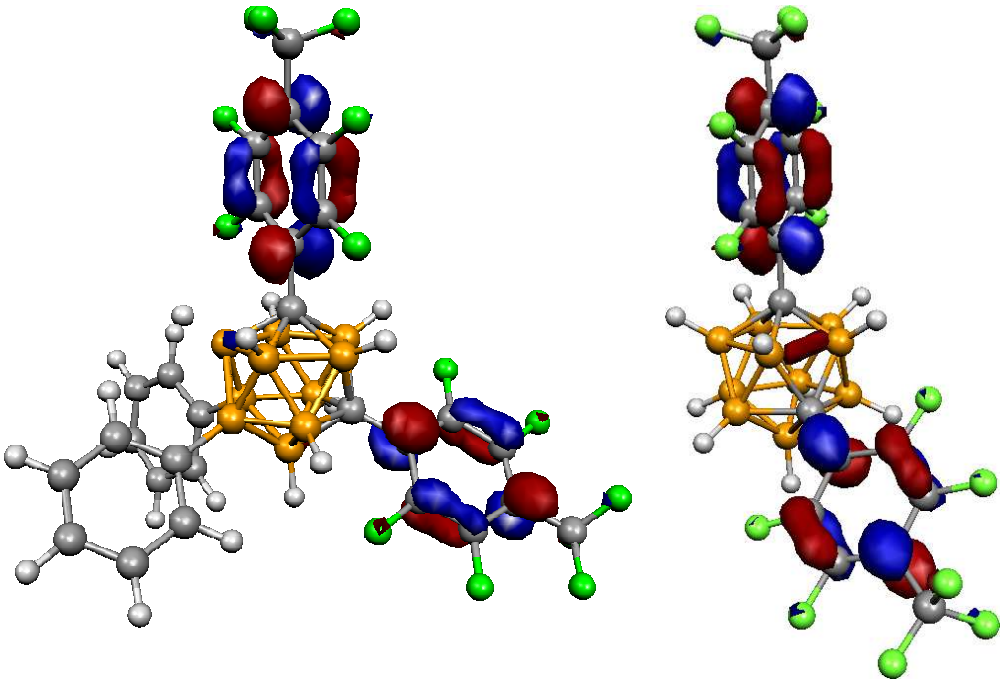

Figure 3.6.3.2 LUMOs of DFT-optimised (B3LYP/6-31G*) compounds 16 and 14.

As figure 3.6.3.2 shows, the addition of phenyl rings to boron vertices B9 and B10 in **14** does not significantly change the LUMO character. The strong electron withdrawing character of the perfluoroaryl groups determines the reduction behaviour of the compounds studied in this chapter and, in conclusion, no perfluorotolyl compounds other than the ortho cages of **10** and **8** are susceptible to the reductive cage opening required for the polyhedral expansion purposes that are described in the following chapter.

3.7 References

3.1 For example: a) N. M. M. Wilson, D. Ellis, A. S. F. Boyd, B. T. Giles, S. A. Macgregor, G. M. Rosair and A. J. Welch, *Chem. Commun.*, 2002, 464; b) S. Zlatogorsky, D. Ellis, G. M. Rosair and A. J. Welch, *Chem. Commun.*, 2007, 2178; c) S. Zlatogorsky, M. J. Edie, D. Ellis, S. Erhardt, M. E. Lopez, S. A. Macgregor, G. M. Rosair and A. J. Welch, *Angew. Chem. Int. Ed.*, 2007, **46**, 6706.

3.2 D. McKay, PhD thesis, *Heriot-Watt University*, 2010.

3.3 W. H. Knoth, H. C. Miller, D. C. England, G. W. Parshall and E. L. Muetterties, *J. Am. Chem. Soc.*, 1962, **84**, 1056.

3.4 S. Kongpricha and H. Schroeder, *Inorg. Chem.*, 1969, **8**, 2449.

3.5 R. J. Lagow and J. L. Margrave, *J. Inorg. Nucl. Chem.*, 1973, **35**, 2084.

3.6 a) B. T. King and J. Michl, *J. Am. Chem. Soc.*, 2000, **122**, 10255; b) A. Herzog, R. P. Callahan, C. L. B. Macdonald, V. M. Lynch, M. F. Hawthorne and R. J. Lagow, *Angew. Chem. Int. Ed.*, 2001, **40**, 2121.

3.7 L. I. Zakharkin and V. N. Lebedev, *Izv. Akad. Nauk. SSSR, Ser. Khim.*, 1970, **4**, 957.

3.8 a) Rh. Ll. Thomas and A. J. Welch, *Acta Crystallogr., Sect. C*, 1996, **52**, 1689; b) A. S. Batsanov, M. A. Fox, J. A. K. Howard and K. Wade, *J. Organomet. Chem.*, 2000, **597**, 157.

3.9 For example: a) L. A. Boyd, W. Clegg, R. C. B. Copley, M. G. Davidson, M. A. Fox, T. G. Hibbert, J. A. K. Howard, A. Mackinnon, R. J. Peace and K. Wade, *Dalton Trans.*, 2004, 2786, b) M. E. Lopez, M. J. Edie, D. Ellis, A. Horneber, S. A. Macgregor, G. M. Rosair and A. J. Welch, *Chem. Commun.*, 2007, 2243.

3.10 C. E. Smith, P. S. Smith, Rh. Ll. Thomas, E. G. Robins, J. C. Collings, C. Dai, A. J. Scott, S. Borwick, A. S. Batsanov, S. W. Watt, S. J. Clark, C. Viney, J. A. K. Howard, W. Clegg and T. B. Marder, *J. Mater. Chem.*, 2004, **14**, 413.

3.11 W. P. Norris, *J. Org. Chem.*, 1972, **37**, 147.

3.12 P. T. Brain, J. Cowie, D. J. Donohoe, D. Hnyk, D. W. H. Rankin, D. Reed, B. D. Reid, H. E. Robertson and A. J. Welch, *Inorg. Chem.*, 1996, **35**, 1701.

3.13 R. Coult, M. A. Fox, W. R. Gill, P. L. Herbertson, J. A. H. MacBride and K. Wade, *J. Organomet. Chem.*,1993, **462**, 19.

3.14 K. Ohta, T. Goto and Y. Endo, *Tetrahedron Lett.*, 2005, **46**, 483.

3.15 A. Kollhofer, T. Pullmann and H. Plenio, *Angew. Chem. Int. Ed.*, 2003, **42**, 1056.

3.16 Z. G. Lewis and A. J. Welch, *Acta Crystallogr., Sect. C*, 1993, **49**, 705.

3.17 T. L. Venable, W. C. Hutton and R. N. Grimes, *J. Am. Chem. Soc.*, 1984, **106**, 29.

3.18 M. A. Fox, C. Nervi, A. Crivello and P. J. Low, *Chem. Commun.*, 2007, 2372.

3.19 M. J. Mio, L. C. Kopel, J. B. Braun, T. L. Gadzikwa, K. L. Hull, R. G. Brisbois, C. J. Markworth and P. A. Grieco, *Org. Lett.*, 2002, **4**, 3199.

3.20 For example: a) H. Lee, C. B. Knobler and M. F. Hawthorne, *Chem. Commun.*, 2000, 2485; b) M. A. Fox, C. Nervi, A. Crivello, A. S. Batsanov, J. A. K. Howard, K. Wade and P. J. Low, *J. Solid State Electrochem.*, 2009, **13**, 1483.

3.21 For example: a) E. S. Alekseyeva, M. A. Fox, J. A. K. Howard, J. A. H. MacBride and K. Wade, *Appl. Organomet. Chem.*, 2003, **17**, 499; b) I. V. Glukhov, M. Y. Antipin and K. A. Lyssenko, *Eur. J. Inorg. Chem.*, 2004, 1379; c) M. Tsuji, *J. Org. Chem.*, 2004, **69**, 4063; d) W. Clegg, R. Coult, M. A. Fox, W. R. Gill, J. A. H. MacBride and K. Wade, *Polyhedron.*, 1993, **12**, 2711; e) R. Kivekäs, R. Sillanpää, F. Teixidor, C. Vinas and R. Nunez, *Acta Crystallogr., Sect. C*, 1994, **50**, 2027.

3.22 For example: a) D. A. Brown, W. Clegg, H. M. Colquhoun, J. A. Daniels, I. R. Stephenson and K. Wade, *J. Chem. Soc., Chem. Commun.*, 1987, 889; b) T. D. Getman, C. B. Knobler and M. F. Hawthorne, *Inorg. Chem.*, 1992, **31**, 101; c) K. Chui, H.-W. Li and Z. Xie, *Organometallics*, 2000, **19**, 5447.

3.23 For example: a) V. I. Stanko, Yu. V. Gol'tyapin and V. A. Brattsev, *J. Gen. Chem. USSR*, 1969, 1142; b) L. I. Zakharkin, V. N. Kalinin, V. A. Antonovich and E. G. Rys, *Bull. Acad. Sci. USSR, Div. Chem. Sci.*, 1976, 1009.

3.24 Z. Zheng, W. Jiang, A. A. Zinn, C. B. Knobler and M. F. Hawthorne, *Inorg. Chem.*, 1995, **34**, 2095.

CHAPTER 4. Polyhedral expansion of selected carboranes.

4.1 Introduction.

The attachment of fluorinated aryl groups (Ar_F) to carborane cages has been presented in the previous chapter. After an extensive investigation, C-substitution of 1,2-*closo*-C_2B_{10} cages with perfluorotolyl groups is expected to afford highly stabilised 7,9-*nido* species after reduction and, as a consequence, 1,2-(4'-$F_3CC_6F_4)_2$-1,2-*closo*-$C_2B_{10}H_{10}$ (**10**) and 1-(4'-$F_3CC_6F_4$)-2-Ph-1,2-*closo*-$C_2B_{10}H_{10}$ (**8**) have been selected as the most appropiate precursors for polyhedral expansion procedures.

Notwithstanding interest in the polyhedral expansion of these compounds, little is known about their reduction chemistry. Electrochemically, compounds **10** and **8** have been subjected to cyclic voltammetric studies to confirm the reversibility of their reduction/oxidation cycles and the stability of the Ar_F groups. However, the experimental reduction of **10** with an excess of sodium metal followed by aerial oxidation revealed evidence for C-F activation or, in other words, the instability of perfluorotolyl units towards sodium metal reduction. Consequently, although the two-electron cage reductive opening of carboranes **10** and **8** is possible, extreme care must be taken during the experimental reduction to prevent C-F activation and consequent side reactions.

The work presented in this chapter is focussed on the polyhedral expansion of compounds **10** and **8** to afford supraicosahedral species. Stoichiometric reductions with two equivalents of sodium naphthalenide are required to obtain 7,9-*nido* dianions and minimise side reactions at the perfluorotolyl unit. The subsequent addition of a suitable fragment, isolobal to {BH}, should afford new 13-vertex heteroboranes. The polyhedral expansion chemistry of compounds **10** and **8** will be compared with that of non-substituted $C_2B_{10}H_{12}$ carboranes in order to evaluate the effect of the perfluorotolyl groups on polyhedral expansion chemistry.

4.2 Expansion to 13-vertex cobaltacarboranes.

The reduction of compounds **10** and **8**, followed by the addition of a suitable metal fragment {M}, isolobal to {BH}, was performed as a preliminary investigation of their polyhedral expansion chemistry. Metallation was performed because, in general, the supraicosahedral metallacarboranes obtained from Reduction/Metallation (Red/Met) processes are air-stable coloured compounds that readily crystallise, allowing their complete characterisation by *X*-ray diffraction. In addition, Red/Met expansions with transition metal fragments generally yield 13-vertex species in good yields, due to the greater overlap between the diffuse molecular orbitals of the metal and the six-atom open face of the nido dianion.

The first supraicosahedral heteroborane was obtained in 1971 by sodium reduction of *ortho*-carborane and the addition of cyclopentadienyl cobalt $\{CpCo\}^{2+}$, generated *in-situ* from sodium cyclopentadienide and cobalt(II) chloride, to afford 4-(η-C_5H_5)-4,1,6-*closo*-$CoC_2B_{10}H_{12}$ after aerial oxidation of the metal centre.[1] After this first synthesis, the use of cobalt for the preparation of supraicosahedral metallacarboranes has been extensively reported.[2] For all the abovementioned reasons, cyclopentadienyl cobalt {CpCo} was selected as the metal fragment in the preliminary studies on the polyhedral expansion of carboranes **10** and **8**.

4.2.1 Reduction/Metallation with {CpCo} of 10.

The reduction of **10** followed by addition of {CpCo} was performed to obtain supraicosahedral cobaltacarboranes bearing perfluorotolyl groups. The success of this reaction would confirm the stability of perfluorotolyl units towards reduction. Whereas the Red/Met expansion of *ortho*-carborane exclusively affords 4,1,6-supraicosahedral metallacarboranes, the expansion of diphenyl *ortho*-carborane has been reported to yield, besides the 4,1,6- isomer, the isomerised 4,1,8- species as a minor product.[3] It has been suggested that the steric demands and electron withdrawing effect of phenyl rings facilitate the 4,1,6- → 4,1,8- isomerisation. Therefore, due to the greater size and electron withdrawing character of perfluorotolyl

groups over phenyl substituents, the 4,1,8-CoC_2B_{10} isomer was expected to be found as a product of the polyhedral expansion of **10**.

Stoichiometric reduction with two equivalents of sodium naphthalenide of 1,2-(4'-$F_3CC_6F_4)_2$-1,2-*closo*-$C_2B_{10}H_{10}$ (**10**) in THF was followed by treatment with excess of NaCp and $CoCl_2$ at low temperature. The crude dark green mixture was filtered and purified by column chromatography. Further purification by preparative TLC revealed an orange compound (**17**) as the single product of the reaction.

Elemental analysis of **17** gave results in good agreement with the expected values for a 13-vertex cobaltacarborane, while mass spectrometry revealed the molecular ion at m/z 701, with typical carborane envelope which is consistent with the formula of compound **17**, $C_{21}H_{15}B_{10}CoF_{14}$.

The ^{1}H-NMR spectrum of compound **17** confirmed the presence of the cyclopentadienyl ligand as a single peak at δ 5.3 and the ^{19}F-NMR spectrum suggested the equivalence of the two perfluorotolyl units. However, the six different resonances found in the ^{11}B-NMR spectrum were not conclusive in assigning the isomeric form of the supraicosahedral cobaltacarborane. Furthermore, the presence of perfluorotolyl groups, and their effect on δ^{11}B, complicated the comparison of the spectrum obtained for **17** to the reported ^{11}B-NMR spectra of supraicosahedral cobaltacarboranes.[2b]

A *X*-ray diffraction study of a single crystal of **17** established the structure as 1,12-(4'-$F_3CC_6F_4)_2$-4-Cp-4,1,12-*closo*-$CoC_2B_{10}H_{10}$ (figure 4.2.1.1). In the structural study the cage is shown to be docosahedral with the metal atom at vertex 4 and carbon atoms at vertices 1 and 12. The carbon atoms are non-equivalent, since C1 occupies a degree-four vertex whilst C12 is in a five-connected position. An interesting feature of the structure is the angle of 10.89º adopted by the Cp ligand, with respect to the cage lower belt, to minimise steric hindrance with the perfluorotolyl group bonded to C1 (figure 4.2.1.1).

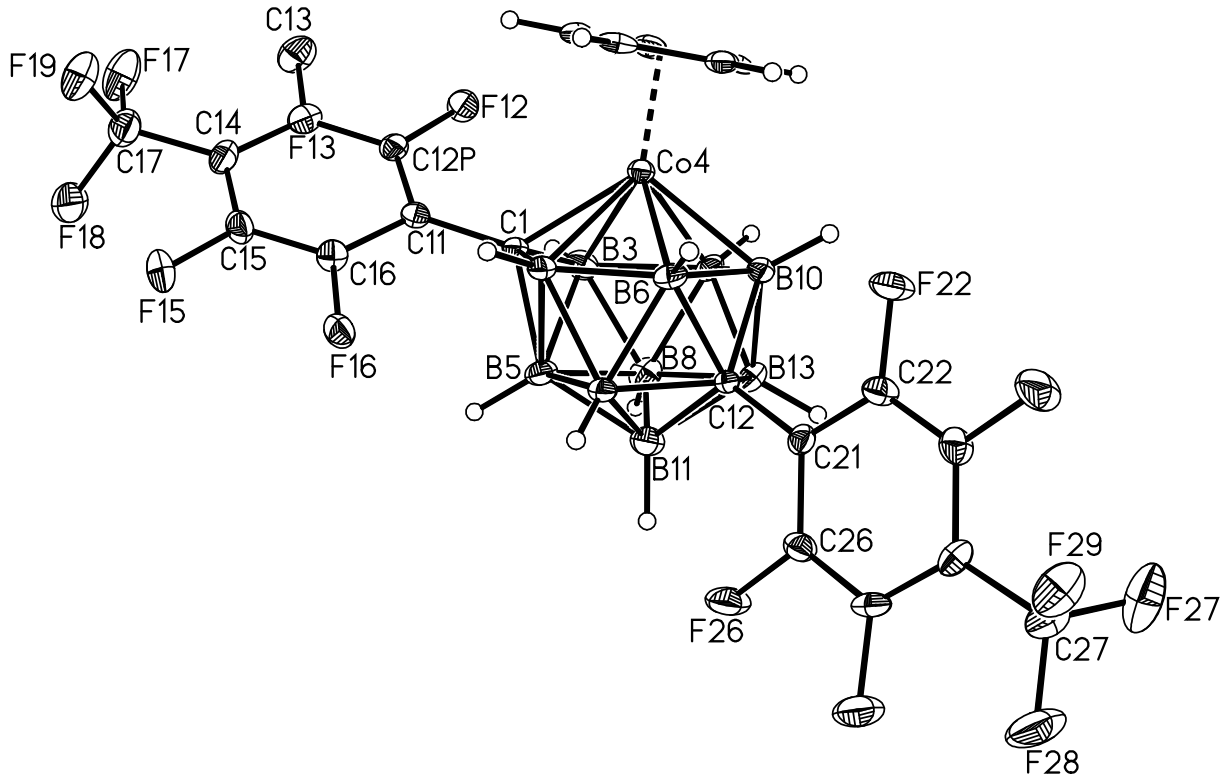

Figure 4.2.1.1 Perspective view of 1,12-(4'-$F_3CC_6F_4)_2$-4-Cp-4,1,12-*closo*-$CoC_2B_{10}H_{10}$ (17). Displacement ellipsoids are drawn at the 50% probability level except for H atoms.

Thus **17** was revealed to be the 4,1,12-CoC_2B_{10} isomer, instead of the expected 4,1,6- or 4,1,8- cobaltacarboranes. Once the structure of **17** has been undoubtedly established, the observed ^{19}F- and ^{11}B-NMR patterns can be rationalised. Since the cage only possesses C_1 symmetry, ten different resonances should be displayed in the ^{11}B-NMR spectrum. Therefore, the six observed peaks must involve some signal coincidences. On the other hand, although the perfluorotolyl groups of **17** have been found to be non equivalent, the δ^{19}F for both fluorinated units were found at the same frequencies and thus only three multiplets, corresponding to CF_3 groups and the two sets of aromatic fluorine atoms, were observed in the ^{19}F-NMR spectrum.

Although the polyhedral expansion of **10** to afford a 13-vertex metallacarborane has been successfully achieved, there is no simple explanation for the direct formation of **17** after reduction and metallation of the carbon atoms adjacent **10**. Generally, 4,1,12-metallacarboranes are obtained as a result of the thermal isomeration sequence 4,1,6-MC_2B_{10} → 4,1,8-MC_2B_{10} → 4,1,12-MC_2B_{10} [2b] that in some cases requires very high temperatures[4] or from direct isomerisation of the more convenient precursor 4,1,10-MC_2B_{10}.[5] The preparation of **17** must involve sequential room temperature

rearrangements to afford the 4,1,12- isomer, the thermodynamically most stable isomer of 13-vertex metallacarboranes. Cluster rearrangements by two different possible mechanisms that could account for the formation of **17** from **10** are summarised in figure 4.2.1.2.

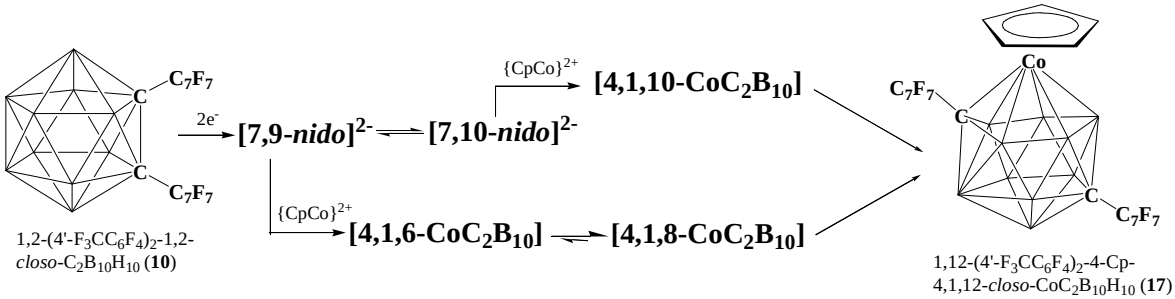

Figure 4.2.1.2 Two possible mechanisms to explain the formation of 17 from the polyhedral expansion of 10.

The main difference between the two proposed isomerisation mechanisms lies in which nido dianion is metallated to generate the first isomer of 13-vertex cobaltacarborane in the isomeration sequences. As described in chapter 1, two electron reduction of *ortho*-carborane affords 7,9-*nido* dianions, metallation of which affords 4,1,6- species. Consequently, the formation of **17** could be the result of a 4,1,6-MC_2B_{10} → 4,1,8-MC_2B_{10} → 4,1,12-MC_2B_{10} isomerisation cascade. However, the electron withdrawing character of phenyl groups has been reported to decrease the energy barrier between 7,9- and 7,10-*nido* species, allowing rearrangements between these dianions even at low temperature.[6] Since the electron withdrawing effect of perfluorotolyl groups is even greater, a 7,10-*nido* dianion could form from the reduction of **10**, metallation of which would afford a 4,1,10- metallacarborane that would readily isomerise to **17**.

In order to elucidate which mechanism accounts for the formation of **17**, the expansion of **10** was repeated at low temperatures and at shorter reaction times in an attempt to isolate and identify the reaction intermediates. Unfortunately, all these experiments were inconclusive since compound **17** was the only metallacarborane isolated, with all other bands corresponding to kinetic isomers observed in chromatography decomposing, making their characterisation impossible. Nevertheless, the synthesis of **17** constitutes the first example of the preparation of 4,1,12-MC_2B_{10} species directly from a 1,2-C_2B_{10} icosahedral carborane.

4.2.2 Reduction/Metallation with {CpCo} of 8.

Since the polyhedral expansion of compound **10** has been successful affording the 13-vertex metallacarborane **17**, the same process was applied to **8** in order to demonstrate the experimental reductive cage opening of this carborane and, at the same time, gather more information about the direct synthesis of 4,1,12- metallacarboranes from 1,2-C_2B_{10} species.

Stoichiometric reduction with two equivalents of sodium naphthalenide of 1-(4'-$F_3CC_6F_4$)-2-Ph-1,2-*closo*-$C_2B_{10}H_{10}$ (**8**) in THF was followed by treatment with excess of NaCp and $CoCl_2$ at low temperature. The crude dark green mixture was filtered and purified by column chromatography. Further purification by preparative TLC revealed three mobile bands, compounds **18**, **19** and **20**.

Mass spectrometric analysis of the red compound **18**, isolated in trace amount, indicated the molecular ion at m/z 538, with typical carborane envelope, which is consistent with the formula of compound **18** as $C_{20}H_{19}B_{10}CoF_6$, revealing the loss of one fluorine atom. Elemental analysis of **18** gave results in good agreement with the formula above, confirming the loss of a fluorine atom.

The four resonances in the ^{19}F-NMR spectrum of compound **18** revealed the presence of three different aromatic fluorine environments in the molecule, instead of the two expected signals for aromatic fluorine atoms in a perfluorotolyl group. This is in good agreement with the loss of an aromatic fluorine atom from the perfluorotolyl unit, making the three remaining aromatic fluorine atoms inequivalent. On the other hand, the ^{1}H-NMR spectrum of **18** revealed, apart from the presence of the phenyl ring in the aromatic range of the spectrum, a set of multiplets corresponding to the cyclopentadienyl ligand. The presence of thirteen different peaks in the ^{11}B-NMR spectrum of the red compound implied the presence of different stereoisomers in solution. In order to characterise compound **18**, a single block crystal was grown from a concentrated solution of **18** in DCM and was subjected to *X*-ray diffraction revealing the solid state molecular structure shown in figure 4.2.2.1.

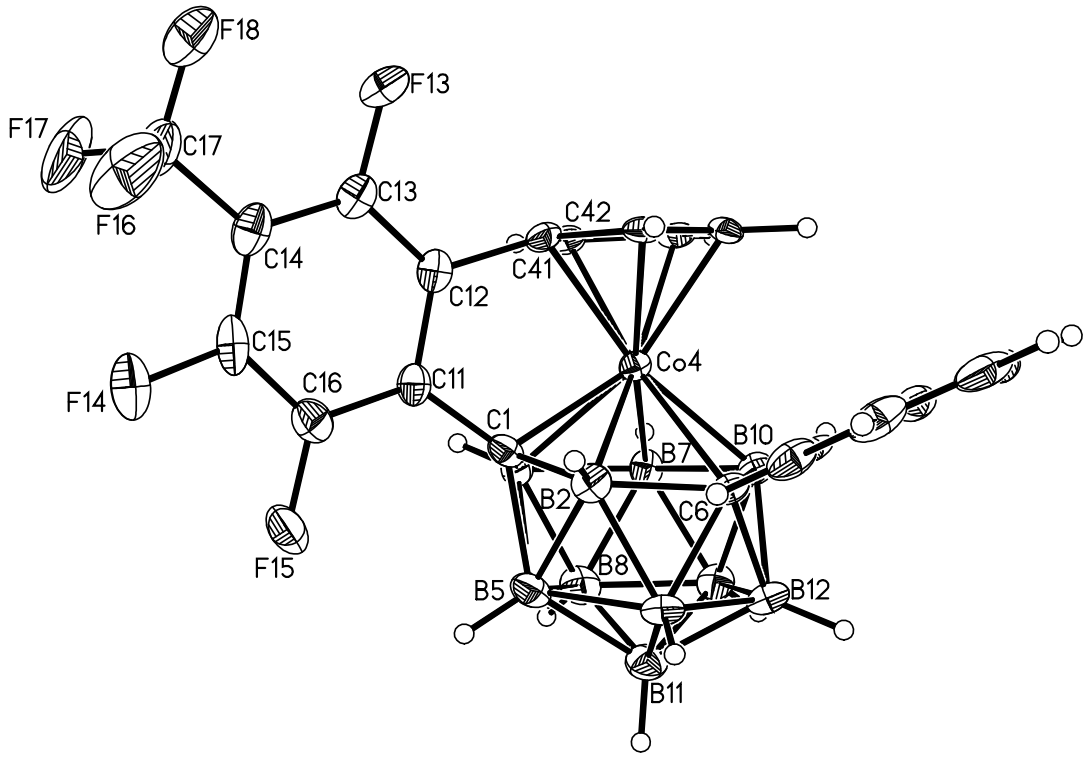

Figure 4.2.2.1 Perspective view of 1,4-μ-[2'-(η-C_5H_4)-4'-CF_3-C_6F_3]-6-Ph-4,1,6-*closo*-$CoC_2B_{10}H_{10}$ (18A). Displacement ellipsoids are drawn at the 50% probability level except for H atoms.

The molecular structure of **18** was revealed to be a 4,1,6- supraicosahedral cobaltacarborane in which the loss of one fluorine atom from the perfluorotolyl group has led to the formation of a new C-C bond between cyclopentadienyl and perfluorotolyl units. The structure is characterised by the presence of a new five-member ring that links a cage carbon vertex with the cyclopentadienyl ligand. The cage is shown to be docosahedral with the metal atom at vertex 4 and carbon atoms at vertices 1 and 6. In the isolated crystal, the perfluorotolyl group is attached to the four-connected carbon vertex C1, however, the spectroscopic analysis suggest that the other diastereoisomer, in which the perfluorotolyl linker is attached to the five-connected carbon vertex C6, is also present in solution. In accord with the high number of resonances observed in the ^{11}B-NMR spectrum, there is no fluxional equilibrium between diastereoisomers (see section 4.2.5) and, consequently, product **18** corresponds to a mixture of 1,4-μ-[2'-(η-C_5H_4)-4'-CF_3-C_6F_3]-6-Ph-4,1,6-*closo*-$CoC_2B_{10}H_{10}$ (**18A**) and 1-Ph-6,4-μ-[2'-(η-C_5H_4)-4'-CF_3-C_6F_3]-4,1,6-*closo*-$CoC_2B_{10}H_{10}$ (**18B**) which, in spite of being two independent reaction products, could not be separated by chromatographic techniques.

The second product isolated from the polyhedral expansion of **8** was the bright yellow compound **19**. Mass spectrometry and elemental analysis of the new cobaltacarborane suggested the formula of compound **19** as $C_{20}H_{20}B_9CoF_7$, i.e. a 12-vertex cobaltacarborane. Whereas the ^{1}H-NMR spectrum of **19** displayed a multiplet and a singlet corresponding to phenyl and cyclopentadienyl rings, respectively, the ^{19}F-NMR spectrum confirmed the presence of the intact perfluorotolyl unit. ^{11}B-NMR spectroscopy of the bright yellow compound showed five independent signals corresponding to nine different boron atoms in a 1:1:4:1:2 pattern of signal ratios.

According to the spectroscopic analysis of **19**, the new compound was predicted to be an icosahedral cobaltacarborane. In addition, cage degradation compounds are commonly found as by-products of Red/Met expansions on *ortho*-carborane.[7] An *X*-ray diffraction study of a single crystal of **19** revealed the molecular structure shown in figure 4.2.2.2.

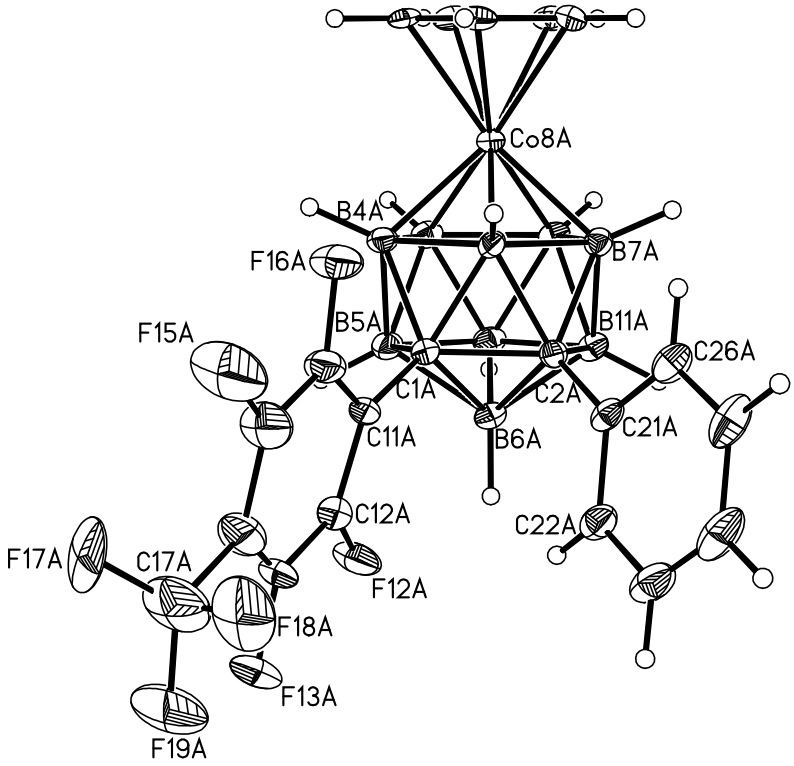

Figure 4.2.2.2 Perspective view of 1-(4'-$F_3CC_6F_4$)-2-Ph-8-Cp-8,1,2-*closo*-$CoC_2B_9H_{11}$ (19) (one of the two crystallographically independent molecules). The minor disordered component of CF_3 has been omitted and displacement ellipsoids have been drawn at the 50% probability level except for hydrogen atoms.

Thanks to crystallographic characterisation, the molecular structure of **19** was revealed to be 1-(4'-$F_3CC_6F_4$)-2-Ph-8-Cp-8,1,2-*closo*-$CoC_2B_9H_9$, the first crystallographically characterised example of a 8,1,2- isomer of the MC_2B_9 icosahedral metallacarborane series. The structure is characterised by the presence of the metal atom at vertex 8 and carbon atoms at vertices 1 and 2 of the icosahedron.

The third product obtained from the polyhedral expansion of **8** was compound **20**. Mass spectrometry (molecular ion at m/z 673) and elemental analysis of the dark brown solid were consistent with the formula of a bimetallacarborane, $C_{25}H_{24}B_9Co_2F_7$.

The ^{1}H-NMR spectrum of **20** displayed, apart from the multiplet corresponding to the phenyl ring, two singlets at δ 5.26 and δ 5.29 for the two predicted cyclopentadienyl ligands. This implies a docosahedral cage that probably features the two metal centres at six-connected vertices 4 and 5 and one of the carbon atoms at the four-connected position 1. On the other hand, the presence of the perfluorotolyl group in the structure of **20** was confirmed by ^{19}F-NMR spectroscopy. Finally, the ^{11}B-NMR spectrum of **20** displayed nine independent signals for the nine boron atoms in the structure. The molecular structure of **20** was ultimately revealed by *X*-ray diffraction and is shown in figure 4.2.2.3.

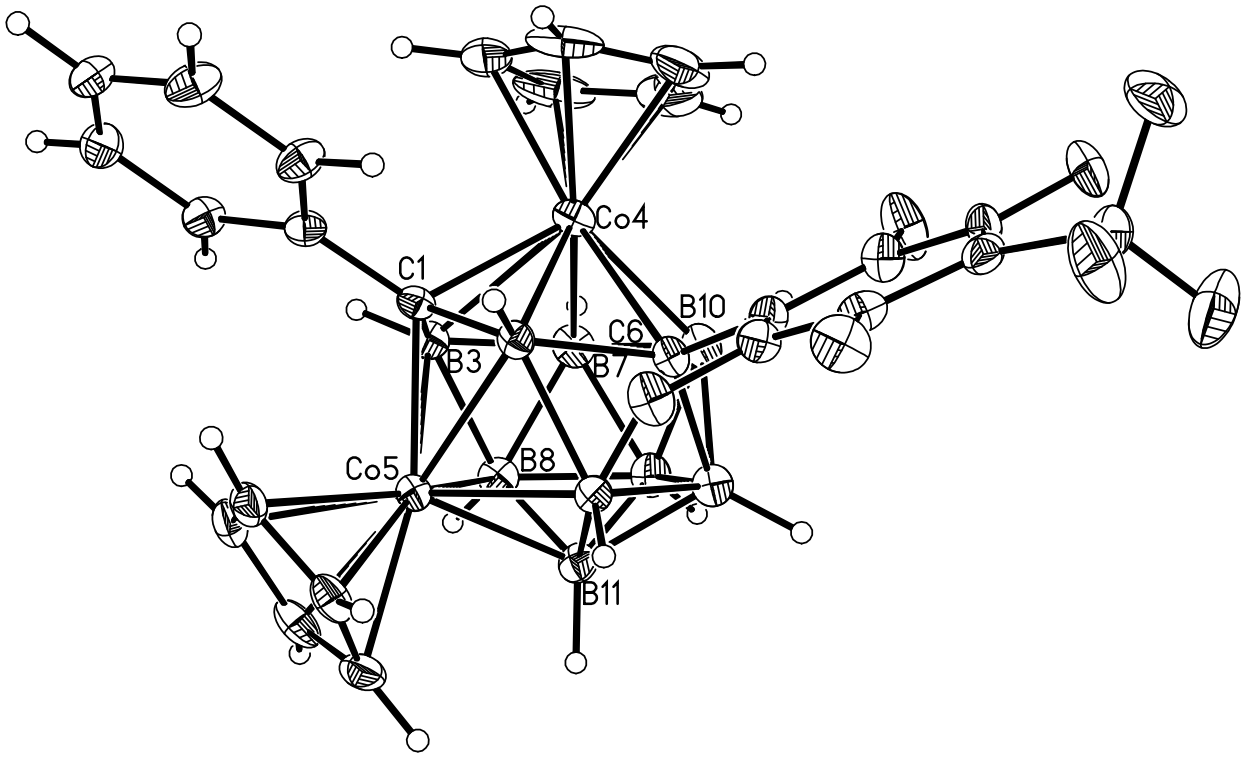

Figure 4.2.2.3 Perspective view of 1-Ph-4,5-Cp_2-6-(4'-$F_3CC_6F_4$)-4,5,1,6-*closo*-$Co_2C_2B_9H_9$ (20). Displacement ellipsoids are drawn at the 50% probability level except for H atoms.

Thus the third isolated metallacarborane from the reduction and subsequent metallation with {CpCo} of **8** was found to be 1-Ph-4,5-Cp_2-6-(4'-$F_3CC_6F_4$)-4,5,1,6-*closo*-$Co_2C_2B_9H_9$. The cage was found to be docosahedral with the metal atoms at vertices 4 and 5 and the carbon atoms at vertices 1 and 6, with the phenyl group attached to the four-connected carbon vertex C1.

Interestingly, none of the three isolated metallacarboranes **18**, **19** and **20** was a regular 4,1,X-CoC_2B_{10} supraicosahedral metallacarborane. From the isolated reaction products, it appears that the first intermediate obtained after metallation is the 4,1,6-isomer, generated after the capitation of a 7,9-*nido* dianion. This was confirmed by the isolation of **18**, whose formation presumably then involves the nucleophilic attack by the cyclopentadienyl ligand coordinated to cobalt on the 4-$F_3CC_6F_4$ unit, leading to the elimination of one of the ortho fluorine atoms from the perfluorotolyl group. The adventitious generation of a new C-C bond and a five-member ring that links positions 1 and 4 of the docosahedron prevents further isomerisation to 4,1,8- or 4,1,12- species and allows the isolation of the 4,1,6- cluster.

Nevertheless, although the intramolecular cyclisation observed in **18** prevents further rearrangements of it, the isolation of compounds **19** and **20** gave good evidence of the formation of a different 4,1,8- intermediate. If the intramolecular cyclisation did not occur, the 4,1,6- isomer would be expected to isomerise in the first step to the 4,1,8- species. This isomer of metallacarborane features a boron atom at the six-connected vertex 5, directly bonded to the cage carbon atoms. It is well known that high connected boron vertices are susceptible to nucleophilic attack,[8] which would be also promoted by the influence of phenyl and perfluorotolyl electron withdrawing groups on the adjacent cage carbon atoms.[9] The elimination of the highest connected boron vertex as a formal $\{BH\}^{2+}$ unit would generate a new open face as shown in figure 4.2.2.4. The nido intermediate generated after the {BH} removal could either undergo an oxidative closure to afford the 8,1,2- icosahedral metallacarborane **19** or, on the other hand, a second metallation with a {CpCo} fragment from the reaction mixture to generate the 13-vertex bimetallacarborane **20**.

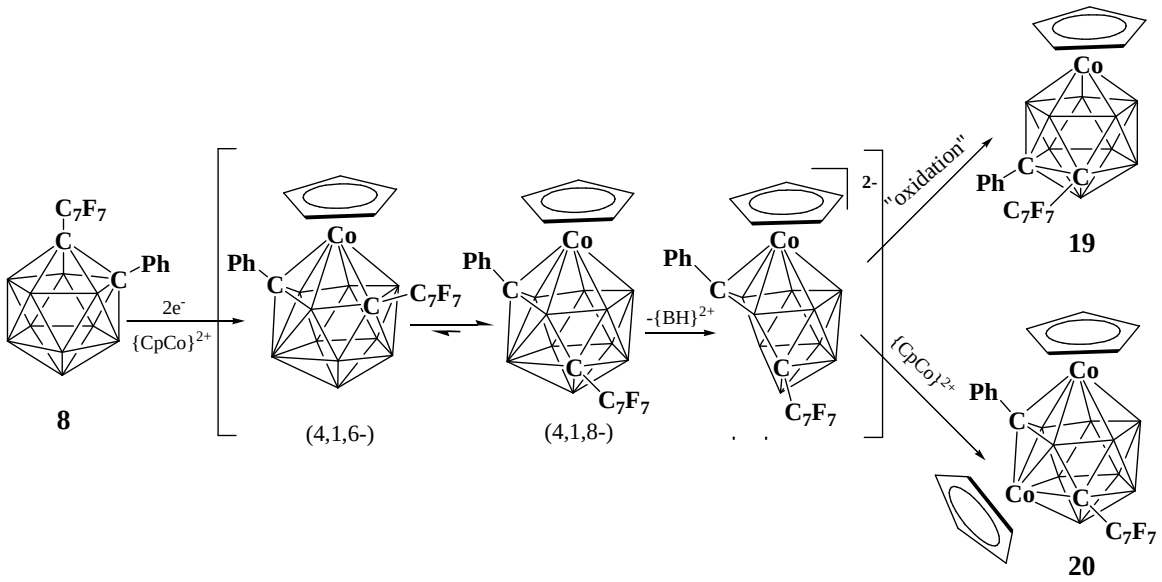

Figure 4.2.2.4 Schematic representation of the reduction and metallation with {CpCo} of 8 to generate compounds 19 and 20.

The reduction and subsequent metallation of compounds **10** and **8** has been found to afford quite different reaction products. Whereas the formation of **17** from **10** is not completely understood although is presumed to proceed by one of two possible mechanisms (figure 4.2.1.2), the unprecedented formation of **19** and **20** from **8** leaves only one plausible mechanism (figure 4.2.2.4).

Regarding the expansion of **8** to cobaltacarboranes, the spontaneous formation of a new C-C linkage between cyclopentadienyl and perfluorotolyl units prevented cage rearrangement and allowed the isolation of a 4,1,6- isomer (**18**), confirming the generation of 7,9-*nido* species as a result of the reduction. The formation of this new type of M-C tethered 13-vertex cobaltacarborane involves the nucleophilic attack of the cyclopentadienyl ligand at position 4 of the docosahedron on the ortho position of the perfluorotolyl unit. This would only be possible after the removal of one proton from the cyclopentadienyl ligand to afford an anion. The excess of NaCp in the reaction mixture could be responsible for the proton abstraction and the catalyst for an intramolecular cyclisation favoured by the elimination of sodium fluoride (figure 4.2.2.5).

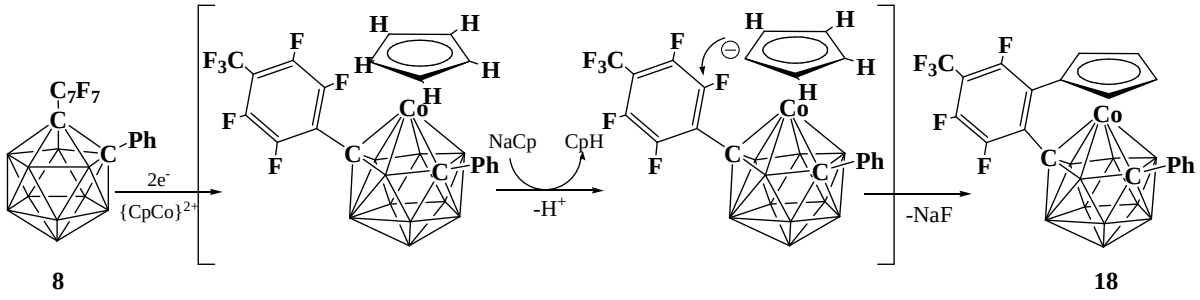

Figure 4.2.2.5 Schematic representation of the proposed NaCp-catalysed intramolecular cyclisation route to afford 1,4-μ-[2'-(η-C_5H_4)-4'-CF_3-C_6F_3]-6-Ph-4,1,6-*closo*-$CoC_2B_{10}H_{10}$ (18A).

Since the adventitious NaCp-catalysed formation of **18** (as a mixture of the two possible diasteroisomers **18A** and **18B**) has allowed the characterisation of reaction intermediates from the polyhedral expansion of **8**, a similar approach might be deliberately used to rationalise the direct formation of **17** from **10** (figure 4.2.1.2). A stronger base such as BuLi could be utilised to favour the intramolecular cyclisation and isolate the first 13-vertex isomer generated after the reduction and metallation of 1,2-(4'-$F_3CC_6F_4)_2$-1,2-*closo*-$C_2B_{10}H_{10}$ (**10**).

4.2.3 Deliberate formation of M-C tethered MC_2B_{10} species by intramolecular cyclisation processes.

The isolation of 1,4-μ-[2'-(η-C_5H_4)-4'-CF_3-C_6F_3]-6-Ph-4,1,6-*closo*-$CoC_2B_{10}H_{10}$ (**18A**) as a result of the polyhedral expansion of compound **8** has been explained in terms of a intramolecular cyclisation promoted by the excess of NaCp in the reaction mixture (figure 4.2.2.5). The formation of the intramolecular five-membered ring prevents further rearrangements allowing the characterisation of the first product of metallation (4,1,6-CoC_2B_{10}) and the consequent identification of the nido dianion generated after the two-electron reduction ([7,9-*nido*-C_2B_{10}]$^{2-}$). In order to confirm the base-catalysed mechanism proposed to explain the formation of **18**, the polyhedral expansion (Red/Met) of compounds **10** and **8** was performed inserting the addition of one equivalent of BuLi between reduction and metallation steps.

The stoichiometric reduction of **8** in THF, followed by the addition of one equivalent of BuLi gave a dark purple solution that was treated with an excess of NaCp and $CoCl_2$ at low temperature. The green residue obtained after aerial oxidation of the reaction mixture was filtered and purified by preparative TLC to reveal a single red band as the unique reaction product. Spectroscopic analysis confirmed the red solid to be the mixture of M-C tethered diastereoisomers previously isolated (**18**). No trace of any other metallacarborane was found after chromatographic purification. The addition of BuLi after reduction of **8** has thus been shown to promote the intramolecular cyclisation. Hence the reaction exclusively affords **18** after metallation, preventing the 4,1,6- → 4,1,8- isomerisation and the consequent formation of compounds **19** and **20**.

The same experiment was performed on compound **10**. Stoichiometric reduction of **10** in THF gave a dark red solution that was treated with one equivalent of BuLi followed by an excess of NaCp and $CoCl_2$. The green solution obtained after aerial oxidation was filtered and purified by preparative TLC. The red major band isolated from the TLC plate was found to be a new compound **21** while a second orange band,

isolated in trace amount, was identified as 1,12-(4'-$F_3CC_6F_4$)$_2$-4-Cp-4,1,12-*closo*-$CoC_2B_{10}H_{10}$ (**17**) according to NMR analysis.

The red major band (**21**) was characterised by elemental analysis and mass spectrometry (molecular ion found at m/z 681 confirming fluorine atom loss) and the obtained results were in good agreement with the molecular formula of **21** as $C_{21}H_{14}B_{10}CoF_{13}$.

The ^{1}H-NMR spectrum of **21** displayed a set of multiplets corresponding to a monosubstituted cyclopentadienyl unit. On the other hand, the ^{19}F-NMR spectrum revealed five different signals in the fluorine-aromatic region, corresponding to the presence of both *ortho*-substituted and non-substituted perfluorotolyl groups. Once again, the ^{11}B-NMR spectrum of the product revealed the presence of the two different diastereoisomers (**21A** and **21B**) in accord with the great number of signals displayed in the spectrum. Although all the analytical techniques confirmed the presence of an intramolecular five-member ring in the structure of **21**, *X*-ray diffraction study of a single crystal of **21** was necessary to ultimately reveal the molecular structure (figure 4.2.3.1).

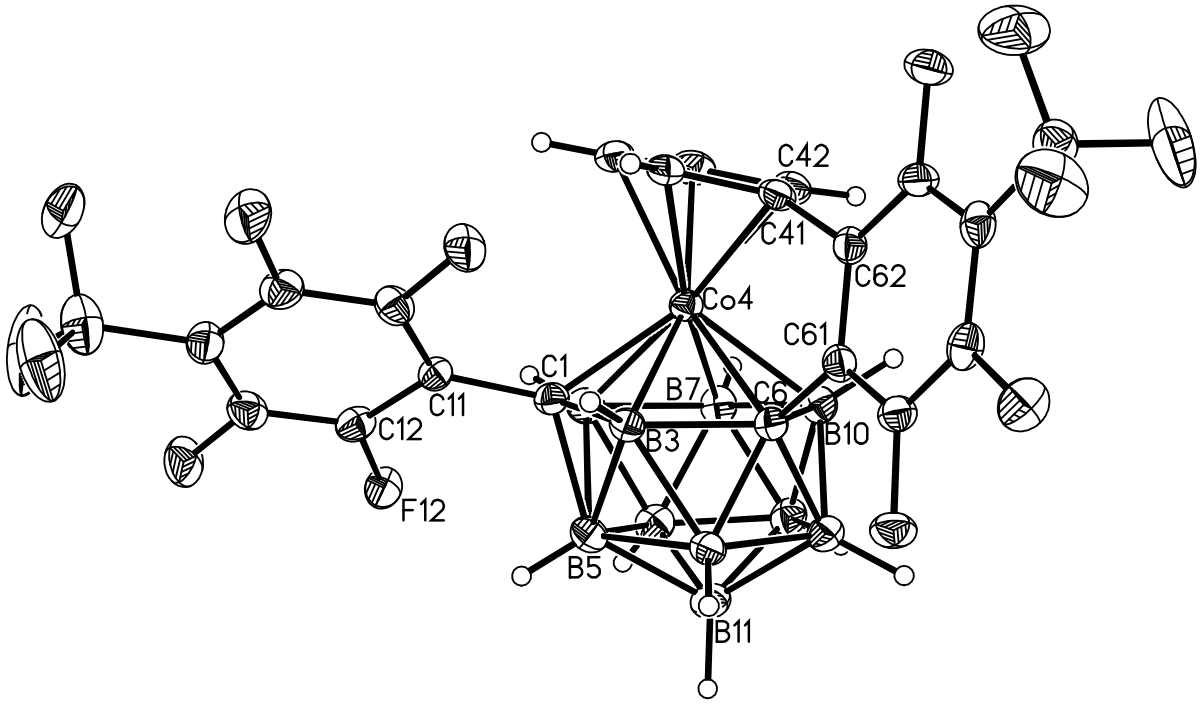

Figure 4.2.3.1 Perspective view of 1-(4'-$F_3CC_6F_4$)-6,4-μ-[2'-(η-C_5H_4)-4'-CF_3-C_6F_3]-4,1,6-*closo*-$CoC_2B_{10}H_{10}$ (21B). Displacement ellipsoids are drawn at the 50% probability level except for H atoms.

From the isolated crystal, the solid state structure of **21** was found to be 1-(4'-$F_3CC_6F_4$)-6,4-μ-[2'-(η-C_5H_4)-4'-CF_3-C_6F_3]-4,1,6-*closo*-$CoC_2B_{10}H_{10}$ (**21B**). The structure is characterised by the presence of a new five-membered ring that links a cage carbon C6 with the cyclopentadienyl ligand. The cage is shown to be docosahedral with the metal atom at vertex 4 and carbon atoms at vertices 1 and 6. Surprisingly, the crystallised diastereoisomer was revealed to be the 6,4-μ-4,1,6-MC_2B_{10} instead of the 1,4-μ-4,1,6-MC_2B_{10} structure found for **18**.

The success of the BuLi experiments to afford **18** and **21** supports the base-catalysed mechanism for the intramolecular cyclisation. The two different crystallised structures and the high number of resonances in the ^{11}B-NMR spectra suggest that M-C tethered compounds **18** and **21** are not fluxional (see section 4.2.5) in solution and are thus obtained as mixtures of diastereoisomers **18A** and **18B** and **21A** and **21B**. Although these diastereoisomers are independent compounds, they could not be separated by chromatographic techniques, thus they are reported in the experimental section as diastereoisomeric mixtures, i.e. product **18** (compounds **18A** and **18B**) and product **21** (compounds **21A** and **21B**).

Finally, the 4,1,6- cage found in the structure of **21** corroborates the formation of a 7,9-*nido* dianion as a consequence of the reduction of **10** and more interestingly, supports the formation of 1,12-(4'-$F_3CC_6F_4)_2$-4-Cp-4,1,12-*closo*-$CoC_2B_{10}H_{10}$ (**17**) as the result of the isomerisation sequence: 4,1,6-MC_2B_{10} → 4,1,8-MC_2B_{10} → 4,1,12-MC_2B_{10}.

4.2.4 Reduction/Metallation with {Cp*Co} of 10.

An interesting reaction encountered during the polyhedral expansion of perfluorotolyl carboranes is the intramolecular cyclisation that affords M-C tethered products **18** and **21**. The addition of BuLi has been shown to promote this reaction and to confirm the base-promoted mechanism. Alternatively, replacement of the acidic protons in the cyclopentadienyl ligand (Cp) by moving to its pentamethylated analogue (Cp*) should totally avoid the formation of M-C tethered compounds and might increase the yield of other metallation products. However, {Cp*Co} metal fragments are bulkier and more electron-rich than {CpCo}, thus different reaction pathways could arise from their use as metal fragments in the expansion of **10**.

Stoichiometric reduction with two equivalents of sodium naphthalenide of 1,2-(4'-$F_3CC_6F_4)_2$-1,2-closo-$C_2B_{10}H_{10}$ (**10**) was followed by treatment with excess of NaCp* and $CoCl_2$ at low temperature. The crude dark green mixture obtained after aerial oxidation was filtered and purified by column chromatography. Further purification by preparative TLC revealed multiple bands, from which only the major three were isolated to afford compounds **22**, **23** and **24**.

Major compound **22** was isolated as a pale yellow solid. Elemental analysis and mass spectrometry (molecular ion at m/z 809) identified **22** as $C_{36}H_{40}B_{10}F_{12}$. This reported molecular formula corresponds to the substitution of two fluorine atoms by Cp* in the structure of the icosahedral starting material **10**.

The suspected structure was corroborated by multinuclear NMR studies. Whilst the presence of the methyl groups from the Cp* ligand was confirmed in the ^{1}H-NMR spectrum, the ^{11}B-NMR spectrum of **22** was found to be very similar to that of **10**, revealing the presence of an icosahedral carborane. Finally, two resonances for aromatic fluorine atoms were shown in the ^{19}F-NMR spectrum of **22** but surprisingly, the signal corresponding to CF_3 groups appeared shifted to lower frequencies, a good indication of the formation of a new C-C bond in that position. In order to confirm the suspected structure, attributed to a side reaction between **10** and $[Cp^*]^-$, a single

crystal of **22** was subjected to a *X*-ray diffraction study to reveal the molecular structure shown in figure 4.2.4.1.

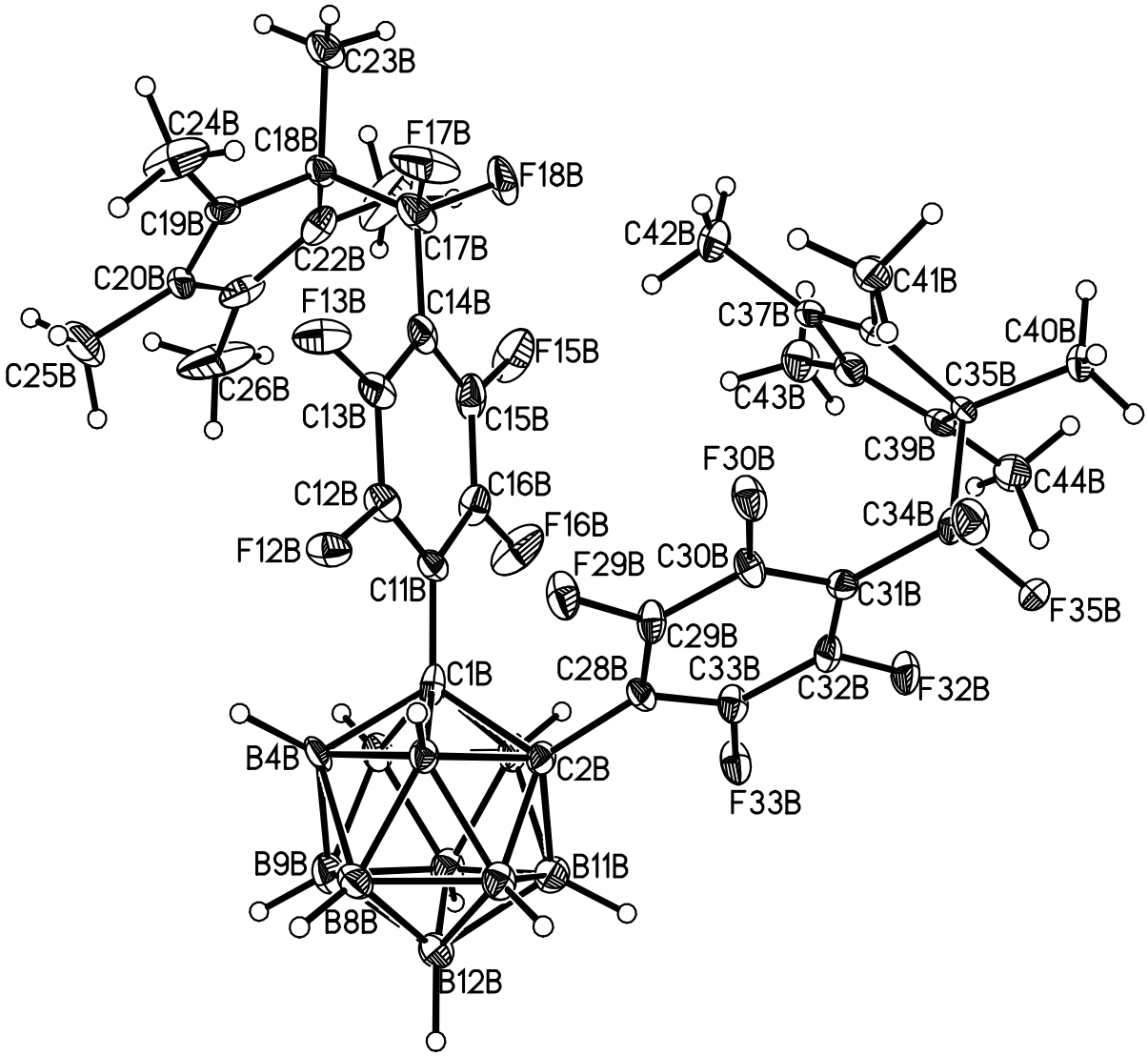

Figure 4.2.4.1 Perspective view of 1,2-(4'-$CF_2C_{10}H_{15}$-C_6F_4)$_2$-1,2-*closo*-$C_2B_{10}H_{10}$ (22). Displacement ellipsoids are drawn at the 50% probability level except for H atoms.

The reaction of $[Cp^*]^-$ with CF_3 groups in both perfluorotolyl units was demonstrated, revealing the vulnerability of these groups towards nucleophilic attack. This side reaction consumes **10** and disfavours the generation of supraicosahedral species. Nevertheless, the expansion of **10** with {Cp*Co} to generate metallacarboranes is possible, according to the other compounds isolated from the reaction mixture.

Compound **23** was characterised by elemental analysis and mass spectrometry (molecular ion at m/z 770) to reveal the presence of a 13-vertex cobaltacarborane of the formula $C_{26}H_{25}B_{10}CoF_{14}$. The ^{1}H-NMR spectrum revealed the presence of the Cp* ligand as a singlet at δ 1.7. Moreover, the perfluorotolyl groups were found intact as only three peaks were present in the ^{19}F-NMR spectrum of **23**. Finally, the ^{11}B-NMR spectrum revealed 8 signals between 8.78 and -14.0 ppm, in a pattern that resembles that obtained for compound **17**.

Unfortunately, although crystals of **23** were produced they were not of suitable quality for *X*-ray diffraction. Therefore, the identity of compound **23** was assigned as 1,12-(4'-$F_3CC_6F_4)_2$-4-Cp*-4,1,12-*closo*-$CoC_2B_{10}H_{10}$ by analogy with the ^{11}B-NMR spectrum of 1,12-(4'-$F_3CC_6F_4)_2$-4-Cp-4,1,12-*closo*-$CoC_2B_{10}H_{10}$ (**17**).

Another product (**24**) was isolated from this reaction. Although mass spectrometric analysis of the dark orange solid revealed the presence of the molecular ion at m/z 795, elemental analysis of **24** gave percentages of carbon and hydrogen that could not be interpreted.

The ^{1}H-NMR spectrum of the unknown compound revealed two distinct peaks corresponding to Cp* units, as if two different {Cp*Co} fragments were inserted in the cluster. In addition, peaks attributed to THF but shifted to higher frequencies were found in the proton spectrum of **24**, implying that a $(THF)^{+}$ unit was bonded to a cage vertex. Although the ^{19}F-NMR spectrum indicated only the presence of perfluorotolyl units, the ^{11}B-NMR spectrum of compound **24** displayed 6 independent signals spread over a wide range of the spectrum (from 20 to -20 ppm), confirming the presence of a metallacarborane. After great efforts, single crystals of **24** suitable for *X*-ray diffraction studies were obtained, allowing its complete structural characterisation (figure 4.2.4.2).

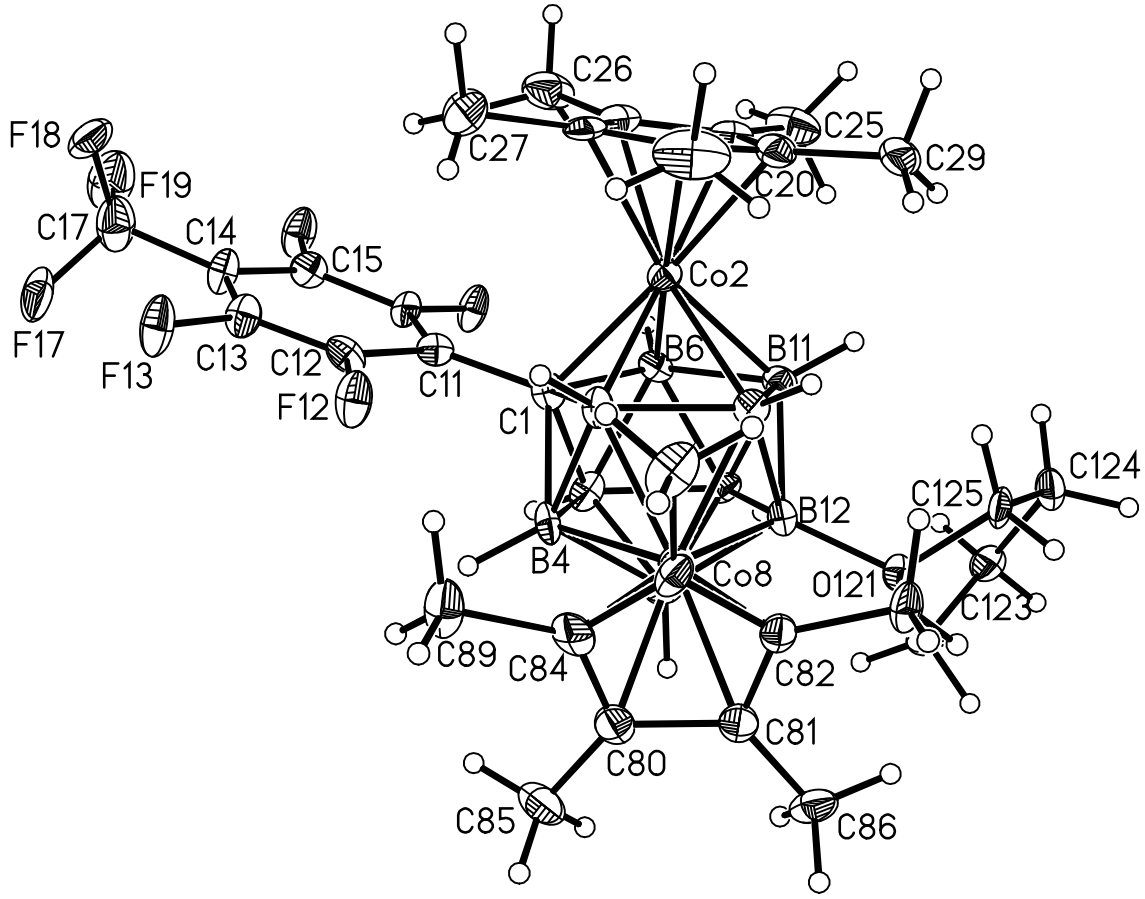

Figure 4.2.4.2 Perspective view of 1-(4'-$F_3CC_6F_4$)-2,8-Cp*$_2$-12-(THF)-2,8,1-*closo*-$Co_2CB_9H_8$ (24). Displacement ellipsoids are drawn at the 50% probability level except for H atoms.

Compound **24** was revealed to be the bimetallacarborane 1-(4'-$F_3CC_6F_4$)-2,8-Cp*$_2$-12-(THF)-2,8,1-*closo*-$Co_2CB_9H_8$. The structure of **24** is characterised by the presence of two {Cp*Co} units and a molecule of THF attached to the boron atom antipodal to the unique carbon vertex of the Co_2CB_9 icosahedron. The cage was found to be icosahedral with the metal atoms at vertices 2 and 8 and the single carbon atom at vertex 1. In accord with the Wade's rules, such an arrangement of atoms in an icosahedral cluster needs an extra electron. This extra electron appears as a negative charge at B12, compensated by the positive charge at the oxygen atom in the attached molecule of THF, leading to the observed zwitterionic **24**. This constitutes the first example of a "decarbonation" process (i.e. extrusion and loss of a carbon vertex) during polyhedral expansion procedures. A summary of the isolated products from the polyhedral expansion of **10** with {Cp*Co} is shown in figure 4.2.4.3.

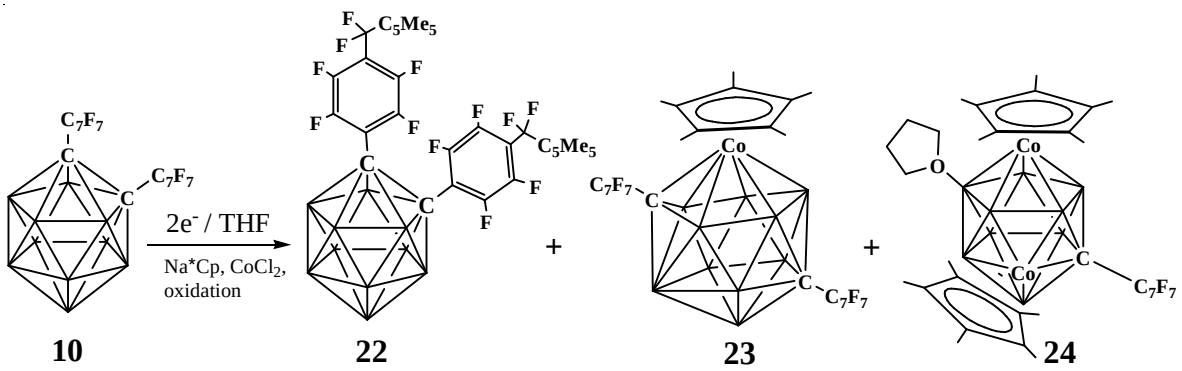

Figure 4.2.4.3 Schematic summary of the reduction and metallation with {Cp*Co} of 10 to afford compounds 22, 23 and 24.

The replacement of Cp by Cp* in the cobalt fragment employed for Red/Met purposes has led to dramatic changes in the expansion chemistry of **10**. Whereas a 4,1,12-species (**17**) was the unique product from Red/Met with {CpCo}, Red/Met with {Cp*Co} led to the formation of **23**, the Cp* analogue of **17**, as a secondary product in low yield. In addition, preliminary experiments on the expansion of **8** with {Cp*Co} led to the formation of an analogue of **22** as the major product of reaction, confirming the vulnerability of perfluorotolyl substituents towards nucleophiles. Due to the side reactions derived from the nucleophilic attack by $[Cp^*]^-$, the use of this ligand is discouraged.

Nevertheless, the steric and electronic nature of the {Cp*Co} fragment has led to the extraordinary compound **24** whose formation involves the unprecedented carbon vertex extrusion or "decarbonation". An exhaustive discussion about the expansion reactions of **10** and **8** to cobaltacarboranes is described in the following section.

4.2.5 Discussion.

The polyhedral expansion of 1,2-(4'-$F_3CC_6F_4)_2$-1,2-*closo*-$C_2B_{10}H_{10}$ (**10**) and 1-(4'-$F_3CC_6F_4$)-2-Ph-1,2-*closo*-$C_2B_{10}H_{10}$ (**8**) to supraicosahedral cobaltacarboranes has been reported in previous sections. Reduction and metallation with {CpCo} of **10** leads to the 4,1,12- metallacarborane (**17**) resulting from the isomerisation sequence 4,1,6- → 4,1,8- → 4,1,12-, as confirmed by the isolation of **21**. Although another 4,1,12- isomer, **23**, is also obtained from the metallation with the bulkier {Cp*Co} fragment, the yields are much lower due to side reactions. Thermolysis is generally required to obtain 4,1,12- species, however, the presence of perfluorotolyl groups appears to facilitate the isomerisation allowing the direct formation of **17** and **23** at even low temperatures and short reaction times.

In general, 4,1,6-MC_2B_{10} metallacarboranes generated from metallation of 7,9-*nido*-C_2B_{10} dianions are fluxional in solution presenting a single signal for both CH groups in ^{1}H- and ^{13}C-NMR spectra. For transition-metal species, the fluxionality can be arrested at low temperature[10] allowing the experimental determination of the activation energy (E_{act}) for certain metallacarboranes (figure 4.2.5.1).[11]

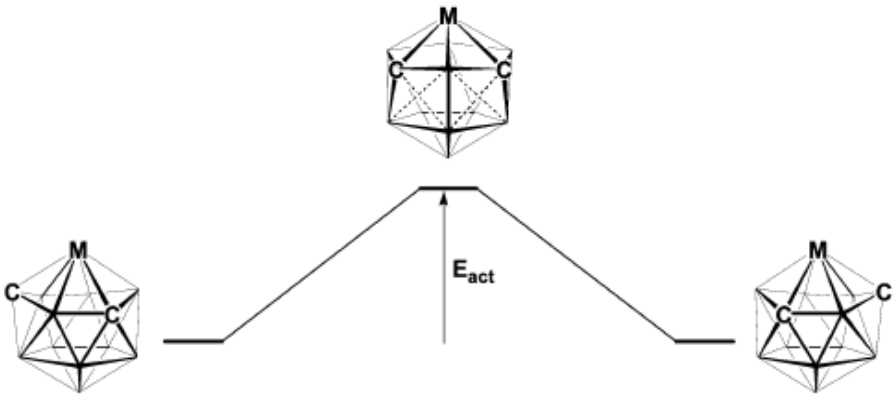

Figure 4.2.5.1 The double DSD process and the activation energy E_{act} involved in the fluxional equilibrium between 4,1,6-MC_2B_{10} species.

Thus the NMR spectra of symmetrically C,C'-substituted 4,1,6-MC_2B_{10} species are simplified due to fluxional equilibrium between enantiomers. However, the only 4,1,6- species obtained from the expansions of **10** and **8** to cobaltacarboranes are the M-C tethered supraicosahedral species **18** and **21**. The high number of signals observed in their ^{11}B-NMR spectra suggests that although regular 4,1,6- species are

fluxional in solution, the intramolecular cyclisation arrests the fluxionality leading to the formation of M-C tethered compounds **18** and **21** as mixtures of their possible diastereoisomers (**18A** and **18B** and **21A** and **21B**).

Therefore, the symmetrically substituted 4,1,6-MC_2B_{10} metallacarborane derived from **10** affords **21** as a mixture of the two possible diastereoisomers [1,4-μ-4,1,6-CoC_2B_{10} (**21A**) and 6,4-4,1,6-μ-CoC_2B_{10} (**21B**)] after the cyclisation, although only crystals of the 6,4-μ-4,1,6-CoC_2B_{10} form (**21B**, figure 4.2.3.1) were isolated. On the other hand, expansion of the asymmetrically substituted carborane **8**, would afford an asymmetrically substituted 4,1,6- metallacarborane which, although it is more likely to possess the electron withdrawing perfluorotolyl group on C1, should be fluxional in solution. Consequently, although the isolated single crystal of **18** was found to be the 1,4-μ-4,1,6-CoC_2B_{10} form (**18A**, figure 4.2.2.1), **18** is formed as a mixture of the two possible diastereoisomers, **18A** and **18B**, both clearly present by NMR. Indeed, the existence of the fluxional process between asymmetric 4,1,6-MC_2B_{10} species derived from **8** was confirmed by the isolation of compounds **18**, **19** and **20** (figure 4.2.5.2).

The fluxional process between 4,1,6- metallacarboranes derived from **8** has been confirmed, however, it appears that each of the fluxional forms prefer to undergo a different rearrangement (figure 4.2.5.2). As described previously, the more favoured isomer in the fluxional equilibrium should be the one that possesses the perfluorotolyl group on the four-connected vertex C1, which was only isolated as the M-C tethered compound **18A**. On the other hand, the less favoured form of the equilibrium, although it also undergoes the intramolecular cyclisation to **18B** (confirmed by NMR, figure 4.2.5.2), is the only fluxional form that appears to undergo isomerisation to a 4,1,8- species that ultimately leads to compounds **19** and **20** after loss of the {BH} unit.

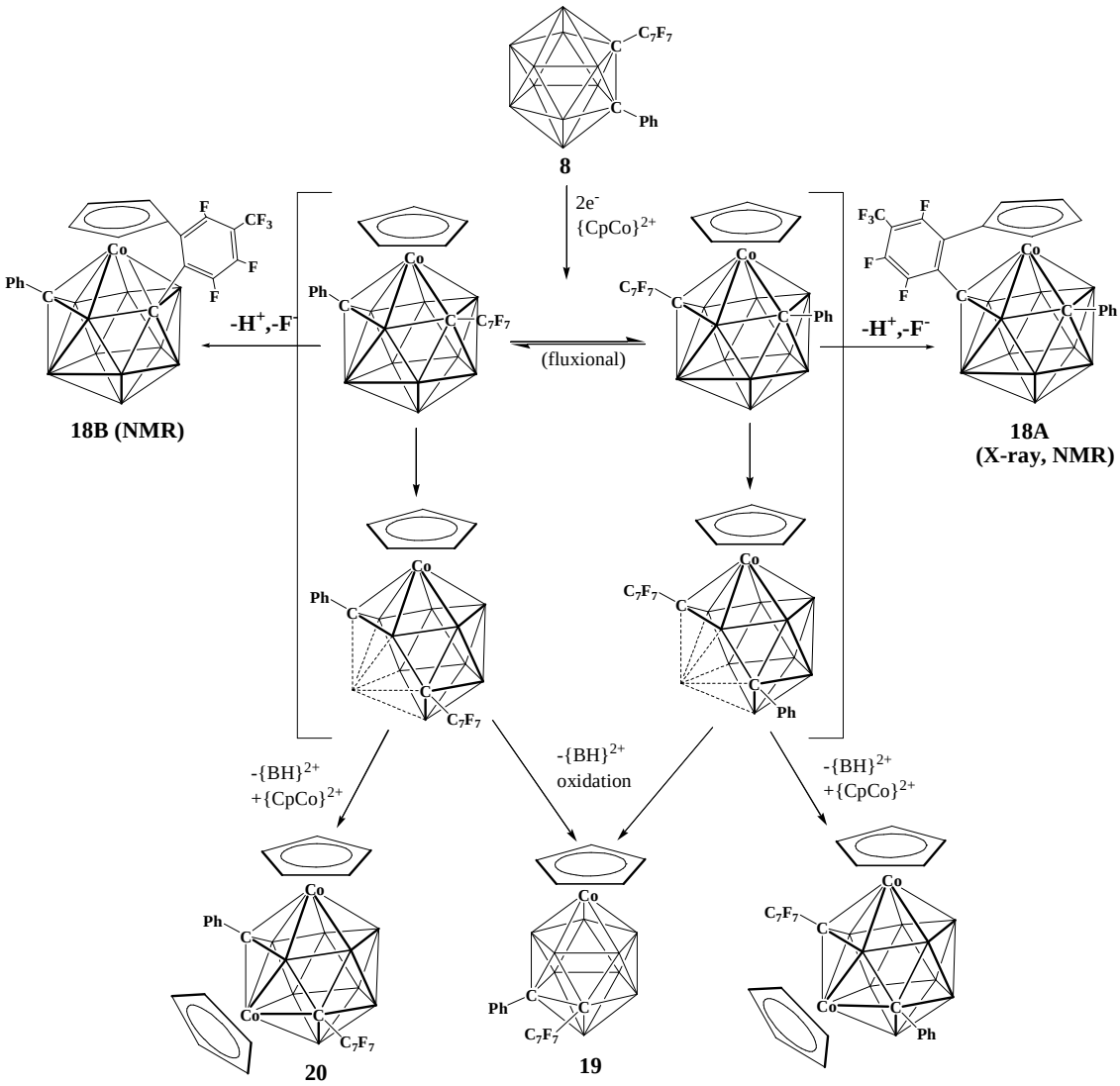

Figure 4.2.5.2 Importance of the fluxional process during the polyhedral expansion of 8 to afford compounds 18, 19 and 20.

In addition to compound **20**, another biscobaltacarborane has been isolated from Red/Met procedures on perfluorotolyl carboranes. Compound **24**, obtained from the reduction of **10** followed by the addition of {Cp*Co} represents the unique example of a "decarbonation" (i.e. extrusion and loss of a carbon vertex) from expansion reactions. In general, the reported examples of M_2CB_9 icosahedral species are the result of oxidative metal insertions to 11-vertex MCB_9 clusters.[12] However, icosahedral compound **24** is very unlikely to be formed from an 11-vertex precursor: since two metal fragments have been inserted into a cage that initially was 12-vertex (**10**), the degradation of a supraicosahedral cobaltacarborane to explain the formation of **24** would be more plausible. In fact, in order to rationalise the formation of **24**, five

independent steps have to be considered to account for the direct generation of a M_2CB_9 structure (**24**) from a regular C_2B_{10} carborane (**10**) (figure 4.2.5.3).

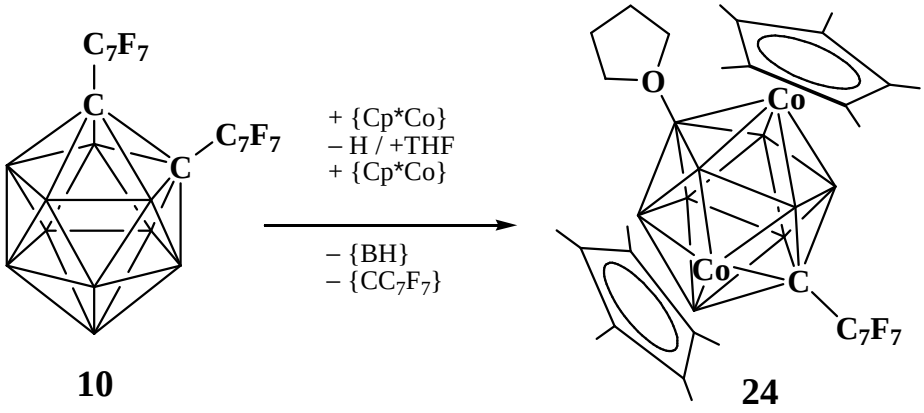

Figure 4.2.5.3 The five individual steps (in an arbitrary order) necessary for the transformation of 10 into 24.

Although five individual steps are necessary to obtain **24** from **10**, three of these steps have already been described in the formation of 1-Ph-4,5-Cp_2-6-(4'-$F_3CC_6F_4$)-4,5,1,6-*closo*-$Co_2C_2B_9H_9$ (**20**). The formation of **20** has been rationalised in terms of Red/Met of **8** to 4,1,6-MC_2B_{10}, followed by isomerisation to 4,1,8-MC_2B_{10}, then extrusion of a $\{BH\}^{2+}$ fragment to generate a new open face that is metallated again to afford a 4,5,1,6-$M_2C_2B_9$ cluster (**20**) (figure 4.2.5.2). Since compounds **20** and **24** are the only two examples of biscobaltacarboranes isolated from expansion of perfluorotolyl carboranes, it is appropriate to consider that their formation might involve some common steps.

The generation of a 4,5,1,6-$M_2C_2B_9$ species from the expansion of **10** with {Cp*Co}, following the mechanism described for **20**, should be disfavoured since the four-connected carbon vertex C1 would be in an extremely crowded position. Perhaps this steric crowding is the driving force that leads to the extraordinary "decarbonation" process. In fact, a closer inspection of 4,5,1,6-$M_2C_2B_9$ and $[M_2CB_9]^-$ structures reveals that both clusters are related by the simple removal of the four-connected C1 from the former and the subsequent making of a new B-B connection (figure 4.2.5.4).

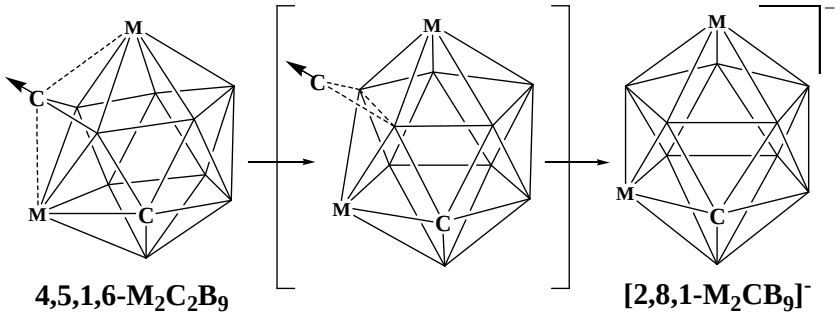

Figure 4.2.5.4 Proposed mechanism for the unprecedented decarbonation process.

Consequently, extrusion of the four-connected carbon vertex C1 (formally as $\{CC_7F_7\}^+$) in a hypothetical and extremely crowded 1,6-(4'-$F_3CC_6F_4)_2$-4,5-Cp*$_2$-4,5,1,6-*closo*-$Co_2C_2B_9H_9$ species could lead directly to the isolated 1-(4'-$F_3CC_6F_4$)-2,8-Cp*$_2$-2,8,1-*closo*-$Co_2CB_9H_8$ anion. Therefore, the only remaining step necessary to account for the formation of **24** would be the attachment of a THF molecule at the expense of a (B)H atom (formally lost as H^-) to stabilise the monocarborane anion and generate the charge-compensated zwitterion. Fortunately, the attachment of a THF solvent molecule to the boron vertex antipodal to carbon in MCB_{10} and M_2CB_9 species is a very well known process.[13] With the formation of **24** thus considered, a summary of the assumed polyhedral reactions of **10** to afford the icosahedral and supraicosahedral cobaltacarboranes isolated is summarised in figure 4.2.5.5.

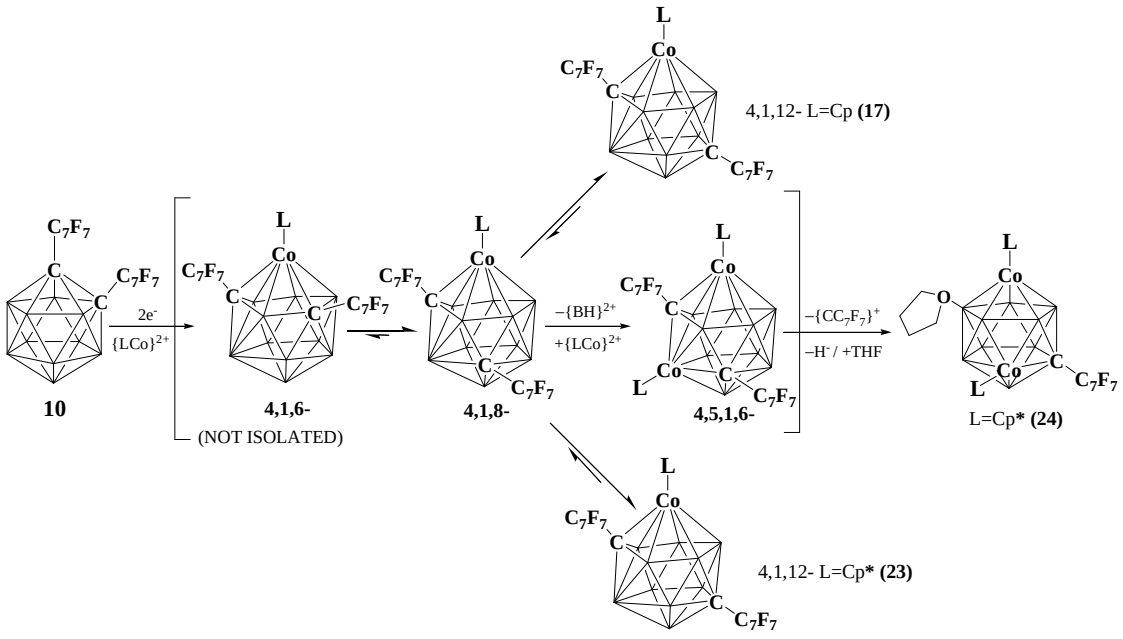

Figure 4.2.5.5 Summary of the expansion reactions of 10 to icosahedral and supraicosahedral cobaltacarboranes. Note the five independent steps required for the formation of 24.

In general, it seems that the presence of two perfluorotolyl groups on 7,9-*nido* dianions leads to rapid rearrangements to 4,1,12-CoC_2B_{10} species upon metallation with cobalt metal fragments. When only one perfluorotolyl group is present, the complete isomeration to 4,1,12- species is not observed, although the polyhedral expansion is possible and some of the generated supraicosahedral species undergo extraordinary decomposition pathways to afford novel icosahedral and supraicosahedral cobaltacarboranes. Interestingly, the presence of base promotes the generation of unprecedented M-C tethered 4,1,6- species when {CpCo} is utilised for metallation. On the other hand, although the use of pentamethylcyclopentadienyl cobalt {Cp*Co} prevents the formation of M-C tethered compounds, the stronger nucleophilic character of $[Cp^*]^-$ anions leads to side reactions in the perfluorotolyl units and consequently to lower yields of the expansion products. Nevertheless, the higher steric demand of {Cp*Co} fragments has been suggested to favour extraordinary reaction pathways such as the unprecedented extrusion of a carbon vertex.

In conclusion, the presence of perfluorotolyl groups allows the polyhedral expansion of icosahedral carboranes to afford 13-vertex cobaltacarboranes. The so-called "flexibility"[2d,4] of cobalt vertices in supraicosahedral metallacarborane chemistry along with the effect of perfluorotolyl groups leads to rapid rearrangements to 4,1,12-species. On the other hand, it appears that, depending on the nature of the ligand coordinated to the metal centre, side reactions with either aromatic or aliphatic fluorine atoms of the perfluorotolyl groups are observed. In order to prevent these side reactions and evaluate the ease of 4,1,6- → 4,1,12- rearrangements, polyhedral expansion with less flexible {ArRu} fragments will be investigated.

4.3 Expansion to 13-vertex ruthenacarboranes.

The experimental reduction of perfluorotolyl carboranes **10** and **8** and their consequent metallation to afford novel supraicosahedral cobaltacarboranes has been described in the previous section. Although the successful polyhedral expansion of these species has been demonstrated, side reactions have been observed due to the nature of Cp and Cp* ligands combined with the susceptibility towards nucleophilic substitution of fluorine atoms in perfluorotolyl groups. In principle, the prevention of side reactions by using different metal fragments would lead to simpler reaction mixtures. On the other hand, the use of different metal fragments could undoubtedly attribute the observed rearrangements between 4,1,X-MC_2B_{10} species to the influence of perfluorotolyl groups. Consequently, ruthenium-(η-arene) metal fragments {ArRu}, isolobal to {BH}, will be utilised in order to obtain new supraicosahedral species.

The use of ruthenium in the expansion of icosahedral carboranes has been extensively reported[14] because it generally affords neutral and air-stable yellow compounds that readily crystallise allowing the complete characterisation of the supraicosahedral species. Experimentally, the ruthenium fragment $\{ArRu\}^{2+}$ is generated in-situ by the cleavage of the stable dimer $[Ru(Ar)Cl_2]_2$. Despite the great scope of ruthenium-(η-arene) dimers, the three most common in metallacarborane chemistry are benzene (C_6H_6), hexamethylbenzene (C_6Me_6) and especially *para*-cymene ($^{i}Pr\text{-}C_6H_4\text{-}CH_3$).[15] Since vertex extrusion pathways due to steric hindrance between metal fragments and perfluorotolyl units have been reported in the previous section, the smallest ruthenium-arene fragment {(η-C_6H_6)Ru} was selected for the expansion of perfluorotolyl carboranes **10** and **8**.

4.3.1 Reduction/Metallation with {(η-C_6H_6)Ru} of 10.

After the selection of the {(η-C_6H_6)Ru} fragment due to its relatively small size, the polyhedral expansion of the bis(perfluorotolyl) carborane **10** was carried out in order to obtain supraicosahedral ruthenacarboranes.

Stoichiometric reduction with two equivalents of sodium naphthalenide of 1,2-(4'-$F_3CC_6F_4)_2$-1,2-*closo*-$C_2B_{10}H_{10}$ (**10**) in THF, was followed by treatment with half an equivalent of $[Ru(\eta\text{-}C_6H_6)Cl_2]_2$ at low temperature. The crude brown mixture was filtered and purified by column chromatography. Further purification by preparative TLC revealed two mobile bands, compounds **25** and **26**.

Mass spectrometric analysis of compound **25**, indicated the molecular ion at m/z 744, with typical carborane envelope, which is consistent with the formula of compound **25** as $C_{22}H_{15}B_9F_{14}Ru$, revealing the loss of one boron vertex. Elemental analysis of **25** gave results in good agreement with the formula above, confirming the loss of a {BH} unit.

Whereas the ^{1}H-NMR spectrum of **25** displayed a single signal corresponding to the η-coordinated benzene ring, the ^{19}F-NMR spectrum confirmed the presence of perfluorotolyl units. ^{11}B-NMR spectroscopy of the pale grey compound showed six independent resonances corresponding to nine different boron atoms in a 1:2:1:2:2:1 ratio pattern. From the spectroscopic analysis of **25**, the new compound was predicted to be a icosahedral cobaltacarborane, since the loss of a boron vertex was confirmed by mass spectrometry and the ^{11}B-NMR spectrum of **25** matches the number of signals expected for a 3,1,2-*closo*-MC_2B_9 structure. However, the ^{11}B-NMR resonances of **25** were found extremely shifted upfield, suggesting the presence of a pseudocloso cluster. An *X*-ray diffraction study of a single crystal of **25** revealed the molecular structure shown in figure 4.3.1.1.

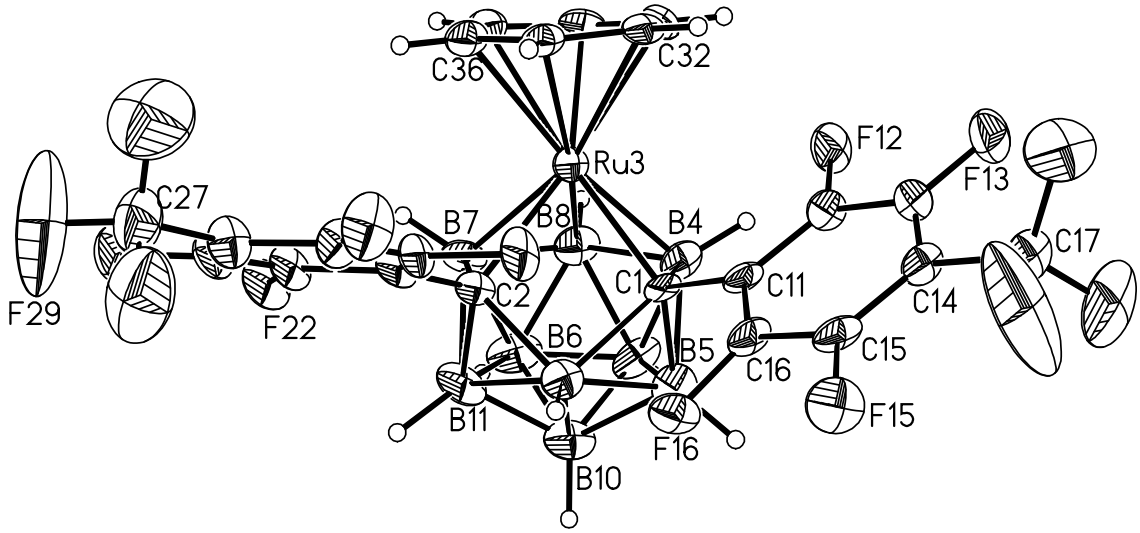

Figure 4.3.1.1 Perspective view of 1,2-(4'-$F_3CC_6F_4)_2$-3-(η-C_6H_6)-3,1,2-*pseudocloso*-$RuC_2B_9H_9$ (25). Displacement ellipsoids are drawn at the 50% probability level except for H atoms.

Compound **25** was found to be 1,2-(4'-$F_3CC_6F_4)_2$-3-(η-C_6H_6)-3,1,2-*pseudocloso*-$RuC_2B_9H_9$ after crystallographic characterisation. The cage was found to be pseudoicosahedral with the metal atom at vertex 3 and the carbon atoms at vertices 1 and 2. The structure is characterised by the missing bond between C1 and C2 vertices, leading to the observed pseudocloso icosahedron (figure 4.3.1.1). As was described previously, the formation of 3,1,2- icosahedral metallacarboranes as by-products of Red/Met expansion of *ortho*-carborane is a known process.[7] On the other hand, pseudocloso species are typically obtained as a result of the attempted synthesis of icosahedral 3,1,2-MC_2B_9 metallacarboranes derived from diphenyl carboranes, due to steric crowding.[16] Therefore, it is not surprising to isolate **25** as a by-product of the polyhedral expansion of **10**. Nevertheless, the isolation of **25** gives strong evidence of the steric demand of perfluorotolyl groups and constitutes another example of vertex extrusion as a result of perfluorotolyl carborane Red/Met procedures.

The crystallographic study of **25** revealed the C1···C2 distance to be 2.534 Å. As the cage carbon atoms C1 and C2 are forced apart by the steric demand of perfluorotolyl substituents, the Ru3 and B6 vertices to which they are both connected, are pulled together and the Ru3···B6 separation is reduced to 2.909 Å. In addition to the structural distortions, pseudocloso metallacarboranes have interesting spectroscopic features. In these clusters, the ^{11}B-NMR resonances appear at higher frequencies than

in closo metallacarboranes and as a result, their averaged ^{11}B chemical shift, $<\delta^{11}B>$, present particularly positive values. For example, the $<\delta^{11}B>$ of the C,C'-diphenyl analogue of **25**, 1,2-Ph_2-3-(η-C_6H_6)-3,1,2-*pseudocloso*-$RuC_2B_9H_9$**,**[16] was reported to be +5.36. In this new pseudocloso ruthenacarborane, **25**, the $<\delta^{11}B>$ was found to be +7.06, which is even more positive due to the influence of the electron withdrawing perfluorotolyl groups.

In addition to **25**, the major compound isolated from reduction and metallation with {(η-C_6H_6)Ru} of **10** was the pale yellow compound **26**. Mass spectrometry (molecular ion at m/z 756) and elemental analysis confirmed **26** to be a 13-vertex ruthenacarborane of formula $C_{22}H_{16}B_{10}F_{14}Ru$.

The ^1H-NMR spectrum of compound **26** confirmed the presence of the coordinated benzene ring as a single resonance at δ 6.2 and the ^{19}F-NMR spectrum suggested the equivalence of the two perfluorotolyl units, showing only the three typical signals. Interestingly, the five independent resonances displayed in the ^{11}B-NMR spectrum of **26**, although not conclusive for the definitive assignment of the expected 4,1,X-MC_2B_{10} species, revealed a pattern rather similar to that obtained for **17**, a 4,1,12-cobaltacarborane. An *X*-ray diffraction study of a single crystal of **26** confirmed the predictions revealing the species to be 1,12-(4'-$F_3CC_6F_4)_2$-4-(η-C_6H_6)-4,1,12-*closo*-$RuC_2B_{10}H_{10}$ (**26**) (figure 4.3.1.2).

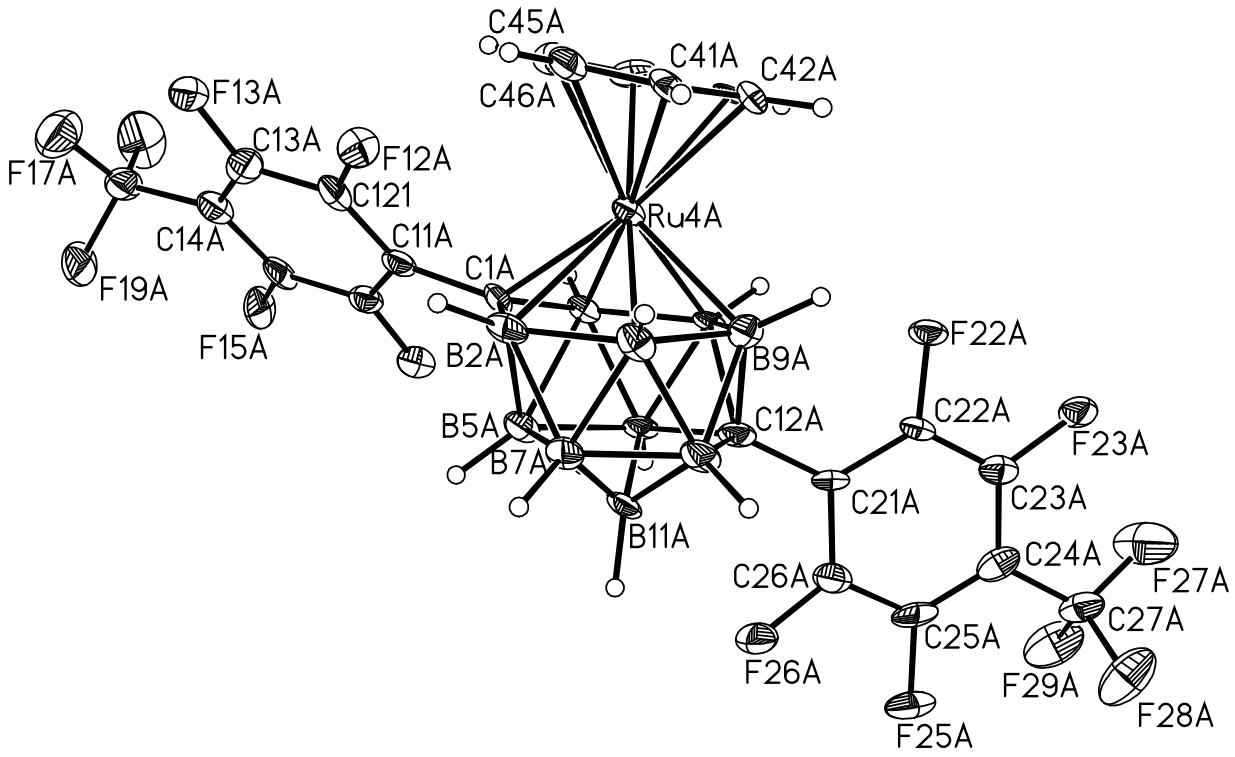

Figure 4.3.1.2 Perspective view of 1,12-(4'-$F_3CC_6F_4)_2$-4-(η-C_6H_6)-4,1,12-*closo*-$RuC_2B_{10}H_{10}$ (26) (one of two crystallographically-independent molecules). Displacement ellipsoids are drawn at the 50% probability level except for H atoms.

Interestingly, the only supraicosahedral product isolated from the expansion of **10** with {(η-C_6H_6)Ru} is compound **26**, a 4,1,12- 13-vertex ruthenacarborane. In the structural study the cage is shown to be docosahedral with the metal atom at vertex 4 and carbon atoms at vertices 1 and 12. An interesting feature of the structure is the angle of 9.41º adopted by the benzene ring, with respect to the cage lower belt, to minimise steric hindrance with the perfluorotolyl group bonded to C1 (figure 4.3.1.2). Although the direct formation of 4,1,12- species is already known from the expansion of **10** to cobaltacarboranes **17** and **23**, the room temperature generation of **26** is more remarkable due to the high temperatures that are normally required for the isomerisation of ruthenacarboranes.[4,9] The three 4,1,12- species (**17**, **23** and **26**) reported in this chapter constitute the first examples of low temperature formation of the most thermodynamically stable isomer of the 4,1,X-MC_2B_{10} series, directly from 1,2-C_2B_{10} carboranes.

Thus far, two perfluorotolyl groups appear to be necessary in order to obtain 4,1,12- species. The expansion with {(η-C_6H_6)Ru} of the asymmetric carborane **8** will be

described in the next section in order to evaluate how important the presence of two Ar_F groups is in the polyhedral expansion of perfluorotolyl carboranes.

4.3.2 Reduction/Metallation with {(η-C_6H_6)Ru} of 8.

The polyhedral expansion of compounds **10** and **8** has been reported in previous sections to afford quite different cobaltacarboranes. Once the expansion of **10** to ruthenacarboranes has been demonstrated to afford **26** (and **25**), it is interesting to study the reaction of **8**, as a means of evaluating the importance of mono- and di-substitution with perfluorotolyl groups towards polyhedral expansion chemistry.

The dark purple solution obtained from the stoichiometric reduction of **8** in THF was treated with half an equivalent of $[Ru(\eta\text{-}C_6H_6)Cl_2]_2$ at low temperature. The resulting brown suspension was filtered and purified by preparative TLC to reveal a single pale yellow band, compound **27**, as the unique metallacarborane product.

Mass spectrometric analysis of **27** showed the parent ion to have a mass of 615 with a broad heteroborane envelope from 611 to 620 whilst elemental analysis was in good agreement with the expected values for $C_{21}H_{21}B_{10}F_7Ru$ (a 13-vertex ruthenacarborane).

The new ruthenacarborane **27** was also analysed by multinuclear NMR spectroscopic techniques. The ^{1}H-NMR spectrum only displayed a multiplet in the aromatic region and a single resonance at δ 5.7, corresponding to phenyl and η-benzene groups of **27**, respectively. Whilst the presence of the single perfluorotolyl group of **27** was also confirmed by ^{19}F-NMR spectroscopy, the ^{11}B-NMR spectrum revealed five independent resonances corresponding to ten boron atoms in a 1:2:4:2:1 pattern of signals. In order to obtain the complete solid state molecular structure of the new ruthenacarborane, a single crystal of **27** was grown by solvent diffusion of petroleum ether and a concentrated solution of **27** in DCM and subjected to a *X*-ray diffraction study, revealing the molecular structure shown in figure 4.3.2.1.

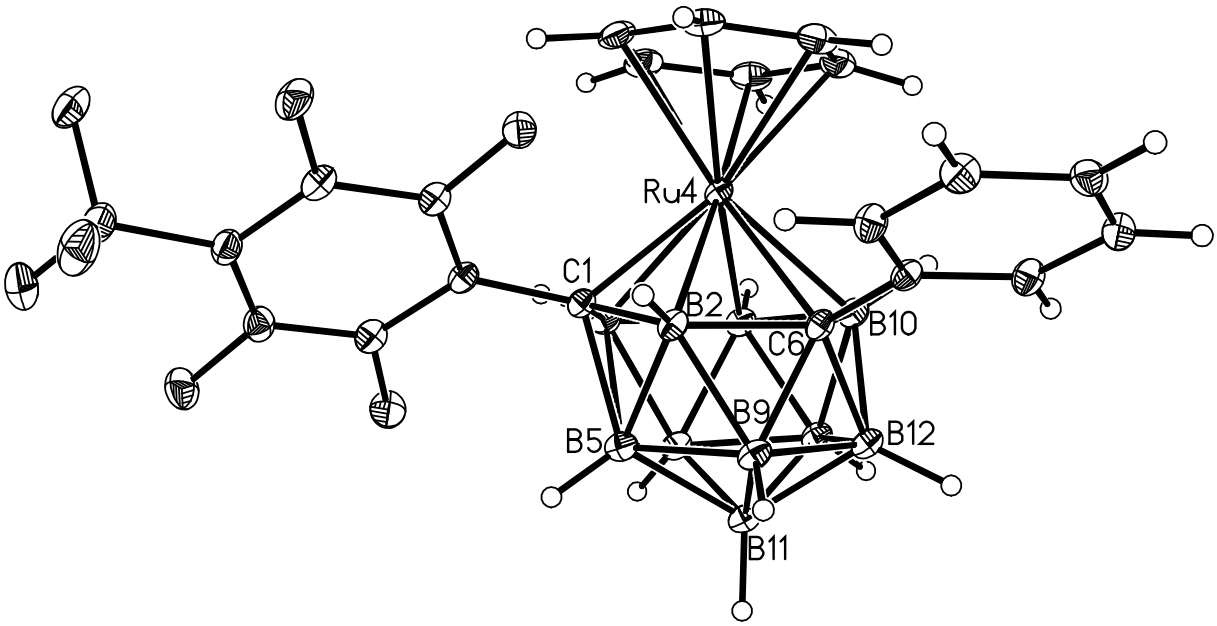

Figure 4.3.2.1 Perspective view of 1-(4'-$F_3CC_6F_4$)-4-(η-C_6H_6)-6-Ph-4,1,6-*closo*-$RuC_2B_{10}H_{10}$ (27). Displacement ellipsoids are drawn at the 50% probability level except for H atoms.

After crystallographic characterisation, the structure of the new compound was undoubtedly confirmed as 1-(4'-$F_3CC_6F_4$)-4-(η-C_6H_6)-6-Ph-4,1,6-*closo*-$RuC_2B_{10}H_{10}$ (**27**). The cage is found to be docosahedral with the metal atom at vertex 4 and carbon atoms at vertices 1 and 6. The solid state structure of **27** is characterised by the presence of the perfluorotolyl group at the four-connected vertex C1 and the angle of 9.54º adopted by the benzene ring, with respect to the cage lower belt, to minimise steric hindrance with perfluorotolyl and phenyl groups bonded to C1 and C6, respectively, in the cage upper belt (figure 4.3.2.1). After the complete characterisation of **27**, the polyhedral expansion of **8** to metallacarboranes has been once more demonstrated and more interestingly, the requirement of two perfluorotolyl groups in order to obtain 4,1,12- supraicosahedral species has been verified.

4.3.3 Discussion.

The expansion of **10** and **8** with {(η-C_6H_6)Ru} fragments to afford supraicosahedral ruthenacarboranes has been successfully accomplished. Whereas reduction and subsequent metallation of **10** leads to a 4,1,12- docosahedral species (**26**) together with a cage partial degradation product (**25**), the same process applied to **8** only affords the direct product that results from the metallation of 7,9-*nido* dianions, a 4,1,6- 13-vertex metallacarborane (**27**) (figure 4.3.3.1).

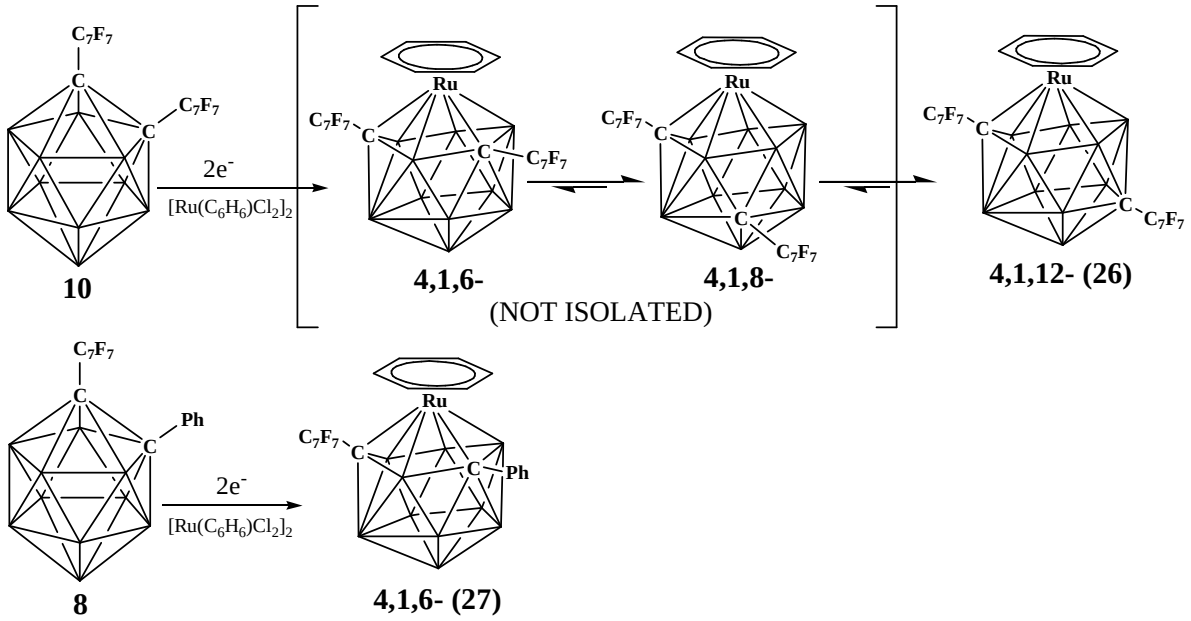

Figure 4.3.3.1 Schematic summary of the supraicosahedral species obtained as a result of the polyhedral expansion of compounds 10 and 8 to ruthenacarboranes.

As predicted, the expansion of **10** and **8** to ruthenacarboranes affords simpler mixtures of products than their expansion to cobaltacarboranes. The expansion of **10** to afford 1,12-(4'-$F_3CC_6F_4$)$_2$-4-(η-C_6H_6)-4,1,12-*closo*-$RuC_2B_{10}H_{10}$ (**26**) is analogous to the formation of supraicosahedral cobaltacarboranes (**17** and **23**) reported in an earlier section (4.2) and is thereby attributed to a rapid 4,1,6-MC_2B_{10} → 4,1,8-MC_2B_{10} → 4,1,12-MC_2B_{10} isomerisation cascade. Although the conditions required for the thermal isomeration of 4,1,6-MC_2B_{10} species generally depend on the nature of the metal, the presence of two perfluorotolyl groups has been found to facilitate the

required rearrangements regardless of which metal occupies position 4 of the docosahedron.

A different situation arises when only one perfluorotolyl group is present in the icosahedral starting material (**8**). The expansion of **8** to a supraicosahedral ruthenacarborane was found to afford 1-(4'-$F_3CC_6F_4$)-4-(η-C_6H_6)-6-Ph-4,1,6-*closo*-$RuC_2B_{10}H_{10}$ (**27**) as the unique isolated product of the reaction. This result is in good agreement with the reported expansions of *ortho*-carborane to 4,1,6-MC_2B_{10} species[1] and confirms the requirement of two perfluorotolyl units as necessary for the direct formation of 4,1,12- metallacarboranes.

Interestingly, no trace of the 4,1,8- isomer was isolated from any expansion experiment with $[Ru(\eta\text{-}C_6H_6)Cl_2]_2$. This isomer is generally obtained from thermal isomerisation of 4,1,6- species, although has also been reported as a by product from the expansion of 1,2-Ph_2-1,2-*closo*-$C_2B_{10}H_{10}$ (**G**).[3] The direct formation of 4,1,8-metallacarboranes from **G** is attributed to steric and electronic effects of the phenyl groups; nevertheless, the main products from reduction and metallation of **G** are always 4,1,6- species, regardless of what metal fragment is employed. Since perfluorotolyl groups are bulkier and much more electron withdrawing than phenyl rings, the isolation of 4,1,8- metallacarboranes from the expansion of compounds **10** and **8** was expected. Regarding the expansion of **10**, the formation of **26** has been rationalised in terms of two subsequent rapid rearrangements starting from the 4,1,6-isomer. Therefore it is reasonable that 4,1,8- species are just intermediates that readily transforms into **26**, making their isolation impossible.

A different situation arises during the polyhedral expansion of **8**. Since the 4,1,6-ruthenacarborane (**27**) was the only isolated product, the expansion chemistry of **8** and **G** to 13-vertex ruthenacarboranes could be regarded as similar processes. However, unlike for the expansion of **G**, no trace of the 4,1,8- isomer was found as result of the expansion of **8**. Decomposition of the missing 4,1,8- species might explain the experimental observations described above. As explained in previous sections, strong electron withdrawing perfluorotolyl groups are expected to favour the extrusion of weakly bonded boron vertices, such as the six-connected boron vertex B5 of 4,1,8-metallacarboranes. Following this principle, the predicted 4,1,8- ruthenacarboranes

derived from **8** would undergo degradation to either icosahedral 8,1,2-RuC_2B_9 or supraicosahedral 4,5,1,6-$Ru_2C_2B_9$ species, as described for the expansion of **8** to cobaltacarboranes. In conclusion, although the 4,1,8- ruthenacarborane derived from **8** was expected to be isolated as a minor product, either of these two predicted degradation pathways would dramatically decrease the reaction yields making the practical isolation and characterisation of any of these species impossible.

4.4 Expansion to 13-vertex carboranes.

The reduction and metallation of perfluorotolyl carboranes **10** and **8** with different metal fragments has been reported in previous sections. These reactions have been successful in preparing 13-vertex metallacarboranes confirming the reductive cage opening of **10** and **8** to afford 7,9-*nido* dianions. However, side reactions on the perfluorotolyl groups have been observed and, in addition, the presence of perfluorotolyl units has been demonstrated to promote the elimination of certain cage vertices, leading to cage degradation by-products. As a result, the yields of supraicosahedral metallacarboranes obtained from the expansion of compounds **10** and **8** are lower that those reported for the expansion of 1,2-Ph_2-1,2-*closo*-$C_2B_{10}H_{10}$ (**G**). Nevertheless, since reduction and metallation (Red/Met) procedures have been proved to be possible, the reduction of perfluorotolyl carboranes and the subsequent capitation (Red/Cap) with boron fragments was attempted in order to prepare supraicosahedral carboranes.

4.1 Attempted expansion of 10 and 8 with {BR} (R = H, Ph).

The polyhedral expansion of **10** and **8** to afford supraicosahedral carboranes was exhaustively attempted in several independent experiments with different solvents and boron fragments. Each perfluorotolyl carborane was first reduced with two equivalents of sodium naphthalenide in “oxygen-free” THF to afford either a dark red or a dark purple coloured solution of the 7,9-*nido* dianion of **10** or **8**, respectively. After the reduction step, solvent was completely removed under reduced pressure to afford oily residues that were taken into “oxygen-free” toluene or DCM. The resulting suspensions were treated with an excess of the corresponding dihaloborane (RBX_2) at low temperature and, finally, the mixture was allowed to warm over a few hours. A summary of the Red/Cap experiments performed is shown in table 4.1.1.

Experiment	Reduction	Capitation	Conditions
1	**10** + $2e^-$ (THF)	2 x $HBBr_2$•SMe_2	Toluene, -78°C
2	**8** + $2e^-$ (THF)	2 x $HBBr_2$•SMe_2	Toluene, -78°C
3	**10** + $2e^-$ (THF)	2 x $PhBCl_2$	Toluene, -78°C
4	**8** + $2e^-$ (THF)	2 x $PhBCl_2$	Toluene, -78°C
5	**10** + $2e^-$ (THF)	2 x $HBBr_2$•SMe_2	DCM, -78°C
6	**8** + $2e^-$ (THF)	2 x $HBBr_2$•SMe_2	DCM, -78°C

Table 4.4.1 Summary of the Red/Cap experiments performed on compounds 10 and 8.

In all the experiments, the dark colours observed for the reduced carboranes slowly disappeared upon the addition of two equivalents of dihaloborane. Interestingly, the red colour observed after reduction of bis(perfluorotolyl) carborane **10** remained after $\{BR\}^{2+}$ addition for longer than the purple colour observed after reduction of **8**, which is good evidence of the higher stability of the 7,9-*nido* species derived from **10**. However, although the oily residues recovered after solvent removal were analysed by mass spectrometry and multinuclear NMR spectroscopy, and in spite of the extreme care taken during these Red/Cap expansions, none of the experiments afforded supraicosahedral species. According to the analyses, the attempted expansion of compounds **10** and **8** to supraicosahedral carboranes only afforded the re-oxidised icosahedral 1,2-*closo*-C_2B_{10} species.

4.5 General summary and conclusions.

The expansion of perfluorotolyl carboranes **10** and **8** to supraicosahedral metallacarboranes has been successful, although in some cases low yields are afforded due to side reactions on the fluorinated substituents. Nevertheless, the steric demand and the electronic influence of perfluorotolyl groups have led to novel isomeration and degradation pathways, previously unknown in metallacarborane chemistry. On the other hand, perfluorotolyl groups have been shown to be robust enough to allow the reductive cage opening necessary for expansion purposes. However, their stabilisation of reduced carborane dianions does not favour boron insertion, or in other words, the expansion to supraicosahedral carboranes. Figures 4.5.1 and 4.5.2 summarise the expansion chemistry of compounds **10** and **8**, respectively.

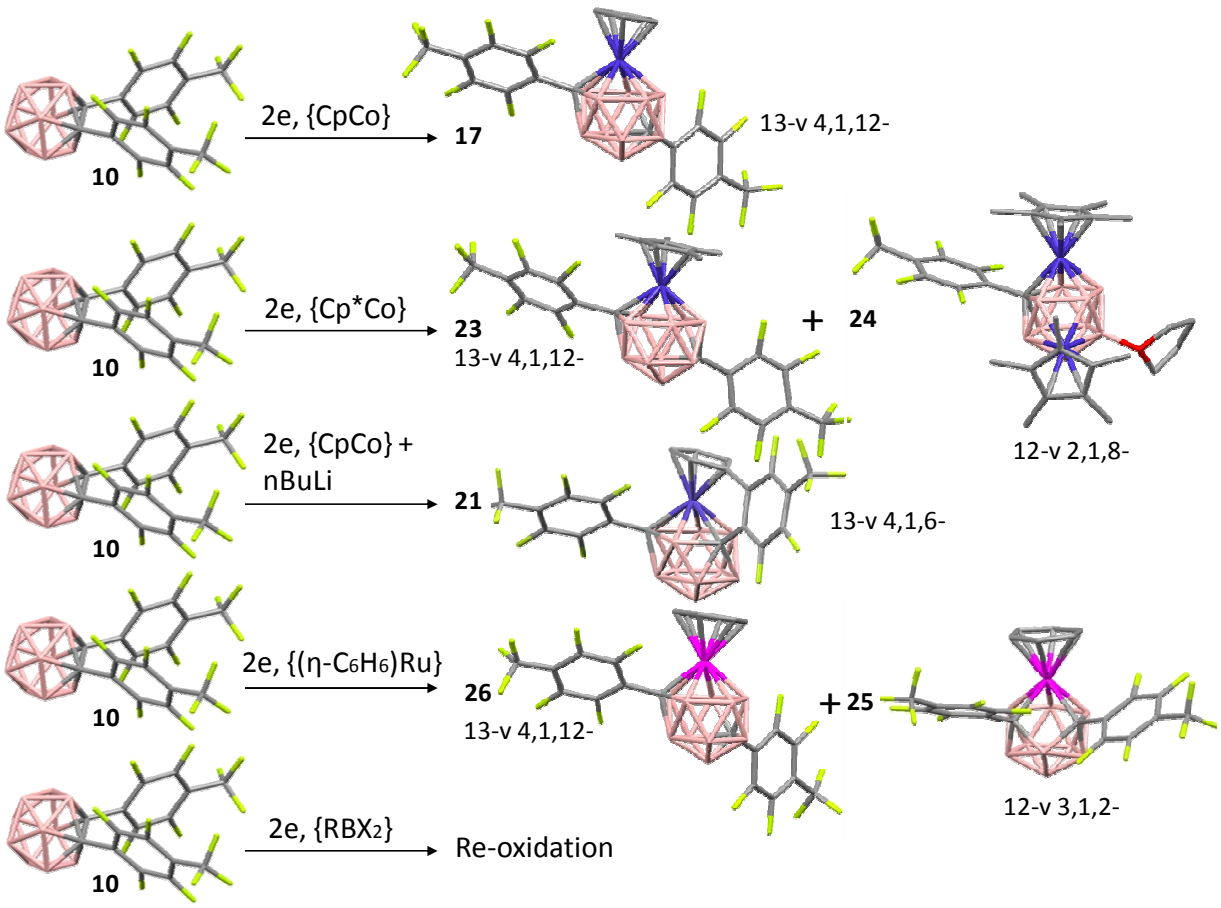

Figure 4.5.1 Schematic summary of the polyhedral expansion experiments on 10 to afford metallacarboranes 17, 21, 23, 24, 25 and 26 and the attempted expansion to 13-vertex carboranes. Hydrogen atoms omitted for clarity.

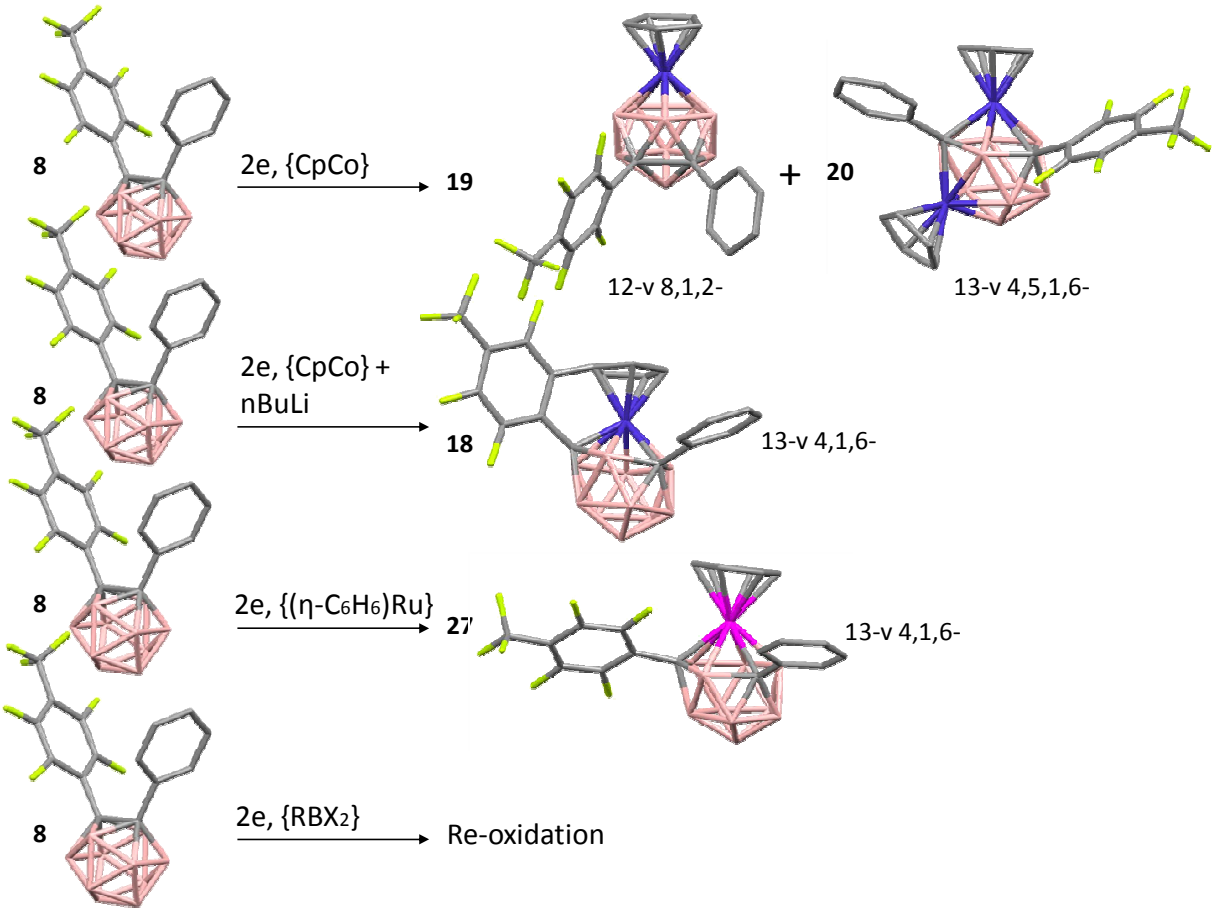

Figure 4.5.2 Schematic summary of the polyhedral expansion experiments on 8 to afford metallacarboranes 18, 19, 20 and 27 and the attempted expansion to 13-vertex carboranes. Hydrogen atoms omitted for clarity.

It can be concluded that the two-electron reduction of perfluorotolyl compounds **10** and **8** leads to 7,9-*nido* dianionic species. These nido intermediates can be treated with a suitable metal fragment, isolobal to {BH}, to obtain metallacarboranes, the derived isomer of which depends on the nature of the metal and the number of perfluorotolyl groups in the starting material. Undesired reactions, mainly due to C-F activation, are also observed.

In the case of **10**, which bears two perfluorotolyl groups, the main product of reduction and metallation is the 4,1,12-MC_2B_{10} 13-vertex metallacarborane, regardless of which metal fragment is utilised. The unprecedented direct formation of 4,1,12- species from a carbon atoms adjacent icosahedral starting material is attributed to a rapid 4,1,6-MC_2B_{10} → 4,1,8-MC_2B_{10} → 4,1,12-MC_2B_{10} isomerisation sequence promoted by the steric demand and the electronic influence of perfluorotolyl

groups. Nevertheless, the rapid isomerisation cascade has to be mainly due to the electronic influence of perfluorotolyl groups as the second rearrangement (4,1,8-MC_2B_{10} → 4,1,12-MC_2B_{10}) is independent of the steric hindrance between the ligand coordinated to the metal and the substituents attached to the cage carbon atoms.

The asymmetrically substituted compound **8**, which has only one perfluorotolyl group in the molecule, undergoes different rearrangements depending on which metal is employed in metallation. Reduction and subsequent metallation with ruthenium-arene fragments leads to 4,1,6-MC_2B_{10} species, the direct product from metallation of the 7,9-*nido* dianion generated after reduction. However, when cobalt fragments are employed in the metallation step, the expected 4,1,6- isomer spontaneously converts to the 4,1,8- form, which undergoes extraordinary degradation routes to either new isomers of icosahedral metallacarboranes or supraicosahedral bimetallacarboranes.

In addition, perfluorotolyl groups have been shown to promote boron atom extrusion, especially the elimination of those six-connected boron vertices directly bonded to two cage carbon atoms. Nevertheless, although these groups favour cage degradation, they also stabilise the resultant anionic nido structures allowing the direct synthesis of bimetallacarboranes.

Finally, whilst the stabilisation of 7,9-*nido* species by the negative inductive effect of electron withdrawing groups attached to the cage carbon atoms reduces re-oxidation as predicted computationally, it does not favour {BR} insertion into the open face and the consequent generation of supraicosahedral carboranes. In fact, it may be that preventing the oxidation of the reduced intermediates actually disfavours the insertion of any fragment into the six-atom open face, based on the yields of 13-vertex metallacarboranes obtained. Many reasons could account for these experimental observations. The greater energy mismatch between stabilised 7,9-*nido* dianions and incoming fragments might disfavour adequate orbital overlap and consequent insertion. Moreover, perfluorotolyl groups have been demonstrated to promote the extrusion of six-connected boron vertices, thus the hypothetical 13-vertex carborane derived from boron insertion into a reduced perfluorotolyl carborane could be really prone to decomposition, which in this case means re-oxidation back to an icosahedral species. Nevertheless, although unsuccessful in preparing 13-vertex carboranes, the

use of perfluorotolyl groups has led to the discovery of novel and unprecedented reactions in metallacarborane chemistry, leading to the isolation of previously unknown species and enhancing our understanding of this particular field of chemistry.

4.5 References.

4.1 G. B. Dunks, M. M. McKown and M. F. Hawthorne, *J. Am. Chem. Soc.*, 1971, **93**, 2541.

4.2 For example: a) M. R. Churchill and B. G. DeBoer, *Chem. Commun.*, 1972, 1326; b) A. Burke, R. McIntosh, D. Ellis, G. M. Rosair and A. J. Welch, *Collect. Czech. Chem. Commun.*, 2002, **67**, 991; c) M. E. Lopez, M. J. Edie, D. Ellis, A. Horneber, S. A. Macgregor, G. M. Rosair and A. J. Welch, *Chem. Commun.*, 2007, 2243; d) G. Scott, A. McAnaw, D. McKay, A. S. F. Boyd, D. Ellis, G. M. Rosair, S. A. Macgregor, A. J. Welch, F. Laschi, F. Rossi and P. Zanello, *Dalton Trans*., 2010, **39**, 5286.

4.3 A. Burke, PhD Thesis, *Heriot-Watt University*, 2002.

4.4 S. Zlatogorsky, D. Ellis, G. M. Rosair and A. J. Welch, *Chem. Commun.*, 2007, 2178.

4.5 D. Ellis, M. E. Lopez, R. McIntosh, G. M. Rosair, A. J. Welch and R. Quenardelle, *Chem. Commun.*, 2005, 1348.

4.6 S. Zlatogorsky, M. J. Edie, D. Ellis, S. Erhardt, M. E. Lopez, S. A. Macgregor, G. M. Rosair and A. J. Welch, *Angew. Chem. Int. Ed.*, 2007, **46**, 6706.

4.7 D. F. Dustin, G. B. Dunks and M. F. Hawthorne, *J. Am. Chem. Soc.*, 1973, **95**, 1109.

4.8 D. F. Dustin and M. F. Hawthorne, *J. Am. Chem. Soc*., 1974, **96**, 3462.

4.9 S. Zlatogorsky, PhD Thesis, *Heriot-Watt University*, 2007.

4.10 E. W. Abel, J. K. Bhargava and K. G. Orrell, *Prog. Inorg. Chem*.,1984, **32**, 1.

4.11 M. A. Laguna, D. Ellis, G. M. Rosair and A. J. Welch, *Inorg. Chim. Acta*, 2003, **347**, 161.

4.12 For example: a) S. Du, J. A. Kautz, T. D. McGrath and F. G. A. Stone, *Inorg. Chem*. 2001, **40**, 6563; b) S. Du, J. A. Kautz, T. D. McGrath and F. G. A. Stone, *Inorg. Chem*. 2002, **41**, 3202; c) T. D. McGrath, A. Franken, J. A. Kautz and F. G. A. Stone, *Inorg. Chem*. 2005, **44**, 8135.

4.13 For example: a) M. Gomez-Saso, D. F. Mullica, E. Sappenfield and F. G. A. Stone, *Polyhedron*, 1996, **15**, 793; b) S. Du, J. A. Kautz, T. D. McGrath and F. G. A. Stone, *Dalton Trans.*, 2001, 2791; c) J. A. Kautz, D. A. Kissounko, N. S. Kissounko and F. G. A. Stone, *Organometallics*, 2002, **21**, 2547; d) X. L. Lu, T. D. McGrath and F. G. A. Stone, *Organometallics*, 2006, **25**, 2590; e) D. D.

Ellis, A. Franken, P. A. Jelliss, F. G. A. Stone and P.-Y. Yu, *Organometallics*, 2009, **19**, 19.

4.14 For example: a) A. Burke, D. Ellis, D. Ferrer, D. L. Ormsby, G. M. Rosair and A. J. Welch, *Dalton Trans.*, 2005, 1716; b) R. McIntosh, D. Ellis, G. M. Rosair and A. J. Welch, *Angew. Chem. Int. Ed.*, 2006, **45**, 4313; J. Zhang, L. Deng, H.-S. Chan and Z. Xie, *J. Am. Chem. Soc.*, 2007, **129**, 18.

4.15 For example: a) M. A. Bennett and A. K. Smith, *Dalton Trans.*, 1974, 233; b) M. A. Bennett, T. N. Huang, T. W. Matheson and A. K. Smith, *Inorg. Synth.*, 1982, **21**, 73.

4.16 P. T. Brain, M. Bühl, J. Cowie, Z. G. Lewis and A. J. Welch, *Dalton Trans.*, 1996, 231.

CHAPTER 5. Experimental Section

5.1 General experimental.

5.1.1 Syntheses.

All experiments were performed under an atmosphere of dry, oxygen free, dinitrogen using standard Schlenk techniques, with some manipulations being completed in the open laboratory. Most of the ultimate compounds reported in this thesis are air stable. Solvents used were freshly distilled over CaH_2 (CH_3CN and CH_2Cl_2) or sodium wire [THF, petroleum ether (b.p. 40-60°C) and toluene] under nitrogen and were degassed (3 x freeze-pump-thaw cycles) prior to use, or were stored over molecular sieves. Preparative thin layer chromatography (TLC) employed 20 x 20 cm Kiesegel 60 F_{254} glass plates.

5.1.2 Analyses.

NMR spectroscopy was carried out on a Bruker DPX400 spectrometer (^1H spectra at 400.1 MHz, ^{11}B spectra at 128.4 MHz and ^{19}F spectra at 376.5 MHz). Unless stated otherwise, spectra were recorded at room temperature (298 K) from $CDCl_3$ solutions; chemical shifts are reported relative to tetramethylsilane (^1H) or BF_3.OEt (^{11}B and ^{19}F). The broad uninformative peaks corresponding to hydrogens attached to cage borons observed in the ^1H-NMR spectra for carboranes and metallacarboranes are not reported in this section.

EI (Low. Res.) mass spectrometry was carried out using a Kratos Concept mass spectrometer and elemental analyses (CHN) were carried out using a Exeter CE-440 Elemental Analyser by the Chemistry Department services of Heriot-Watt University.

5.1.3 Hazards.

Standard principles of safe handling and good general laboratory practice were followed, including the wearing of protective clothing and safety glasses. Extra care and attention was employed when handling flammable solvents, volatile compounds, sodium and lithium metals and toxic carboranes.

5.1.4 Standard Preparations.

Compounds 1,7-$(CH_2OH)_2$-1,7-*closo*-$C_2B_{10}H_{10}$,[1] 1,8-$(C{\equiv}CH)_2$-$C_{14}H_8$,[2] C_6F_5-C≡C-Ph,[3] 1-Ph-1,2-*closo*-$C_2B_{10}H_{11}$,[4] 1,2-Ph_2-1,2-*closo*-$C_2B_{10}H_{10}$,[5] 4-$F_3CC_6H_4$-C≡C-Ph,[6] 4-$F_3CC_6H_4$-C≡C-4'-$C_6H_4CF_3$,[7] 9,10-Ph_2-1,7-*closo*-$C_2B_{10}H_{10}$[8] and $[Ru(\eta\text{-}C_6H_6)Cl_2]_2$[9] were prepared using literature methods or slight variants thereof. All other reagents and solvents were supplied commercially and used as received.

5.1.5 Electrochemistry measurements.

Electrochemical studies (Cyclic Voltammetry) were performed by Prof. P. Zanello and co-workers (University of Siena, Italy) in a standard three-electrode cell having a gold working electrode surrounded by a platinum-spiral counter electrode and the aqueous saturated calomel reference electrode (SCE) mounted with a Luggin capillary. The different carboranes were analysed in a solution of anhydrous THF for electrochemical measurements. Electrochemical grade $[NBu_4][PF_6]$ from Fluka was used as the supporting electrolyte. Either a BAS 100A electrochemical analyzer or a multipurpose Amel instrument (Model 566 analog function generator and a Model 552 potentiostat) were used as polarizing units. All the potential values are referred to the saturated calomel electrode (SCE). Under the present experimental conditions the one electron oxidation of ferrocene occurs at E°' = +0.53 V in THF solution. The different compounds were analysed at different scan rates (0.1, 0.2, 0.4, 0.8 and 1 $V\ s^{-1}$) in order to determine the reversibility of the redox processes.

5.1.6 Crystallographic data collection and analysis.

X-ray diffraction quality single crystals were mounted in inert oil on a glass fibre and cooled to 100K by an Oxford Cryosystems Cryostream. All measurements were made on a Bruker X8 APEX2 diffractometer,[10] employing graphite-monochromated Mo-K_α *X*-radiation (λ = 0.71069 Å) and were corrected for absorption semi-empirically from symmetry–equivalent and repeated reflections. Structures were solved by direct and difference Fourier methods and refined by full-matrix least-squares against F^2 using the SHELXTL program suite.[11] Refinement was completed with all non-hydrogen atoms assigned anisotropic displacement parameters. Geometric measurements were made using Mercury software.[12]

5.2 Chapter 2. Stabilisation by control of the carbon atoms movement in reduced carboranes

5.2.1 Synthesis of 1,7-$(CH_2OSO_2CF_3)_2$-1,7-*closo*-$C_2B_{10}H_{10}$ (1)

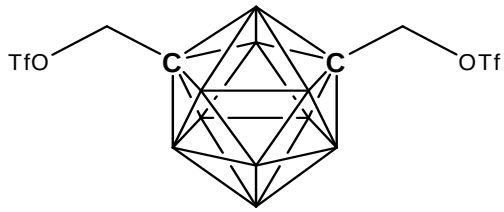

A solution of Tf_2O (1.24 g, 4.4 mmol) in CH_2Cl_2 (5 ml) was added dropwise to a mixture of 1,7-$(CH_2OH)_2$-1,7-$C_2B_{10}H_{10}$ **(D)** (0.408 g, 2 mmol) and pyridine (0.313 g, 4 mmol) in CH_2Cl_2 (15 ml) at 0ºC. The resultant mixture was stirred for 2 hours at room temperature and then water (15 ml) was added. The organic layer was separated, washed with water and dried over anhydrous $MgSO_4$. The solvent was removed under vacuum, affording 0.92 g (98%) of **1** as a colourless oil.

^{1}H-NMR (400.1 MHz, $CDCl_3$, 298 K): δ = 4.52 (s, 4H, -CH_2-)

^{11}B{^{1}H}-NMR (128.4 MHz, $CDCl_3$, 298 K): δ = -5.90 (2B), -10.30 (2B), -11.65 (4B), -16.03 (2B)

^{19}F-NMR (376.5 MHz, $CDCl_3$, 298 K): δ = -74.24 (s, 3F, -CF_3)

Mass Spectrometry (low res. EI): FW $C_6H_{14}B_{10}F_6O_6S_2$ = 468.40 g/mol
M^+ = m/z 466 (with typical carborane envelope from 463 to 469). Fragment ion: m/z 315 (loss of one -OTf group)

CHN: $C_6H_{14}B_{10}F_6O_6S_2$ requires C 15.39%, H 3.01%; found C 15.51%, H 3.05%

5.2.2 Synthesis of

1,7-$(CH_2I)_2$-1,7-*closo*-$C_2B_{10}H_{10}$ (2)

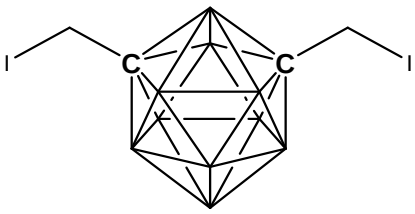

A suspension of 1,7-$(CH_2OSO_2CF_3)_2$-1,7-$C_2B_{10}H_{10}$ **(1)** (1.0 g, 2.14 mmol) and NaI (0.64 g, 4.28 mmol) in THF (30 ml) was vigorously stirred and heated to reflux for 10 hours. The solvent was removed and the residue was taken up in 10 ml of Et_2O. This solution was washed with water and dried over anhydrous $MgSO_4$. The solvent was removed under vacuum, affording a colourless oil. Recrystallisation at -30ºC afforded 0.86 g (95%) of **2** as white solid.

^{1}H-NMR (400.1 MHz, $CDCl_3$, 298 K): δ = 3.65 (s, 4H, -CH_2-)

^{11}B{^{1}H}-NMR (128.4 MHz, $CDCl_3$, 298 K): δ = -6.18 (2B), -10.30 (6B), -11.75 (2B)

Mass Spectrometry (low res. EI): FW $C_4H_{14}B_{10}I_2$= 423.92 g/mol
M^+ = m/z 424 (with typical carborane envelope from 420 to 426). Fragment ion: m/z 295 (loss of one I atom)

CHN: $C_4H_{14}B_{10}I_2$ requires C 11.33%, H 3.33%; found C 12.04%, H 3.62%

5.2.3 Synthesis of 1,8-bis[(hydroxymethyl)ethynyl]-anthracene (3)

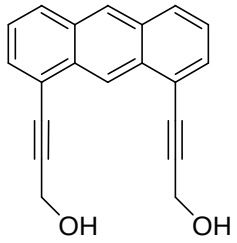

2 g of 1,8-diethynylanthracene **(C)** (8.8 mmol) was dissolved in 30 ml of THF in a Schlenk tube. This solution was cooled to -78ºC. Then 7.92 ml (19.8 mmol) of n-BuLi were added by syringe through a rubber septum. The solution turned a dark brown colour. This mixture was stirred for 2 hours at -78ºC. At this point the solution was frozen in liquid N_2 at -196ºC and 0.594 g (19.8 mmol) of paraformaldehyde were then added to the mixture in one portion. The solution was stirred at -78ºC for 2 additional hours and was then quenched by the addition of 15 ml of saturated aqueous NH_4Cl. The orange organic layer was extracted, washed with more NH_4Cl solution (2 x 10ml) and then with NaCl solution. The organic layer was then extracted, dried over anhydrous $MgSO_4$ and concentrated at reduced pressure to afford a yellow solid. Recrystallisation from hexane-THF (3:1) afforded 0.93 g (37% yield) of analytically pure **3** as yellow needles.

^{1}H-NMR (400.1 MHz, $CDCl_3$, 298 K): δ = 9.56 (s, 1H, 9-anth), 8.47 (s, 1H, 10-anth), 8.15 (d, 2H, 4,5-anth), 7.74 (d, 2H, 3,6-anth), 7.52 (dd, 2H, 2,7-anth), 4.78 (s, 4H, -CH_2-), 3.05 (bs, 2H, -OH)

Mass Spectrometry (low res. EI): FW $C_{20}H_{14}O_2$ = 286.33 g/mol
M^+ = m/z 286. Fragment ion: m/z 256 (loss of one -CH_2OH group)

CHN: $C_{20}H_{14}O_2$ requires C 83.9%, H 4.93%; found C 84.25%, H 4.90%

5.2.4 Synthesis of 1,8-bis[(bromomethyl)ethynyl]-anthracene (4)

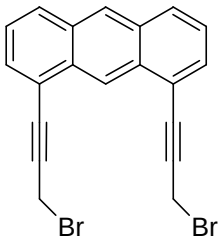

To a solution of 1,8-bis[(hydroxymethyl)ethynyl]-anthracene **(3)** (1.971 g, 6.89 mmol) in 25 ml of dry and degassed THF was added 0.8 ml of pyridine by syringe. This solution was stirred for 5 min under nitrogen and a THF solution (15ml) of PBr_3 (1.62 ml, 17.22 mmol) was added dropwise over a period of 30 min. The resultant mixture was stirred at room temperature under nitrogen for 3 additional hours. At this point the organic solution was quenched by the addition of 10 ml of aqueous saturated NaCl. The organic phase was collected, washed with more NaCl solution and dried over anhydrous $MgSO_4$. Then the solution was filtered and the solvent was removed at reduced pressure affording a yellow solid. Purification by column chromatography (silica/DCM) afforded 2.49 g (6.06 mmol, 88%) of **4** as bright yellow crystals.

^{1}H-NMR (400.1 MHz, $CDCl_3$, 298 K): δ = 9.32 (s, 1H, 9-anth), 8.45 (s, 1H, 10-Anth), 8.02 (d, 2H, 4,5-anth), 7.73 (d, 2H, 3,6-anth), 7.46 (dd, 2H, 2,7-anth), 4.48 (s, 4H, CH_2)

Mass Spectrometry (low res. EI): FW $C_{20}H_{12}Br_2$ = 411.8 g/mol
M^+ = m/z 412 (with typical isotopic signal of bromine at M+2). Fragment ion: m/z 333 (loss of bromine atom). Fragment ion: m/z 250 (loss of the second bromine atom)

CHN: $C_{20}H_{12}Br_2$ requires C 58.29%, H 2.93%; found C 56.61%, H 2.80%

5.2.5 Synthesis of 1,7-μ-[1',8'-$(C_2CH_2)_2$-$C_{14}H_8$]-1,7-*closo*-$C_2B_{10}H_{10}$ (5)

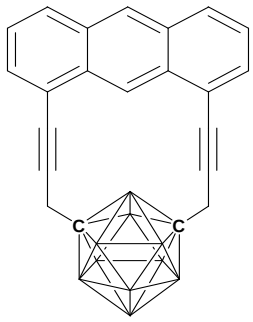

In a Schlenk tube, 0.204 g (1.42 mmol) of 1,7-*closo*-$C_2B_{10}H_{12}$ was dissolved in 20 ml of dry and degassed THF. This solution was cooled with an ice bath, n-BuLi (2.84 mmol) was added by syringe and the mixture was stirred for 18 hours allowing the solution to reach room temperature. Thereafter, the cloudy solution of the deprotonated carborane was cooled with a dry ice/acetone bath at -78ºC and a solution of 0.584 g of 1,8-bis[(bromomethyl)ethynyl]-anthracene **(4)** (1.42 mmol) in 10 ml of THF was added by syringe. The resulting dark solution was stirred for 4 hours at -78ºC and 2 additional hours at room temperature. The solvent was removed at reduced pressure and the orange residue was washed with diethyl ether (3 x 10 ml). The yellow organic solutions were concentrated at reduced pressure and purified by preparative TLC (DCM: 40-60 petroleum ether) (1:9) afforded 0.050 g (8.9 % yield) of **5** as a pale yellow solid.

^{1}H-NMR (400.1 MHz, $CDCl_3$, 298 K): δ = 9.68 (s, 1H, 9-anth), 8.42 (s, 1H, 10-anth), 7.95 (d, 2H, 4,5-anth), 7.63 (d, 2H, 3,6-anth), 7.40 (dd, 2H, 2,7-anth), 3.23 (s, 4H, -CH_2)

^{11}B-{^{1}H}-NMR (128.4 MHz, $CDCl_3$, 298 K): δ = -8.20 (2B), -10.09 (6B), -15.09 (2B)

Mass Spectrometry (low res. EI): FW $C_{22}H_{22}B_{10}$ = 394.53 g/mol
M^+ = m/z 394 (with typical carborane envelope from 390 to 397). Fragment ion: m/z 178 (anthracene ring).

CHN: $C_{22}H_{22}B_{10}$ requires C 66.98%, H 5.62%; found C 68.32%, H 5.64%

5.3 Chapter 3. Stabilisation of reduced carboranes by inductive effect

5.3.1 Synthesis of

1-C_6F_5-2-Ph-1,2-*closo*-$C_2B_{10}H_{10}$ (6)

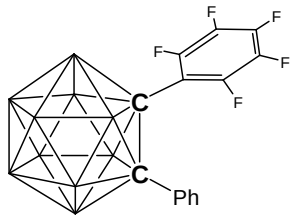

In a 100 ml round bottom flask, 0.32 g (2.62 mmol) of decaborane ($B_{10}H_{14}$) was dissolved in 20 ml of dry and degassed toluene. To this solution were added 2 ml of N,N-dimethylaniline (excess) and the solution was then stirred under nitrogen at 50ºC for an hour in order to generate the arachno species. To the resulting solution were added 0.77 g of 1-pentafluorophenyl-phenylacetylene (**E**) (2.88 mmol) in one portion and the solution was then heated to reflux under nitrogen for 18 hours. The yellow solution was concentrated under reduced pressure (heating at 50ºC was necessary to remove the N,N-dimethylaniline) leaving a bright yellow oil. Purification by column chromatography (silica/40-60 petroleum ether) afforded 0.62 g (61% yield) of pure **6** as a white powder.

^{1}H-NMR (400.1 MHz, $CDCl_3$, 298 K): δ = 7.55 (m, 2H, *ortho* phenyl), 7.36 (m, 3H, *para* and *meta* phenyl)

^{11}B{^{1}H}-NMR (128.4 MHz, $CDCl_3$, 298 K): δ = 0.61 (1B), -3.46 (1B), -9.34 (8B)

^{19}F-NMR (376.5 MHz, $CDCl_3$, 298 K): δ = -136.06 (m, 2F, *meta* F), -152.84 (m, 1F, *para* F), -161.94 (m, 2F, *ortho* F)

Mass Spectrometry (low res. EI): $C_{14}H_{15}B_{10}F_5$ FW = 386.39 g/mol
M^+ = m/z 386 (with typical carborane envelope from 382 to 389). Fragment ion: m/z 366 (loss of one fluorine atom)

CHN: $C_{14}H_{15}B_{10}F_5$ requires C 43.52%, H 3.91%; found C 43.46%, H 4.00%

5.3.2 Synthesis of

1-(4'-$H_3CC_6F_4$)-2-Ph-1,2-*closo*-$C_2B_{10}H_{10}$ (7)

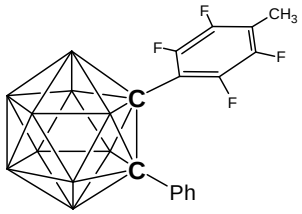

In a Schlenk tube, 0.3 g (0.78 mmol) of 1-C_6F_5-2-Ph-1,2-*closo*-$C_2B_{10}H_{10}$ (**6**) was dissolved in 20 ml of dry and degassed Et_2O. The solution was cooled at 0ºC and then 0.54 mmol of MeLi solution (1.1 eqs) were slowly added by syringe. After 1 hour stirring at room temperature, the mixture was heated to reflux for 2 further hours. Then, the reaction was quenched by addition of 10 ml of distilled water. The organic layer was extracted, washed with brine (3 x 10 ml) and dried over anhydrous $MgSO_4$. The yellowish solution was concentrated under reduced pressure leaving a pale yellow solid. Purification by column chromatography (silica/40-60 petroleum ether) afforded 0.26 g (86% yield) of pure **7** as a white crystalline powder.

^{1}H-NMR (400.1 MHz, $CDCl_3$, 298 K): δ = 7.58 (m, 2H, *ortho* phenyl), 7.30 (m, 1H, *para* phenyl), 7.22 (m, 2H, *meta* phenyl), 2.18 (s, 3H, -CH_3)

^{11}B{^{1}H}-NMR (128.4 MHz, $CDCl_3$, 298 K): δ = 0.27 (1B) -3.58 (1B), -9.50 (8B)

^{19}F-NMR (376.5 MHz, $CDCl_3$, 298 K): δ = -132.86 (m, 2F, *ortho* F), -141.46 (m, 2F, *meta* F)

Mass Spectrometry (low res. EI): $C_{15}H_{18}B_{10}F_4$ FW = 382.4 g/mol
M^+ = m/z 382 (with typical carborane envelope from 378 to 386). Fragment ion: m/z 362 (loss of one fluorine atom)

CHN: $C_{15}H_{18}B_{10}F_4$ requires C 47.11%, H 4.74%; found C 48.09%, H 4.47%

5.3.3 Synthesis of 1-(4'-$F_3CC_6F_4$)-2-Ph-1,2-*closo*-$C_2B_{10}H_{10}$ (8)

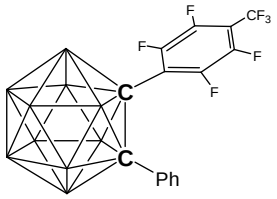

In a Schlenk tube under nitrogen, 0.5 g (2.27 mmol) of 1-Ph-1,2-*closo*-$C_2B_{10}H_{11}$ was dissolved in 20 ml of dry and degassed THF. This solution was cooled to 0ºC and then n-BuLi (1ml, 2.5 mmol) was slowly added by syringe. Then the mixture was stirred for 2 hours allowing the solution to reach room temperature. The resulting orange solution of deprotonated phenylcarborane was cooled at 0ºC with an ice bath then 0.35 ml of octafluorotoluene (2.5 mmol) were added by syringe and the deep red solution was stirred at room temperature for 18 hours. Thereafter, the reaction was quenched with saturated aqueous NH_4Cl (10 ml). The organic layer was extracted and the aqueous layer was washed with Et_2O (10 ml). The combined organic fractions were concentrated under reduced pressure. The resulting dark brown residue was filtered through silica with 40-60 petroleum ether and the colourless solution was concentrated under reduced pressure to afford 0.84 g (85% yield) of **8** as a colourless oil that slowly crystallised at room temperature to afford a white solid.

^{1}H-NMR (400.1 MHz, $CDCl_3$, 298 K): δ = 7.58 (m, 2H, *ortho* phenyl), 7.47 (m, 1H, *para* phenyl), 7.39 (m, 2H *meta* phenyl)

^{11}B{^{1}H}-NMR (128.4 MHz, $CDCl_3$, 298 K): δ = 1.19 (1B), -3.48 (1B), -9.13 (8B)

^{19}F-NMR (376.5 MHz, $CDCl_3$, 298 K): δ = -56.93 (m, 3F, $-CF_3$), -128.07 (m, 2F, *ortho* F), -137.95 (m, 2F, *meta* F)

Mass Spectrometry (low res. EI): $C_{15}H_{15}B_{10}F_7$ FW = 436.39 g/mol
M^+ = m/z 436 (with typical carborane envelope from 431 to 439). Fragment ion: m/z 416 (loss of one fluorine atom)

CHN: $C_{15}H_{15}B_{10}F_7$ requires C 41.29%, H 3.46%; found C 40.64%, H 3.52%

5.3.4 Synthesis of

1-(4'-$F_3CC_6H_4$)-2-Ph-1,2-*closo*-$C_2B_{10}H_{10}$ (9)

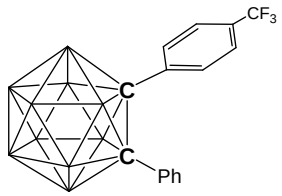

In a 100 ml round bottom flask, 0.4 g (3.28 mmol) of decaborane ($B_{10}H_{14}$) was dissolved in 20 ml of dry and degassed toluene. To this solution was added 2 ml of N,N-dimethylaniline (excess) and the solution was then stirred under nitrogen at 50ºC for an hour in order to generate the arachno species. To the resulting solution was added 0.81 g of 1-[(4'-trifluoromethyl)phenyl]-phenylacetylene (**F**) (3.28 mmol) in one portion. The solution was heated to reflux under nitrogen for 18 hours. The yellow solution was concentrated under reduced pressure (heating at 50ºC was necessary to remove the N,N-dimethylaniline) leaving a bright yellow oil. Purification by column chromatography (silica/40-60 petroleum ether) afforded 0.74 g (62% yield) of **9** as a white powder.

^{1}H-NMR (400.1 MHz, $CDCl_3$, 298 K): δ = 7.55 (m, 2H, phenyl *ortho* to CF_3), 7.39 (m, 2H, phenyl *meta* to CF_3), 7.25 (d, 2H, *ortho* phenyl), 7.14 (m, 3H, *meta* and *para* phenyl)

^{11}B{^{1}H}-NMR (128.4 MHz, $CDCl_3$, 298 K): δ = -2.48 (2B), -9.30 (2B), -10.30 (4B), -11.65 (2B)

^{19}F-NMR (376.5 MHz, $CDCl_3$, 298 K): δ = -63.15 (m, 3F, -CF_3)

Mass Spectrometry (low res. EI): $C_{15}H_{19}B_{10}F_3$ FW = 364.42 g/mol
M^+ = m/z 364 (with typical carborane envelope from 359 to 467)

CHN: $C_{15}H_{19}B_{10}F_3$ requires C 49.44%, H 5.26%; found C 49.16%, H 5.35%

5.3.5 Synthesis of 1,2-(4'-$F_3CC_6F_4)_2$-1,2-*closo*-$C_2B_{10}H_{10}$ (10)

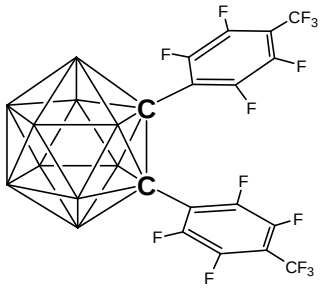

In a Schlenk tube under nitrogen, 0.4 g (2.78 mmol) of 1,2-*closo*-$C_2B_{10}H_{12}$ was dissolved in 20 ml of dry and degassed Et_2O. This solution was cooled to 0ºC and n-BuLi (2.4 ml, 5.84 mmol) was slowly added by syringe and the mixture stirred for 2 hours allowing the solution to reach room temperature. The white suspension of the deprotonated carborane was cooled with an ice bath and 0.83 ml of octafluorotoluene (5.84 mmol) was added by syringe through a rubber septum. The deep red solution was stirred at room temperature for 18 hours. Then, the reaction was quenched with saturated aqueous NH_4Cl (10 ml). The organic layer was separated and the aqueous layer was washed with Et_2O (10 ml). The combined organic fractions were concentrated under vacuum. The dark brown residue was filtered through a pad of silica with 40-60 petroleum ether and the colourless solution was concentrated at reduced pressure to afford 0.66 g (41 % yield) of **10** as a white crystalline powder.

$^{11}B\{^1H\}$-NMR (128.4 MHz, $CDCl_3$, 298 K): δ = 0.39 (2B), -7.46 (4B), -8.58 (4B)

^{19}F-NMR (376.5 MHz, $CDCl_3$, 298 K): δ = -56.87 (m, 6F, $-CF_3$), -127.79 (m, 4F, *ortho* F), -136.32 (m, 4F, *meta* F)

Mass Spectrometry (low res. EI): $C_{16}H_{10}B_{10}F_{14}$ FW = 576.34 g/mol
M^+ = m/z 576 (with typical carborane envelope from 573 to 579). Fragment ion: m/z 557 (loss of one fluorine atom)

CHN: $C_{16}H_{10}B_{10}F_{14}$ requires C 33.34%, H 1.75%; found C 33.61%, H 1.99%

5.3.6 Synthesis of 1-(4'-$F_3CC_6F_4$)-1,2-*closo*-$C_2B_{10}H_{11}$ (11)

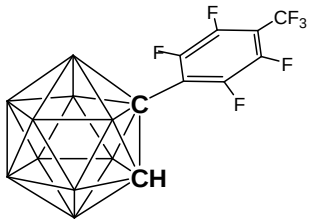

In a Schlenk tube under nitrogen, 0.4 g (2.78 mmol) of 1,2-*closo*-$C_2B_{10}H_{12}$ was dissolved in 20 ml of a 1:1 mixture of dry and degassed Et_2O and toluene. To this solution was added 0.39 ml of octafluorotoluene (2.78 mmol) by syringe and the mixture was then stirred for 5 min. The solution was cooled to 0ºC with an ice bath and n-BuLi (1.17 ml, 2.92 mmol) was added by syringe. The resulting deep red mixture was stirred for 3 hours allowing the solution to reach room temperature. Then the reaction was quenched with saturated aqueous NH_4Cl (10 ml). The organic layer was extracted and the aqueous layer was washed with Et_2O (3 x 10 ml). The combined organic washes were concentrated at reduced pressure leaving a dark brown residue. Purification by column chromatography (silica/40-60 petroleum ether) afforded the di- (**10**) and mono-substituted (**11**) products in 11% and 68% yields, respectively. 1-(4'-$F_3CC_6F_4$)-1,2-*closo*-$C_2B_{10}H_{11}$ (**11**) was isolated as a colourless oil that crystallised as a white solid over 48 hours at room temperature.

^{1}H-NMR (400.1 MHz, $CDCl_3$, 298 K): δ = 4.87 (br, 1H, C_{cage}-H)

^{11}B{^{1}H}-NMR (128.4 MHz, $CDCl_3$, 298 K): δ = -0.60 (1B), -2.09 (1B), -8.35 (2B), -9.87 (2B), -11.41 (2B), -13.09 (2B)

^{19}F-NMR (376.5 MHz, $CDCl_3$, 298 K): δ = -56.71 (m, 3F, $-CF_3$), -135.19 (m, 2F, *ortho* F), -137.29 (m, 2F, *meta* F)

Mass Spectrometry (low res. EI): $C_9H_{11}B_{10}F_7$ FW = 360.29 g/mol
M^+ = m/z 361 (with typical carborane envelope from 355 to 363). Fragment ion: m/z 342 (loss of one fluorine atom)

CHN: $C_9H_{11}B_{10}F_7$ requires C 30.00%, H 3.08%; found C 30.26%, H 3.47%

5.3.7 Synthesis of

1-(4'-$F_3CC_6H_4$)-1,2-*closo*-$C_2B_{10}H_{11}$ (12)

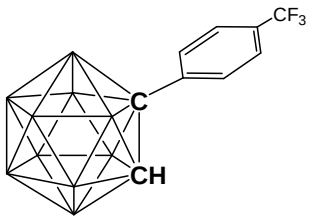

In a Schlenk tube under nitrogen, 0.4 g (2.78 mmol) of 1,2-*closo*-$C_2B_{10}H_{12}$ was dissolved in 15 ml of dry and degassed DME. The solution was cooled with an ice bath and n-BuLi (2.45 ml, 6.12 mmol) was added by syringe. The resulting white suspension was stirred for 1 hour at room temperature and then cooled again at 0ºC with an ice bath. To this cold suspension 0.49 ml of pyridine (6.12 mmol) was added followed by the addition of 0.69 g of CuCl (6.94 mmol) in one portion. The solution, which turned black, was stirred at room temperature for one hour and then heated to 60°C for 15 min and then 0.86 ml of 4-iodobenzotrifluoride (5.84 mmol) was added by syringe. The resulting mixture, which had turned dark red, was heated to reflux for 48 hours. Then, the dark brown suspension was cooled, diluted with 20 ml of Et_2O and quenched with brine. The organic layer was extracted and concentrated under reduced pressure leaving a yellow oily residue. Purification by column chromatography (silica/40-60 petroleum ether) afforded 0.52 g of **12** (65% yield) as a colourless oil. Colourless needles were obtained from recrystallisation in MeOH.

^{1}H-NMR (400.1 MHz, $CDCl_3$, 298 K): δ = 7.63 (m, 4H, phenyl), 3.97 (br, 1H, C_{cage}-H)

^{11}B{^{1}H}-NMR (128.4 MHz, $CDCl_3$, 298 K): δ = -2.03 (1B), -3.97 (1B), -8.86 (2B), -11.07 (2B), -12.84 (2B), -13.85 (2B)

^{19}F-NMR (376.5 MHz, $CDCl_3$, 298 K): δ = -63.08 (m, 3F, -CF_3)

Mass Spectrometry (low res. EI): $C_9H_{15}B_{10}F_3$ FW = 288.33 g/mol
M^+ = m/z 288 (with typical carborane envelope from 283 to 291). Fragment ion: m/z 143 (loss of –$C_6H_4CF_3$ group)

CHN: $C_9H_{15}B_{10}F_3$ requires C 37.49%, H 5.24%; found C 36.61%, H 5.40%

5.3.8 Synthesis of

1,2-(4'-$F_3CC_6H_4)_2$-1,2-*closo*-$C_2B_{10}H_{10}$ (13)

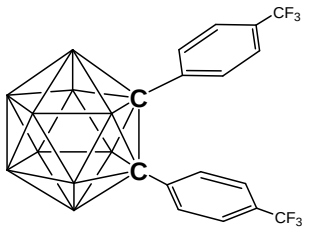

In a 100 ml round bottom flask, 0.22 g (1.80 mmol) of decaborane ($B_{10}H_{14}$) was dissolved in 20 ml of dry and degassed toluene. To this solution was added 2 ml of N,N-dimethylaniline (excess) and the solution was then stirred under nitrogen at 50ºC for an hour in order to generate the arachno species. To the resulting solution was added 0.57 g of bis[4'-(trifluoromethyl)phenyl]acetylene (**H**) (1.80 mmol) in one portion and the mixture was then heated to reflux under nitrogen for 18 hours. The yellow solution was concentrated under reduced pressure (heating at 50ºC was necessary to remove the N,N-dimethylaniline) leaving a bright yellow oil. Purification by column chromatography (silica/40-60 petroleum ether) afforded 0.45 g (58% yield) of pure **13** as a white powder.

^{1}H-NMR (400.1 MHz, $CDCl_3$, 298 K): δ = 7.58 (m, 4H, phenyl *meta*), 7.42 (m, 4H, phenyl *ortho*)

^{11}B{^{1}H}-NMR (128.4 MHz, $CDCl_3$, 298 K): δ = -1.93 (2B), -9.26 (2B), -9.93 (4B), -11.67 (2B)

^{19}F-NMR (376.5 MHz, $CDCl_3$, 298 K): δ = -63.22 (m, 6F, $-CF_3$)

Mass Spectrometry (low res. EI): $C_{16}H_{18}B_{10}F_6$ FW = 432.41 g/mol
M^+ = m/z 432 (with typical carborane envelope from 429 to 436)

CHN: $C_{16}H_{18}B_{10}F_6$ requires C 44.44%, H 4.20%; found C 44.75%, H 4.37%

5.3.9 Synthesis of 1,7-(4'-$F_3CC_6F_4)_2$-1,7-*closo*-$C_2B_{10}H_{10}$ (14)

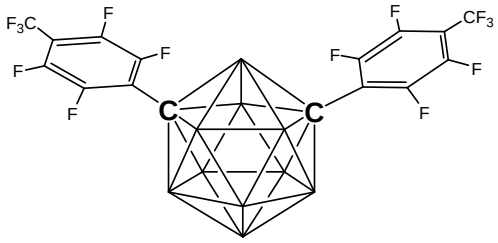

In a Schlenk tube under nitrogen, 0.4 g (2.78 mmol) of 1,7-*closo*-$C_2B_{10}H_{12}$ was dissolved in 20 ml of dry and degassed Et_2O. This solution was cooled with an ice bath, n-BuLi (2.34 ml, 5.84 mmol) was slowly added by syringe and the mixture was stirred for 6 hours allowing the solution to reach room temperature. The white suspension of deprotonated carborane was then cooled with an ice bath and 0.83 ml of octafluorotoluene (5.84 mmol) was added by syringe. The dark mixture was stirred at room temperature for 18 hours. Then the reaction was quenched with saturated aqueous NH_4Cl (10 ml). The organic layer was extracted and the aqueous layer was washed with Et_2O (10 ml). The combined organic fractions were concentrated under vacuum. The dark brown residue was filtered through a pad of silica with 40-60 petroleum ether and the colourless solution was concentrated at reduced pressure to afford 1.31 g (82 % yield) of **14** as a white crystalline powder.

$^{11}B\{^1H\}$-NMR (128.4 MHz, $CDCl_3$, 298 K): δ = -1.77 (2B), -9.96 (6B), -11.89 (2B)

^{19}F-NMR (376.5 MHz, $CDCl_3$, 298 K): δ = -56.86 (m, 6F, $-CF_3$), -127.93 (m, 4F, *ortho* F), -136.42 (m, 4F, *meta* F)

Mass Spectrometry (low res. EI): $C_{16}H_{10}B_{10}F_{14}$ FW = 576.34 g/mol
M^+ = m/z 576 (with typical carborane envelope from 573 to 579). Fragment ion: m/z 557 (loss of one fluorine atom)

CHN: $C_{16}H_{10}B_{10}F_{14}$ requires C 33.34%, H 1.75%; found C 33.83%, H 1.96%

5.3.10 Synthesis of 1,12-(4'-$F_3CC_6F_4)_2$-1,12-*closo*-$C_2B_{10}H_{10}$ (15)

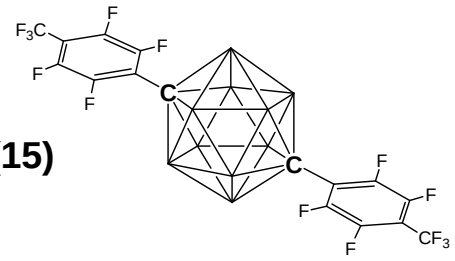

In a Schlenk tube under nitrogen, 0.3 g (2.08 mmol) of 1,12-*closo*-$C_2B_{10}H_{12}$ was dissolved in 20 ml of dry and degassed Et_2O. This solution was cooled with an ice bath and n-BuLi (1.83 ml, 4.58 mmol) was slowly added by syringe and the mixture stirred for 18 hours allowing the solution to reach room temperature. The white suspension of deprotonated carborane was then cooled with an ice bath and 0.59 ml of octafluorotoluene (4.16 mmol) was added by syringe through a rubber septum. The resulting yellow solution was stirred at room temperature for 18 hours. Thereafter, the reaction was quenched with saturated aqueous NH_4Cl (10 ml). The organic layer was extracted and the aqueous layer was washed with Et_2O (10 ml). The combined organic fractions were concentrated under vacuum. The brown residue was filtered through silica with 40-60 petroleum ether and the colourless solution was concentrated at reduced pressure to afford 1.09 g (91 % yield) of **15** as a white crystalline powder. Sometimes heating the resulting white solid at 50ºC under reduced pressure was necessary to remove traces of unreacted *p*-carborane.

$^{11}B\{^1H\}$-NMR (128.4 MHz, $CDCl_3$, 298 K): δ = -11.90 (10B)

^{19}F-NMR (376.5 MHz, $CDCl_3$, 298 K): δ = -56.83 (m, 6F, $-CF_3$), -131.21 (m, 4F, *ortho* F), -139.05 (m, 4F, *meta* F)

Mass Spectrometry (low res. EI): $C_{16}H_{10}B_{10}F_{14}$ FW = 576.34 g/mol
M^+ = m/z 576 (with typical carborane envelope from 573 to 579). Fragment ion: m/z 557 (loss of one fluorine atom)

CHN: $C_{16}H_{10}B_{10}F_{14}$ requires C 33.34, H 1.75%; found C 33.65, H 1.89%

5.3.11 Synthesis of 1,7-(4'-$F_3CC_6F_4)_2$-9,10-Ph_2-1,7-*closo*-$C_2B_{10}H_8$ (16)

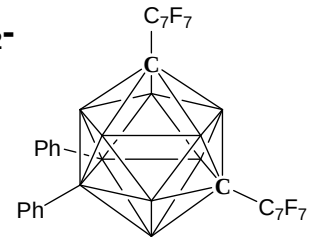

In a Schlenk tube under nitrogen, 0.23 g (0.78 mmol) of 9,10-Ph_2-1,7-*closo*-$C_2B_{10}H_{10}$ was dissolved in 20 ml of dry and degassed Et_2O. This solution was cooled with an ice bath and n-BuLi (0.68 ml, 1.71 mmol) was added by syringe and the mixture was stirred for 6 hours allowing the solution to reach room temperature. The pink suspension of deprotonated carborane was cooled again with an ice bath and 0.22 ml of octafluorotoluene (1.55 mmol) was added by syringe. The solution turned red and this mixture was stirred at room temperature for 18 hours. Then, the reaction was quenched with saturated aqueous NH_4Cl (10 ml). The organic layer was extracted and the aqueous layer was washed with Et_2O (10 ml). The combined organic fractions was concentrated at reduced pressure. The dark brown residue was filtered through a pad of silica with 40-60 petroleum ether and the colourless solution was concentrated at reduced pressure to afford 0.37 g (65 % yield) of **16** as a white crystalline powder.

^{1}H-NMR (400.1 MHz, $CDCl_3$, 298 K): δ = 7.38 (m, 4H, *ortho* phenyl), 7.15 (m, 6H, *para* and *meta* phenyl)

^{11}B{^{1}H}-NMR (128.4 MHz, $CDCl_3$, 298 K): δ = 0.90 (2B), -2.60 (2B), -9.96 (4B), -14.92 (2B)

^{19}F-NMR (376.5 MHz, $CDCl_3$, 298 K): δ = -56.73 (m, 6F, $-CF_3$), -136.42 (m, 4F, *ortho* F), -138.33 (m, 4F, *meta* F)

Mass Spectrometry (low res. EI): $C_{28}H_{18}B_{10}F_{14}$ FW = 728.54 g/mol
M^+ = m/z 728 (with typical carborane envelope from 724 to 732). Fragment ion: m/z 512 (loss of one perfluorotolyl group)

CHN: $C_{28}H_{18}B_{10}F_{14}$ requires C 46.16%, H 2.49%; found C 47.75%, H 3.00%

5.4 Chapter 4. Polyhedral expansion of selected carboranes

5.4.1 Reduction/Metallation with {CpCo} of 10.

In a Schlenk tube, 0.4 g (0.69 mmol) of 1,2-(4'-$F_3CC_6F_4)_2$-1,2-*closo*-$C_2B_{10}H_{10}$ (**10**) in 10 ml of THF was treated with 2.1 equivalents (1.39 mmol) of sodium naphthalenide added by syringe. 2.82 mmol of a 2M solution of NaCp in THF were added to the dark red solution of the reduced carborane and the resulting mixture was stirred for 15 min at room temperature. The reaction was then frozen in liquid nitrogen (-196°C) and $CoCl_2$ (2.57 mmol) was added in one portion. The stirred mixture was left to warm to room temperature. After 18 hours, air was bubbled through the solution for 30 minutes and the resulting green solution was concentrated at reduced pressure. The brown/green solid was washed with 40-60 petroleum ether in order to remove naphthalene and unreacted carborane. Further purification by preparative TLC eluting with DCM: 40-60 petroleum ether (1:1) revealed a unique orange mobile band. Compound **17** (R_F = 0.55, 0.054 g, 11.1% yield) was isolated. Dark orange crystals were grown by slow diffusion of 40-60 petroleum ether and a DCM solution of **17.**

1,12-(4'-$F_3CC_6F_4)_2$-4-Cp-4,1,12-*closo*-$CoC_2B_{10}H_{10}$ (17)

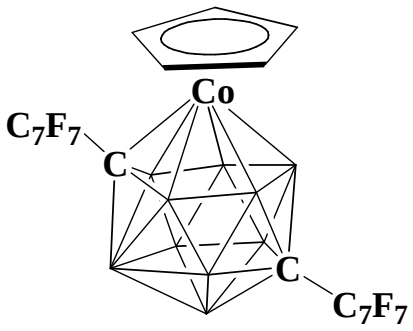

^{1}H-NMR (400.1 MHz, $CDCl_3$, 298 K): δ = 5.51 (s, 5H, η-C_5H_5).

^{11}B{^{1}H}-NMR (128.4 MHz, $CDCl_3$, 298 K): δ = 7.93 (2B), 3.32 (2B), 0.26 (1B), -2.99 (1B), -8.25 (2B), -12.81 (2B)

^{19}F-NMR (376.5 MHz, $CDCl_3$, 298 K): δ = -56.58 (m, 6F, -CF_3), -132.04 (m, 4F, *ortho* F), -140.82 (m, 4F, *meta* F)

Mass Spectrometry (low res. EI): $C_{21}H_{15}B_{10}CoF_{14}$ FW = 700.37 g/mol
M^+ = m/z 701 (with typical carborane envelope from 696 to 704)

CHN: $C_{21}H_{15}B_{10}CoF_{14}$ requires C 36.01%, H 2.16%; found C 36.01%, H 2.10%

5.4.2 Reduction/Metallation with {CpCo} of 8.

In a Schlenk tube, 0.4 g (0.92 mmol) of 1-(4'-$F_3CC_6F_4$)-2-Ph-1,2-*closo*-$C_2B_{10}H_{10}$ (**8**) in 10 ml of THF was treated with 2.1 equivalents (1.932 mmol) of sodium naphthalenide by syringe. 2.75 mmol of a 2M solution of NaCp in THF was added to the dark purple solution of the reduced carborane and the mixture was stirred for 15 min at room temperature. The reaction was then frozen in liquid nitrogen (-196°C) and $CoCl_2$ (3.45 mmol) was added in one portion. The stirred mixture was left to warm to room temperature. After 18 hours, air was bubbled through the solution for 30 minutes and the resulting brown solution was concentrated at reduced pressure. The brown/green solid was washed with 40-60 petroleum ether in order to remove naphthalene and unreacted carborane. Further purification by preparative TLC eluting with DCM: 40-60 petroleum ether (1:1) revealed three mobile bands, compounds **18** (trace), **19** and **20**. The yellow compound **19** (R_F = 0.75, 0.067 g, 13.3% yield) and brown compound **20** (R_F = 0.48, 0.034 g, 5.6% yield) were isolated and characterised. *X*-ray quality crystals were grown by slow diffusion of 40-60 petroleum ether and a concentrated DCM solution of either **19** or **20**. Full data on compound **18** are given in section 5.4.3.

1-(4'-$F_3CC_6F_4$)-2-Ph-8-Cp-8,1,2-*closo*-$CoC_2B_9H_9$ (19)

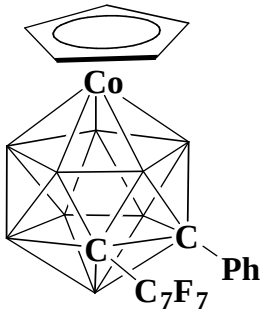

^{1}H-NMR (400.1 MHz, $CDCl_3$, 298 K): δ = 7.55-7.31 (m, 5H, phenyl), 5.48 (s, 5H, η-C_5H_5).

^{11}B{^{1}H}-NMR (128.4 MHz, $CDCl_3$, 298 K): δ = 8.27 (1B), 3.82 (1B), -0.65 (4B), -9.24 (1B), -11.70 (2B)

^{19}F-NMR (376.5 MHz, $CDCl_3$, 298 K): δ = -56.82 (m, 3F, -CF_3), -128.41 (m, 2F, *ortho* F), -139.72 (m, 2F, *meta* F)

Mass Spectrometry (low res. EI): $C_{20}H_{20}B_9CoF_7$ FW = 549.6 g/mol
M^+ = m/z 549 (with typical carborane envelope from 545 to 551)

CHN: $C_{20}H_{20}B_9CoF_7$ requires C 43.71%, H 3.67%; found C 45.04%, H 3.44%

1-Ph-4,5-Cp_2-6-(4'-$F_3CC_6F_4$)-4,5,1,6-*closo*-$Co_2C_2B_9H_9$ (20)

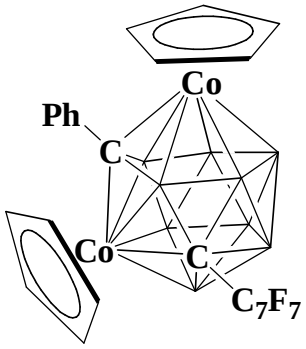

^{1}H-NMR (400.1 MHz, $CDCl_3$, 298 K): δ = 7.58-7.30 (m, 5H, phenyl), 5.29 (s, 5H, η-C_5H_5), 5.26 (s, 5H, η-C_5H_5)

^{11}B{^{1}H}-NMR (128.4 MHz, $CDCl_3$, 298 K): δ = 19.97 (1B), 14.01 (1B), 12.06 (1B), 8.29 (1B), 4.22 (1B), 0.61 (1B), -1.55 (1B), -5.69 (1B), -9.01 (1B)

^{19}F-NMR (376.5 MHz, $CDCl_3$, 298 K): δ = -56.46 (m, 3F, -CF_3), -126.51 (m, 2F, *ortho* F), -139.12 (m, 2F, *meta* F)

Mass Spectrometry (low res. EI): $C_{25}H_{24}B_9Co_2F_7$ FW = 672.62 g/mol
M^+ = m/z 673 (with typical carborane envelope from 668 to 677)

CHN: $C_{25}H_{24}B_9Co_2F_7$ requires C 44.64%, H 3.6%; found C 45.30%, H 3.71%

5.4.3 Reduction/Metallation with {CpCo} of 8 in the presence of n-BuLi.

In a Schlenk tube, 0.4 g (0.92 mmol) of 1-(4'-$F_3CC_6F_4$)-2-Ph-1,2-*closo*-$C_2B_{10}H_{10}$ (**8**) in 10 ml of THF was treated with 2.1 equivalents (1.932 mmol) of sodium naphthalenide by syringe. 2.75 mmol of a 2M solution of NaCp in THF was added to the dark purple solution of the reduced carborane and this mixture was stirred for 15 min at room temperature. Then the solution was cooled in an ice bath and one equivalent of n-BuLi (0.92 mmol) was added dropwise. Finally, the reaction was frozen in liquid nitrogen (-196°C) and $CoCl_2$ (3.45 mmol) was added in one portion. The stirred mixture was left to warm to room temperature. After 18 hours, air was bubbled through the solution for 30 min and the resulting brown suspension was concentrated at reduced pressure. The brown/green solid was washed with 40-60 petroleum ether in order to remove naphthalene and unreacted carborane. Further purification by preparative TLC eluting with DCM: 40-60 petroleum ether (1:1) gave a unique red mobile band. Product **18** (R_F = 0.62, 0.051 g, 10.2% yield) was isolated (as a mixture of two possible diastereoisomers, compounds **18A** and **18B**) and characterised. *X*-ray quality crystals were grown by slow diffusion of 40-60 petroleum ether and a concentrated DCM solution of **18**.

1,4-μ-[2'-(η-C_5H_4)-4'-CF_3-C_6F_3]-6-Ph-4,1,6-*closo*-$CoC_2B_{10}H_{10}$ (18A) and 1-Ph-6,4-μ-[2'-(η-C_5H_4)-4'-CF_3-C_6F_3]-4,1,6-*closo*-$CoC_2B_{10}H_{10}$ (18B)

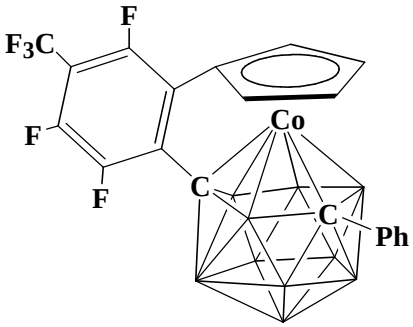

18A

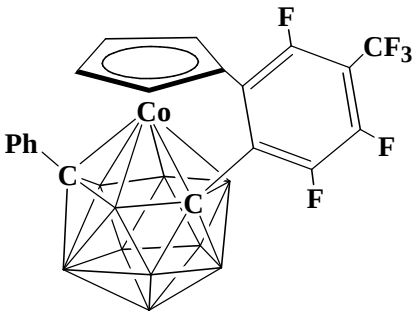

18B

^{1}H-NMR (400.1 MHz, $CDCl_3$, 298 K): δ = 7.95-7.42 (m, 5H, phenyl), 5.92 (m, 2H, η-C_5H_4), 5.58 (m, 2H, η-C_5H_4)

^{11}B{^{1}H}-NMR (128.4 MHz, $CDCl_3$, 298 K): δ = 15.94, 14.82, 11.82, 4.84, 1.47, -2.40, -3.87, -6.49, -10.67, -13.94, -16.13 (mixture of two diastereoisomers **18A** and **18B**)

^{19}F-NMR (376.5 MHz, $CDCl_3$, 298 K): δ = -56.20 (m, 3F, -CF_3), -119.28 (m, 1F), -129.12 (m, 1F), -144.40 (m, 1F)

Mass Spectrometry (low res. EI): $C_{20}H_{19}B_{10}CoF_6$ FW = 540.41 g/mol
M^+ = m/z 538 (with typical carborane envelope from 535 to 543)

CHN: $C_{20}H_{19}B_{10}CoF_6$ requires C 44.45%, H 3.54%; found C 44.70%, H 3.88%

5.4.4 Reduction/Metallation with {CpCo} of 10 in the presence of n-BuLi.

In a Schlenk tube, 0.5 g (0.87 mmol) of 1,2-(4'-$F_3CC_6F_4)_2$-1,2-*closo*-$C_2B_{10}H_{10}$ (**10**) in 10 ml of THF was treated with 2.1 equivalents (1.82 mmol) of sodium naphthalenide by syringe. 2.61 mmol of a 2M solution of NaCp in THF were added to the dark red solution of the reduced carborane and the resulting mixture was stirred for 15 min at room temperature. The solution was then cooled in an ice bath and one equivalent of n-BuLi (0.87 mmol) was added dropwise. Then the reaction was frozen in liquid nitrogen (-196°C) and $CoCl_2$ (3.45 mmol) was added in one portion. The stirred mixture was left to warm to room temperature. After 18 hours, air was bubbled through the solution for 30 minutes and the resulting brown suspension was concentrated at reduced pressure. The resulting residue was washed with 40-60 petroleum ether. Further purification by preparative TLC eluting with DCM: 40-60 petroleum ether (2:3) allowed the isolation of two mobile bands, compounds **17** (R_F = 0.64, trace) and **21** (R_F = 0.52, 0.056 g, 9.5% yield). The new product **21** (isolated as a mixture of two possible diastereoisomers, compounds **21A** and **21B**) was characterised. *X*-ray quality crystals were grown by slow diffusion of 40-60 petroleum ether and a concentrated DCM solution of **21**.

1,4-μ-[2'-(η-C_5H_4)-4'-CF_3-C_6F_3]-6-(4'-$F_3CC_6F_4$)-4,1,6-*closo*-$CoC_2B_{10}H_{10}$ (21A) and 1-(4'-$F_3CC_6F_4$)-6,4-μ-[2'-(η-C_5H_4)-4'-CF_3-C_6F_3]-4,1,6-*closo*-$CoC_2B_{10}H_{10}$ (21B)

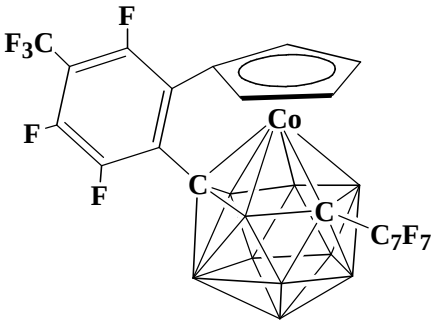

21A

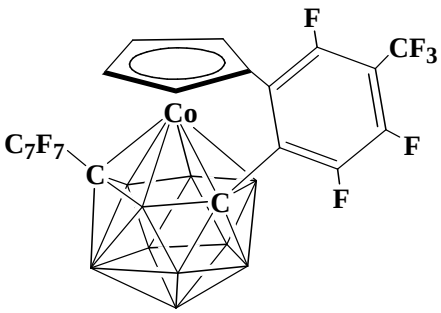

21B

^{1}H-NMR (400.1 MHz, $CDCl_3$, 298 K): δ = 6.02 (m, 2H, η-C_5H_4), 5.49 (m, 2H, η-C_5H_4)

^{11}B{^{1}H}-NMR (128.4 MHz, $CDCl_3$, 298 K): δ = 29.10, 13.27, 9.07, 3.85, 0.63, -3.25, -4.99, -7.43, -12.44, -16.54 (mixture of two diastereoisomers **21A** and **21B**)

^{19}F-NMR (376.5 MHz, $CDCl_3$, 298 K): δ = -56.42 (m, 6F, -CF_3), -118.27 (m, 1F, C_5H_4-perfluorotolyl), -128.83 (m, 1F, C_5H_4-perfluorotolyl), -132.03 (m, 2F, *ortho* perfluorotolyl), -134.01 (m, 2F, *meta* perfluorotolyl), -140.64 (m, 1F, C_5H_4-perfluorotolyl)

Mass Spectrometry (low res. EI): $C_{21}H_{14}B_{10}CoF_{13}$ FW = 680.37 g/mol
M^+ = m/z 679 (with typical carborane envelope from 674 to 684)

CHN: $C_{21}H_{14}B_{10}CoF_{13}$ requires C 37.07%, H 2.07%; found C 36.76%, H 2.44%

5.4.5 Reduction/Metallation with {Cp*Co} of 10.

In a Schlenk tube, 0.5 g (0.87 mmol) of 1,2-(4'-$F_3CC_6F_4)_2$-1,2-*closo*-$C_2B_{10}H_{10}$ (**10**) in 10 ml of THF was treated with 2.1 equivalents (1.82 mmol) of sodium naphthalenide by syringe and the mixture was stirred for 15 min at room temperature. Then, 2.60 mmol of a 0.5M solution of NaCp* in THF were added and the solution was stirred for 10 min. The reaction was then frozen in liquid nitrogen (-196°C) and $CoCl_2$ (3.45 mmol) was added in one portion. The stirred mixture was left to warm to room temperature. After 18 hours, air was bubbled through the solution for 30 min and the resulting brown suspension was concentrated at reduced pressure. The brown/green residue was washed with 40-60 petroleum ether in order to remove naphthalene and unreacted carborane. Chromatography column (DCM: 40-60 petroleum ether, 1:1) afforded pale yellow compound **22** (0.169 g, 24% yield) and a mixture of cobaltacarboranes that was further purified by preparative TLC (DCM: 40-60 petroleum ether, 2:3) to isolate orange compounds **23** (R_F = 0.75, 0.037 g, 5.5% yield) and **24** (R_F = 0.27, 0.058 g, 8.4% yield). *X*-ray quality crystals of **22** and **24** were grown by slow diffusion of 40-60 petroleum ether in a concentrated DCM solution of the appropriate compound.

1,2-(4'-$CF_2C_{10}H_{15}$-C_6F_4)$_2$-1,2-*closo*-$C_2B_{10}H_{10}$ (22)

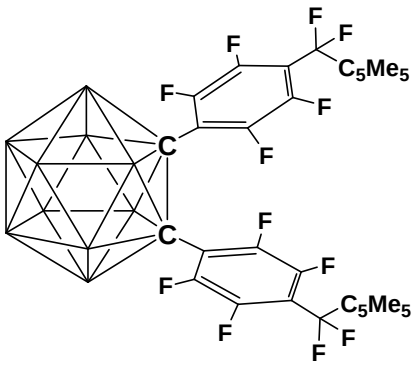

^{1}H-NMR (400.1 MHz, $CDCl_3$, 298 K): δ = 1.85 (s, 12H, C_5Me_5), 1.46 (s, 12H, C_5Me_5), 1.25 (s, 6H, C_5Me_5)

^{11}B{^{1}H}-NMR (128.4 MHz, $CDCl_3$, 298 K): δ = -1.97 (2B), -9.89 (8B)

^{19}F-NMR (376.5 MHz, $CDCl_3$, 298 K): δ = -94.92 (m, 4F, -CF_2-), -135.29 (m, 4F, *ortho* F), -138.03 (m, 4F, *meta* F)

Mass Spectrometry (low res. EI): $C_{36}H_{40}B_{10}F_{12}$ FW = 808.81 g/mol
M^+ = m/z 809 (with typical carborane envelope from 804 to 812)

CHN: $C_{36}H_{40}B_{10}F_{12}$ requires C 53.46%, H 4.98%; found C 52.95%, H 4.85%

1,12-(4'-$F_3CC_6F_4)_2$-4-Cp*-4,1,12-*closo*-$CoC_2B_{10}H_{10}$ (23)

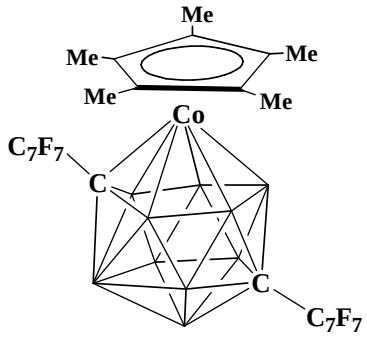

^{1}H-NMR (400.1 MHz, $CDCl_3$, 298 K): δ = 1.71 (s, 15H, η-C_5Me_5)

^{11}B{^{1}H}-NMR (128.4 MHz, $CDCl_3$, 298 K): δ = 8.78 (1B), 4.73 (1B), 1.93 (1B), 0.12 (1B), -2.21 (1B), -7.98 (2B), -9.76 (1B), -14.00 (2B)

^{19}F-NMR (376.5 MHz, $CDCl_3$, 298 K): δ = -56.55 (m, 6F, -CF_3), -131.31 (m, 4F, *ortho* F), -141.26 (m, 4F, *meta* F)

Mass Spectrometry (low res. EI): $C_{26}H_{25}B_{10}CoF_{14}$ FW = 770.51 g/mol
M^+ = m/z 771 (with typical carborane envelope from 765 to 774)

CHN: $C_{26}H_{25}B_{10}CoF_{14}$ requires C 40.53%, H 3.27%; found C 41.22%, H 3.28%

1-(4'-$F_3CC_6F_4$)-2,8-Cp^*_2-12-THF-2,8,1-*closo*-$Co_2CB_9H_8$ (24)

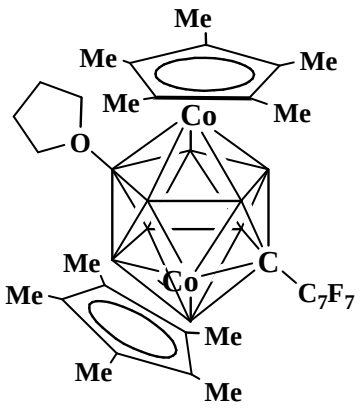

^{1}H-NMR (400.1 MHz, $CDCl_3$, 298 K): δ = 4.33 (m, 4H, THF), 2.12 (m, 4H, THF), 1.76 (s, 15H, η-C_5Me_5), 1.48 (s, 15H, η-C_5Me_5)

^{11}B{^{1}H}-NMR (128.4 MHz, $CDCl_3$, 298 K): δ = 27.15 (1B, B-THF), 19.17 (1B), 17.32 (1B), 4.04 (2B), 0.57 (2B), -18.74 (2B)

^{19}F-NMR (376.5 MHz, $CDCl_3$, 298 K): δ = -56.07 (m, 3F, -CF_3), -128.05 (m, 2F, *ortho* F), -144.39 (m, 2F, *meta* F)

Mass Spectrometry (low res. EI): $C_{32}H_{46}B_9Co_2F_7O$ FW = 794.88 g/mol
M^+ = m/z 795 (with typical carborane envelope from 791 to 798). Fragment ion: m/z 723 (loss of THF group)

CHN: $C_{32}H_{46}B_9Co_2F_7O$ requires C 48.35%, H 5.83%; found C 48.57%, H 5.83%

5.4.6 Reduction/Metallation with {(η-C_6H_6)Ru} of 10.

In a Schlenk tube, 0.4 g (0.69 mmol) of 1,2-(4'-$F_3CC_6F_4)_2$-1,2-*closo*-$C_2B_{10}H_{10}$ (**10**) in 10 ml of THF were treated with 2.1 equivalents (1.39 mmol) of sodium naphthalenide added by syringe. The resultant dark red solution of the reduced carborane was stirred at room temperature for 15 min, then frozen in liquid nitrogen (-196ºC) and 0.174 g of $[Ru(\eta\text{-}C_6H_6)Cl_2]_2$ (0.35 mmol) were added in one portion. The stirred mixture was left to warm to room temperature. After 18 hours, the solvent was removed under reduced pressure and the brown/orange residue was washed with 40-60 petroleum ether in order to remove naphthalene and unreacted carborane. Further purification by preparative TLC eluting with DCM: 40-60 petroleum ether (1:1) revealed two mobile bands. A pale grey compound **25** (R_F = 0.32, 0.019 g, 3.8% yield) and a pale yellow compound **26** (R_F = 0.20, 0.049 g, 9.3% yield) were isolated. *X*-ray quality crystals of **25** and **26** were grown by slow diffusion of 40-60 petroleum ether and a concentrated DCM solution of the compound.

1,2-(4'-$F_3CC_6F_4)_2$-3-(η-C_6H_6)-3,1,2-*pseudocloso*-$RuC_2B_9H_9$ (25)

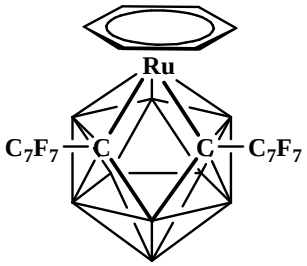

^{1}H-NMR (400.1 MHz, $CDCl_3$, 298 K): δ = 6.09 (s, 6H, η-C_6H_6)

^{11}B{^{1}H}-NMR (128.4 MHz, $CDCl_3$, 298 K): δ = 33.71 (1B), 20.15 (2B), 14.15 (1B), 3.07 (2B), 1.23 (2B), -16.61 (1B)

^{19}F-NMR (376.5 MHz, $CDCl_3$, 298 K): δ = -56.78 (m, 6F, -CF_3), -129.56 (m, 4F, *ortho* F), -141.13 (m, 4F, *meta* F)

Mass Spectrometry (low res. EI): $C_{22}H_{15}B_9F_{14}Ru$ FW = 743.71 g/mol
M^+ = m/z 744 (with typical carborane envelope from 737 to 749)

CHN: $C_{22}H_{15}B_9F_{14}Ru$ requires C 35.53%, H 2.03%; found C 36.29%, H 1.95%

1,12-(4'-$F_3CC_6F_4)_2$-4-(η-C_6H_6)-4,1,12-*closo*-$RuC_2B_{10}H_{10}$ (26)

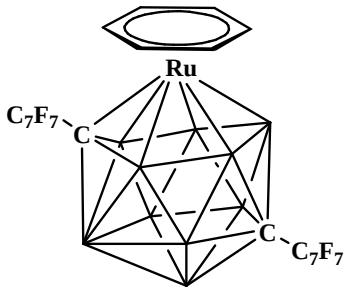

^{1}H-NMR (400.1 MHz, $CDCl_3$, 298 K): δ = 6.16 (s, 6H, η-C_6H_6)

^{11}B{^{1}H}-NMR (128.4 MHz, $CDCl_3$, 298 K): δ = 9.12 (1B), 1.72 (2B), -7.61 (4B), -18.39 (2B), -20.51 (1B)

^{19}F-NMR (376.5 MHz, $CDCl_3$, 298 K): δ = -56.47 (m, 6F, $-CF_3$), -130.86 (m, 4F, *ortho* F), -140.67 (m, 4F, *meta* F)

Mass Spectrometry (low res. EI): $C_{22}H_{16}B_{10}F_{14}Ru$ FW = 755.53 g/mol
M^+ = m/z 756 (with typical carborane envelope from 751 to 760)

CHN: $C_{22}H_{16}B_{10}F_{14}Ru$ requires C 34.97%, H 2.13%; found C 34.13%, H 3.05%

5.4.7 Reduction/Metallation with {(η-C_6H_6)Ru} of 8.

In a Schlenk tube, 0.56 g (1.28 mmol) of 1-(4'-$F_3CC_6F_4$)-2-Ph-1,2-*closo*-$C_2B_{10}H_{10}$ (**8**) in 10 ml of THF was treated with 2.1 equivalents (2.70 mmol) of sodium naphthalenide added by syringe. The resultant dark purple solution of the reduced carborane was stirred at room temperature for 15 min, then frozen in liquid nitrogen (-196ºC) and 0.320 g of $[Ru(\eta\text{-}C_6H_6)Cl_2]_2$ (0.64 mmol) was added in one portion. The stirred mixture was left to warm to room temperature. After 18 hours, the solvent was removed under reduced pressure and the brown/orange residue was washed with 40-60 petroleum ether in order to remove naphthalene and unreacted carborane. Further purification by preparative TLC eluting with DCM: 40-60 petroleum ether (1:1) revealed a pale yellow mobile band. Compound **27** (R_F = 0.20, 0.065 g, 8.2% yield) was isolated. *X*-ray quality crystals were grown by slow diffusion of 40-60 petroleum ether and a concentrated DCM solution of **27**.

1-(4'-$F_3CC_6F_4$)-4-(η-C_6H_6)-6-Ph-4,1,6-*closo*-$RuC_2B_{10}H_{10}$ (27)

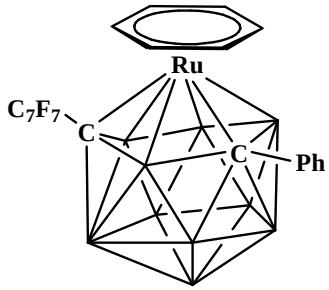

^{1}H-NMR (400.1 MHz, $CDCl_3$, 298 K): δ = 7.61-7.18 (m, 5H, phenyl), 5.68 (s, 6H, η-C_6H_6)

^{11}B{^{1}H}-NMR (128.4 MHz, $CDCl_3$, 298 K): δ = 8.60 (1B), 2.50 (2B), -6.50 (4B), -9.54 (2B), -17.83 (1B)

^{19}F-NMR (376.5 MHz, $CDCl_3$, 298 K): δ = -56.30 (m, 3F, -CF_3), -131.63 (m, 2F, *ortho* F), -139.94 (m, 2F, *meta* F)

Mass Spectrometry (low res. EI): $C_{21}H_{21}B_{10}F_7Ru$ FW = 615.57 g/mol
M^+ = m/z 615 (with typical carborane envelope from 611 to 620)

CHN: $C_{21}H_{21}B_{10}F_7Ru$ requires C 40.98%, H 3.44%; found C 41.07%, H 3.41%

5.5 References

5.1 A. M. Spokoyny, M. G. Reuter, C. L. Stern, M. A. Ratner, T. Seideman and C. A. Mirkin, *J. Am. Chem. Soc.*, 2009, **131**, 9482.

5.2 H. E. Katz, *J. Org. Chem.*, 1989, **54**, 2179.

5.3 C. E. Smith, P. S. Smith, Rh. Ll. Thomas, E. G. Robins, J. C. Collings, C. Dai, A. J. Scott, S. Borwick, A. S. Batsanov, S. W. Watt, S. J. Clark, C. Viney, J. A. K. Howard, W. Clegg and T. B. Marder, *J. Mater. Chem.*, 2004, **14**, 413.

5.4 P. T. Brain, J. Cowie, D. J. Donohoe, D. Hnyk, D. W. H. Rankin, D. Reed, B. D. Reid, H. E. Robertson and A. J. Welch, *Inorg. Chem.*, 1996, **35**, 1701.

5.5 Z. G. Lewis and A. J. Welch, *Acta Crystallogr., Sect. C*, 1993, **49**, 705.

5.6 A. Kollhofer, T. Pullmann and H. Plenio, *Angew. Chem. Int. Ed.*, 2003, **42**, 1056.

5.7 M. J. Mio, L. C. Kopel, J. B. Braun, T. L. Gadzikwa, K. L. Hull, R. G. Brisbois, C. J. Markworth and P. A. Grieco, *Org. Lett.*, 2002, **4**, 3199.

5.8 Z. Zheng, W. Jiang, A. A. Zinn, C. B. Knobler and M. F. Hawthorne, *Inorg. Chem.*, 1995, **34**, 2095.

5.9 M. A. Bennett and A. K. Smith, *J. Chem. Soc. Dalton Trans.*, 1974, 233.

5.10 Bruker *AXS APEX2*, version 1.0-8; Bruker AXS Inc., Madison, WI, USA, 2003.

5.11 *SHELXTL*, version 6.10; Bruker AXS Inc., Madison, WI, USA, 2000.

5.12 Mercury, version 1.4.2, Cambridge Crystallographic Data Centre, Cambridge, UK, 2006.

APPENDIX 1

CRYSTAL DATA AND STRUCTURE REFINEMENT

Crystal data and structure refinement for compound **4**.

Identification code	x82091_0m
Empirical formula	C_{20} H_{12} Br_2
Formula weight	412.12
Temperature	100(2) K
Wavelength	0.71073 Å
Crystal system	Triclinic
Space group	P-1
Unit cell dimensions	a = 7.4578(12) Å, α= 114.452(5)°. b = 10.3401(19) Å, β= 93.817(6)°. c = 11.582(2) Å, γ = 106.144(6)°.
Volume	763.9(2) $Å^3$
Z	2
Density (calculated)	1.792 Mg/m^3
Absorption coefficient	5.298 mm^{-1}
F(000)	404
Crystal size	0.38 x 0.20 x 0.16 mm^3
Theta range for data collection	2.25 to 32.56°.
Index ranges	-11<=h<=8, -13<=k<=15, -17<=l<=16
Reflections collected	15829
Independent reflections	4921 [R(int) = 0.0438]
Completeness to theta = 25.00°	98.3 %
Absorption correction	Semi-empirical from equivalents
Max. and min. transmission	0.4844 and 0.2380
Refinement method	Full-matrix least-squares on F^2
Data / restraints / parameters	4921 / 0 / 199
Goodness-of-fit on F^2	1.067
Final R indices [I>2sigma(I)]	R1 = 0.0384, wR2 = 0.0970
R indices (all data)	R1 = 0.0565, wR2 = 0.1036
Largest diff. peak and hole	0.692 and -0.657 e.$Å^{-3}$

Crystal data and structure refinement for compound **5**.

Identification code	x82670_0m
Empirical formula	C_{22} H_{22} B_{10}
Formula weight	394.50
Temperature	100(2) K
Wavelength	0.71073 Å
Crystal system	Orthorhombic
Space group	P2(1)2(1)2(1)
Unit cell dimensions	a = 6.5541(19) Å, α= 90°. b = 16.871(5) Å, β= 90°. c = 18.748(6) Å, γ = 90°.
Volume	2073.0(11) $Å^3$
Z	4
Density (calculated)	1.264 Mg/m^3
Absorption coefficient	0.064 mm^{-1}
F(000)	816
Crystal size	0.38 x 0.20 x 0.08 mm^3
Theta range for data collection	2.49 to 26.73°.
Index ranges	-8<=h<=8, -21<=k<=21, -23<=l<=23
Reflections collected	35462
Independent reflections	2521 [R(int) = 0.1062]
Completeness to theta = 25.00°	99.9 %
Absorption correction	Semi-empirical from equivalents
Max. and min. transmission	0.9949 and 0.8237
Refinement method	Full-matrix least-squares on F^2
Data / restraints / parameters	2521 / 0 / 323
Goodness-of-fit on F^2	1.084
Final R indices [I>2sigma(I)]	R1 = 0.0678, wR2 = 0.1636
R indices (all data)	R1 = 0.1260, wR2 = 0.2233
Largest diff. peak and hole	0.881 and -0.347 e.$Å^{-3}$

Crystal data and structure refinement for compound **6**.

Identification code	hut299
Empirical formula	C_{14} H_{15} B_{10} F_5
Formula weight	386.36
Temperature	100(2) K
Wavelength	0.71073 Å
Crystal system	Monoclinic
Space group	P 21/c
Unit cell dimensions	a = 7.9262(10) Å, α= 90°. b = 16.625(2) Å, β= 97.880(2)°. c = 13.5738(17) Å, γ = 90°.
Volume	1771.8(4) $Å^3$
Z	4
Density (calculated)	1.448 Mg/m^3
Absorption coefficient	0.112 mm^{-1}
F(000)	776
Crystal size	0.31 x 0.17 x 0.09 mm^3
Theta range for data collection	1.95 to 30.12°.
Index ranges	-11<=h<=11, -20<=k<=23, -14<=l<=19
Reflections collected	14612
Independent reflections	5171 [R(int) = 0.0669]
Completeness to theta = 25.00°	99.9 %
Absorption correction	Semi-empirical from equivalents
Max. and min. transmission	0.986 and 0.970
Refinement method	Full-matrix least-squares on F^2
Data / restraints / parameters	5171 / 0 / 292
Goodness-of-fit on F^2	1.016
Final R indices [I>2sigma(I)]	R1 = 0.0593, wR2 = 0.1151
R indices (all data)	R1 = 0.1143, wR2 = 0.1359
Largest diff. peak and hole	0.378 and -0.297 e.$Å^{-3}$

Crystal data and structure refinement for compound **7**.

Identification code	2856m
Empirical formula	C_{15} H_{18} B_{10} F_4
Formula weight	382.39
Temperature	100(2) K
Wavelength	0.71073 Å
Crystal system	Monoclinic
Space group	P2(1)/c
Unit cell dimensions	a = 20.395(4) Å, α= 90°. b = 10.841(2) Å, β= 116.36(3)°. c = 18.920(4) Å, γ = 90°.
Volume	3748.3(13) $Å^3$
Z	8
Density (calculated)	1.355 Mg/m^3
Absorption coefficient	0.097 mm^{-1}
F(000)	1552
Crystal size	0.54 x 0.38 x 0.20 mm^3
Theta range for data collection	2.15 to 26.00°.
Index ranges	-25<=h<=25, -13<=k<=13, -22<=l<=23
Reflections collected	41788
Independent reflections	7318 [R(int) = 0.0552]
Completeness to theta = 25.00°	99.9 %
Absorption correction	Semi-empirical from equivalents
Max. and min. transmission	0.9808 and 0.9054
Refinement method	Full-matrix least-squares on F^2
Data / restraints / parameters	7318 / 0 / 525
Goodness-of-fit on F^2	1.017
Final R indices [I>2sigma(I)]	R1 = 0.0475, wR2 = 0.1030
R indices (all data)	R1 = 0.0744, wR2 = 0.1138
Largest diff. peak and hole	0.220 and -0.254 e.$Å^{-3}$

Crystal data and structure refinement for compound **8**.

Identification code	x82696
Empirical formula	C_{15} H_{15} B_{10} F_7
Formula weight	436.37
Temperature	100(2) K
Wavelength	0.71073 Å
Crystal system	Triclinic
Space group	P-1
Unit cell dimensions	a = 7.1669(11) Å, α= 101.887(5)°. b = 10.7348(15) Å, β= 98.662(5)°. c = 13.205(2) Å, γ = 91.230(5)°.
Volume	981.3(3) $Å^3$
Z	2
Density (calculated)	1.477 Mg/m^3
Absorption coefficient	0.124 mm^{-1}
F(000)	436
Crystal size	0.78 x 0.34 x 0.18 mm^3
Theta range for data collection	2.24 to 28.33°.
Index ranges	-9<=h<=9, -13<=k<=13, 0<=l<=17
Reflections collected	29038
Independent reflections	4547 [R(int) = 0.0440]
Completeness to theta = 25.00°	95.8 %
Absorption correction	Semi-empirical from equivalents
Max. and min. transmission	0.9780 and 0.5777
Refinement method	Full-matrix least-squares on F^2
Data / restraints / parameters	4547 / 6 / 339
Goodness-of-fit on F^2	1.028
Final R indices [I>2sigma(I)]	R1 = 0.0614, wR2 = 0.1414
R indices (all data)	R1 = 0.1034, wR2 = 0.1662
Largest diff. peak and hole	0.690 and -0.560 e.$Å^{-3}$

Crystal data and structure refinement for compound **9**.

Identification code	x82704_0m
Empirical formula	C_{15} H_{19} B_{10} F_3
Formula weight	364.40
Temperature	100(2) K
Wavelength	0.71073 Å
Crystal system	Monoclinic
Space group	P2(1)/n
Unit cell dimensions	a = 10.1887(11) Å, α= 90°. b = 12.3835(12) Å, β= 103.201(4)°. c = 15.3510(17) Å, γ = 90°.
Volume	1885.7(3) $Å^3$
Z	4
Density (calculated)	1.284 Mg/m^3
Absorption coefficient	0.086 mm^{-1}
F(000)	744
Crystal size	0.78 x 0.12 x 0.06 mm^3
Theta range for data collection	2.63 to 23.70°.
Index ranges	-11<=h<=11, -13<=k<=13, -17<=l<=17
Reflections collected	25735
Independent reflections	2847 [R(int) = 0.0732]
Completeness to theta = 23.70°	99.7 %
Absorption correction	Semi-empirical from equivalents
Max. and min. transmission	0.9949 and 0.8252
Refinement method	Full-matrix least-squares on F^2
Data / restraints / parameters	2847 / 0 / 284
Goodness-of-fit on F^2	1.032
Final R indices [I>2sigma(I)]	R1 = 0.0378, wR2 = 0.0824
R indices (all data)	R1 = 0.0772, wR2 = 0.1028
Largest diff. peak and hole	0.184 and -0.228 e.$Å^{-3}$

Crystal data and structure refinement for compound **10**.

Identification code	x82649_0m
Empirical formula	C_{16} H_{10} B_{10} F_{14}
Formula weight	576.34
Temperature	100(2) K
Wavelength	0.71073 Å
Crystal system	Monoclinic
Space group	P2(1)/n
Unit cell dimensions	a = 10.8344(14) Å, α= 90°. b = 27.098(3) Å, β= 91.132(7)°. c = 14.8774(19) Å, γ = 90°.
Volume	4367.0(10) $Å^3$
Z	8
Density (calculated)	1.753 Mg/m^3
Absorption coefficient	0.179 mm^{-1}
F(000)	2256
Crystal size	0.48 x 0.40 x 0.14 mm^3
Theta range for data collection	1.50 to 26.51°.
Index ranges	-13<=h<=13, -33<=k<=33, -18<=l<=18
Reflections collected	83652
Independent reflections	8933 [R(int) = 0.0601]
Completeness to theta = 25.00°	99.9 %
Absorption correction	Semi-empirical from equivalents
Max. and min. transmission	0.9754 and 0.8910
Refinement method	Full-matrix least-squares on F^2
Data / restraints / parameters	8933 / 0 / 721
Goodness-of-fit on F^2	1.128
Final R indices [I>2sigma(I)]	R1 = 0.0827, wR2 = 0.2709
R indices (all data)	R1 = 0.1009, wR2 = 0.2840
Largest diff. peak and hole	0.941 and -0.620 e.$Å^{-3}$

Crystal data and structure refinement for compound **12**.

Identification code	x82679_0m
Empirical formula	C_9 H_{15} B_{10} F_3
Formula weight	288.31
Temperature	100(2) K
Wavelength	0.71073 Å
Crystal system	Monoclinic
Space group	P2(1)/c
Unit cell dimensions	a = 7.1953(12) Å, α= 90°. b = 10.1655(17) Å, β= 96.818(6)°. c = 20.213(3) Å, γ = 90°.
Volume	1468.0(4) $Å^3$
Z	4
Density (calculated)	1.304 Mg/m^3
Absorption coefficient	0.091 mm^{-1}
F(000)	584
Crystal size	0.62 x 0.14 x 0.06 mm^3
Theta range for data collection	2.85 to 25.23°.
Index ranges	-8<=h<=8, -10<=k<=12, -24<=l<=24
Reflections collected	15421
Independent reflections	2645 [R(int) = 0.0522]
Completeness to theta = 25.00°	99.9 %
Absorption correction	Semi-empirical from equivalents
Max. and min. transmission	0.9946 and 0.8536
Refinement method	Full-matrix least-squares on F^2
Data / restraints / parameters	2645 / 0 / 202
Goodness-of-fit on F^2	1.016
Final R indices [I>2sigma(I)]	R1 = 0.0484, wR2 = 0.1181
R indices (all data)	R1 = 0.0813, wR2 = 0.1367
Largest diff. peak and hole	0.253 and -0.344 e.$Å^{-3}$

Crystal data and structure refinement for compound **13.**

Identification code	x82870o
Empirical formula	C_{16} H_{18} B_{10} F_6
Formula weight	432.40
Temperature	100(2) K
Wavelength	0.71073 Å
Crystal system	Orthorhombic
Space group	Pna2(1)
Unit cell dimensions	a = 9.9377(6) Å, α= 90°. b = 14.8567(9) Å. β= 90°. c = 14.0881(8) Å. γ = 90°.
Volume	2080.0(2) $Å^3$
Z	4
Density (calculated)	1.381 Mg/m^3
Absorption coefficient	0.110 mm^{-1}
F(000)	872
Crystal size	0.38 x 0.24 x 0.04 mm^3
Theta range for data collection	2.47 to 25.62°.
Index ranges	-12<=h<=12, -18<=k<=17, -17<=l<=17
Reflections collected	38169
Independent reflections	2035 [R(int) = 0.0374]
Completeness to theta = 25.00°	99.9 %
Absorption correction	Semi-empirical from equivalents
Max. and min. transmission	0.9956 and 0.9372
Refinement method	Full-matrix least-squares on F^2
Data / restraints / parameters	2035 / 55 / 317
Goodness-of-fit on F^2	1.141
Final R indices [I>2sigma(I)]	R1 = 0.0398, wR2 = 0.1035
R indices (all data)	R1 = 0.0440, wR2 = 0.1068
Largest diff. peak and hole	0.204 and -0.205 e.$Å^{-3}$

Crystal data and structure refinement for compound **14.**

Identification code	x82678_0m
Empirical formula	C_{16} H_{10} B_{10} F_{14}
Formula weight	576.34
Temperature	100(2) K
Wavelength	0.71073 Å
Crystal system	Monoclinic
Space group	P2(1)/n
Unit cell dimensions	a = 7.3776(14) Å, α= 90°. b = 11.542(2) Å. β= 98.164(7)°. c = 25.729(5) Å. γ = 90°.
Volume	2168.6(7) $Å^3$
Z	4
Density (calculated)	1.765 Mg/m^3
Absorption coefficient	0.180 mm^{-1}
F(000)	1128
Crystal size	0.62 x 0.38 x 0.04 mm^3
Theta range for data collection	1.60 to 24.77°.
Index ranges	-8<=h<=8, -13<=k<=13, -30<=l<=30
Reflections collected	29696
Independent reflections	3682 [R(int) = 0.1019]
Completeness to theta = 24.77°	98.7 %
Absorption correction	Semi-empirical from equivalents
Max. and min. transmission	0.993 and 0.7975
Refinement method	Full-matrix least-squares on F^2
Data / restraints / parameters	3682 / 0 / 362
Goodness-of-fit on F^2	1.660
Final R indices [I>2sigma(I)]	R1 = 0.1820, wR2 = 0.4721
R indices (all data)	R1 = 0.2127, wR2 = 0.4885
Extinction coefficient	0.27(3)
Largest diff. peak and hole	1.149 and -1.070 e.$Å^{-3}$

Crystal data and structure refinement for compound **15**.

Identification code	x83029
Empirical formula	C_{16} H_{10} B_{10} F_{14}
Formula weight	576.34
Temperature	100(2) K
Wavelength	0.71073 Å
Crystal system	Monoclinic
Space group	P2(1)/n
Unit cell dimensions	a = 12.259(4) Å, α= 90°. b = 7.194(2) Å, β= 91.861(10)°. c = 24.414(8) Å, γ = 90°.
Volume	2152.1(12) $Å^3$
Z	4
Density (calculated)	1.779 Mg/m^3
Absorption coefficient	0.182 mm^{-1}
F(000)	1128
Crystal size	0.78 x 0.62 x 0.04 mm^3
Theta range for data collection	1.88 to 26.02°.
Index ranges	-14<=h<=15, -8<=k<=8, -29<=l<=29
Reflections collected	28720
Independent reflections	4153 [R(int) = 0.0640]
Completeness to theta = 25.00°	99.9 %
Absorption correction	Semi-empirical from equivalents
Max. and min. transmission	0.9928 and 0.8713
Refinement method	Full-matrix least-squares on F^2
Data / restraints / parameters	4153 / 0 / 361
Goodness-of-fit on F^2	1.089
Final R indices [I>2sigma(I)]	R1 = 0.0570, wR2 = 0.1444
R indices (all data)	R1 = 0.0880, wR2 = 0.1597
Largest diff. peak and hole	0.349 and -0.308 e.$Å^{-3}$

Crystal data and structure refinement for compound **16**.

Identification code	x83061
Empirical formula	C_{28} H_{18} B_{10} F_{14}
Formula weight	728.52
Temperature	100(2) K
Wavelength	0.71073 Å
Crystal system	Triclinic
Space group	P-1
Unit cell dimensions	a = 8.0105(9) Å, α= 61.228(5)°. b = 14.6893(17) Å, β= 78.048(6)°. c = 14.7775(17) Å, γ = 88.155(6)°.
Volume	1486.5(3) $Å^3$
Z	2
Density (calculated)	1.628 Mg/m^3
Absorption coefficient	0.151 mm^{-1}
F(000)	724
Crystal size	0.58 x 0.34 x 0.08 mm^3
Theta range for data collection	2.61 to 27.40°.
Index ranges	-10<=h<=10, -19<=k<=18, -18<=l<=19
Reflections collected	23809
Independent reflections	6485 [R(int) = 0.0315]
Completeness to theta = 25.00°	98.3 %
Absorption correction	Semi-empirical from equivalents
Max. and min. transmission	0.9880 and 0.9177
Refinement method	Full-matrix least-squares on F^2
Data / restraints / parameters	6485 / 15 / 497
Goodness-of-fit on F^2	1.043
Final R indices [I>2sigma(I)]	R1 = 0.0390, wR2 = 0.0938
R indices (all data)	R1 = 0.0554, wR2 = 0.1031
Largest diff. peak and hole	0.297 and -0.332 e.$Å^{-3}$

Crystal data and structure refinement for compound **17**.

Identification code	x82929
Empirical formula	C_{21} H_{15} B_{10} Co F_{14}
Formula weight	700.36
Temperature	100(2) K
Wavelength	0.71073 Å
Crystal system	Monoclinic
Space group	Cc
Unit cell dimensions	a = 24.237(3) Å, α= 90°. b = 12.4207(17) Å, β= 105.478(7)°. c = 9.0234(12) Å, γ = 90°.
Volume	2617.9(6) $Å^3$
Z	4
Density (calculated)	1.777 Mg/m^3
Absorption coefficient	0.771 mm^{-1}
F(000)	1376
Crystal size	0.32 x 0.12 x 0.10 mm^3
Theta range for data collection	2.80 to 25.65°.
Index ranges	-29<=h<=29, -15<=k<=15, -10<=l<=10
Reflections collected	17205
Independent reflections	4860 [R(int) = 0.0499]
Completeness to theta = 25.00°	99.9 %
Absorption correction	Semi-empirical from equivalents
Max. and min. transmission	0.9269 and 0.7904
Refinement method	Full-matrix least-squares on F^2
Data / restraints / parameters	4860 / 2 / 446
Goodness-of-fit on F^2	1.022
Final R indices [I>2sigma(I)]	R1 = 0.0376, wR2 = 0.0603
R indices (all data)	R1 = 0.0532, wR2 = 0.0645
Absolute structure parameter	0.251(12)
Largest diff. peak and hole	0.246 and -0.251 e.$Å^{-3}$

Crystal data and structure refinement for compound **18**.

Identification code	x82958
Empirical formula	C_{20} H_{19} B_{10} Co F_6
Formula weight	540.38
Temperature	100(2) K
Wavelength	0.71073 Å
Crystal system	Monoclinic
Space group	P2(1)/c
Unit cell dimensions	a = 15.3592(11) Å, α= 90°. b = 8.3208(6) Å, β= 92.862(4)°. c = 17.3907(13) Å, γ = 90°.
Volume	2219.8(3) $Å^3$
Z	4
Density (calculated)	1.617 Mg/m^3
Absorption coefficient	0.834 mm^{-1}
F(000)	1080
Crystal size	0.28 x 0.18 x 0.10 mm^3
Theta range for data collection	2.64 to 24.97°.
Index ranges	-18<=h<=18, 0<=k<=9, 0<=l<=20
Reflections collected	29038
Independent reflections	4007 [R(int) = 0.0989]
Completeness to theta = 24.97°	99.4 %
Absorption correction	None
Max. and min. transmission	0.9213 and 0.8001
Refinement method	Full-matrix least-squares on F^2
Data / restraints / parameters	4007 / 0 / 366
Goodness-of-fit on F^2	1.045
Final R indices [I>2sigma(I)]	R1 = 0.0548, wR2 = 0.1174
R indices (all data)	R1 = 0.0958, wR2 = 0.1342
Largest diff. peak and hole	0.737 and -0.436 e.$Å^{-3}$

Crystal data and structure refinement for compound **19**.

Identification code	x82910
Empirical formula	C_{20} H_{20} B_9 Co F_7
Formula weight	550.82
Temperature	100(2) K
Wavelength	0.71073 Å
Crystal system	Triclinic
Space group	P-1
Unit cell dimensions	a = 8.9537(6) Å, α= 97.643(3)°. b = 14.7491(10) Å, β= 99.295(3)°. c = 18.7783(13) Å, γ = 102.812(3)°.
Volume	2349.3(3) $Å^3$
Z	4
Density (calculated)	1.557 Mg/m^3
Absorption coefficient	0.796 mm^{-1}
F(000)	1101
Crystal size	0.42 x 0.40 x 0.04 mm^3
Theta range for data collection	1.12 to 27.49°.
Index ranges	-11<=h<=11, -19<=k<=19, -24<=l<=24
Reflections collected	47566
Independent reflections	10555 [R(int) = 0.0447]
Completeness to theta = 25.00°	99.4 %
Absorption correction	Semi-empirical from equivalents
Max. and min. transmission	0.9689 and 0.8950
Refinement method	Full-matrix least-squares on F^2
Data / restraints / parameters	10555 / 57 / 704
Goodness-of-fit on F^2	1.043
Final R indices [I>2sigma(I)]	R1 = 0.0435, wR2 = 0.1147
R indices (all data)	R1 = 0.0751, wR2 = 0.1389
Largest diff. peak and hole	0.743 and -0.566 e.$Å^{-3}$

Crystal data and structure refinement for compound **20.**

Identification code	x83224
Empirical formula	C_{25} H_{24} B_9 Co_2 F_7
Formula weight	672.59
Temperature	100(2) K
Wavelength	0.71073 Å
Crystal system	Monoclinic
Space group	P2(1)/n
Unit cell dimensions	a = 8.0211(5) Å, α= 90°. b = 26.0503(18) Å, β= 94.026(3)°. c = 12.5510(8) Å, γ = 90°.
Volume	2616.1(3) $Å^3$
Z	4
Density (calculated)	1.708 Mg/m^3
Absorption coefficient	1.337 mm^{-1}
F(000)	1344
Crystal size	0.38 x 0.14 x 0.04 mm^3
Theta range for data collection	2.26 to 26.48°.
Index ranges	-9<=h<=9, -32<=k<=32, -15<=l<=14
Reflections collected	37965
Independent reflections	5314 [R(int) = 0.0453]
Completeness to theta = 25.00°	99.7 %
Absorption correction	Semi-empirical from equivalents
Max. and min. transmission	0.9485 and 0.6306
Refinement method	Full-matrix least-squares on F^2
Data / restraints / parameters	5314 / 60 / 413
Goodness-of-fit on F^2	1.039
Final R indices [I>2sigma(I)]	R1 = 0.0343, wR2 = 0.0731
R indices (all data)	R1 = 0.0537, wR2 = 0.0798
Largest diff. peak and hole	0.518 and -0.438 e.$Å^{-3}$

Crystal data and structure refinement for compound **21**.

Identification code	x83113
Empirical formula	C_{21} H_{14} B_{10} Co F_{13}
Formula weight	701.58
Temperature	100(2) K
Wavelength	0.71073 Å
Crystal system	Rhombohedral
Space group	R-3
Unit cell dimensions	a = 23.6037(12) Å, α= 90°. b = 23.6037(12) Å, β= 90°. c = 24.7385(15) Å, γ = 120°.
Volume	11936.1(11) $Å^3$
Z	18
Density (calculated)	1.757 Mg/m^3
Absorption coefficient	0.805 mm^{-1}
F(000)	6201
Crystal size	0.38 x 0.24 x 0.06 mm^3
Theta range for data collection	2.76 to 26.40°.
Index ranges	-29<=h<=29, -29<=k<=28, -30<=l<=20
Reflections collected	38491
Independent reflections	5409 [R(int) = 0.0406]
Completeness to theta = 25.00°	99.6 %
Absorption correction	Semi-empirical from equivalents
Max. and min. transmission	0.9533 and 0.7496
Refinement method	Full-matrix least-squares on F^2
Data / restraints / parameters	5409 / 17 / 455
Goodness-of-fit on F^2	1.064
Final R indices [I>2sigma(I)]	R1 = 0.0439, wR2 = 0.1314
R indices (all data)	R1 = 0.0710, wR2 = 0.1523
Largest diff. peak and hole	0.793 and -0.504 e.$Å^{-3}$

Crystal data and structure refinement for compound **22**.

Identification code	X83097
Empirical formula	C_{36} H_{40} B_{10} F_{12}
Formula weight	808.78
Temperature	100(2) K
Wavelength	0.71073 Å
Crystal system	Triclinic
Space group	P-1
Unit cell dimensions	a = 14.5973(13) Å, α= 70.015(4)°. b = 16.0164(14) Å, β= 79.973(4)°. c = 18.3603(16) Å, γ = 89.535(4)°.
Volume	3966.3(6) $Å^3$
Z	4
Density (calculated)	1.354 Mg/m^3
Absorption coefficient	0.113 mm^{-1}
F(000)	1656
Crystal size	0.72 x 0.68 x 0.40 mm^3
Theta range for data collection	1.20 to 25.49°.
Index ranges	-17<=h<=17, -18<=k<=19, 0<=l<=22
Reflections collected	69711
Independent reflections	18020 [R(int) = 0.0605]
Completeness to theta = 25.00°	95.0 %
Absorption correction	Semi-empirical from equivalents
Max. and min. transmission	0.9561 and 0.9229
Refinement method	Full-matrix least-squares on F^2
Data / restraints / parameters	18020 / 202 / 1125
Goodness-of-fit on F^2	1.146
Final R indices [I>2sigma(I)]	R1 = 0.0835, wR2 = 0.2115
R indices (all data)	R1 = 0.1091, wR2 = 0.2268
Largest diff. peak and hole	0.583 and -0.544 e.$Å^{-3}$

Crystal data and structure refinement for compound **24**.

Identification code	j5we36k
Empirical formula	C_{32} H_{46} B_9 Co_2 F_7 O
Formula weight	794.84
Temperature	173(2) K
Wavelength	0.71073 Å
Crystal system	Orthorhombic
Space group	Pbca
Unit cell dimensions	a = 12.8521(5) Å, α= 90°. b = 16.2817(6) Å, β= 90°. c = 33.9667(12) Å, γ = 90°.
Volume	7107.7(5) $Å^3$
Z	8
Density (calculated)	1.486 Mg/m^3
Absorption coefficient	0.998 mm^{-1}
F(000)	3264
Crystal size	0.15 x 0.06 x 0.01 mm^3
Theta range for data collection	3.02 to 25.68°.
Index ranges	-15<=h<=13, -17<=k<=19, -41<=l<=34
Reflections collected	39726
Independent reflections	6737 [R(int) = 0.1167]
Completeness to theta = 25.00°	99.8 %
Absorption correction	Semi-empirical from equivalents
Max. and min. transmission	0.9901 and 0.8647
Refinement method	Full-matrix least-squares on F^2
Data / restraints / parameters	6737 / 77 / 532
Goodness-of-fit on F^2	1.422
Final R indices [I>2sigma(I)]	R1 = 0.0899, wR2 = 0.1459
R indices (all data)	R1 = 0.1341, wR2 = 0.1601
Largest diff. peak and hole	0.686 and -0.562 e.$Å^{-3}$

Crystal data and structure refinement for compound **25**.

Identification code	x83004
Empirical formula	C_{22} H_{15} B_9 F_{14} Ru
Formula weight	743.70
Temperature	100(2) K
Wavelength	0.71073 Å
Crystal system	Monoclinic
Space group	P2(1)/c
Unit cell dimensions	a = 8.7173(11) Å, α= 90°. b = 18.314(2) Å, β= 96.509(6)°. c = 17.055(2) Å, γ = 90°.
Volume	2705.3(6) $Å^3$
Z	4
Density (calculated)	1.826 Mg/m^3
Absorption coefficient	0.692 mm^{-1}
F(000)	1448
Crystal size	0.38 x 0.16 x 0.08 mm^3
Theta range for data collection	1.64 to 25.68°.
Index ranges	-10<=h<=10, 0<=k<=21, 0<=l<=20
Reflections collected	50659
Independent reflections	8442 [R(int) = 0.1039]
Completeness to theta = 25.00°	98.8 %
Absorption correction	Semi-empirical from equivalents
Max. and min. transmission	0.9467 and 0.7788
Refinement method	Full-matrix least-squares on F^2
Data / restraints / parameters	8442 / 145 / 464
Goodness-of-fit on F^2	1.095
Final R indices [I>2sigma(I)]	R1 = 0.1081, wR2 = 0.2554
R indices (all data)	R1 = 0.1623, wR2 = 0.2890
Largest diff. peak and hole	2.800 and -1.548 e.$Å^{-3}$

Crystal data and structure refinement for compound **26**.

Identification code	x82990
Empirical formula	C_{22} H_{16} B_{10} F_{14} Ru
Formula weight	802.49
Temperature	100(2) K
Wavelength	0.71073 Å
Crystal system	Triclinic
Space group	P1
Unit cell dimensions	a = 9.0549(6) Å, α= 108.044(4)°. b = 11.4599(8) Å, β= 93.812(4)°. c = 16.0093(12) Å, γ = 90.151(4)°.
Volume	1575.59(19) $Å^3$
Z	2
Density (calculated)	1.692 Mg/m^3
Absorption coefficient	0.683 mm^{-1}
F(000)	783
Crystal size	0.42 x 0.38 x 0.10 mm^3
Theta range for data collection	1.34 to 27.62°.
Index ranges	-11<=h<=11, -14<=k<=14, -20<=l<=20
Reflections collected	28551
Independent reflections	12765 [R(int) = 0.0435]
Completeness to theta = 25.00°	99.9 %
Absorption correction	Semi-empirical from equivalents
Max. and min. transmission	0.9348 and 0.7623
Refinement method	Full-matrix least-squares on F^2
Data / restraints / parameters	12765 / 5 / 853
Goodness-of-fit on F^2	1.019
Final R indices [I>2sigma(I)]	R1 = 0.0592, wR2 = 0.1497
R indices (all data)	R1 = 0.0642, wR2 = 0.1543
Absolute structure parameter	0.02(3)
Largest diff. peak and hole	3.960 and -1.078 e.$Å^{-3}$

Crystal data and structure refinement for compound **27**.

Identification code	x83093
Empirical formula	C_{21} H_{21} B_{10} F_7 Ru
Formula weight	734.92
Temperature	100(2) K
Wavelength	0.71073 Å
Crystal system	Triclinic
Space group	P-1
Unit cell dimensions	a = 9.184(2) Å, α= 112.229(9)°. b = 11.658(3) Å, β= 90.328(10)°. c = 13.897(3) Å, γ = 90.640(10)°.
Volume	1377.2(5) $Å^3$
Z	2
Density (calculated)	1.772 Mg/m^3
Absorption coefficient	0.925 mm^{-1}
F(000)	724
Crystal size	0.42 x 0.40 x 0.38 mm^3
Theta range for data collection	2.22 to 31.60°.
Index ranges	-12<=h<=13, -16<=k<=17, -20<=l<=20
Reflections collected	33166
Independent reflections	8873 [R(int) = 0.0324]
Completeness to theta = 25.00°	99.3 %
Absorption correction	Semi-empirical from equivalents
Max. and min. transmission	0.7201 and 0.6974
Refinement method	Full-matrix least-squares on F^2
Data / restraints / parameters	8873 / 10 / 410
Goodness-of-fit on F^2	1.067
Final R indices [I>2sigma(I)]	R1 = 0.0273, wR2 = 0.0664
R indices (all data)	R1 = 0.0311, wR2 = 0.0685
Largest diff. peak and hole	1.394 and -1.308 e.$Å^{-}$